# KoG

No. 26. (2022)
ISSN 1331-1611

SCIENTIFIC - PROFESSIONAL JOURNAL
OF CROATIAN SOCIETY FOR GEOMETRY AND GRAPHICS

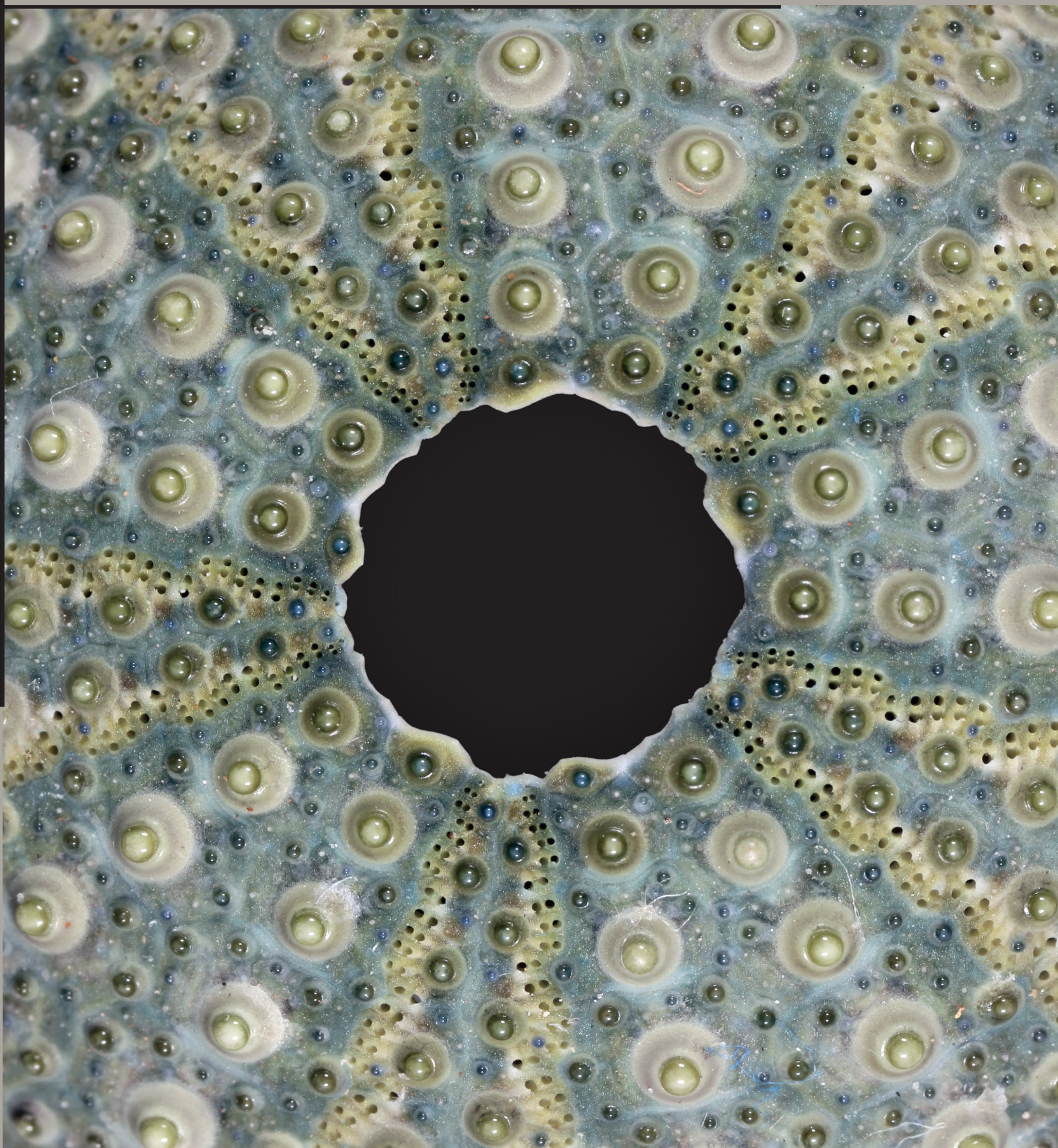

Official publication of the Croatian Society for Geometry and Graphics publishes scientific and professional papers from the fields of geometry, applied geometry and computer graphics.

**Founder and Publisher**

Croatian Society for Geometry and Graphics



**Design**

Miroslav Ambruš-Kiš

**Layout**

Sonja Gorjanc, Ema Jurkin

**Cover Illustration**

Georg Glaeser, photography

**Print**

SAND d.o.o., Zagreb

**URL address**

http://www.hdgg.hr/kog
http://hrcak.srce.hr

**Edition**

150

**Published annually**

**Guide for authors**
Please, see the page 79.

**KoG** is reviewed by zbMATH.

---

This issue has been financially supported by the Foundation of the Croatian Academy of Sciences and Arts.

ISSN 1331–1611

# KoG

SCIENTIFIC AND PROFESSIONAL JOURNAL OF
CROATIAN SOCIETY FOR GEOMETRY AND GRAPHICS

No. 26
Zagreb, 2022

# CONTENTS

## ORIGINAL SCIENTIFIC PAPERS



## REVIEWS

ISSN 1331–1611

BROJ 26
Zagreb, 2022

ZNANSTVENO-STRUČNI ČASOPIS
HRVATSKOG DRUŠTVA ZA GEOMETRIJU I GRAFIKU

# SADRŽAJ

## ORIGINALNI ZNANSTVENI RADOVI



## PREGLEDNI RADOVI

https://doi.org/10.31896/k.26.1
Original scientific paper
Accepted 24. 1. 2022.

FILIPE BELLIO
RONALDO GARCIA
DAN REZNIK

# Parabola-Inscribed Poncelet Polygons Derived from the Bicentric Family

**Parabola-Inscribed Poncelet Polygons Derived from the Bicentric Family**

**ABSTRACT**

We study loci and properties of a Parabola-inscribed family of Poncelet polygons whose caustic is a focus-centered circle. This family is the polar image of a special case of the bicentric family with respect to its circumcircle. We describe closure conditions, curious loci, and new conserved quantities.

**Key words:** Poncelet, closure, porism, parabola, bicentric, conservation, invariants

**MSC2020:** 37M05, 00A72, 51N20, 37-04

**Ponceletovi poligoni upisani paraboli i dobiveni iz bicentričkih familija**

**SAŽETAK**

Proučavamo geometrijska mjesta i svojstva familija Ponceletovih poligona upisanih paraboli koji omataju kružnicu sa središtem u fokusu parabole. Ova familija je polarna slika specijalnog slučaja bicentrične familije s obzirom na svoju opisanu kružnicu. Opisujemo uvjete zatvaranja, geometrijska mjesta, i nove invarijante.

**Ključne riječi:** Poncelet, zatvaranje, porizam, parabola, bicentričan, očuvanost, invarijante

## 1 Introduction

This is a continuation of our investigation of Euclidean phenomena of Poncelet families [11, 12, 14, 20]. Recall Poncelet's porism: specially-chosen pairs of conics $\mathcal{C}, \mathcal{C}'$ admit a one-parameter family of polygons inscribed in $\mathcal{C}$ while simultaneously circumscribed about $\mathcal{C}'$ [5, 7, 8].

Here we consider a certain family such that $\mathcal{C}$ is a parabola $\mathcal{P}$ while $\mathcal{C}'$ is a circle centered on the focus of $\mathcal{P}$. As shown in Figure 1, this is simply the polar image of the *bicentric family* (interscribed between two circles) with respect to its circumcircle, see Appendices A and B for construction details. We derive closure conditions for this new family for $N = 3,4,5,6$ cases ($N$ is the number of sides) and describe some of its properties and loci of associated points. Also considered is its polar image with respect to $\mathcal{P}$.

**Main results**

- The loci of vertex, perimeter, and area centroids are parabolas. Recall that in general, the locus of the perimeter centroid is not a conic [22].
- The loci of vertex and area centroids of polar polygons are straight lines, whereas that of the perimeter centroid is a non-conic.
- In the $N = 3$ case, the locus of the orthocenter is a straight line as are those of many triangle centers of the polar family. The Euler line of the polar family always passes through the parabola's focus.
- Several centers of the $N = 3$ polar family are stationary and/or sweep circles. In the latter case, they all belong to a single parabolic pencil.
- We prove that the quantity $\sum \sin\theta_i/2$ is conserved, where $\theta_i$ are the interior angles of parabola-inscribed polygons. In fact, this quantity is conserved by any conic-inscribed polar image of the bicentric family.

Most of the above properties were first noticed via simulation [25], and later proved with a computer-algebra system (CAS) [17], using the explicit parametrizations given in Appendix A. For brevity, we omit any CAS-based proofs.

**Related work**

We can roughly divide it into three groups: (i) the study of point loci over certain triangle families [18, 19, 27], (ii) proving that loci of certain Poncelet triangle families are of a given curve type [9, 13, 21, 23], and (iii) proving properties and invariants over $N \geq 3$ Poncelet families [2, 4, 6, 22]. Also related is the Steiner-Soddy Poncelet family which are the polar image of the so-called Brocard porism with respect to the circumcircle [10].

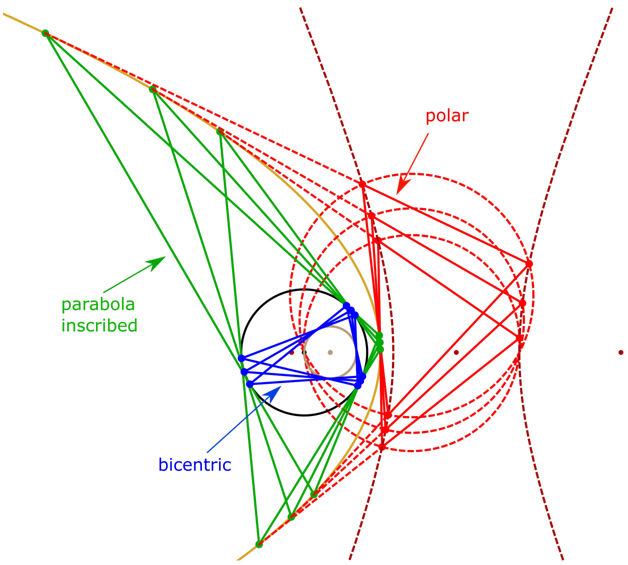


Figure 1: *Several configurations of the parabola-inscribed Poncelet family (green), obtainable as the polar image of the bicentric family (blue) with respect to the outer circle (black), provided the bicentric incircle passes through the circumcenter, see Apendix B. Also shown is the polar family (red) of the parabola-inscribed one with respect to the parabola itself. This family is inscribed in a hyperbola (dark dashed red). So you can think of this trio (blue, green, red) as successive polar images with respect to the outer conic of each preceding family.*

**Article organization**

In Sections 2 and 3 we examine parabola-inscribed Poncelet triangles (as well as its polar polygons with respect to the parabola), deriving closure conditions and expressions for many of its their triangle center loci. In Section 4 we derive geometric closure conditions for $N = 4, 5, 6$ families, respectively, detecting the abovementioned pattern for the loci of their centroids (as well as in the polar family), followed by conjectured generalizations in Section 7. In Section 8 we describe a new quantity conserved by the parabola-inscribed family (and variations thereof).

In Appendix A we provide explicit parametrizations for the vertices of both the $N = 3$ and $N = 4$ families, as well as their respective polar families. In Appendix B we explore the relation of parabola-inscribed families with the traditional bicentric family.

## 2 Loci of parabola-inscribed triangles

Referring to Figure 2, consider a Poncelet family $T$ of triangles inscribed in a parabola $\mathcal{P}$, and circumscribed about a focus-centered circle. Let $F = [-f, 0]$ and $V = [0, 0]$ denote focus and vertex, respectively, where $f$ is the focal distance. Consider a circle $\mathcal{C}$ centered at $F$ with radius $r$.

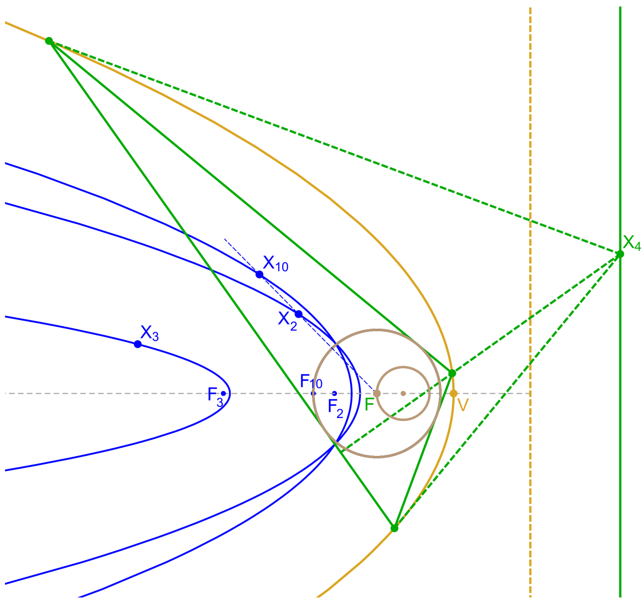


Figure 2: *A Poncelet triangle (green) is shown inscribed in a parabola $\mathcal{P}$ (gold), circumscribed about a focus-centered circle $\mathcal{C}'$ (brown). Over the family, $X_4$ sweeps a line (solid green) parallel to the directrix (dashed gold). The loci of barycenter $X_2$, circumcenter $X_3$, and Spieker center $X_{10}$ are coaxial parabolas (blue); their foci are labeled $F_2$, $F_3$, and $F_{10}$, respectively. Notice the latter is on an intersection of $\mathcal{C}'$ and the axis of the $\mathcal{P}$ (dashed gray). Since the family circumscribes a circle centered on $F$, $F, X_2, X_{10}$ are collinear (dashed blue) and $X_{10} = F + (3/2)(X_2 - F)$, see Remark 1.*

**Proposition 1** *$\mathcal{P}$ and $\mathcal{C}$ will admit a Poncelet family of triangles if, and only if, $r/f = 2(\sqrt{2} - 1)$.*

**Proof.** Consider the Poncelet triangle with two parallel sides shown in Figure 3, inscribed in the parabola $y = x^2/(4f)$, where $f$ is the focal length. At $x = r$ the parabola must be at $y = f - r$, i.e., $f - r = r^2/(4f)$, and the result follows. $\square$

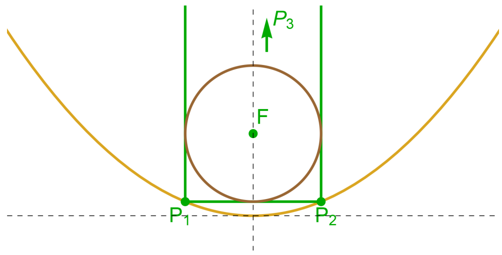


Figure 3: *Construction used to derive $r/f$ in Proposition 1. Side $P_1P_2$ of the Poncelet triangle is perpendicular to the axis while the other two sides are parallel to it, i.e., vertex $P_3$ lies on the line at infinity.*

### 2.1 Straight-line orthocenter locus

let $\mathcal{T}$ denote our parabola-inscribed triangle family and $\mathcal{D}$ the directrix of $\mathcal{P}$. Henceforth we shall adopt Kimberling's notation $X_k$ to refer to triangle centers [16].

**Proposition 2** *Over $\mathcal{T}$, the locus of the orthocenter $X_4$ is the line parallel to $\mathcal{D}$ given by $x = (5-2\sqrt{2})f$, with $y \in \mathbb{R}\backslash\{\pm 2(\sqrt{2}-1)f\}$.*

The proof below was kindly contributed by Alexey Zaslavsky [26]:

**Proof.** Let $\mathcal{C}$ be the unit circle in the complex plane and $A$, $B$, $C$ the touching points with the sides of the parabola-inscribed triangles. The polar transformation with center $F$ maps the parabola to a circle with center $I$ passing through $F$ and touching $AB$, $BC$, $CA$. Using Euler's formula $|FI|^2 = r^2 = R(R-2r)$ [24], with $R = 1$ its radius, and $r = \sqrt{2}-1$. Consider the line $FI$ as the real axis. Since $I$ is self-conjugated with respect to $ABC$, we have $a+b+c = 2\sqrt{2}-2+(3-2\sqrt{2})abc$, $ab+bc+ca = 3-\sqrt{2}+(2\sqrt{2}-2)abc$. The polar images of the altitudes of the original triangle are the common points of $BC$, $CA$, $AB$ with the lines passing through $F$, and perpendicular to $FA$, $FB$, $FC$ respectively. We have to calculate the common point of the line passing through these three points and the real axis. The coordinate functions of this point are symmetric functions in $a, b, c$, so we can express them as elementary symmetric functions on said variables, and verify that they are constant. The restriction on $y$ coordinates are poles in the parametric equation that describes the locus. □

Note that in [10, Section 4] a more general result was proved: the locus of the orthocenter $X_4$ of any Poncelet triangle family inscribed in a parabola $\mathcal{P}$ whose caustic is a circle centered on the axis of $\mathcal{P}$, is a straight line parallel to the directrix of $\mathcal{P}$.

In Appendix B we describe how the parabola-inscribed family is the polar image of the bicentric family with respect to its circumcircle. Referring to Figure 4, Proposition 2 is actually a special case of:

**Proposition 3** *The locus of $X_4$ of an family which is the polar image of $N = 3$ bicentrics with respect to its outer circle is an ellipse, straight line, or hyperbola if the circumcenter of the bicentric triangle lies in the interior, on top, or outside its incircle.*

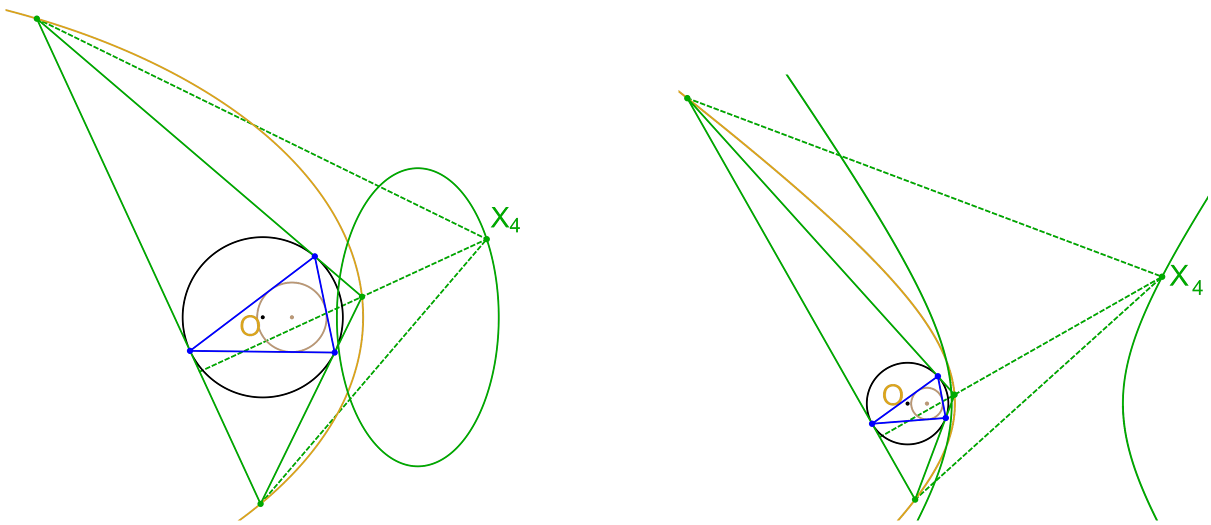


Figure 4: *Consider perturbing to the bicentric family (blue) such that the circumcenter $O$ is interior (resp. exterior) to the incircle, as shown on the left (resp. right). The tangential family (green) becomes ellipse- (resp. hyperbola-) inscribed (gold curve). In the former (resp. latter) case, the locus of the orthocenter $X_4$ is an ellipse (resp. hyperbola).*

### 2.2 Three parabolic loci

Referring to Figure 2, we show below that over $\mathcal{T}$, the loci of the barycenter, circumcenter, and Spieker centers are all parabolas. The first and last correspond to the vertex and perimeter centroids of a triangle. This is curious since, in general, the locus of the perimeter centroid of a Poncelet family is not a conic [22].

**Proposition 4** *Over $\mathcal{T}$, the locus of the barycenter $X_2$ is a parabola coaxial with $\mathcal{P}$, with focus $F_2 = [-f/3, 0]$, and vertex $V_2 = [2f(1-2\sqrt{2})/3, 0]$.*

**Proposition 5** *Over $\mathcal{T}$, the locus of the circumcenter $X_3$ of $T$ is a parabola coaxial with $\mathcal{P}$, with focus $F_3 = [-f(2\sqrt{2}-3)/2, 0]$, and vertex $V_3 = [-f(2\sqrt{2}+3)/2, 0]$.*

**Proposition 6** *Over $\mathcal{T}$, the locus of the Spieker center $X_{10}$ is a parabola coaxial with $\mathcal{P}$, with focus $F_{10} = [(1-2\sqrt{2})f, 0]$ and vertex $V_{10} = [f(3/2-2\sqrt{2}), 0]$. In particular, $F_{10} = [-f-r, 0]$, i.e., it lies on the left extreme of $\mathcal{C}$.*

Note that $X_{10}$ is the perimeter centroid of a triangle, while $X_2$ doubles up as both the vertex and area centroid. A. Akopyan has reminded us of the following general fact:

**Remark 1** *If a polygon circumscribes a circle (let its center be $O$), then $C_1, C_2, O$ are collinear and $(C_1 - O) = (3/2)(C_2 - O)$.*

Therefore:

**Corollary 1** *Over $\mathcal{T}$, $X_{10}$ is collinear with $X_2$ and $X_{10} = F + (3/2)(X_2 - F)$.*

## 3 The polar $N = 3$ family

Referring to Figure 5, let $T'$ denote the *polar* triangle of a triangle $T$ in $\mathcal{T}$, i.e., whose sidelines are the polars of $T$ with respect to $\mathcal{P}$. Since $T$ is inscribed in $\mathcal{P}$ these are simply the tangents.

Recall some known properties of the polar triangle with respect to any parabola [3]: (i) the circumcircle of $T'$ passes through the focus $F$; (ii) the orthocenter of $T'$ is on the directrix; (iii) its area is half that of the reference triangle.

**Proposition 7** *The $T'$ family is Ponceletian. It is circumscribed about $\mathcal{P}$ and is inscribed in a hyperbola $\mathcal{H}$ with center $[f, 0]$. Its axes are the axis and directrix of $\mathcal{P}$. Its implicit equation reads*

$$\mathcal{H}: \left(\sqrt{2}+\frac{3}{2}\right)(x-f)^2 - \frac{y^2}{2} - 2f^2 = 0.$$

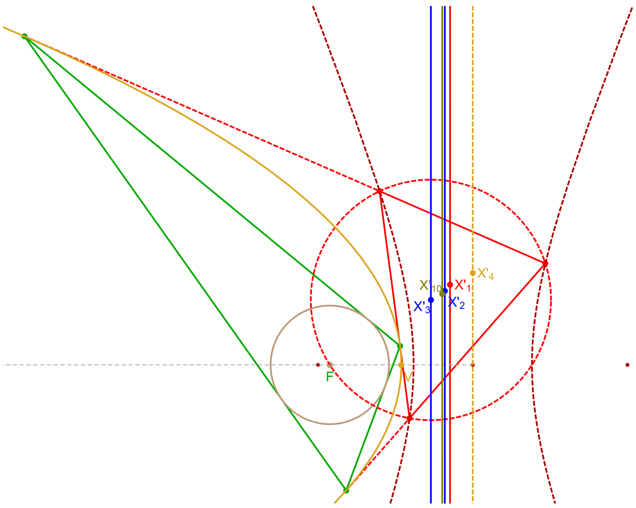


Figure 5: *The polar triangle $T'$ (red) with respect to the parabola $\mathcal{P}$ (gold) to which our Poncelet family (green) is inscribed. It is Ponceletian as it is inscribed in a hyperbola (dashed dark red). Well-know properties include (i) the circumcircle (dashed red) passes through the focus $F$, and (ii) the orthocenter $X_4'$ lies (and therefore sweeps) the directrix of $\mathcal{P}$ [3]. Also shown are the visually-straight, though quartic loci of the polar incenter $X_1'$ and Spieker center $X_{10}'$ (red and olive, respectively). The loci of $X_k'$, $k = 2,3,4$ are straight lines parallel to the directrix (red, red, and dashed gold), the latter the directrix itself.*

### 3.1 Straight and nearly-straight loci

An enduring conjecture has been that the locus of the incenter $X_1$ of a Poncelet triangle family can only be a conic if the pair is confocal [15].

As shown in Figure 5, over the polars, the locus of the incenter is, to the naked eye, a straight line. However, upon an algebraic investigation:

**Proposition 8** *The locus of the incenter $X_1'$ of $T'$ is one of four branches of the following quartic:*

$$X_1' : (-5\sqrt{2}-6)x^2y^2 + (4\sqrt{2}+2)f^2x^2 + (10\sqrt{2}+12)fxy^2 + (8\sqrt{2}+4)f^3x + (3\sqrt{2}-16)f^2y^2 - 14f^4 = 0.$$

*Specifically, the branch*

$$X_1' = \left[\frac{\sqrt{2}y^2+2+2y^2-\sqrt{-4y^2+4y^4+8\sqrt{2}+8\sqrt{2}y^2-2\sqrt{2}y^4}}{y^2(\sqrt{2}+2)-2}, y\right],$$

*where $y \neq \pm\sqrt{2-\sqrt{2}}$.*

The locus of $X_1'$ is bounded by two lines parallel to the directrix and approximately $f/850$ apart, see Figure 6.

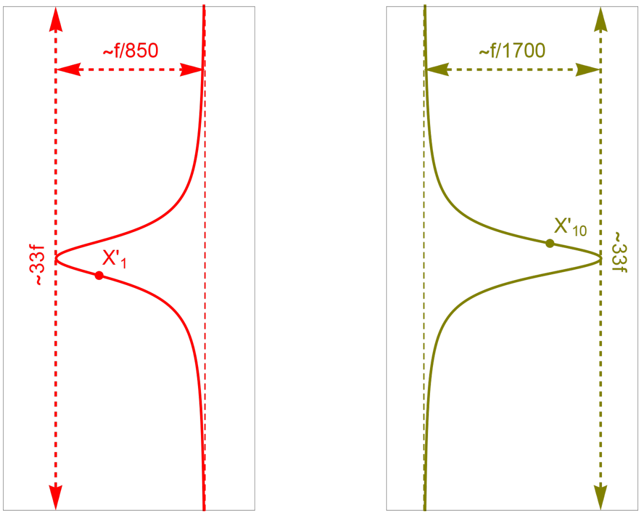


Figure 6: ***Left:*** *The locus of the polar incenter $X_1'$ is the branch of a quartic which visually is a straight line. It fits within to lines parallel to the directrix and at a distance of $f/850$. In the figure the curve is shown at aspect ratio of 28,000.* ***Right:*** *The locus of the polar Spieker center $X_{10}'$ (perimeter centroid) is an algebraic curve of degree at least four, bounded by two vertical lines separated by $f/1700$. The aspect ratio of the figure is 56,000.*

Still referring to Figure 5:

**Proposition 9** *The locus of the barycenter $X_2'$ of $T'$ is a line parallel to $\mathcal{D}$ and parametrized by*

$$X_2' = \frac{1}{3}\left[\left(2\sqrt{2}-1\right)f, \frac{(4-8\sqrt{2})f^2y+y^3}{(8\sqrt{2}-12)f^2+y^2}\right].$$

**Proposition 10** *The locus of the circumcenter $X_3'$ of $T'$ is a line parallel to $\mathcal{D}$ and parametrized by*

$$X_3' = \left[(\sqrt{2}-1)f, \frac{(3\sqrt{2}+2)(2\sqrt{2}y^2-28f^2+y^2)y}{14(y\sqrt{2}-2f+y)(y\sqrt{2}+2f+y)}\right].$$

Referring to Figure 7, the above expressions for $X_2'$ and $X_3'$ yield:

**Corollary 2** *The (varying) Euler line $X_2'X_3'$ of the polar family passes through the focus $F=[-f,0]$ of $\mathcal{P}$.*

Still referring to Figure 7, the next 4 propositions were obtains from experimental evidence and verification by CAS:

**Proposition 11** *The locus of the symmedian point $X_6'$ of $T'$ is a line parallel to $\mathcal{D}$ and parametrized by*

$$X_6' = \left[(5-3\sqrt{2})f, \frac{(3\sqrt{2}+4)(2\sqrt{2}y^2-28f^2+y^2)y}{14(y\sqrt{2}-2f+y)(y\sqrt{2}+2f+y)}\right].$$

**Proposition 12** *The locus of $X_{10}'$ of the polar family is an algebraic curve of degree four given by*

$$\begin{aligned} X_{10}' : 4\left(11\sqrt{2}+16\right)x^4 - 4\left(3\sqrt{2}+5\right)x^2y^2 - 4\left(37\sqrt{2}+50\right)fx^3 \\ +8\left(2\sqrt{2}+1\right)fxy^2 + 21\left(5\sqrt{2}+8\right)f^2x^2 - 4\left(9\sqrt{2}+8\right)f^3x \\ -\left(\sqrt{2}+4\right)f^2y^2 + 7f^4 = 0 \end{aligned}$$

*This locus is tightly bound by the following two lines parallel to the directrix:*

$$x = \left(\sqrt{2}-1+\frac{\sqrt{10-7\sqrt{2}}}{2}\right)f \text{ and } x = \left(\sqrt{2}-2^{-1/4}\right)f.$$

*The distance between these lines is approx. $f/1700$.*

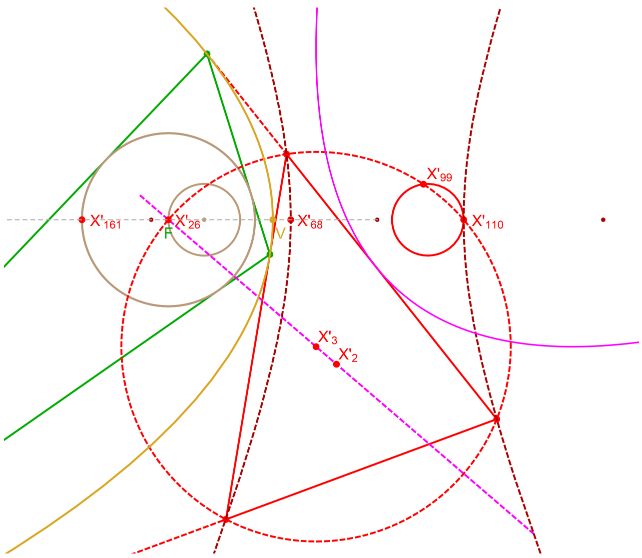


Figure 7: *Over the polar family (red), the Euler line (dashed magenta) will always pass through the focus $F$ of the parabola-inscribed family (green). $X_{26}'$ (resp. $X_{68}'$ and $X_{110}'$) remain stationary at the focus $F$ (resp. the two vertices of the hyperbola to which the polar family is inscribed). Experimentally, $X_{161}$ is stationary at the intersection of the caustic with the parabola axis farthest from the latter's vertex. Also shown is the Kiepert inparabola (magenta), whose focus is $X_{110}$ and directrix is the Euler line. Thus the polar family simultaneously inscribes the original parabola (gold) and the Kiepert (magenta). Finally, the figure depicts the circular locus of Steiner point $X_{99}'$ of the polar family.*

### 3.2 Stationary points

The circumcenter of the tangential triangle appears as $X_{26}$ on [16].

**Proposition 13** *Point $X'_{26}$ of $T'$ is stationary at the focus $F$ of $\mathcal{P}$.*

Note $X_{26}$ does not lie in general on the circumcircle of a reference triangle. In our case it does since, as mentioned above, the circumcircle of the polar contains the focus.

The Kiepert parabola of a triangle is an inscribed parabola whose focus is labeled $X_{110}$ on [16]. Its directrix is the Euler line [24]. Referring to Figure 7:

**Proposition 14** *The focus $X'_{110}$ of the Kiepert parabola (resp. the Prasolov point $X'_{68}$) of the polar family is stationary at the vertex of $\mathcal{H}$ farthest (resp. closest) to the focus of $\mathcal{P}$. Furthermore, $X'_{161}$ is stationary at the intersection of the incircle with the parabola axis farthest from the parabola vertex, i.e., at $[(1-2\sqrt{2})f,0]$.*

**Observation 1** *Over the polar family, the vertex of its Kiepert parabola sweeps a circle.*

### 3.3 Linear loci galore

Referring to Figure 8:

**Observation 2** *Over the first 1000 triangle centers in [16], the following triangle centers of $T'$ sweep linear loci parallel to $\mathcal{D}$: $X'_k, k=$2, 3, 4, 5, 6, 20, 22, 23, 24, 25, 49, 51, 52, 54, 64, 66, 67, 69, 74, 113, 125, 140, 141, 143, 146, 154, 155, 156, 159, 182, 184, 185, 186, 193, 195, 206, 235, 265, 323, 343, 368, 370, 373, 376, 378, 381, 382, 389, 394, 399, 403, 427, 428, 468, 546, 547, 548, 549, 550, 567, 568, 569, 575, 576, 578, 597, 599, 631, 632, 858, 895, 973, 974.*

### 3.4 A pencil of circular loci

Referring to Figure 7:

**Proposition 15** *The locus of the Steiner point $X'_{99}$ is a circle whose center $O'_{99}$ lies on the axis of $\mathcal{P}$ of radius $R'_{99}$ such that at its right endpoint it touches $X'_{110}$. Explicitly,*

$$O'_{99}=\left[(6\sqrt{2}-7)f,0\right],\quad R'_{99}=2f\sqrt{17-12\sqrt{2}}\,.$$

Referring to Figure 9:

**Observation 3** *Over the first 1000 triangle centers in [16], the following triangle centers of $T'$ sweep circular loci with centers on the axis of $\mathcal{P}$ and passing through $X'_{110}$: $X'_k, k=$99, 107, 112, 249, 476, 691, 827, 907, 925, 930, 933, 935.*

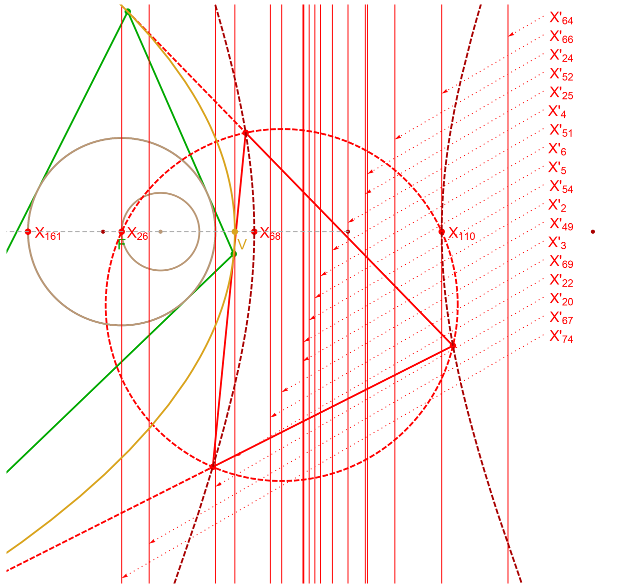


Figure 8: *Many triangle centers of the polar family sweep lines parallel to the directrix. The following are shown: $X_k$, $k=$2, 3, 4, 5, 6, 20, 22, 24, 25, 49, 51, 52, 54, 64, 66, 67, 69, 74.*

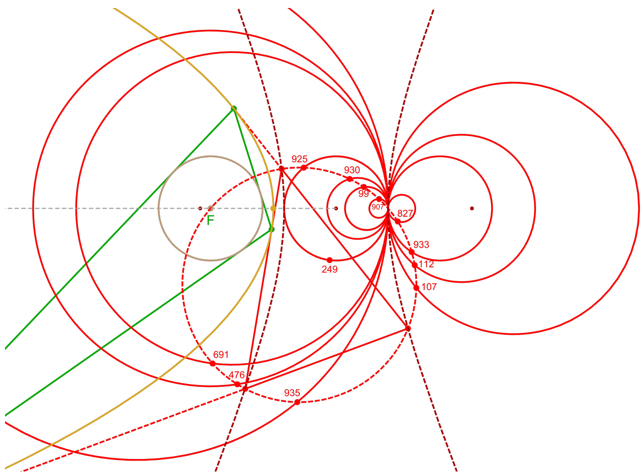


Figure 9: *Over the polar family we find that if a certain triangle center sweeps a circular locus, said locus will be an element of a parabolic pencil with $X_{110}$ as their common point (not labeled). In the figure the circular loci of $X_k$, $k=$99, 107, 112, 249, 476, 691, 827, 907, 925, 930, 933, 935 are shown. Notice all lie on the dynamically-moving circumcircle (dashed red) except for $X_{249}$.*

This gives credence to:

**Conjecture 1** *If the locus of $X'_k$ is a circle with nonzero radius, it is in the parabolic pencil with $X_{110}$ as a common point.*

# 4 Parabola-inscribed quadrilaterals

Referring to Figure 10, consider a Poncelet family $\mathcal{Q}$ of quadrilaterals inscribed in a parabola $\mathcal{P}$, and circumscribed about a focus-centered circle $\mathcal{C}$ of radius $r$. As before, let $f$ denote the parabola's focal distance, and $V=[0,0]$, $F=[-f,0]$, its vertex and focus, respectively.

**Proposition 16** *$\mathcal{P}$ and $\mathcal{C}$ will admit a Poncelet family of convex quadrilaterals if, and only if, $r/f=2\sqrt{\sqrt{5}-2}$.*

**Proof.** Referring to Figure 11, consider the symmetric Poncelet quadrilateral $P_i=[x_i,y_i]$, $i=1,\ldots,4$, inscribed in the parabola $y=x^2/(4f)$, i.e., $x=2\sqrt{fy}$. Clearly, $y_1=f-r$, and $y_2=f+r$. Requiring that $P_1P_2$ be tangent to $\mathcal{C}$ yields the quartic $r^2+4f\sqrt{f^2-r^2}=0$. The claim is the one positive root of this quartic. □

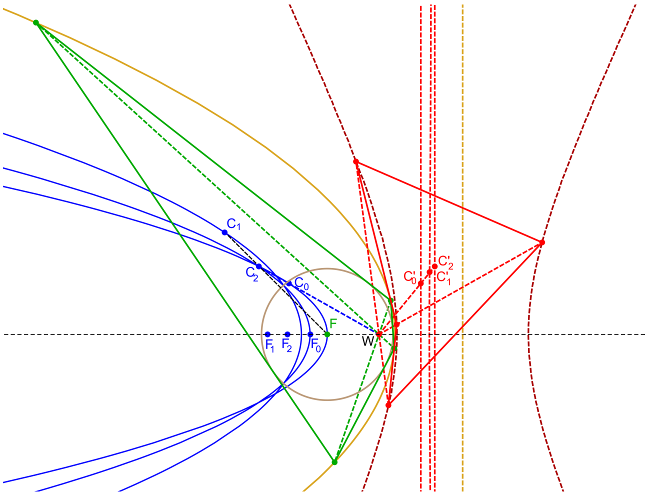


Figure 10: *A Poncelet quadrilateral (green) is shown inscribed in a parabola $\mathcal{P}$ (gold) and circumscribed about a focus-centered circle (brown). Over the family, (i) the intersection $W$ of its diagonals (dashed green) is stationary; (ii) the loci of vertex $C_0$, perimeter $C_1$, and area $C_2$, centroids sweep 3 distinct parabolas (blue) coaxial with $\mathcal{P}$ with foci on $F_0$, $F_1$ and $F_2$. Notice the vertex of $C_0$ is $F$ and that of $C_1$ is $F_0$. (iv) As predicted by Remark 1, $C_1$ is collinear with $F$ and $C_2$ (dashed black); (v) $C_0,C_2,W$ are collinear (dashed blue). Also shown is the polar quadrilateral $\mathcal{Q}'$ (red) with respect to $\mathcal{P}$, inscribed in a hyperbola (dashed, red) centered at $[f,0]$. One observes that: (a) its diagonals (dashed red) also intersect at $W$; (b) the loci of its vertex $C_0'$ and area $C_2'$ centroids are lines (dashed orange) perpendicular to the axis of $\mathcal{P}$, (c) $C_0',C_2',W$ are collinear (dashed red); (d) the locus of the polar perimeter centroid $C_1'$ is algebraic and of degree 10.*

Note: more generally, Cayley's conditions may be used to include the non-convex case, see [8].

The next 3 propositions, first identified experimentally, were then confirmed via CAS.

**Proposition 17** *Over $\mathcal{Q}$, the two diagonals $P_1P_3$ and $P_2P_4$ intersect at a stationary point $W=[(2-\sqrt{5})f,0]$.*

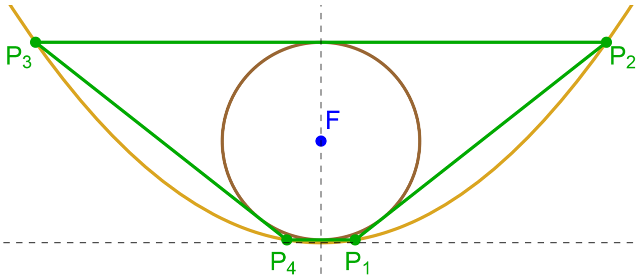


Figure 11: *Construction used to derive $r/f$ in for parabola-inscribed convex quadrilaterals in Proposition 16.*

## 4.1 The three centroids

Referring to Figure 10, let $C_0$, $C_1$, and $C_2$ denote the vertex, perimeter, and area centroids of the quadrilaterals in $\mathcal{Q}$, respectively.

**Proposition 18** *Over the family, $C_0$, $C_2$, and $W$ are collinear.*

**Proposition 19** *Over the Poncelet family, the loci of $C_0,C_2$ are parabolas coaxial with $\mathcal{P}$, whose foci and vertices locations are listed in Table 1.*

From Remark 1:

**Corollary 3** *The locus of $C_1$ is a $3/2$-scaled version of the locus of $C_2$ with $F$ as the homothety center.*

| centroid (N=4) | focal dist. | vertex $x/f$ | vtx. $x/f$ (num) |
|---|---|---|---|
| $C_0$ | $f/4$ | $-1$ | $-1$ |
| $C_1$ | $f/2$ | $(\sqrt{5}-5)/2$ | $-1.381966$ |
| $C_2$ | $f/3$ | $\sqrt{5}/3-2$ | $-1.25464$ |

Table 1: *Location of centroids $C_0,C_1,C_2$ in the convex $N=4$ family.*

### 4.2 The polar quadrilateral

Referring to Figure 10, consider the polar quadrilateral whose sides are the tangents to $\mathcal{P}$ at the vertices of the original family. Let $P_i'$, $i = 1, \ldots, 4$ denote its vertices and $C_0'$, $C_1'$, and $C_2'$ denote its vertex, perimeter, and area centroids.

**Proposition 20** *The locus of the polar quadrilateral's vertices is the hyperbola $\mathcal{H}$ given by*

$$\mathcal{H}: \frac{(x-f)^2}{4(\sqrt{5}-2)f^2} - \frac{y^2}{4f^2} - 1 = 0.$$

*with center at $[f, 0]$ and foci $[f(1 \pm 2\sqrt{\sqrt{5}-1}), 0]$.*

Let $W$ be defined as in Proposition 17. The next two propositions result from visual (and numerical) detection, followed by verification by CAS.

**Proposition 21** *The two diagonals of the polar quadrilateral intersect at $W$.*

**Proposition 22** *Over the polar quadrilateral family, $C_0'$, $C_2'$, and $W$ are collinear.*

**Proposition 23** *Over $Q$, the loci of $C_0'$ and $C_2'$ are lines parallel to the parabola's directrix and given by $C_0' : x = (3-\sqrt{5})f/2$, and $C_2' : x = (4-\sqrt{5})f/3$.*

Rather laborious CAS manipulation yields:

**Proposition 24** *Over $Q$, the locus of $C_1'$ is one connected component of an algebraic curve of degree ten, given by the following equation:*

$$\begin{aligned}
C_1' :\ & -\left(1457008\sqrt{5}+3257968\right) f x^7 y^2 + \left(122156\sqrt{5}+273148\right) f^2 x^4 y^4 \\
& + \left(465164\sqrt{5}+1040132\right) f^2 x^6 y^2 - \left(96506\sqrt{5}+215698\right) f^6 x^2 y^2 \\
& - \left(119256\sqrt{5}+266664\right) f^3 x^3 y^4 + \left(505052\sqrt{5}+1129268\right) f^5 x^3 y^2 \\
& + \left(8564\sqrt{5}+19204\right) f^7 x y^2 - \left(881712\sqrt{5}+1971568\right) x^{10} \\
& + \left(43955\sqrt{5}+98289\right) f^4 x^2 y^4 + \left(24568\sqrt{5}+54936\right) f x^5 y^4 \\
& - \left(7250\sqrt{5}+16210\right) f^5 x y^4 - \left(1274930\sqrt{5}+2850838\right) f^4 x^4 y^2 \\
& + \left(1235568\sqrt{5}+2762832\right) f^3 x^5 y^2 + \left(4457696\sqrt{5}+9967712\right) f x^9 \\
& - \left(7787152\sqrt{5}+17412608\right) f^2 x^8 + \left(5470456\sqrt{5}+12232344\right) f^3 x^7 \\
& - \left(1690535+755997\sqrt{5}\right) f^4 x^6 - \left(812098\sqrt{5}+1815898\right) f^5 x^5 \\
& + \left(330322\sqrt{5}+738968\right) f^6 x^4 + \left(1002+448\sqrt{5}\right) f^6 y^4 \\
& - \left(228\sqrt{5}+672\right) f^8 y^2 - \left(7300\sqrt{5}+16956\right) f^7 x^3 \\
& + \left(2750\sqrt{5}+7150\right) f^9 x - \left(16145\sqrt{5}+36103\right) f^8 x^2 \\
& - \left(84196\sqrt{5}+188268\right) x^6 y^4 + \left(544928\sqrt{5}+1218496\right) x^8 y^2 - 726 f^{10} = 0.
\end{aligned}$$

*Furthermore, $C_1'$ is bound by the following two lines parallel to the directrix and approximately $f/25$ apart: $x = \left(5+\sqrt{2}-\sqrt{5}\sqrt{2}-\sqrt{5}\right)f/2$, and $x = \left(\sqrt{5}\sqrt{2}-\sqrt{5}-2\sqrt{2}+3\right)f/2$.*

## 5 Parabola-inscribed pentagons

Referring to Figure 12, consider a family of pentagons inscribed in a parabola $\mathcal{P}$ of focal distance $f$, and circumscribed about a focus-centered circle $\mathcal{C}$ of radius $r$.

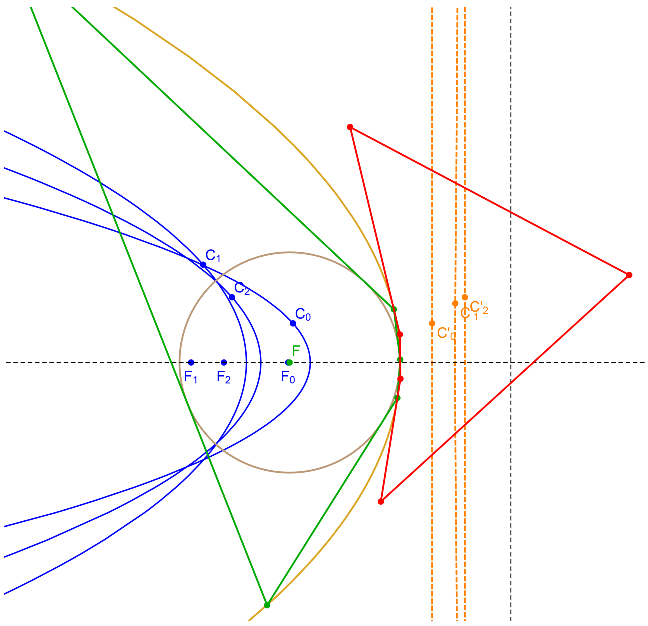


Figure 12: *Parabola-inscribed pentagons (green), and their polar polygon (red). The loci of vertex $C_0$, perimeter $C_1$, and area centroids $C_1$ are parabolas (blue) coaxial with $\mathcal{P}$ (gold). Over the polar family, $C_0'$ and $C_2'$ are straight lines (dashed orange) perpendicular to the directrix (dashed black). Though the locus of the perimeter centroid $C_1'$ is indistinguishable from a straight line, it is an algebraic curve of degree likely much higher than 10 (since that is the degree for $C_1'$ on $N = 4$).*

**Proposition 25** *The pair $\mathcal{P}, \mathcal{C}$ will admit a Poncelet family of pentagons if, and only if, $r/f$ is the only positive root of the following sextic polynomial ($r/f \approx 0.995219$):*

$$x^6 + 12x^5 - 28x^4 + 32x^3 + 112x^2 - 64x - 64 = 0.$$

**Proof.** Referring to Figure 13, without loss of generality, let $\mathcal{P}$ be the unit parabola $y = x^2$ with focus $F = [0, 1/4]$

and let $\mathcal{C}$ be a circle of radius $r$ centered at $F$. Consider the Poncelet pentagon $P_i$, $i = 1, \ldots, 5$ with $P_4$ at infinity, and $P_1P_2$ horizontal and tangent to $\mathcal{C}$ at $[0, 1/4 - r]$. Compute the next Poncelet vertex $P_3 = [x_3, y_3]$ as the intersection of a tangent to $\mathcal{C}$ from $P_2$ with $\mathcal{P}$. By requiring that $x_3 = r$, we obtain the sextic in the claim. □

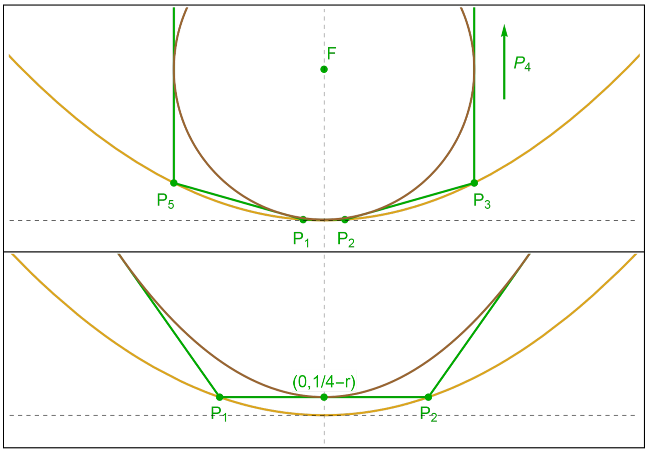


Figure 13: *Construction used to derive $r/f$ in Proposition 25. Top (resp. bottom) shows the complete picture (resp. a detailed view near the vertex)*

Referring to Figure 12:

**Conjecture 2** *Over the parabola-inscribed pentagon family, the loci of vertex, perimeter, and area centroids are parabolas coaxial with $\mathcal{P}$.*

**Conjecture 3** *Over the family of polar polygons to parabola-inscribed pentagons, the locus of vertex and area vertices are lines perpendicular to the directrix while that of the perimeter centroid is an algebraic curve of degree at least four.*

## 6 Parabola-inscribed hexagons and summary

### 6.1 Hexagons and summary

Referring to Figure 14, we can also consider a family of parabola-inscribed hexagons.

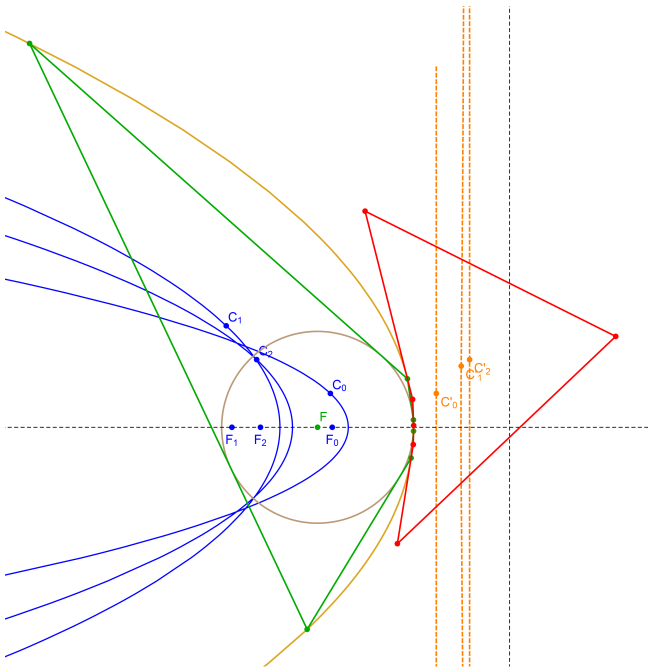


Figure 14: *Hexagons (green) inscribed in a parabola $\mathcal{P}$. As before, the loci of $C_0$, $C_1$, and $C_2$ are parabolas (blue) coaxial $\mathcal{P}$. Over the polar family (red), the loci of $C'_0, C'_2$ are lines perpendicular to the axis while that of $C'_1$ is algebraic, and though visually a straight line, its degree is likely much higher than 10 (since that is the degree for $C'_1$ on $N = 4$).*

An analogous construction (based on symmetric configurations) was used to obtain $r/f$ required for convex $N = 6$. A summary of all $r/f$ thus obtained appears in Table 2.

| $N$ | $r/f$ | $r/f$ (num.) | Cayley |
|---|---|---|---|
| 3 | $2(\sqrt{2}-1)$ | 0.828427 | 4 |
| 4 | $2\sqrt{\sqrt{5}-2}$ | 0.971737 | 4 |
| 5 | n/a | 0.995219 | 8 |
| 6 | n/a | 0.999183 | 8 |

Table 2: *Table of $r/f$ required for closure of convex $N$-gons inscribed in a parabola, and circumscribed about a focus-centered circle. Algebraic expressions (2nd column) are only possible for $N = 3, 4$. The last column shows the number of possible solutions for $r/f$ if one were to include cases where circle and parabola intersect (the Poncelet polygon may be self-intersecting and/or non-convex). For Cayley's conditions in the general case, see [8].*

## 7 Generalizing centroidal loci

Let $\mathcal{R}$ be a Poncelet family of $N$-gons inscribed to a parabola $\mathcal{P}$, and circumscribed about a focus-centered circle

$\mathcal{C}$. Experimental the evidence for the $N = 3,4,5,6$ cases, we propose the following generalizations (reader contributions are encouraged):

**Conjecture 4** *Over $\mathcal{R}$, for any $N \geq 3$, the loci of vertex, perimeter, and area centroids are parabolas coaxial with $\mathcal{P}$.*

**Conjecture 5** *Over $\mathcal{R}$ and for any $N \geq 3$, the loci of vertex and area centroids of the polar polygons with respect to $\mathcal{P}$ are straight lines parallel to the directrix of $\mathcal{P}$.*

Let $\mathcal{B}'$ be the conic-inscribed polar image of a generic bicentric family of $N$-gons with respect to the bicentric circumcircle (see Appendix B).

Recall that the locus of vertex and area centroids $C_0, C_2$ are conics over any Poncelet family, while that of the perimeter centroid $C_1$ is not, in general, a conic [22]. A consequence of Remark 1, analogously exploited in [10, Corollary 2], is that:

**Corollary 4** *Over $\mathcal{B}'$, the locus of the perimeter centroid is a conic.*

Let $\mathcal{P}'$ be the conic to which $\mathcal{B}'$ is inscribed.

**Conjecture 6** *Over the polar polygons of $\mathcal{B}'$ with respect to $\mathcal{P}'$, the locus of the perimeter centroid is never a conic.*

## 8 A conserved quantity

As in Appendix B, let $\mathcal{B}$ denote a bicentric family of $N$-gons inscribed to a circle $\mathcal{C} = (O,R)$, and circumscribed about a second, nested circle $\mathcal{C}'$. Let $d_i$ denote the perpendicular distance from the bicentric circumcenter $O$ to side $P_iP_{i+1}$.

Referring to Figure 15:

**Lemma 1** *Over $\mathcal{B}$, the quantity $\sum d_i$ is conserved.*

The argument below was kindly provided by A. Akopyan [1].

**Proof.** The above statement is equivalent to stating that over $\mathcal{B}$ the sum of unit vectors from a point $P$ in the direction perpendicular to bicentric sides is constant. In turn, the latter is a corollary of the well-known fact that over $\mathcal{B}$, the centroid of the touchpoints of sidelines with $\mathcal{C}'$ is stationary. □

Let $\theta_i$, $i = 1,\ldots,N$, denote the angles interior to a polygon $\mathcal{B}$.

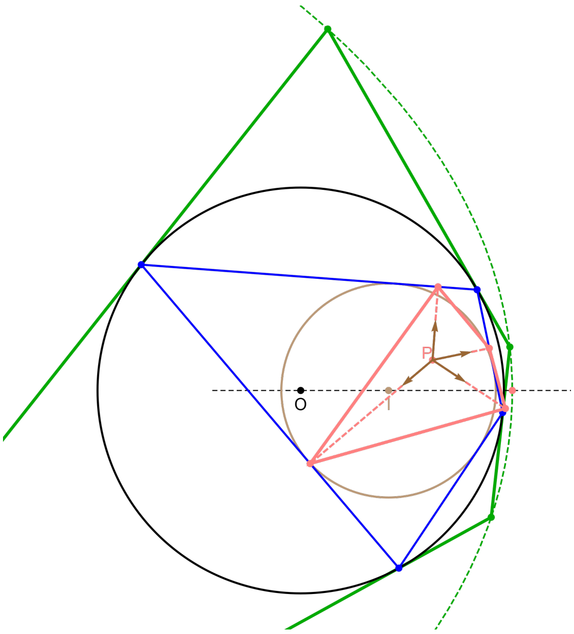


Figure 15: *An $N = 4$ bicentric polygon is shown (blue). Without loss of generality, in the case shown the circumcenter $O$ is interior to the incircle, i.e., the polar family (green) is ellipse-inscribed. Also shown is the pedal polygon (pink) with respect to a point $P$ in the interior of the circumcircle and the unit vectors (brown) along each perpendicular dropped from $P$ onto the sides.*

**Proposition 26** *For all $N$, the porism of polygons polar to $\mathcal{B}$ with respect to its circumcenter conserves $\sum_{i=1}^{N} \sin\theta_i/2 = (1/R)\sum d_i$.*

**Proof.** The vertices of the tangential polygon are the poles of each side of $\mathcal{B}$ with respect to the circumcircle. Therefore, said vertices are at a distance $D_i = R^2/d_i$ from the $O$. Since $\sin\theta_i/2 = R/D_i = d_i/R$, per Lemma 1, the claim follows. □

Note that in general, $\theta_i$ is the directed angle $P_{i-1}P_iP_{i+1}$. In the case when $r < d$, the tangential polygon will be inscribed in two branches of a hyperbola. There are only two cases: Either (i) all vertices lie on a first proximal branch of the hyperbola, or (ii) all but one vertex $P_k$ will lie on said branch, with $P_k$ lying on the distal branch. In case (i), all $\theta_i$ are positive whereas in (ii) all are positive except for $\theta_k$. Furthermore, in this case, the supplement of angles $\theta_{k-1}$ and $\theta_{k+1}$ need to be used in the sum. So the invariant sum becomes

$$\sin\frac{\theta_1}{2} + \ldots + \sin\frac{\pi - \theta_{k-1}}{2} - \sin\frac{\theta_k}{2}$$
$$+ \sin\frac{\pi - \theta_{k+1}}{2} + \ldots + \sin\frac{\theta_N}{2} =$$
$$\sin\frac{\theta_1}{2} + \ldots + \cos\frac{\theta_{k-1}}{2} - \sin\frac{\theta_k}{2} + \cos\frac{\theta_{k+1}}{2} + \ldots + \sin\frac{\theta_N}{2}.$$

## Acknowledgements

We would like to thank A. Akopyan, B. Gibert, P. Moses, and A. Zaslavsky for their invaluable help with questions and proofs. We are grateful to the detailed corrections and suggestions made by the referee. The second author is fellow of CNPq and coordinator of Project PRONEX/ CNPq/ FAPEG 2017 10 26 7000 508.

## Appendix A. Vertex parametrizations

### A.1. Parabola-inscribed triangles

A 3-periodic orbit $P_i = [x_i, y_i] = [-y_i^2/(4f), y_i]$ is such that

$$y_2 = \frac{2\left(1-\sqrt{2}\right)(4fy_1+\Delta)f}{8f^2\sqrt{2}-12f^2+y_1^2},$$

$$y_3 = \frac{2\left(\sqrt{2}-1\right)f\Delta}{8f^2\sqrt{2}-12f^2+y_1^2},$$

where $\Delta = \sqrt{16(8\sqrt{2}-11)f^4+8f^2y_1^2+y_1^4}$.

### A.2. Hyperbola-inscribed polar triangles

A 3-periodic orbit $Q_i = [q_{1,i}, q_{2,i}]$ is such that

$$Q_1 = \left(1+\sqrt{2}\right)\cdot \left[\frac{(4fy_1+\Delta)y_1}{2(2\sqrt{2}+3)y_1^2-8f^2}, \frac{\left(1+\sqrt{2}\right)y_1^3-4\left(1+\sqrt{2}\right)f^2y_1-2\Delta f}{2(2\sqrt{2}+3)y_1^2-8f^2}\right],$$

$$Q_2 = \left(1+\sqrt{2}\right)\cdot \left[\frac{(4fy_1-\Delta)y_1}{2(2\sqrt{2}+3)y_1^2-8f^2}, \frac{\left(1+\sqrt{2}\right)y_1^3-4\left(1+\sqrt{2}\right)f^2y_1+2\Delta f}{2(2\sqrt{2}+3)y_1^2-8f^2}\right],$$

$$Q_3 = \left(1+\sqrt{2}\right)\cdot \left[\frac{\left(5-3\sqrt{2}\right)\left((1+2\sqrt{2})y_1^2-28f^2\right)f}{7((3+2\sqrt{2})y_1^2-4f^2)}, -\frac{8f^2y_1}{(3+2\sqrt{2})y_1^2-4f^2}\right],$$

where $\Delta = \sqrt{y_1^4+8f^2y_1^2+16(8\sqrt{2}-11)f^4}$.

### A.3. Parabola-inscribed quadrilaterals

A 4-periodic orbit $P_i = [x_i, y_i] = [-\frac{1}{4f}y_i^2, y_i]$ is such that:

$$y_2 = \frac{\left(2\sqrt{\sqrt{5}-2}\,\Delta_1+4fy_1\left(3-\sqrt{5}\right)\right)f}{4f^2\sqrt{5}-8f^2-y_1^2},$$

$$y_3 = \frac{4\left(2-\sqrt{5}\right)f^2}{y_1},$$

$$y_4 = -\frac{\left(2\sqrt{\sqrt{5}-2}\,\Delta_1+4fy_1\left(\sqrt{5}-3\right)\right)f}{4f^2\sqrt{5}-8f^2-y_1^2},$$

where $\Delta_1 = \sqrt{y_1^4+8f^2y_1^2+16\left(9-4\sqrt{5}\right)f^4}$.

### A.4. Hyperbola-inscribed polar quadrilaterals

A 4-periodic orbit $P_i = [p_i, q_i]$ is such that:

$$p_1 = \frac{\sqrt{\sqrt{5}-2}\left(\Delta_1+6fy_1\sqrt{5}\sqrt{\sqrt{5}-2}+14fy_1\sqrt{\sqrt{5}-2}\right)y_1}{4y_1^2+2y_1^2\sqrt{5}-8f^2}$$

$$q_1 = \frac{\left(2\sqrt{\sqrt{5}+2}\,\Delta_1 f+4f^2y_1-yl^3\right)\left(4f^2\sqrt{5}+8f^2+y_1^2\right)}{32f^4-32f^2y_1^2-2y_1^4}$$

$$p_2 = \frac{2\sqrt{\sqrt{5}-2}\left(\Delta_1+2\sqrt{2}(\sqrt{5}-1)y_1\right)\left(\left(\sqrt{5}-2\right)y_1^2+4f^2\right)f^2}{y_1\left(16f^4-16f^2y_1^2-y_1^4\right)}$$

$$q_2 = \sqrt{\sqrt{5}+2}\left(y_1\Delta_1+2\sqrt{\sqrt{5}+2}fy_1^2-8\left(\sqrt{5}-2\right)^{3/2}f^3\right)\cdot \left((\sqrt{5}-2)y_1^2+4f^2\right)f$$

$$p_3 = \frac{-2\sqrt{\sqrt{5}-2}\left(\Delta_1-2\sqrt{2}\sqrt{\sqrt{5}-1}fy_1\right)}{y_1\left(16f^4-16f^2y_1^2-y_1^4\right)}\cdot \left(y_1^2\sqrt{5}+4f^2-2y_1^2\right)f^2$$

$$q_3 = \frac{-\sqrt{\sqrt{5}+2}\left(yl\,\Delta_1-2\sqrt{\sqrt{5}+2}fy_1^2+8\left(\sqrt{5}-2\right)^{3/2}f^3\right)}{y_1\left(16f^4-16f^2y_1^2-y_1^4\right)}\cdot \left((\sqrt{5}-2)y_1^2+4f^2\right)f$$

$$p_4 = \frac{\sqrt{\sqrt{5}-2}\left(\Delta_1-2\sqrt{2}(\sqrt{5}-1)fy_1\right)\left((\sqrt{5}-2)y_1^2+4f^2\right)y_1}{y_1\left(16f^4-16f^2y_1^2-y_1^4\right)}$$

$$q_4 = \frac{\left(-2f\Delta_1\sqrt{\sqrt{5}-2}+4f^2y_1-y_1^3\right)\left(4f^2\sqrt{5}+8f^2+y_1^2\right)}{y_1\left(16f^4-16f^2y_1^2-y_1^4\right)}$$

## Appendix B. Relation to the bicentric family

Referring to 16, the bicentric family $\mathcal{B}$ of $N$-gons is a family of Poncelet $N$-gons inscribed in a circles $\mathcal{C} = (O, R_b)$, and circumscribed about another circle $\mathcal{C}' = (O', r_b)$. Let $d = |O - O'|$. Relations between $d, R, r_b$ are known for many "low N" and are listed in [24, Poncelet's porism].

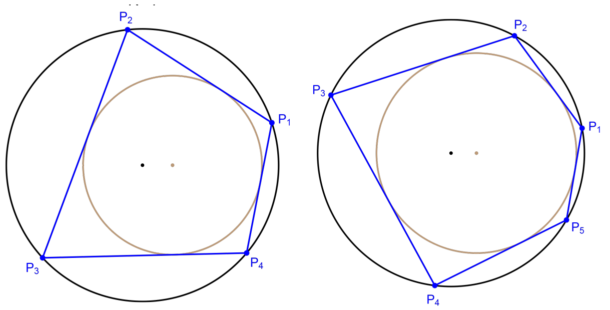


Figure 16: *The bicentric family is a family of Poncelet polygons interscribed between two circles. Shown are the $N = 4$ (left) and $N = 5$ (right) convex cases.*

**Definition 1 (Polar polygon)** *Given a polygon P, its* polar polygon *$P'$ with respect to a conic $\mathcal{C}$ is bounded by the tangents to $\mathcal{C}$ at the vertices of $\mathcal{P}$.*

**Proposition 27** *The polar family $\mathcal{B}'$ of $\mathcal{B}$ with respect to $\mathcal{C}$ is an ellipse, parabola, or hyperbola-inscribed if d is smaller, equal, or greater than $R'$, respectively (O is interior, on the boundary, or exterior to $\mathcal{C}'$, respectively). Furthermore, one of the foci coincides with $O'$.*

As shown in Figure 17, when the polar family is hyperbola-inscribed, there are two layouts for its vertices: either (i) all lie on the branch of the hyperbola closest to the incenter of the family, or (ii) all but one lie on said branch, while the remaining one lies on the "other" branch.

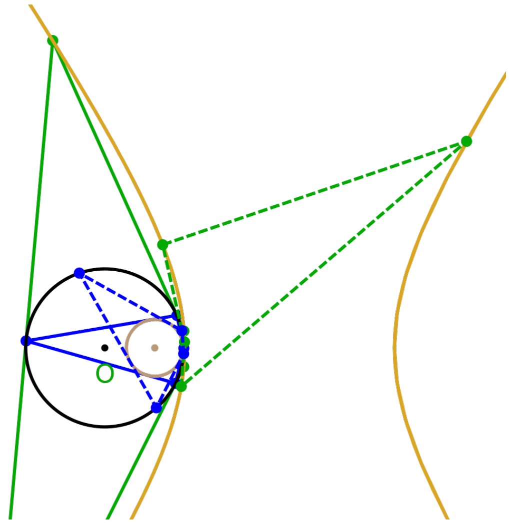


Figure 17: *If the circumcenter O is exterior to the incircle of a bicentric polygon (blue), the polar (i.e., tangential) family will be hyperbola (gold) inscribed. Over the family there are two configurations: (i) solid green: all vertices lie on one branch of the hyperbola; (ii) dashed green: all but one vertex lie on the branch proximal to the incenter, while a lone one lies on the opposite branch.*

**Proposition 28** *The parabola $\mathcal{P}$ which is the polar image of $\mathcal{B}$ with $d = r_b$, has focal distance $f = R_b^2/(2r_b)$.*

**Proof.** Let $O = (0,0)$. Consider a polygon in $\mathcal{B}$ with a vertical side $P_1P_2$ tangent to the incircle at $(2r_b, 0)$. The vertex $V$ of $\mathcal{P}$ is the pole of said side which can be obtained as the inversion of point $(2r_b, 0)$ with respect to the circumcircle. This yields the result. □

## References


[1] AKOPYAN, A., Private communication, 2021.

[2] AKOPYAN, A., SCHWARTZ, R., TABACHNIKOV, S., Billiards in ellipses revisited, *Eur. J. Math.*, 2020, `https://doi.org/10.1007/s40879-020-00426-9`

[3] AKOPYAN, A. V., ZASLAVSKY, A. A., *Geometry of Conics*, Mathematical World - Volume 26, AMS, 2007, `https://doi.org/10.1090/mawrld/026`

[4] BIALY, M., TABACHNIKOV, S., Dan Reznik's identities and more, *Eur. J. Math.* (2020), `https://doi.org/10.1007/s40879-020-00428-7`

[5] BOS, H. J. M., KERS, C., RAVEN, D. W., Poncelet's Closure Theorem, *Expo. Math.* **5** (1987), 289–364.

[6] CHAVEZ-CALIZ, A., More about areas and centers of Poncelet polygons, *Arnold Math J.* **7** (2020), 91–106, `https://doi.org/10.1007/s40598-020-00154-8`

[7] DEL CENTINA, A., Poncelet's porism: a long story of renewed discoveries, I, *Arch. Hist. Exact Sci.*

**70** (2016), 1–122, `https://doi.org/10.1007/s00407-015-0163-y`

[8] DRAGOVIĆ, V., RADNOVIĆ, M., *Poncelet Porisms and Beyond: Integrable Billiards, Hyperelliptic Jacobians and Pencils of Quadrics*, Frontiers in Mathematics, Basel, Springer, 2011, `https://doi.org/10.1007/978-3-0348-0015-0`

[9] FIEROBE, C., On the circumcenters of triangular orbits in elliptic billiard, *J. Dyn. Control Syst.* **27** (2021) 693–705, `https://doi.org/10.1007/s10883-021-09537-2`

[10] GARCIA, R., GHEORGHE, L., REZNIK, D., Exploring the Steiner-Soddy Porism, In: Cheng, LY. (eds) ICGG 2022 - *Proceedings of the 20th International Conference on Geometry and Graphics*. ICGG 2022. Lecture Notes on Data Engineering and Communications Technologies, vol 146. Springer, Cham. `https://doi.org/10.1007/978-3-031-13588-0_3`

[11] GARCIA, R., REZNIK, D., *Euclidean Properties of Poncelet Triangles: Experimental Discovery and Analysis*, Rio de Janeiro, IMPA, isbn:978-65-89124-43-6, 2021.

[12] GARCIA, R., REZNIK, D., Family ties: Relating Poncelet 3-periodics by their roperties, *KoG* **25** (2021), 3–18, `https://doi.org/10.31896/k.25.1`

[13] GARCIA, R., REZNIK, D., KOILLER, J., Loci of 3-periodics in an elliptic billiard: why so many ellipses?, arXiv:2001.08041, 2020.

[14] GARCIA, R., REZNIK, D., KOILLER, J., New properties of triangular orbits in elliptic billiards, *Amer. Math. Monthly* **128**(10) (2021), 898–910, `https://doi.org/10.1080/00029890.2021.1982360`

[15] HELMAN, M., LAURAIN, D., GARCIA, R., REZNIK, D., Invariant center power and loci of Poncelet triangles, *J. Dyn. Control Syst.* (2021), `https://doi.org/10.1007/s10883-021-09580-z`

[16] KIMBERLING, C., *Encyclopedia of triangle centers*, `https://faculty.evansville.edu/ck6/encyclopedia/ETC.html`, 2020.

[17] MAPLESOFT, *Maple*, A division of Waterloo Maple Inc., 2019.

[18] ODEHNAL, B., Poristic loci of triangle centers, *J. Geom. Graph.* **15**(1) (2011), 45–67.

[19] PAMFILOS, P., On some actions of $D_3$ on a triangle, *Forum Geom.* **4** (2014), 157–176.

[20] REZNIK, D., GARCIA, R., KOILLER, J., The ballet of triangle centers on the elliptic billiard, *J. Geom. Graph.* **24**(1) (2020), 79–101.

[21] ROMASKEVICH, O., On the incenters of triangular orbits on elliptic billiards, *Enseign. Math.* **60**(3-4) (2014), 247–255, `https://doi.org/10.4171/LEM/60-3/4-2`

[22] SCHWARTZ, R., TABACHNIKOV, S., Centers of mass of Poncelet polygons, 200 years after, *Math. Intelligencer* **38**(2) (2016), 29–34, `https://doi.org/10.1007/s00283-016-9622-9`

[23] SKUTIN, A., On rotation of an isogonal point, *J. Classical Geom.* **2** (2013), 66–67.

[24] WEISSTEIN, E. W., *CRC concise encyclopedia of mathematics (2nd edition)*, Boca Raton, FL: Chapman and Hall/CRC, 2002, `https://doi.org/10.1201/9781420035223`

[25] WOLFRAM, S., *Mathematica*, Version 10.0, 2019.

[26] ZASLAVSKY, A., Private communication, 2021.

[27] ZASLAVSKY, A., KOSOV, D., MUZAFAROV, M., Trajectories of remarkable points of the Poncelet triangle (in Russian), *Kvant* **2** (2003), 22–25.

**Filipe Bellio**
orcid.org/0000-0003-4059-9292
e-mail: filipe.bellio.nobrega@gmail.com

ENS-Lyon, France

**Ronaldo Garcia**
orcid.org/0000-0001-8876-6956
e-mail: ragarcia@ufg.br

Universidade Federal de Goiás
Instituto de Matemática e Estatística
BR-74001970 Goiânia, GO, Brazil

**Dan Reznik**
orcid.org/0000-0002-0542-6014
e-mail: dreznik@gmail.com

Data Science Consulting, Rio De Janeiro, Brazil

https://doi.org/10.31896/k.26.2
Original scientific paper
Accepted 24. 6. 2022.

Ronaldo Garcia
Liliana G. Gheorghe
Peter Moses
Dan Reznik

# Triads of Conics Associated with a Triangle

Dedicated to Paul Yiu

**Triads of Conics Associated with a Triangle**

**ABSTRACT**

We revisit constructions based on triads of conics with foci at pairs of vertices of a reference triangle. We find that their 6 vertices lie on well-known conics, whose type we analyze. We give conditions for these to be circles and/or degenerate. In the latter case, we study the locus of their center.

**Key words:** triangle, conic, Carnot, Soddy circles

**MSC2010:** 51M04, 51N20, 51N35, 68T20

**Trijade konika pridruženih trokutu**

**SAŽETAK**

Podsjećamo na konstrukcije temeljene na trijadama konika sa žarištima u parovima vrhova referetnog trokuta. Nalazimo da njihovih 6 vrhova leži na dobro poznatim konikama čiji tip analiziramo. Za ove konike dajemo uvjete da budu kružnice i/ili degenerirane konike. U slučaju degeneriranih konika proučavamo geometrijsko mjesto njihovog središta.

**Ključne riječi:** trokut, konika, Carnot, Soddyjeve kružnice

## 1 Introduction

Paraphrasing a passage in [13], "new tools of interactive geometry enable the discovery of properties in a way mathematicians in the past could only have dreamed about". Aided by interactive simulation (mostly Mathematica and GeoGebra), and inspired by a construction by Paul Yiu [17, Sec. 12.4, p. 148], we tour curious dynamic phenomena manifested by triads of ellipses (or hyperbolas) naturally associated with a triangle. Namely, we attach their foci to a pair of vertices and impose that the conic pass through either (i) the remaining vertex, or (ii), some chosen point $P$. We call these "V-" or "P"-conics, respectively, see Figure 1.

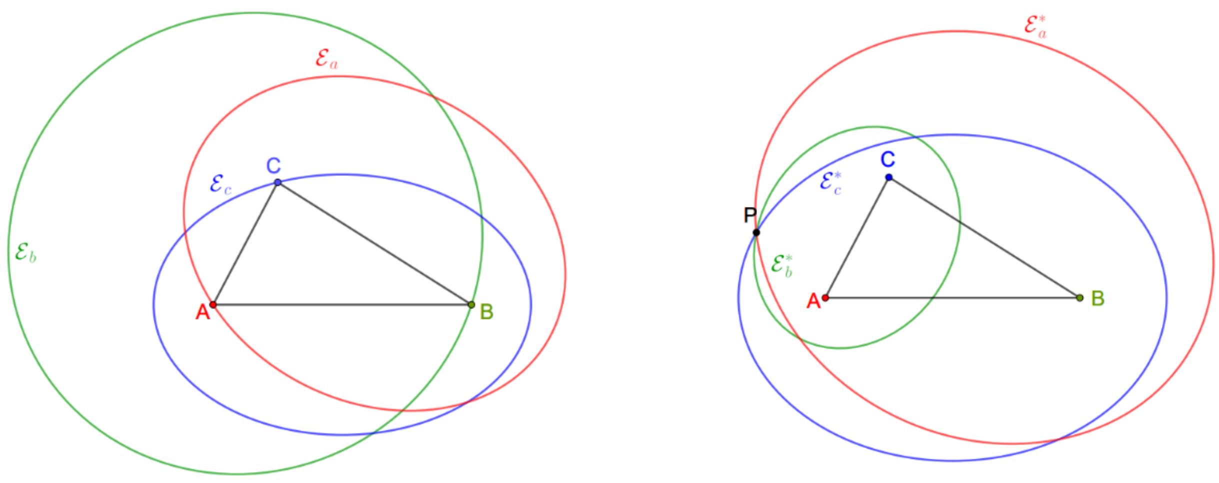


Figure 1: ***Left:*** *A $\triangle ABC$, and a V-triad of ellipses passing through a vertex and with foci on the remaining pair.* ***Right:*** *in the P-triad case, ellipses still have foci on pairs of vertices but now pass through a given point $P$.*

Some of our main results include:

- The 6 vertices of V-ellipses always lie on a conic; this conic is degenerate iff the reference triangle is a right triangle.
- The conic passing through the 6 $P$-ellipse vertices is degenerate iff $P$ lies on the circumcircle.
- The locus of the center of the 6-point conic over the degenerate family is a quartic in the V-ellipse case, and the union of three arcs of ellipses in the P-ellipse case; we derive expressions for them.
- We specify the regions such that various 6-point conics are of a given type (hyperbola, ellipse, parabola, or degenerate).
- We derive conditions such that various 6-point conics are a circle.
- We derive conditions (and loci) under which the co-vertices of conic triad lie on a conic.

Some of the above are done for the case of hyperbola triads as well. Most of our results have been obtained through experimentation with dynamic geometry software first, and later confirmed geometrically and/or algebraically. See [6] for details.

Some long, symbolic proofs are omitted, with some expressions appearing in Section 6. Throughout the paper we will be using $X_k$ notation for triangle centers, after [8].

**Related Work**

We have been inspired by the idea of erecting identical geometrical objects to the sides of a triangle, e.g., [3, 5, 10, 11]. Triads of "Artzt" parabolas, conceived in the XIX century, have been revisited in [4, 9, 15]. In [13], new properties of Artzt parabolas are detected via dynamic geometry software. Properties of conic triads with a shared focus are studied in [1]. A 6-point conic passing through the tangency point of the excircles (which turns out to coincide with the vertices of V-ellipses) is described in [2, 18]. A Construction of 3 "Soddy" hyperbolas (called here V-hyperbolas) with foci on vertices appears in [17, Sec. 12.4, p. 148]. Properties of a triad of circles tangent to the nine-point circle are studied in [12].

[1] These refer to the intersection of a conic with the focal axis.

**Article organization**

Properties of triads of V-ellipses, P-ellipses, V-hyperbolas, and P-hyperbolas, are covered in Sections 2 to 5, respectively. In last section we pose to the reader a few open questions. The last section contains some long-form symbolic expressions for a construction appearing in Section 2.

## 2 A triad of V-ellipses

Referring to Figure 1:

**Definition 1 (V-ellipses)** *Given a triangle $\triangle ABC$, a triad of V-ellipses $\mathcal{E}_a, \mathcal{E}_b, \mathcal{E}_c$ have foci on $(B,C)$, $(C,A)$, $(A,B)$ and pass through A, B, and C, respectively.*

**Proposition 1** *The V-ellipses $\mathcal{E}_a, \mathcal{E}_b, \mathcal{E}_c$ are centered at the midpoints of $\triangle ABC$'s sides. Their vertices[1] are the (external) tangency points of the excircles with triangle's sidelines and lie on a conic, $\mathcal{Y}$.*

**Proof.** Let $a,b,c$ be the sidelengths of $\triangle ABC$. Let $(I_a),(I_b),(I_c)$ the escribed circles and let $A_1$, $A_2$, $B_1$, $B_2$, $C_1$, $C_2$ their (external) tangency points with the lines $BC$, $CA$, $AB$, as shown in Figure 2. We shall prove that these points are the intersection of the V-ellipses with their focal axis $BC$, $CA$, $AB$, hence their vertices. Elementary properties of tangents from a point to a circle yield:

$$\begin{aligned}
AC_2 =& AB_1 = BA_2 = BC_1 = CA_1 = CB_2 = p,\\
BA_1 =& CA_2 = p-a,\\
AB_2 =& CB_1 = p-b,\\
AC_1 =& BC_2 = p-c,
\end{aligned} \tag{1}$$

where $p=(a+b+c)/2$ is the semi-perimeter. Hence:

$$\begin{aligned}
&A_1A_2 = A_1B + BC + CA_2 =\\
&\quad = (p-a)+a+(p-a) = 2p-a = b+c.
\end{aligned}$$

Since $A_1B = A_2C$, and since points $A_1$, $A_2$, $B$ and $C$ are collinear, the former are precisely the two vertices of $\mathcal{E}_a$. Furthermore, the segments $BC$ and $A_1A_2$ share their midpoint, the center of $\mathcal{E}_a$. The proof for $\mathcal{E}_b$ and $\mathcal{E}_c$ is similar.

In order to prove that their six vertices are on a conic, by Carnot's Theorem, it is enough to check that

$$\frac{AC_1}{BC_1}\cdot\frac{AC_2}{BC_2}\cdot\frac{BA_1}{CA_1}\cdot\frac{BA_2}{CA_2}\cdot\frac{CB_1}{AB_1}\cdot\frac{CB_2}{AB_2} = 1. \tag{2}$$

This claim is obtained by substituting (1) into (2). $\square$

**Remark 1** *The fact that a conic passes through the six external tangency points with the excircles was discovered by Paul Yiu [18]. In [8] its center is labeled $X_{478}$.*

It can be shown that the Yiu conic $\mathcal{Y}$ can never be a circle except when $\triangle ABC$ is an equilateral.

**Proposition 2** *Each V-ellipse $\mathcal{E}_a, \mathcal{E}_b, \mathcal{E}_c$ is respectively tangent at $A, B, C$ to the sides of the excentral triangle.*

**Proof.** Referring to Figure 2, since $I_a, I_b, I_c$ are the centers of the escribed circles, the lines $I_bI_c$, $I_cI_a$, $I_aI_b$ are the external bisectors of $\angle BAC$, $\angle ACB$, and $\angle BCA$; thus $AI_a$, $BI_b$ $CI_c$ are altitudes in $\triangle I_aI_bI_c$ as well as (internal) bisectors of $\triangle ABC$. By the optic propriety of conics, lines $I_bI_c$, $I_cI_a$, $I_aI_b$ are also the tangents in $A$, $B$, $C$ to the ellipses $\mathcal{E}_a$, $\mathcal{E}_b$, $\mathcal{E}_c$. □

Referring to Figure 2, let $(A', A'')$, $(B', B'')$, and $(C', C'')$ denote the pairwise intersections between $(\mathcal{E}_b, \mathcal{E}_c)$, $(\mathcal{E}_a, \mathcal{E}_c)$, and $(\mathcal{E}_a, \mathcal{E}_b)$, respectively.

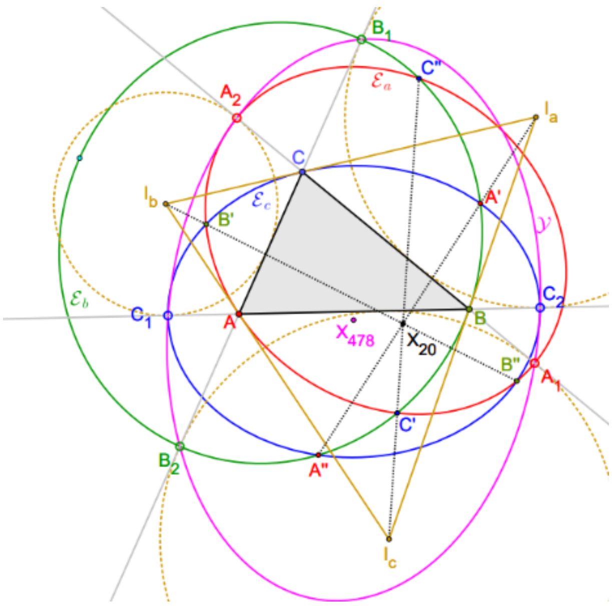


Figure 2: *Properties of a V-ellipses $\mathcal{E}_a, \mathcal{E}_b, \mathcal{E}_c$ (red, green, blue) with respect to a $\triangle ABC$ (black). (i) Its vertices are at the tangency points of the excircles (dashed gold) with the sidelines; hence they lie on the Yiu conic (magenta) [18]. (ii) Each ellipse is tangent at $A, B, C$ to a side of the excentral triangle $\triangle I_aI_bI_c$. (iii) The 3 chords $A'A''$, $B'B''$, and $C'C''$ between the intersections of $(\mathcal{E}_b, \mathcal{E}_c)$, $(\mathcal{E}_c, \mathcal{E}_a)$, $(\mathcal{E}_a, \mathcal{E}_b)$ pass through $I_a, I_b, I_c$, and concur at $X_{20}$.*

**Proposition 3** *The lines through $A', A''$, $B', B''$, $C', C''$ pass through the 3 excenters $I_a, I_b, I_c$, respectively, and concur at the de Longchamps' point $X_{20}$.*

**Proof.** It can be shown that the $\mathcal{E}_a$ is given by the following implicit equation in barycentric coordinates $[x, y, z]$:

$$\begin{aligned}\mathcal{E}_a:\ & 4c(b+c)xy - (a-b-c)(a+b+c)y^2 + \\ & +\ 4b(b+c)xz + 2(a^2+b^2+2bc+c^2)yz - \\ & -\ (a-b-c)(a+b+c)z^2 = 0\end{aligned}$$

$\mathcal{E}_b, \mathcal{E}_c$ can be obtained cyclically on $a, b, c$. The barycentrics for the vertices of $\mathcal{E}_a$ are $A_1 = [0, a+b+c, a-b-c]$ and $A_2 = [0, a-b-c, a+b+c]$. Let $S$ be twice the area of $\triangle ABC$. The two real intersections $A', A''$ between $\mathcal{E}_b, \mathcal{E}_c$ are given by:

$$\begin{aligned}A' = [&(a-b-c)(a+b-c)(a-b+c)\ \cdot \\ &\cdot (3a^2+2ab-b^2+2ac+2bc-c^2)+ \\ &+4(-2a^3-a^2b-b^3-a^2c+b^2c+bc^2-c^3)S, \\ &(a-b-c)(a-b+c)(a+b+c)\cdot \\ &\cdot (a^2-2ab-3b^2+2ac+2bc+c^2)+ \\ &+4(a^3+ab^2+2b^3+a^2c-b^2c-ac^2-c^3)S, \\ &(a-b-c)(a+b-c)(a+b+c)\cdot \\ &\cdot (a^2+2ab+b^2-2ac+2bc-3c^2)+ \\ &+4(a^3+a^2b-ab^2-b^3+ac^2-bc^2+c^3)S]\end{aligned}$$

and $A''$ is obtained as above but with $S \to -S$. The intersections $B', B''$ and $C', C''$ are obtained cyclically. The line $A'A''$ is then given by:

$$\begin{aligned}&-(b-c)(a+b+c)^2x - (a+b-c)^2(a+c)y + \\ &+(a+b)(a-b+c)^2z = 0\end{aligned}$$

It can be shown this line passes through excenter $I_a$. The other lines can be obtained cyclically. It can also be shown these meet at $X_{20}$, whose first barycentric coordinate is given by [8]: $[-3a^4 + 2a^2(b^2+c^2) + (b^2-c^2)^2]$, with the other two obtained cyclically. □

Referring to Figure 3:

**Proposition 4** *When $\triangle ABC$ is a right triangle, the V-ellipses pass through the reflection of the orthocenter on the circumcenter, the de Longchamps point $X_{20}$.*

**Proof.** Let $C$ denote the right-angle vertex of $\triangle ABC$, and $C'$ its reflection about the circumcenter $X_3$. We shall prove that each V-ellipse passes through $C'$. Due to central symmetry, this is trivially true for $\mathcal{E}_c$. Consider $\mathcal{E}_a$: since its foci are $B, C$ and it passes through $A$, its major axis has length $|AC| + |AB|$. Since $ACBC'$ is a rectangle, $|AC| = |BC'|$, and $|BC| = |C'A|$. Hence $|C'B| + |CC'| = |AC| + |AB|$, which ensures that $C' \in \mathcal{E}_a$. Similarly $C' \in \mathcal{E}_b$. □

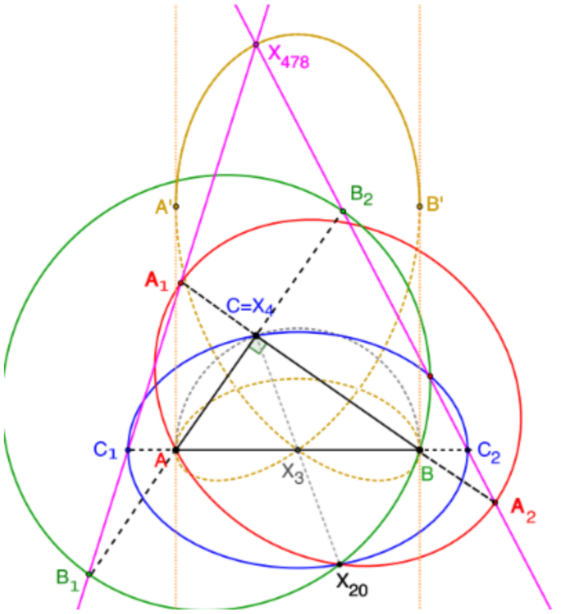


Figure 3: *If $\triangle ABC$ is a right triangle, the Yiu conic $\mathcal{Y}$ (magenta) is degenerate, and the V-ellipses intersect at $X_{20}$. Furthermore, over all C on a semicircle with AB as a diameter, the locus of the center $X_{478}$ of $\mathcal{Y}$ is an arc (solid gold) of a quartic (dashed gold). The lines through $A,B$ perpendicular to AB (dotted gold) are tangent to the locus at its endpoints $A'$, $B'$, and $|AA'| = |BB'| = |AB|$.*

**Degenerate six-point conic:**

Still referring to Figure 3:

**Proposition 5** *$\mathcal{Y}$ is degenerate iff $\triangle ABC$ is a right triangle.*

**Proof.** Let $A_1,A_2,B_1,B_2,C_1,C_2$ the intersection points of the ellipses, with the lines $BC$, $CA$, $AB$, as in Figure 3. We shall prove that $A_1,B_1,C_1$ are collinear iff $\triangle ABC$ is right-angled. To do so, by Menelaus' theorem, we need to check that

$$\frac{A_1C}{A_1B}\cdot\frac{C_1B}{C_1A}\cdot\frac{B_1A}{B_1C}=1. \tag{3}$$

Let $x = CA_1 = BA_2,\; y = AB_1 = CB_2,\; z = AC_1 = BC_2$.

Since the $V-$ ellipses pass through one of triangle's vertices and have their foci into the other two, $a+2x = b+c,\quad b+2y = a+c,\quad c+2z = a+b$, hence

$$x = p-a,\; y = p-b,\; z = p-c,$$

where $p = \frac{a+b+c}{2}$ is the semi-perimeter. Substituting this into (3), we obtain:

$$\frac{x}{p}\cdot\frac{p}{z}\cdot\frac{y}{p}=1$$

hence $(p-a)\cdot(p-b) = p\cdot(p-c)$, which is equivalent to $c^2 = a^2+b^2$. The result follows by Pythagoras' theorem. □

Assume, without loss of generality, that $A = (1/2,0)$ and $B = (-1/2,0)$.

**Proposition 6** *Over C on the semicircle whose diameter is AB, $y>0$, the locus of the center of the degenerate $\mathcal{Y}$ is the arc of a quartic given by:*

$$4(x^2+y^2)^2-8y^3-x^2+2y^2=0,\quad y>1$$

*The semicircle with $y<0$ produces a locus which is symmetric about the x-axis.*

**Proof.** The claim was obtained via manipulation and simplification with a Computer Algebra System (CAS). □

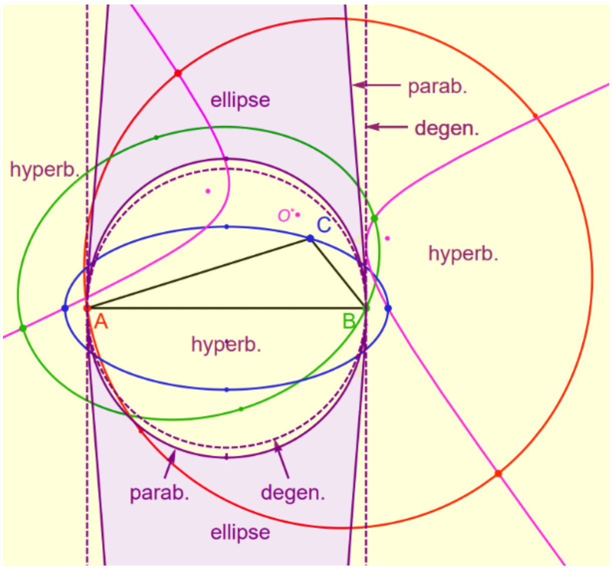


Figure 4: *With $A,B$ fixed, the solid (resp. dashed) purple lines are the locus of C such that the Yiu conic $\mathcal{Y}$ is a parabola (resp. degenerate). As indicated, in between said boundaries, the conic is either an ellipse or a hyperbola. A particular $\triangle ABC$ is shown with C interior to the circumcircle, where $\mathcal{Y}$ is a hyperbola (magenta).*

Referring to Figure 4:

**Proposition 7** *With A, B fixed, the Yiu conic $\mathcal{Y}$ of $\triangle ABC$ is (i) degenerate if C lies on the union of the circumcircle with the two lines tangent to it at A and B; (ii) a parabola if C lies on a curve whose barycentrics satisfy the following degree-8 implicit equation:*

$$\begin{aligned}&a^8+b^8+c^8-2(a^4b^4+a^4c^4+b^4c^4)+\\&+4abc(a^5+b^5+c^5-a^4b-ab^4-a^4c-ac^4-\\&\qquad -bc^4-b^4c+a^3bc+ab^3c+abc^3)=0.\end{aligned}$$

**Proof.** The claim was obtained via manipulation and simplification with a Computer Algebra System (CAS). □

**What about the co-vertices?**

It turns out that for $A, B$ fixed, there is a locus of $C$ such that the 6 co-vertices of the V-ellipses lie on a conic. Without loss of generality, let $A = (-1, 0)$, and $B = (1, 0)$. Referring to Figure 5:

**Proposition 8** *The locus of $C$ such that the 6 co-vertices of $\mathcal{E}_a$, $\mathcal{E}_b$, and $\mathcal{E}_c$ lie on a conic is given by:*

$$
\begin{aligned}
&\left(x^6-(2y^2+3)x^4-\;(3y^4-8y^2-3)x^2+11y^4-6y^2-1\right)\rho_1\rho_2+\\
&+\Big(-2x^6-(22y^2-6)x^4-(14y^4-36y^2+6)x^2+6y^6+22y^4-\\
&\qquad -14y^2+2\Big)\,(\rho_1+\rho_2)+\\
&+2x\left(x^6+(3y^2-3)x^4+(3y^4-2y^2+3)x^2+y^6-7y^4-y^2-1\right)\cdot\\
&\qquad\cdot(\rho_1-\rho_2)+\\
&+2(x^2+y^2-1)\left(5x^4+2(y^2-5)x^2-3y^4-14y^2+5\right)(x^2-1)=0
\end{aligned}
$$

*where* $\rho_1 = \sqrt{x^2+y^2+2x+1}$, *and* $\rho_2 = \sqrt{x^2+y^2-2x+1}$.

**Proof.** Computer algebra system-based manipulation. □

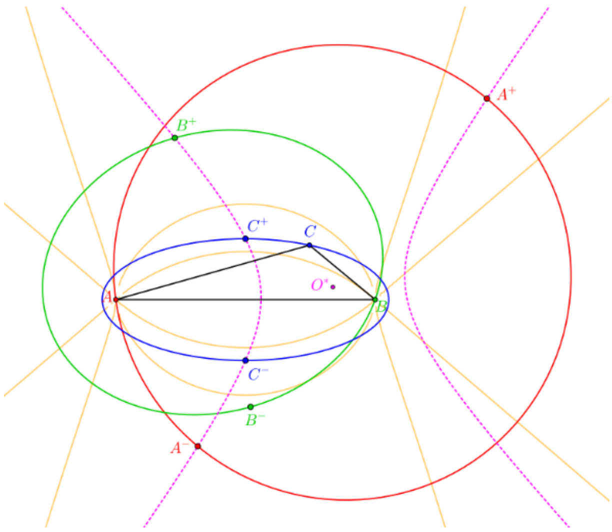


Figure 5: *A $\triangle ABC$ is shown, as well as its 3 P-ellipses (red, green, blue) with co-vertices $A^+, A^-$, $B^+, B^-$, $C^+, C^-$. Also shown is the locus of $C$ (yellow) such that the co-vertices lie on a conic. Notice that for the triangle shown, $C$ does lie on said locus. For illustration, a hyperbola is shown (dashed magenta) which passes through 5 co-vertices but misses $B^-$.*

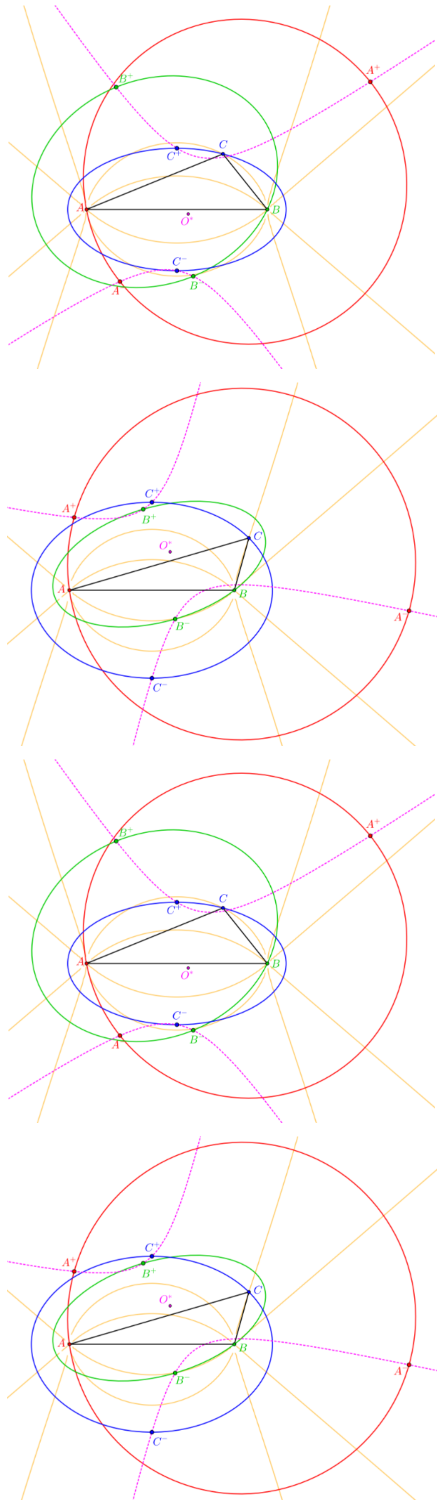

Figure 6: *Four choices for $C$ on the locus (yellow) such that the co-vertices $A^+, A^-$, $B^+, B^-$, and $C^+, C^-$ of V-ellipses (red, green, blue) of $\triangle ABC$ lie on a conic (dashed magenta). In the top two cases (resp. bottom two), the co-vertices are split 3x3 (resp. 5x1) on each branch of the conic.*

Notice that a full 8 branches of the locus converge on either $A$ or $B$. Also note that if one attempts to eliminate the square roots in the implicit, one obtains a degree-36 polynomial.

Examples of the 6-point co-vertex conic for different locations of $C$ on the above locus appear in Figure 6, suggesting that (i) this conic is always a hyperbola, and that (ii) depending on the branch of the locus of $C$ is on, co-vertices are split as 3:3 or 5:1 along the two branches of the hyperbola.

## 3 A triad of P-ellipses

Referring to Figure 7:

**Definition 2 (P-ellipses)** *A triad of P-ellipses $\mathcal{E}_a^*, \mathcal{E}_b^*, \mathcal{E}_c^*$ have foci on $(B,C)$, $(C,A)$, $(A,B)$ and pass through a given point $P$.*

Consider a triad of P-ellipses as in Definition 2.

**Theorem 1** *The six vertices of a triad of P-ellipses lie on a conic $\mathcal{Y}^*$.*

**Proof.** Referring to Figure 7, let $A_1,A_2$ (resp. $B_1,B_2$, and $C_1,C_2$) denote the vertices of $\mathcal{E}_a^*$ (resp. $\mathcal{E}_b^*$ and $\mathcal{E}_c^*$). Note that $A_1A_2$ shares its midpoint with $BC$, and so on cyclically. Therefore: $AC_2 = BC_1$, $BA_2 = A_1C$, and $CB_1 = B_2A$. To finish the proof, we apply Carnot's theorem as in Proposition 1. □

Let $a,b,c$ denote the sidelengths of $\triangle ABC$. Let $\delta_a = |PB|+|PC|$, $\delta_b = |PC|+|PA|$, $\delta_c = |PA|+|PB|$. Referring to Figure 8 (left).

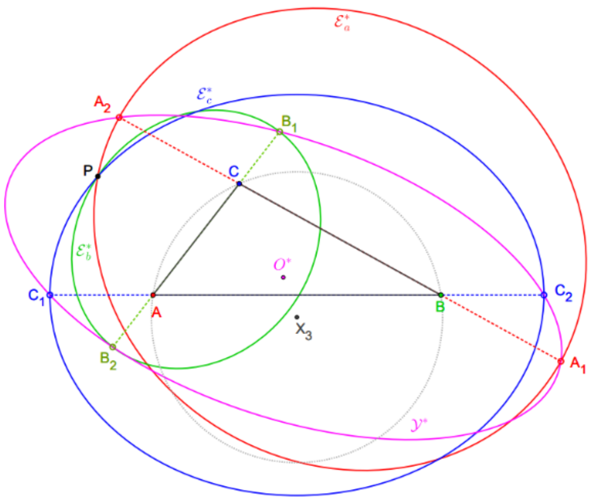


Figure 7: *The six vertices $A_1$, $A_2$, $B_1$, $B_2$, $C_1$, and $C_2$ of P-ellipses $\mathcal{E}_a^*, \mathcal{E}_b^*, \mathcal{E}_c^*$ are on a conic $\mathcal{Y}^*$. For reference, the circumcenter $X_3$ of $\triangle ABC$ and the center $O^*$ of $\mathcal{Y}^*$ are also shown.*

**Proposition 9** *There is a unique point $P^*$ such that $\mathcal{Y}^*$ is a circle given by:*

$$\left[(a^2-\delta_a^2)(c^2-b^2+\delta_b^2-\delta_c^2)\right]^2+$$
$$\left[(b^2-\delta_b^2)(a^2-c^2+\delta_c^2-\delta_a^2)\right]^2+$$
$$\left[(c^2-\delta_c^2)(b^2-a^2+\delta_a^2-\delta_b^2)\right]^2=0$$

*Furthermore, $\mathcal{Y}^*$ is concentric with the circumcircle of $\triangle ABC$.*

Level curves of the above function for a particular triangle are shown in Figure 8 (left). Interestingly, there is a straightforward way to construct a triangle whose $\mathcal{Y}^*$ is a circle.

**Definition 3 (anticevian triangle)** *Given $\triangle ABC$ and a point $Q$, the $Q$-*anticevian *$\triangle A'B'C'$ is such that $\triangle ABC$ is its $Q$-cevian [16].*

Referring to Figure 8 (right), a first "needle in a haystack" find is:

**Proposition 10** *Given a reference triangle $\triangle ABC$, its $X_3$ is the $P^*$ of its $X_3$-anticevian $\triangle A'B'C'$. Furthermore, (i) $\mathcal{Y}^*$ of the the latter is concentric with its circumcircle, and (ii) its center lies on the $X_4X_6$ line of $\triangle ABC$.*

**Proof.** This needle-in-a-haystack phenomenon was discovered experimentally and then verified using CAS. □

Barycentric coordinates for the circumcenter $X_3'$ of the $X_3$-anticevian appear in Section 6.

While it can be shown that given a generic $\triangle A'B'C'$, there is always a triangle $\triangle ABC$ which is the former's $X_3$-cevian (map is invertible), we don't yet have a geometric construction for the latter.

### A degenerate 6-point conic:

As shown in Figure 9 (left), a simple condition renders $\mathcal{Y}^*$ degenerate, namely:

**Proposition 11** *If $P$ is on the circumcircle of $\triangle ABC$, $\mathcal{Y}^*$ is degenerate (two straight lines).*

**Proof.** Via CAS, it can be verified that the 3x3 discriminant of the homogeneous equation for the conic vanishes. □

Referring to Figure 9 (left):

**Proposition 12** *Over $P$ on the circumcircle, the locus of the center $O^*$ of $\mathcal{Y}^*$ is the union of arcs of three distinct ellipses $\mathcal{L}_a, \mathcal{L}_b, \mathcal{L}_c$, all of which pass through the midpoints of $ABC$. The endpoints of $\mathcal{L}_a$ are one vertex of V-ellipse $\mathcal{E}_b$ and one of $\mathcal{E}_c$, and so on cyclically for the endpoints of $\mathcal{L}_b$, $\mathcal{L}_c$.*

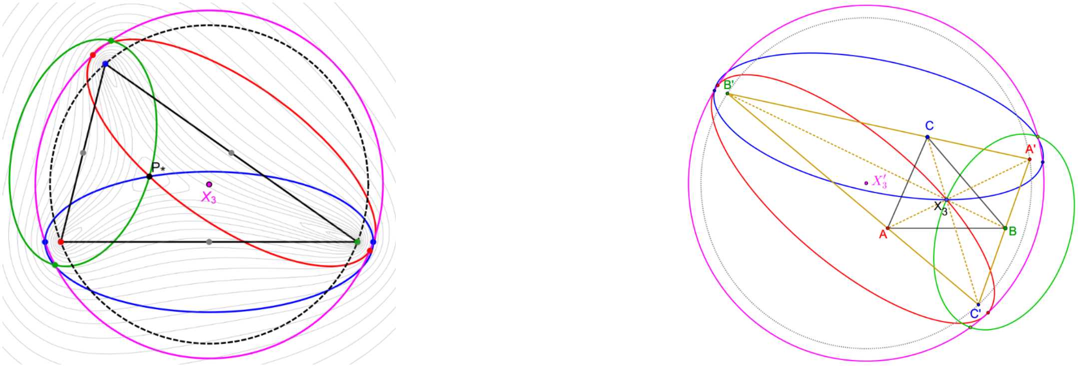


Figure 8: ***Left:*** *Given a triangle, there is a unique $P^*$ such that the 6-point conic (magenta) of a triad of P-ellipses is a circle. The latter is concentric with the circumcircle (dashed black). Also shown are level curves of the functional in Proposition 9: $P^*$ is its unique zero.* ***Right:*** *The vertices of a P-ellipse with foci on vertices of the $X_3$-anticevian $\triangle A'B'C'$ of $\triangle ABC$, and passing through the latter's $X_3$ lie on a circle (magenta). The latter is concentric with the circumcircle of $\triangle A'B'C$ (dashed black) at $X_3'$.*

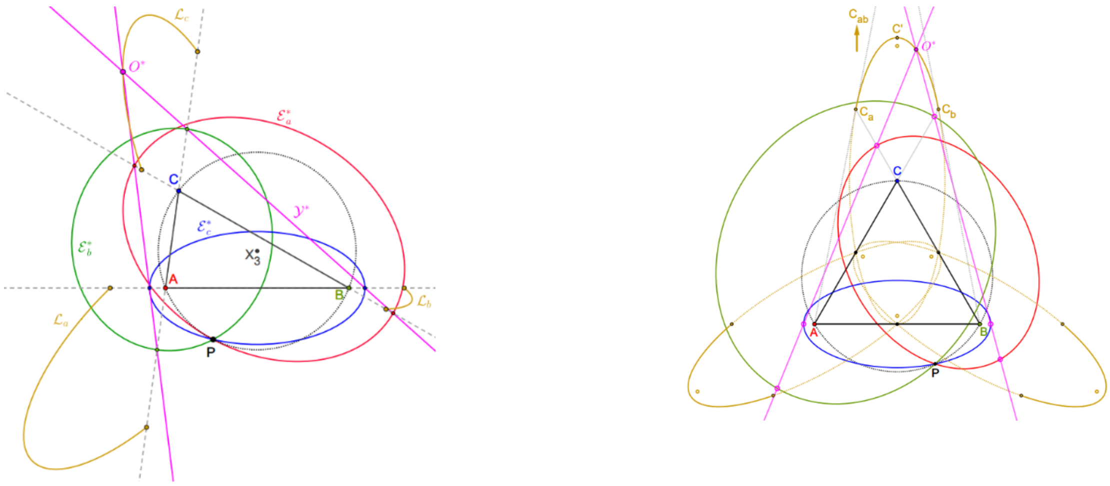


Figure 9: ***Left:*** *If P lies on the circumcircle of $\triangle ABC$, the Yiu conic $\mathcal{Y}^*$ (magenta) is degenerate. Over P on the circumcircle, the locus (gold) of the center $O^*$ of the degenerate conic (magenta lines) is the union of three arcs of ellipse $\mathcal{L}_a, \mathcal{L}_b, \mathcal{L}_c$.* ***Right:*** *Over all P on the circumcircle of an equilateral $\triangle ABC$, the locus of the center $O^*$ of the degenerate 6-pt conic (magenta) is the union of 3 elliptic arcs (solid gold) centered on $A,B,C$, whose major axes are the altitudes of $\triangle ABC$. The major (resp. minor) semi-axes measure $|AB| = \sqrt{3}/2$ (resp. $|AB| = \sqrt{3}/6$).*

**Proof.** Referring to Figure 10, that the endpoints of $\mathcal{L}_c$ are a vertex $A''$ of $\mathcal{E}_a$ and a vertex $B''$ of $\mathcal{E}_b$ can be seen from the fact that the limit of $\mathcal{E}_a^*$ (resp. $\mathcal{E}_b^*$) as $P$ approaches $A$ (resp. $B$) is $\mathcal{E}_a$ (resp. $\mathcal{E}_b$) and that the center $O^*$ of the degenerate $\mathcal{Y}^*$ will approach the intersection of $AA''$ and $BC$. The same argument applies for the endpoints of $\mathcal{L}_a, \mathcal{L}_b$, cyclically. To show that the locus of $O^*$ is the union of three elliptic arcs, we (i) restrict $P$ to a given "third" of the circumcircle, e.g., the arc between $A$ and $B$. Then (ii) we obtain, via a CAS, a (rather long) symbolic expression for the implicit function $f(x,y)$ representing the ellipse which passes through the 5 proposed points, namely, two vertices of V-ellipses and the midpoints of the sides of $\triangle ABC$. We then (iii) obtain a parametric expression for $O^*$ as a function of $P$ and plug it into $f(x,y)$, and notice via a CAS, that this simplifies to zero, independent of $P$. (iv) The same can be repeated cyclically for the other 3 portions of the circumcircle. □

Referring to Figure 9 (right):

**Corollary 1** *Let $\triangle ABC$ be an equilateral of side 1. Over $P$ on the circumcircle, the locus of the center $O^*$ of the degenerate $\mathcal{Y}^*$ is the union of arcs of three congruent ellipses with semi-axes $a = \sqrt{3}/2$ and $b = \sqrt{3}/6$, centered on $A,B,C$.*

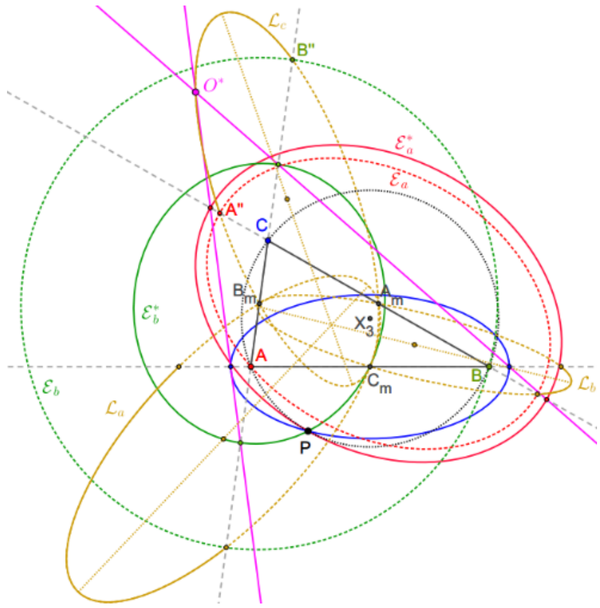


Figure 10: *Definitions used in Proposition 12. The locus of $O^*$ is the union of three arcs of ellipse (solid gold) $\mathcal{L}_a, \mathcal{L}_b, \mathcal{L}_c$, each of which passes through the 3 midpoints $A_m, B_m, C_m$ of $\triangle ABC$. The endpoints $A'', B''$ of $\mathcal{L}_c$ are vertices of V-ellipses $\mathcal{E}_a$ and $\mathcal{E}_b$ (dashed red, green). The major axes (dashed gold) of the three loci nearly concur, though not exactly.*

Let $C_a$ and $C_b$ denote the endpoints of the elliptic locus of $O^*$, over $P$ on the arc of the circumcircle below $AB$. Let $C'$ denote the locus' top vertex. Referring to Figure 9 (right), the following can be shown:

- $C_a$ and $C_b$ are the reflections of the midpoints of $AC$ and $BC$ about $C$
- lines $AC_a$ and $BC_b$ are tangent to the locus. Let $C_{ab}$ denote their intersection.
- $C'$ is the midpoint between $C$ and $C_{ab}$.
- Therefore, $C_aC_b$ is the mid-base of $\triangle AC_{ab}B$, therefore the latter is 3 times the area of $\triangle ABC$.

**Regions of conic type:**

It turns out the type of $\mathcal{Y}^*$ (ellipse, parabola, hyperbola, degenerate) depends on the position of $P$. The case of an equilateral $\triangle ABC$ is illustrated in Figure 11.

**Remark 2** *If $\triangle ABC$ is an equilateral, it can be shown that the portions of the locus of $P$ such that $\mathcal{Y}^*$ is: (i) degenerate (deltoid interior to $\triangle ABC$) are branches of 3 regular cubics; (ii) a parabola: branches of a degree-20 polynomial on $x, y$.*

**Remark 3** *If $\mathcal{Y}^*$ is a hyperbola it can never be a rectangular one.*

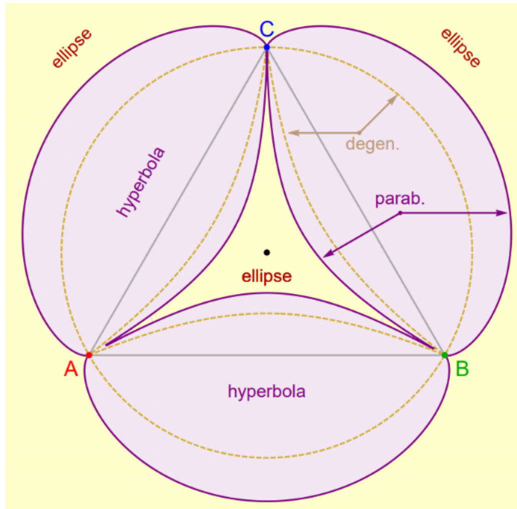


Figure 11: *For $\triangle ABC$ an equilateral, the figure illustrated regions of $P$ such that the $\mathcal{Y}^*$ conic is of a given type.*

**What about the co-vertices?**

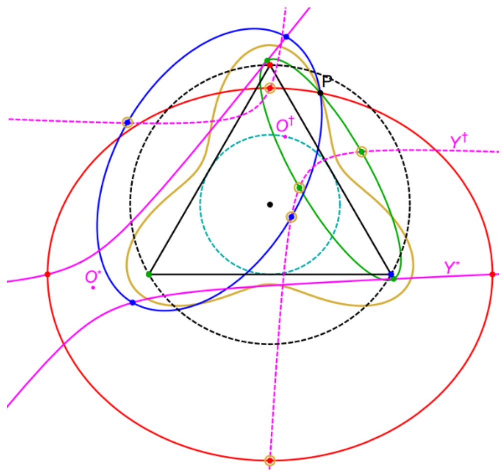


Figure 12: *Given an equilateral (black), the locus for $P$ such that the 6 co-vertices of the 3 $P$-ellipses lie on a conic is a degree-10 algebraic curve (gold) woven symmetrically about the equilateral (there is an isolated point at the centroid as well). The three $P$-ellipses (red, green, blue) are shown for a specific choice of $P$ on said locus. Also shown are (i) the conic $\mathcal{Y}^*$ (solid magenta, center $O^*$) through the major vertices, and (ii) the conic $\mathcal{Y}^\dagger$ (dashed magenta, center $O^\dagger$) through the 6 co-vertices (highlighted by small gold circles). Notice that if $P$ is on the locus, $O^\dagger$ lies on the incircle of the equilateral.*

It turns out that for given $\triangle ABC$, there is a 1d locus for $P$ such that the 6 co-vertices lie on a conic. As before, let Let $\delta_a = |PB|+|PC|$, $\delta_b = |PC|+|PA|$, $\delta_c = |PA|+|PB|$.

Referring to Figure 12:

**Proposition 13** *If $\triangle ABC$ is an equilateral, the locus for $P$ such that the 6 co-vertices lie on a conic $\mathcal{Y}^\dagger$ is given by:*

$$\delta_a^2\delta_b^2+\delta_a^2\delta_c^2+\delta_b^2\delta_c^2-8(\delta_a^2+\delta_b^2+\delta_c^2)+48=0$$

*Furthermore, the center $O^\dagger$ of $\mathcal{Y}^\dagger$ lies on the incircle of the equilateral.*

Note: if one eliminates all square roots involved in computing $\delta_a, \delta_b, \delta_c$, the above becomes a degree-10 equation on $x, y$.

## 4 A triad of V-hyperbolas

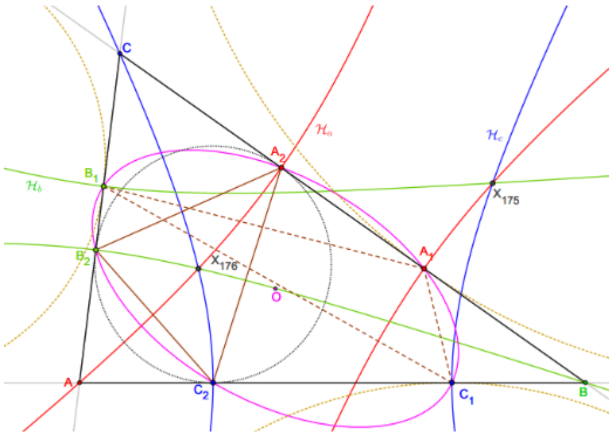


Figure 13: *A triad of V-hyperbolas $\mathcal{H}_a, \mathcal{H}_b, \mathcal{H}_c$ (red, green, blue) is shown with foci on $(B,C)$, $(C,A)$, and $(A,B)$ passing through $A, B, C$, respectively. Notice (i) their vertices taken as triples $A_1B_1C_1$ and $A_2B_2C_2$ are the vertices of the extouch (dashed brown) and intouch (solid brown) triangles; (ii) these 6 points are known to lie on the Privalov conic (magenta), whose center $O$ is $X_{5452}$ on [8]; (iii) the 3 hyperbolas pass through both the "isoperimeteric" and "equal detour" points, i.e., $X_{175}$ and $X_{176}$, respectively. Note: these coincide when the outer Soddy circle is external to the three mutually tangent circles.*

In this section we describe properties – some old, some new – of a special triad of hyperbolas, described in [17, Sec. 12.4, p. 148] where they are called "Soddy" hyperbolas. Referring to Figure 13:

**Definition 4 (V-hyperbolas)** *Given a triangle $\triangle ABC$, a triad of V-hyperbolas $\mathcal{H}_a, \mathcal{H}_b, \mathcal{H}_c$ have foci on $(B,C)$, $(C,A)$, $(A,B)$ and pass through $A$, $B$, and $C$, respectively.*

[2] These pass through the vertices of the intouch triangle.

Let $A_1, A_2$ be the vertices of $\mathcal{H}_a$. Define $B_1, B_2$ and $C_1, C_2$ for $\mathcal{H}_b, \mathcal{H}_c$, respectively. Recall the extouch (resp. intouch) triangle is where the 3 excircles (resp. incircle) touch a triangle's sides.

**Remark 4** *Let $\lambda_a = |AB| - |AC|$. In barycentric coordinates for the vertices of $\mathcal{H}_a$ are given by: $A_1 = [0, a+\lambda_a, a-\lambda_a]$, and $A_2 = [0, a-\lambda_a, a-\lambda_a]$, with the others computed cyclically.*

**Corollary 2** *$\triangle A_1B_1C_1$ (resp. $\triangle A_2B_2C_2$) is the extouch (resp. intouch) triangle of $\triangle ABC$.*

Recall that for any triangle, the intouch and extouch triangles have the same area [16, extouch triangle]. Referring to [8, X(5452)]:

**Corollary 3** *$A_1, A_2, B_1, B_2, C_1, C_2$ lie on the Privalov conic centered on $X_{5452}$, and whose barycentric coordinates $x, y, z$ satisfy:*

$$k_1k_2k_3(x^2+y^2+z^2)+$$
$$+2\left[k_2(k_4-2ab)xy+k_3(k_4-2ac)xz-k_1(k_4-2bc)yz\right]=0$$

*where $a, b, c$ are the sidelengths of $\triangle ABC$, $k_1 = (a-b-c)$, $k_2 = (a+b-c)$, $k_3 = (a-b+c)$, and $k_4 = a^2+b^2+c^2$.*

**Remark 5** *When $\triangle ABC$ is isosceles, one of the V-hyperbolas is degenerate, namely, a pair of coinciding lines at the perpendicular bisector of the base. In this case, the Privalov conic is tangent to the base at its midpoint.*

**Intersections between V-hyperbolas:**

Referring to Figure 15, recall that given a triangle, one can construct[2] three "kissing" circles $\mathcal{C}_A$, $\mathcal{C}_B$, and $\mathcal{C}_C$ centered each on each vertex, and externally tangent to each other [14].

The Apollonius' problem for this triple has (as usual) eight distinct solutions, two of which have the same tangency type (tangent externally or internally to all three circles).

**Definition 5 (Soddy circles of a triangle)** *The two solutions for the Apollonius' problem with the same tangency type are the so-called "Soddy circles". The inner Soddy circle is the one whose center is inside the triangle and whose interior does not intersect any of the three kissing circles; the other one is the outer Soddy circle.*

Note that the outer Soddy circle, always tangent to the 3 kissing circles, can either (i) contain them (see Figure 15), (ii) be a line tangent to them, or (iii) be externally tangent to them. For (ii) and (iii) see Figure 16.

The centers of Soddy circles correspond to a pair of triangle centers found in [8] and derived in [7]. Namely:

**Definition 6 (Isoperimetric point)** *The center of the outer Soddy circle ($X_{175}$ in [8]). Equivalently, the unique point $X$ such that:*

$$|XB|+|XC|\pm|BC|=|XC|+|XA|\pm|CA|=|XA|+|XB|\pm|AB|$$

*where the positive (resp. negative) sign is chosen if the outer Soddy circle contains (resp. is external to) the three mutually tangent circles in Definition 5. As derived in [7], containment corresponds to:*

$$\tan\frac{A}{2}+\tan\frac{B}{2}+\tan\frac{C}{2}<2.$$

In [7] it is shown that if the sum of half-tangents is exactly 2, then the outer Soddy circle degenerates to a line. Referring to Figure 14, it can be shown that:

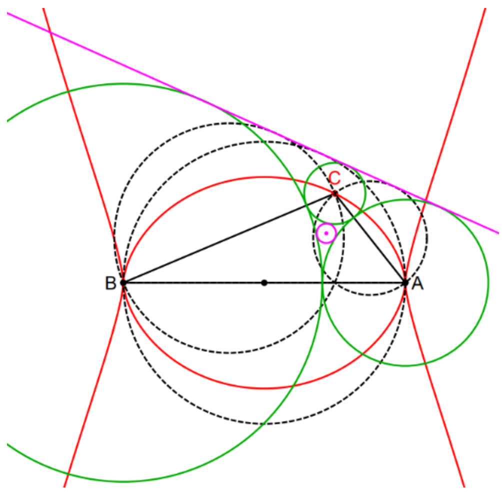


Figure 14: *When A and B are fixed, the locus of C (red) such that the outer Soddy circle degenerates to a line (magenta) is given by the degree-6 implicit equation in Proposition 14. This line is also tangent to the 3 circles (dashed black) whose diameters are the sides of $\triangle ABC$.*

**Proposition 14** *Without loss of generality, let $A=(-1,0)$, $B=(1,0)$, the locus of $C$ such that the sum of half-tangents of $\triangle ABC$ is 2 is given by the union of the following degree-6 polynomial and its reflection about the x-axis:*

$$-4x^6-4x^4(2y^2+2y+1)-4x^2(y^4+y^3-4y-5)+$$
$$+4y^5+13y^4+20y^3+8y^2-8y-12=0.$$

**Definition 7 (Equal detour point)** *The center of the inner Soddy circle ($X_{176}$ in [8]), always internal to a triangle. Also the unique point $X$ in $\triangle ABC$ such that:*

$$|XB|+|XC|-|BC|=|XC|+|XA|-|CA|=|XA|+|XB|-|AB|.$$

**Proposition 15** *The three V-hyperbolas intersect at the centers of the two Soddy circles, i.e., $X_{175}$ and $X_{176}$, respectively.*

**Proof.** Assume that $a>c>b$ as in Figure 13. Then $r_a<r_c<r_b$. $\mathcal{C}_a$ and $\mathcal{C}_b$ are two circles centered at $A$ and $B$ and of radii $r_a<r_b$, which are externally tangent at $C_2$. The locus of the centers of the circles that are externally tangent to both $\mathcal{C}_a$ and $\mathcal{C}_b$ is the branch of the hyperbola with foci on $A$ and $B$, that passes through their tangency point $C_2$. The other branch contains the centers of the circles that are internally tangent (i.e., contain both). The internal Soddy circle is externally tangent to the three circles $\mathcal{C}_a$, $\mathcal{C}_b$, and $\mathcal{C}_c$; hence its center is necessarily the intersection of the three branches of hyperbolas passing through $A_2, B_2, C_2$, the vertices of the intouch triangle. Since $r_a<r_c<r_b$, we may specify those branches as $\mathcal{H}_a^+=\{P : |PB|-|PC|=r_b-r_c\}$, $\mathcal{H}_b^+=\{P : |PC|-|PA|=r_c-r_a\}$, and $\mathcal{H}_c^+=\{P : |PA|-|PB|=r_a-r_b\}$.

Thus, if a point $P\in\mathcal{H}_a^+\bigcap\mathcal{H}_c^+$ then $PA-PC=r_a-r_c$ hence it is on $\mathcal{H}_b^+$ as well. Since $r_c+r_a=b$ and $r_b+r_a=c$, $P$ verifies the equal-detour definition of $X_{176}$.

The points on the other branches contain centers of circles that are internally tangent to the other two; therefore, if two branches, say $\mathcal{H}_a^-$ and $\mathcal{H}_b^-$ have a common point $P$, then, as above, $P$ is also on the third branch and is the (unique) center of an external Soddy circle, that contains $\mathcal{C}_a$, $\mathcal{C}_b$, and $\mathcal{C}_c$. In this case, $P$ verifies the isoperimetric definition of $X_{175}$.

In contrast, if $\mathcal{H}_a^-$ and $\mathcal{H}_b^-$ do not intersect, then there will be no "negative branch" intersection. In this case, the three positive branches will intersect in two distinct points: the centers of the inner and outer Soddy circles. Note that each pair $(\mathcal{H}_a,\mathcal{H}_b)$, $(\mathcal{H}_b,\mathcal{H}_c)$, and $(\mathcal{H}_c,\mathcal{H}_a)$ have one common focus $C, A, B$ respectively; hence they necessarily have four (real) intersections. This guarantees the existence of both detour and isoperimetric points. □

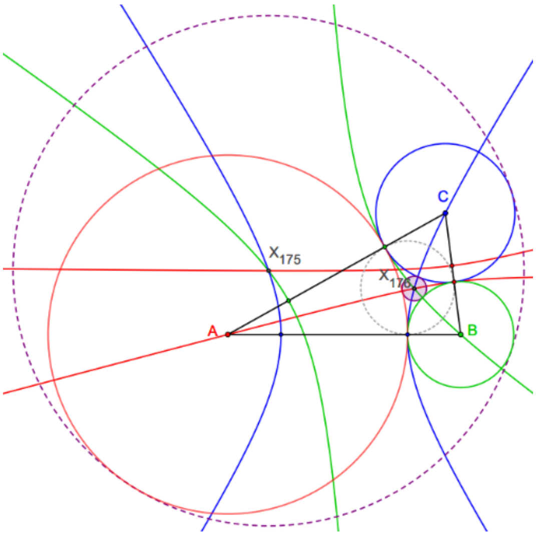


Figure 15: *A construction found in [17, Sec. 12.4, p. 148]: 3 mutually-tangent circles (red, green, blue) of $\triangle ABC$ touch at the contact points of the incircle (dashed gray) with the sides. In turn, these coincide with a vertex of each the 3 V-hyperbolas. Notice the latter intersect at the centers $X_{176}$ and $X_{175}$ of the inner (shaded purple), and outer (dashed purple) Soddy circles, respectively.*

Referring to Figure 17:

**Proposition 16** *The $\mathcal{H}_a$ V-hyperbola passes through the intersections $A'$ and $A''$ of V-ellipses $\mathcal{E}_b$, and $\mathcal{E}_c$. The same holds for $\mathcal{H}_b$, $\mathcal{H}_c$, cyclically.*

**Proof.** Referring to Figure 17, let $A''$ denote an intersection of $\mathcal{E}_b$ with $\mathcal{E}_c$. Then:

$$|A''A|+|A''B|=|CA|+|CB|,\quad |A''A|+|A''C|=|BA|+|BC|.$$

Subtracting, $|A''C|-|A''B|=|BA|-|CA|$, meaning that $A''$ lies on the branch of hyperbola $\mathcal{H}_a$ not containing $A$. □

Still referring to Figure 17, let $A_1$ and $A_2$ denote the two 2-branch intersections between $\mathcal{H}_b$ and $\mathcal{H}_c$, define $B_1,B_2$ and $C_1,C_2$ cyclically.

**Proposition 17** *The three lines $A_1A_2$, $B_1B_2$ and $C_1C_2$ concur at the Nagel point $X_8$ of $\triangle ABC$.*

**Proof.** Let $a,b,c$ denote the sidelines. The barycentrics of $A_1$ are given by:

$$\begin{aligned}A_1:[\,&(L-2a)(3a^2+2ab-b^2+2ac-2bc-c^2+2(b-c)\gamma),\\ &(L-2c)(3a-3b+c)L+2(a^2-c^2-2b^2+ab-bc)\gamma,\\ &(L-2b)(3a+b-3c)L-2(a^2-b^2-2c^2+ac+bc)\gamma\,]\end{aligned}$$

where $L=a+b+c$ and $\gamma=3a^2+2ab-b^2+2ac-2bc-c^2$. The barycentrics of $A_2$ are obtained by replacing $\gamma$ with $-\gamma$. The barycentrics of points on $A_1A_2$ satisfy:

$$\begin{aligned}&(-2a^2+ab+b^2+ac-2bc+c^2)x+\\ &+(a-c)(L-2a)y+(a-b)(L-2a)z=0\end{aligned}$$

and cyclically for $B_1B_2$ and $C_1C_2$. It can be shown that the 3 lines pass through $X_8$, whose barycentric coordinates are $[b+c-a,a+c-b,a+b-c]$, see [8]. □

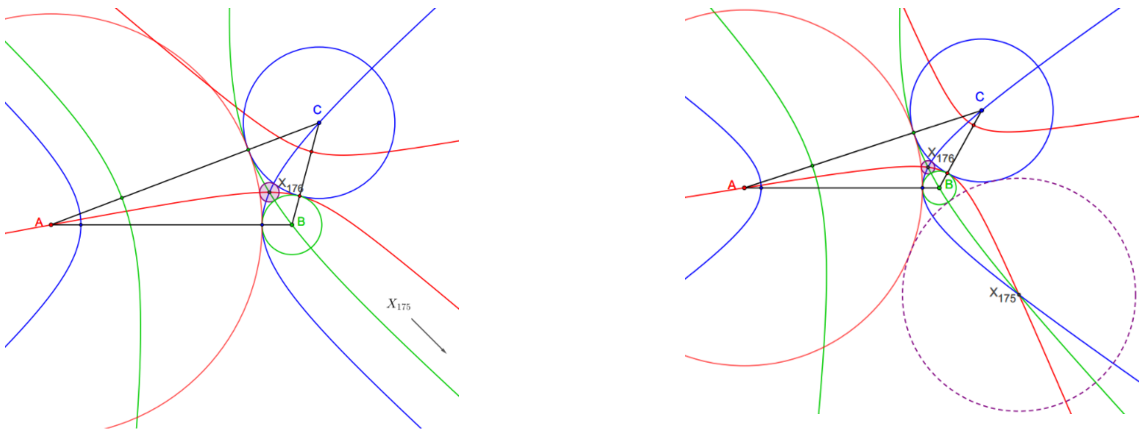


Figure 16: *Two cases of $\triangle ABC$ such that the external Soddy circle (dashed purple) is: (left) a straight line ($\sum\tan(\theta_i)=2$), and (right) does not contain the three kissing circles. Notice that in both cases the three V-hyperbolas (red, green and blue) intersect at the center $X_{176}$ of the inner Soddy circle (shaded purple), interior to the triangle. In the first case their second intersection is at infinity (in the direction perpendicular to the Soddy line), while in the second case they intersect along the same branches where their $X_{176}$ intersection lies.*

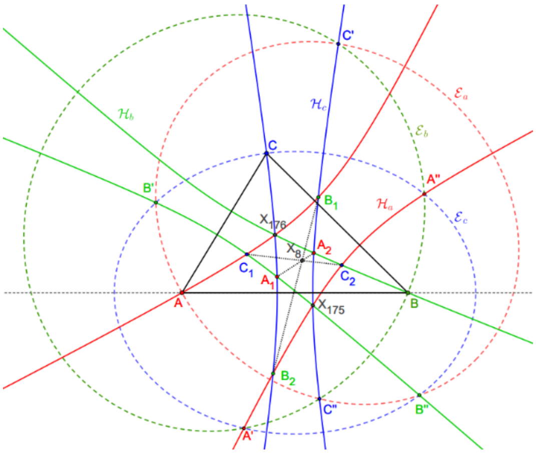


Figure 17: *Each V-hyperbola passes through the two intersections between pairs of V-ellipses. As an example, consider $A''$, common to $\mathcal{H}_a$, $\mathcal{E}_b$, and $\mathcal{E}_c$. Also shown is the fact that the 3 segments $A_1A_2$, $B_1B_2$, and $C_1C_2$ connecting opposing 2-branch intersections of the 3 V-hyperbolas concur at $X_8$.*

Referring to Figure 18:

**Remark 6** *On side BC there lie the 2 vertices of $\mathcal{E}_a$ and the 2 of $\mathcal{H}_a$. Consider the degenerate cubic which is the union of the sidelines of $\triangle ABC$. It is a 15-point cubic since it passes through (i) the three vertices of the triangle, (ii) the 6 vertices of the V-ellipses, and (iii) the 6 vertices of the V-hyperbolas.*

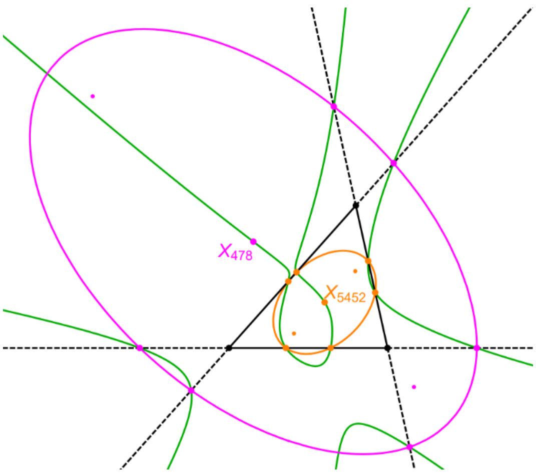


Figure 18: *Given a triangle (black), the union of the 3 sidelines (dashed black) can be regarded as a 15-point degenerate cubic. It passes through (i) the triangle vertices, (ii) the 6 points on the Yiu conic (magenta), and (iii) the 6 points on the Privalov conic (orange). Just for fun, also shown are branches of the 14-point quartic (green) that passes through the 12 points on the Yiu+Privalov as well as their centers $X_{478}$ and $X_{5452}$, respectively.*

Referring to Figure 14:

**Proposition 18** *When the external Soddy circle degenerates to a line, the three circles whose diameters are the sides of $\triangle ABC$ are also tangent to it.*

**Proof.** Let $A_T$, $B_T$ be the tangency points of the degenerate Soddy circle $\mathcal{L}$ (a line) with circles $\mathcal{C}_a, \mathcal{C}_b$, and let $T$ be the tangency point between the latter two. The perpendicular dropped from $T$ onto line $AB$ meets $\mathcal{L}$ at $M$. Then, owing to properties of tangents from a points to a circle, $|MT| = |MA_T| = |MB_T|$. Since $B_T, M, A_T$ are collinear, then $\angle A_T T B_T = 90°$. On the other hand, since $MT$ and $MA_T$ are tangents from $M$ to $\mathcal{C}_a$, $MA \perp TA_T$ and similarly, $MB \perp TB_T$. $\angle AMB = 90°$. Hence, if $O$ is the midpoint of $AB$ then $OM = AO = OB$. Finally, the quadrilateral $[ABB_TA_T]$ is a trapezium ($AA_T$, $BB_T$ are perpendicular to $\mathcal{L}$) and $OM$ is its mid-base. Hence $OM$ is also perpendicular to $\mathcal{L}$ at the midpoint $M$ of $A_TB_T$. Therefore the circle of diameter $AB$ is tangent to $\mathcal{L}$ at $M$, and so on cyclically for $(\mathcal{C}_b, \mathcal{C}_c)$ and $(\mathcal{C}_a, \mathcal{C}_c)$. □

## 5 A triad of P-hyperbolas

We now extend V-hyperbolas to a trio with respect to a point $P$. Referring to Figure 19:

**Definition 8 (P-hyperbolas)** *A triad of P-hyperbolas $\mathcal{H}_a^*, \mathcal{H}_b^*, \mathcal{H}_c^*$ with respect to $\triangle ABC$ have foci on $(B,C)$, $(C,A)$, $(A,B)$ and pass through a given point $P$.*

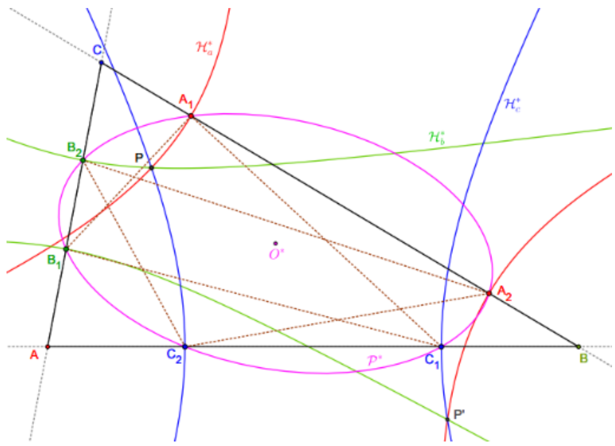


Figure 19: *Given a point P, (i) the triad of P-hyperbolas $\mathcal{H}_a^*, \mathcal{H}_b^*, \mathcal{H}_c^*$ has a second common point $P'$; (ii) their vertices $A_1, A_2, B_1, B_2, C_1, C_2$ lie on a conic $\mathcal{P}^*$ (magenta), not necessarily an ellipse; (iii) $\triangle A_1B_1C_1$ has the same area as $\triangle A_2B_2C_2$.*

Still referring to Figure 19:

**Proposition 19** *Besides $P$, the triad of P-hyperbolas meets at a second real point $P'$.*

**Proof.** Let $\mathcal{H}_a^{*+}$, $\mathcal{H}_b^{*+}$, $\mathcal{H}_c^{*+}$ denote the three branches that pass through $P$. We need to prove that the other three branches $\mathcal{H}_a^{*-}$, $\mathcal{H}_b^{*-}$, $\mathcal{H}_c^{*-}$ also meet at some point.

First, let us show that two other branches $\mathcal{H}_b^{*-}$ and $\mathcal{H}_c^{*-}$ must intersect. To prove it, we perform a polar dual with respect to a circle centered at their common focus $A$, as shown in Figure 20. The polar dual of each hyperbola will be a circle, whose diameter is delimited by the inverses of hyperbola vertices. By polarity, the intersection points of the original hyperbolas are sent to the common tangents of their reciprocal circles and vice-versa; since, by hypothesis, $\mathcal{H}_b^*$ and $\mathcal{H}_c^*$ intersect at a point $P$, these reciprocal circles admit (at least) one common tangent. Hence, they are either externally tangent or secant. Therefore, these circles admit at least two common tangents. One of these tangents is precisely the polar of $P$; the other one, passing through the same homothety center, is the polar of a point $P'$ which is the intersection of the other two branches, $\mathcal{H}_b^{*-}$ and $\mathcal{H}_c^{*-}$. Similarly, branches $\mathcal{H}_a^{*-}$ and $\mathcal{H}_c^{*-}$ also intersect. Now, as in Figure 19, if a point $P' \in \mathcal{H}_b^{*-} \bigcap \mathcal{H}_c^{*-}$, then it satisfies $P'C - P'A = B_1B_2$ and $P'A - P'B = C_1C_2$. Hence, by adding these two relations, we obtain $P'C - P'B = B_1B_2 + C_1C_2$. Nevertheless, by hypothesis $P$ is the common point of three branches: $\mathcal{H}_a^{*+}, \mathcal{H}_b^{*+}, \mathcal{H}_c^{*+}$. Then three similar relations can be written for $P: PA - PC = B_1B_2$, $PB - PA = C_1C_2$, and $PB - PC = A_1A_2$. By adding the first two, we obtain $PB - PC = B_1B_2 + C_1C_2$, hence $B_1B_2 + C_1C_2 = A_1A_2$. The later relation ensures that $P'C - P'B = A_1A_2$, hence $P' \in \mathcal{H}_a^{*-}$ finishing the proof. □

**Proposition 20** *The 6 vertices of the 3 P-hyperbolas lie on a conic $\mathcal{P}^*$.*

**Proof.** Referring to Figure 19, by definition, the center of the P-hyperbola $\mathcal{H}_a^*$ is at the midpoint of $BC$, and so on cyclically. Hence:

$$|A_1C| = |A_2B| = x, \quad |B_1A| = |B_2C| = y, \quad |BC_1| = |AC_2| = z. \tag{4}$$

We obtain the claim using Carnot's theorem. □

Recall the classic result that for any triangle, the intouch and extouch triangles have the same area (we saw this in Colloraly 2 in the context of V-hyperbolas). The analogous result for P-hyperbolas still holds:

**Proposition 21** *Let $A_1, A_2$ denote the vertices of $\mathcal{H}_a^*$, and $B_1, B_2$, $C_1, C_2$, those of $\mathcal{H}_b^*$ and $\mathcal{H}_c*$, respectively. Then $\triangle A_1B_1C_1$ and $\triangle A_2B_2C_2$ have the same area.*

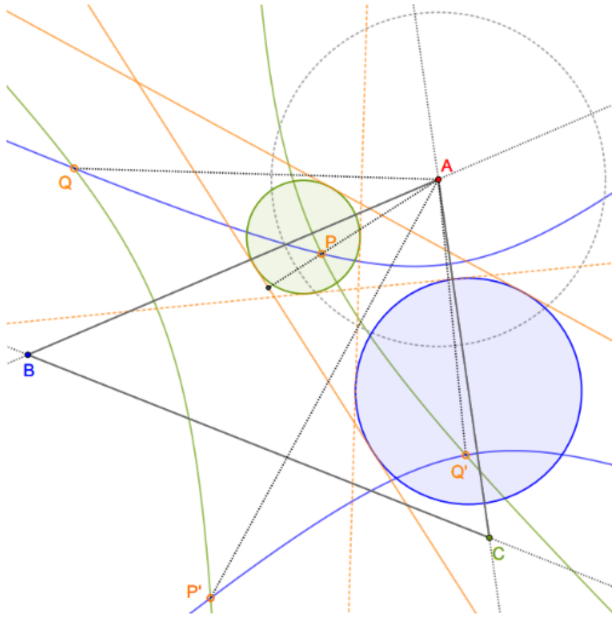


Figure 20: *Two P-hyperbolas (green, blue) sharing a focus at A are shown as well as their reciprocals (shaded green and blue circles) with respect to an inversion circle centered at A (dashed black). The branches closer (resp. further) to A always intersect; their intersection points $P$ and $P'$ are the poles of the common external tangents to their reciprocal circles. When these circles are disjoint (as in the figure), the poles of the internal common tangents are intersections between alternate branches.*

**Proof.** This is again a consequence of (4). Specifically, let $\vec{a} = \overrightarrow{BC}$, $\vec{b} = \overrightarrow{CA}$, $\vec{c} = \overrightarrow{AB}$. Let $\alpha$, $\beta$, and $\gamma$ be such that:

$$\overrightarrow{BA_1} = \alpha\vec{a}, \quad \overrightarrow{CB_1} = \beta\vec{b}, \quad \overrightarrow{AC_1} = \gamma\vec{c};$$

In order to prove that $S_{A_1B_1C_1} = S_{A_2B_2C_2}$, we simply show that they represent the same fraction of $S = S_{ABC}$. In fact, $S_{A_1B_1C_1} = S - [S_A + S_B + S_C]$, where $S_A = S_{AB_1C_1}$, $S_B = S_{BA_1C_1}$, and $S_C = S_{CA_1B_1}$. A direct computation yields:

$$S_A = S_{AB_1C_1} =$$
$$= \frac{1}{2}\|\overrightarrow{AB_1} \times \overrightarrow{AC_1}\| = \frac{1}{2}\|(1-\beta)\vec{b} \times (\gamma\vec{c})\| = \gamma(1-\beta)S.$$

Cyclically, $S_B = \alpha(1-\gamma)S$, and $S_C = \beta(1-\alpha)S$. Therefore:

$$S_{A_1B_1C_1} = S - \left[S_A + S_B + S_C\right] =$$
$$= S\left[1 - \gamma(1-\beta) - \alpha(1-\gamma) - \beta(1-\alpha)\right].$$

Similarly:

$$S_{A_2B_2C_2} = S - \left[S'_A + S'_B + S'_C\right]$$

where $S'_A = S_{AB_2C_2}$, $S'_B = S_{BA_2C_2}$, $S'_C = S_{CA_2B_2}$. Then:

$$S'_A = S_{AB_2C_2} =$$
$$= \frac{1}{2}\|\overrightarrow{AB_2} \times \overrightarrow{AC_2}\| = \frac{1}{2}\|\beta\vec{b} \times ((1-\gamma)\vec{c})\| = \beta(1-\gamma)$$

and cyclically for $S'_B$, $S'_C$. Thus, the area of $S_{A_2B_2C_2}$ can be computed as $S_{A_1B_1C_1}$, where $\alpha, \beta, \gamma$ are replaced at each occurrence by $(1-\alpha)$, $(1-\beta)$, $(1-\gamma)$. Thus:

$$S_{A_2B_2C_2} = S - \left[S'_A + S'_B + S'_C\right] =$$
$$= S\left[1 - (1-\gamma)\beta - (1-\alpha)\gamma - \alpha(1-\beta)\right].$$

Referring to Figure 21:

**Proposition 22** *Given a $\triangle ABC$ there is a unique pair of distinct points $P^*$ and $Q^*$ such that the 6-point conic $\mathcal{P}^*$ is a circle. These are a pair of common intersections of the triad of P-hyperbolas. It can be shown their barycentrics satisfy:*

$$\left[(c^2-\lambda_c^2)(-a^2+b^2+\lambda_a^2-\lambda_b^2)\right]^2 +$$
$$\left[(b^2-\lambda_b^2)(-a^2+c^2+\lambda_a^2-\lambda_c^2)\right]^2 +$$
$$\left[(a^2-\lambda_a^2)(-b^2+c^2+\lambda_b^2-\lambda_c^2)\right]^2 = 0$$

*where $\lambda_a = |PB| - |PC|$, $\lambda_b = |PC| - |PA|$, and $\lambda_c = |PA| - |PB|$.*

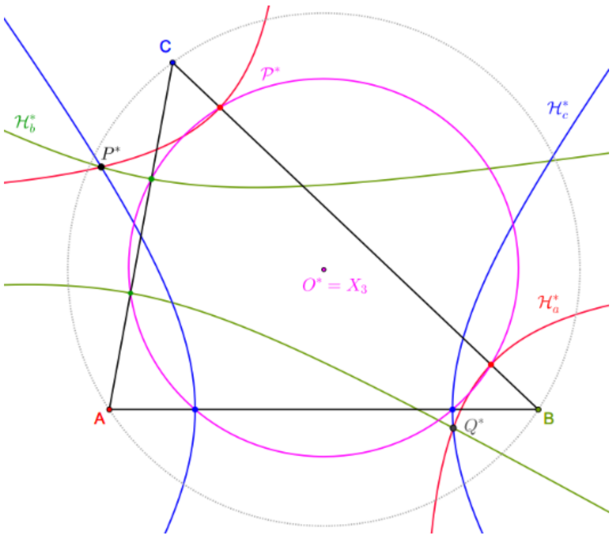


Figure 21: *Given $\triangle ABC$, there is a pair $P^*$ and $Q^*$ such that $\mathcal{P}^*$ (magenta) is a circle. Furthermore the latter is concentric with the circumcircle (dashed black) of $\triangle ABC$.*

**Definition 9 (reflection triangle)** *The reflections $A', B', C'$ of a point $Q$ on the sides of $\triangle ABC$ are the vertices of the Q-reflection triangle.*

Surprisingly, we can construct a triangle such that the vertices of the 6 P-hyperbolas lie on a circle. In [8], center $X_{55}$ is the internal center of similitude of the incircle and circumcircle.

Referring to Figure 22, experimental evidence supports the following "needle in a haystack" phenomenon:

**Conjecture 1** *Let $T'$ be the $X_{55}$-reflection triangle of a reference triangle $T$. The 6 vertices of the P-hyperbolas of $T'$ passing through $X_{55}$-of-$T$ lie on a circle, concentric with the circumcircle of $T'$ which coincides with $X_7$-of-$T$*

,

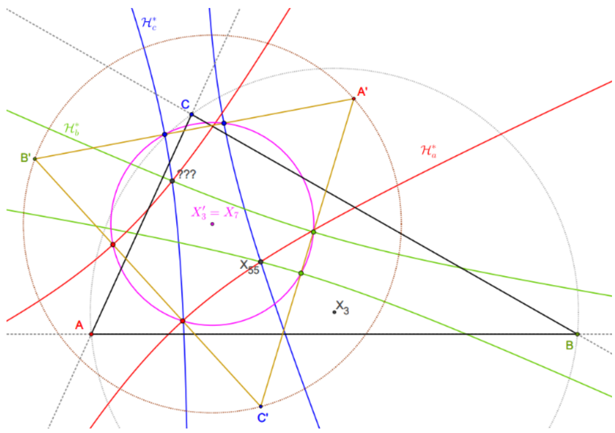


Figure 22: *The vertices of P-hyperbolas $\mathcal{H}_a^*$, $\mathcal{H}_b^*$, and $\mathcal{H}_c^*$ (red, green, blue) passing through $X_{55}$ of $\triangle ABC$, with foci on pairs of vertices of the $X_{55}$-reflection triangle $\triangle A'B'C'$ (gold), lie on a circle (magenta), concentric with the circumcircle (dotted brown) of $\triangle A'B'C'$, whose circumcenter is the Gergonne point $X_7$ of the reference. Note that said 3 hyperbolas meet at a second mystery point "???".*

Referring to Figure 23:

**Proposition 23** *The $\mathcal{H}_a^*$ P-hyperbola passes through the non-P intersection $A'$ between P-ellipses $\mathcal{E}_b^*$, and $\mathcal{E}_c^*$. The same holds for $\mathcal{H}_b^*, \mathcal{H}_c^*$, cyclically.*

**Proof.** Referring to Figure 23, let $A' \in \mathcal{E}_b^*$; then $A'A + A'C = PA + PC$. If $A'$ is also contained in $\mathcal{E}_c^*$, then $A'A + A'B = PA + PB$. Subtracting $A'B - A'C = PB - PC$, i.e., both $A'$ and $P$ lie on the same branch of $\in \mathcal{H}_a^*$. □

As before, let $a, b, c$ be the sidelengths, and $\lambda_a$, $\lambda_b$, and $\lambda_c$ as above. As shown in Figure 24, the plane of a $\triangle ABC$ can be split into zone where $\mathcal{P}^*$ is an ellipse, a hyperbola, or a parabola. In particular:

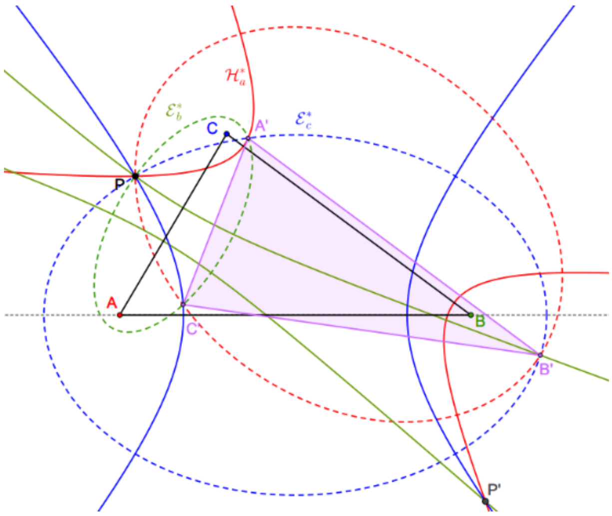


Figure 23: *The 3 P-hyperbolas (solid red, green, blue) also pass through the 3 non-P intersections $A', B', C'$ between pairs of P-ellipses, e.g., $\mathcal{H}_a^*$ passes through the intersection $A'$ of $\mathcal{E}_b^*$ and $\mathcal{E}_c^*$. The triangle with vertices on $A', B', C'$ is shown (purple).*

**Proposition 24** *The conic $\mathcal{P}^*$ through the 6 vertices of the P-hyperbolas is a parabola if:*

$$
\begin{aligned}
&(c^2\lambda_a^2\lambda_b^2)^2 + (b^2\lambda_a^2\lambda_c^2)^2 + (a^2\lambda_b^2\lambda_c^2)^2 + \\
&+\mu(\mu(-3+4(\lambda_a^2/a^2+\lambda_b^2/b^2+\lambda_c^2/c^2))+ \\
&+2\lambda_a^2\lambda_b^2\lambda_c^2(6-\lambda_a^2/a^2-\lambda_b^2/b^2-\lambda_c^2/c^2)- \\
&-6(c^2\lambda_a^2\lambda_b^2+b^2\lambda_a^2\lambda_c^2+a^2\lambda_b^2\lambda_c^2))=0
\end{aligned}
$$

*where $\mu = (abc)^2$. Furthermore, $\mathcal{P}^*$ is degenerate if $P$ lies on either (infinite extension) of the sidelines of the triangle.*

## 6 Open Questions

- Figure 4: what is the locus of the focus of the Yiu conic over $C$ along the parabola locus?
- Figure 6: prove the 6-point co-vertex conic is always a hyperbola and explain why there are two (3:3 and 5:1) distributions of co-vertices over the branches of the conic.
- Figure 8 (left): Prove $P^*$ is unique.
- Figure 8 (right): given $\triangle A'B'C'$ can one always find an inscribed $\triangle ABC$ such that the former is its $X_3$-anticevian triangle?
- Figure 11: how do the zones of 6-vertex conic type deform as one moves $C$ away from the equilateral configuration? What is the locus of the center $O^*$ of the degenrate conic over $P$ on the 3 branches of the inner deltoid? What is the locus of the focus of the conic over the 6 arcs where the conic is a parabola? Prove if a hyperbola, said conic can never be rectangular.
- Figure 12: Prove that if $P$ is on the locus, the center $O\dagger$ of the co-vertex conic is on the incircle. What does the locus of $P$ look like if $\triangle ABC$ is not an equilateral? Over $P$ on said locus, what is the locus of $O\dagger$?

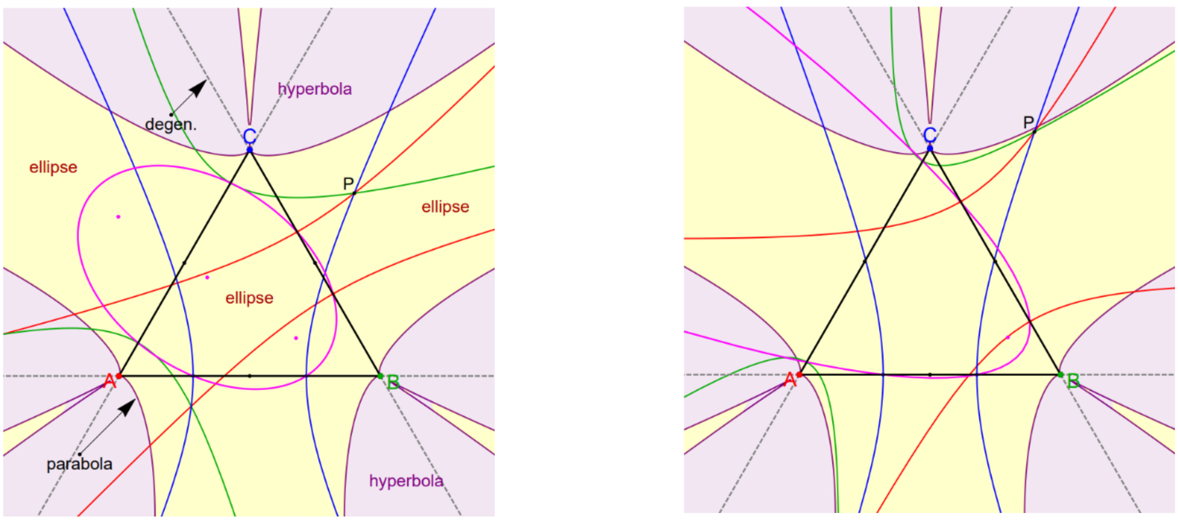


Figure 24: *The 6-point conic $P^*$ (magenta) through the vertices of P-hyperbolas (red, green, blue) is an ellipse if P lies in the yellow (resp.) purple region. It is degenerate if P is on any sideline (dashed black). In the left (resp. right) P is in the yellow region (at the interface) and therefore $P^*$ (magenta) is an ellipse (resp. parabola).*

- prove Conjecture 1. Provide an expression for the second triple intersection point of the 3 P-hyperbolas.
- Figure 18: What are interesting loci for $C$ (with $A, B$ fixed) with respect to properties and/or degeneracies of the 14-point quartic?
- Figure 19: describe the map $P \to P'$ and/or $P \to O^*$? What is the image of a lattice under it?
- Figure 22: given $\triangle A'B'C'$ can one always find a $\triangle ABC$ such that the former is its $X_{55}$-reflection triangle?

## Acknowledgements

We would like to thank Arseniy Akopyan and Boris Odehnal for useful discussions. The first author is fellow of CNPq and coordinator of Project PRONEX/ CNPq/ FAPEG 2017 10 26 7000 508.

## Long Barycentric Equations

Here we provide barycentric equations and coordinates (with respect to the reference $\triangle ABC$) of various associated objects. Let $a, b, c$ be the reference's sidelengths. Let $\mathcal{E}_a^\dagger$ denote the ellipse with foci on $B'C'$, and through $A$ of the reference. Note: the long expression below were kept verbatim so as to facilitate copy-paste.

### A-ellipse:

The barycentrics $[x, y, z]$ of $\mathcal{E}_a^\dagger$ satisfy:

```
8*b^4*c^4*(a^2+b^2-c^2)*(a^2-b^2+c^2)*(a^6*b^4-3*a^4*b^6+
3*a^2*b^8-b^10+3*a^4*b^4*c^2-6*a^2*b^6*c^2+3*b^8*c^2+a^6*c^4+
3*a^4*b^2*c^4+6*a^2*b^4*c^4-2*b^6*c^4-3*a^4*c^6-6*a^2*b^2*c^6-
2*b^4*c^6+3*a^2*c^8+3*b^2*c^8-c^10)*x^2+4*b^2*c^4*(a^2+b^2-
c^2)^2*(a^2-b^2+c^2)*(a^8*b^2-2*a^6*b^4+2*a^2*b^8-b^10-a^8*c^2-
2*a^6*b^2*c^2+10*a^4*b^4*c^2-10*a^2*b^6*c^2+3*b^8*c^2+4*a^6*c^4+
4*a^4*b^2*c^4+10*a^2*b^4*c^4-2*b^6*c^4-6*a^4*c^6-6*a^2*b^2*c^6-
2*b^4*c^6+4*a^2*c^8+3*b^2*c^8-c^10)*x*y+a^2*c^4*(a^2-b^2-c^2)*
(a^2+b^2-c^2)*(a^12-7*a^8*b^4+16*a^6*b^6-21*a^4*b^8+16*a^2*b^10-
5*b^12-6*a^10*c^2-4*a^8*b^2*c^2+12*a^6*b^4*c^2+24*a^4*b^6*c^2-
38*a^2*b^8*c^2+12*b^10*c^2+15*a^8*c^4+16*a^6*b^2*c^4+6*a^4*b^4*
c^4+32*a^2*b^6*c^4-5*b^8*c^4-20*a^6*c^6-24*a^4*b^2*c^6-20*a^2*
b^4*c^6-8*b^6*c^6+15*a^4*c^8+16*a^2*b^2*c^8+9*b^4*c^8-6*a^2*c^10-
4*b^2*c^10+c^12)*y^2-4*b^4*c^2*(a^2+b^2-c^2)*(a^2-b^2+c^2)^2*(a^8
*b^2-4*a^6*b^4+6*a^4*b^6-4*a^2*b^8+b^10-a^8*c^2+2*a^6*b^2*c^2-
4*a^4*b^4*c^2+6*a^2*b^6*c^2-3*b^8*c^2+2*a^6*c^4-10*a^4*b^2*c^4-
10*a^2*b^4*c^4+2*b^6*c^4+10*a^2*b^2*c^6+2*b^4*c^6-2*a^2*c^8-
3*b^2*c^8+c^10)*x*z-2*a^2*b^2*c^2*(a^2-b^2-c^2)*(a^2+b^2-c^2)*
(a^2-b^2+c^2)*(a^10-3*a^8*b^2+2*a^6*b^4+2*a^4*b^6-3*a^2*b^8+
b^10-3*a^8*c^2+8*a^6*b^2*c^2-14*a^4*b^4*c^2+16*a^2*b^6*c^2-7*
b^8*c^2+2*a^6*c^4-14*a^4*b^2*c^4-26*a^2*b^4*c^4+6*b^6*c^4+2*a^4*
c^6+16*a^2*b^2*c^6+6*b^4*c^6-3*a^2*c^8-7*b^2*c^8+c^10)*y*z+a^2*
b^4*(a^2-b^2-c^2)*(a^2-b^2+c^2)*(a^12-6*a^10*b^2+15*a^8*b^4-
20*a^6*b^6+15*a^4*b^8-6*a^2*b^10+b^12-4*a^8*b^2*c^2+16*a^6*b^4*
c^2-24*a^4*b^6*c^2+16*a^2*b^8*c^2-4*b^10*c^2-7*a^8*c^4+12*a^6*
b^2*c^4+6*a^4*b^4*c^4-20*a^2*b^6*c^4+9*b^8*c^4+16*a^6*c^6+24*a^4*
b^2*c^6+32*a^2*b^4*c^6-8*b^6*c^6-21*a^4*c^8-38*a^2*b^2*c^8-5*b^4*
c^8+16*a^2*c^10+12*b^2*c^10-5*c^12)*z^2 = 0
```

### Major vertices:

Let $S$ be twice the area of the reference and:

```
rt = sqrt(a^6-3*a^2*b^4+2*b^6+6*a^2*b^2*c^2-2*b^4*c^2-
3*a^2*c^4-2*b^2*c^4+2*c^6))
```

The two major vertices of $\mathcal{E}_a^\dagger$ are given by:

```
[(a*(a^2-b^2-c^2)*((b^2-c^2)*(a^4*b^2-2*a^2*b^4+b^6+a^4*c^2
+4*a^2*b^2*c^2-b^4*c^2-2*a^2*c^4-b^2*c^4+c^6)+/-2*a^3*S*rt))/
(a*(a^4*b^2-2*a^2*b^4+b^6+a^4*c^2+4*a^2*b^2*c^2-b^4*c^2-
2*a^2*c^4-b^2*c^4+c^6)+/-2*(b^2-c^2)*S*rt),b^2*(-a^2+b^2-c^2),
-(c^2*(-a^2-b^2+c^2))]
```

### P-ellipse 6-point circle

The center $X_3'$ of the 6-point circle of Proposition 10 lies on the Van Aubel line ($X_4X_6$) of the reference. It can be regarded as the circumcenter of the $X_3$-anticevian and is given by barycentrics $[f(a,b,c), f(b,c,a), f(c,a,b)]$ where $f(a,b,c)$ is given by:

```
(a^14-5*a^12*b^2+9*a^10*b^4-5*a^8*b^6-5*a^6*b^8+9*a^4*b^10-
5*a^2*b^12+b^14-5*a^12*c^2+10*a^10*b^2*c^2-13*a^8*b^4*c^2+
28*a^6*b^6*c^2-31*a^4*b^8*c^2+10*a^2*b^10*c^2+b^12*c^2+
9*a^10*c^4-13*a^8*b^2*c^4-30*a^6*b^4*c^4+22*a^4*b^6*c^4+
21*a^2*b^8*c^4-9*b^10*c^4-5*a^8*c^6+28*a^6*b^2*c^6+
22*a^4*b^4*c^6-52*a^2*b^6*c^6+7*b^8*c^6-5*a^6*c^8-
31*a^4*b^2*c^8+21*a^2*b^4*c^8+7*b^6*c^8+9*a^4*c^10+
10*a^2*b^2*c^10-9*b^4*c^10-5*a^2*c^12+b^2*c^12+c^14)*a^2
```

### P-hyperbolas

Let $La = |PB| - |PC|$, $Lb = |PC| - |PA|$, and $Lc = |PA| - |PB|$. Points on the $\mathcal{H}_a^*$ P-hyperbola satisfy:

```
(2*(b^2-c^2-La^2)*p*q+(a^2-La^2)*q^2-2*(b^2-c^2+La^2)*p*r-
2*(a^2+La^2)*q*r+(a^2-La^2)*r^2)*x^2-2*(b^2-c^2-La^2)*p^2*x*y-
(a^2-La^2)*p^2*y^2+2*(b^2-c^2+La^2)*p^2*x*z+2*(a^2+La^2)*p^2*y*z-
(a^2-La^2)*p^2*z^2 = 0
```

The conic $\mathcal{P}^*$ throught the vertices of the 3 P-hyperbolas is given by:

```
x^2+y^2+z^2-(2*(a^2+La^2)*y*z)/(a^2-La^2)-(2*(b^2+Lb^2)*z*x)/
(b^2-Lb^2)-(2*(c^2+Lc^2)*x*y)/(c^2-Lc^2)=0
```

The first barycentric coordinate for its center $X_{5452}$ is given by:

```
(a^2*((-2*La^2)/(a^2-La^2)+(b^2+Lb^2)/(b^2-Lb^2)+(c^2+Lc^2)/
(c^2-Lc^2)))/(a^2-La^2)
```

With the other two computed cyclically.

## References

[1] BOGDANOV, I., Two theorems on the focus-sharing ellipses: a three dimensional view, *J. Classical Geom.* **1** (2012), 1–5.

[2] BRADLEY, C., Conics in the Ex-circle Configuration (article 79), 2005, `https://bit.ly/3aQiu4G`

[3] ČERIN, Z., Loci Related to Variable Flanks, *Forum Geom.* **2** (2002), 105–113.

[4] DERGIADES, N., Conics Tangent at the Vertices to Two Sides of a Triangle, *Forum Geom.* **10** (2010), 41–53.

[5] DOSA, T., Some Triangle Centers Associated with the Excircles, *Forum Geom.* **7** (2007), 151–158.

[6] GARCIA, R., REZNIK, D., KOILLER, J., Loci of 3-periodics in an elliptic billiard: why so many ellipses?, *J. Symb. Computation* **114**(4) (2023), 336–358, `https://doi.org/10.1016/j.jsc.2022.06.001`

[7] HAJJA, M., YFF, P., The isoperimetric Point and the point of equal detour in a triangle, *J. of Geom.* **87**(7) (2007), 76–82, `https://doi.org/10.1007/s00022-007-1906-y`

[8] KIMBERLING, C., *Encyclopedia of triangle centers*, 2020, `http://bit.ly/3mOOver`

[9] KLAOUDATOS, N., The parabolas of Artzt in the solution of a geometric problem of minimum length, *Intl. J. of Math. Educ. in Sci. and Tech.* **42**(2) (2011), 239–245, `https://doi.org/10.1080/0020739X.2010.519794`

[10] VAN LAMOEN, F., Friendship Among Triangle Centers, *Forum Geom.* **1** (2001), 1–6.

[11] MOSES, P., REZNIK, D., A Web of Confocal Parabolas in a Grid of Hexagons, *Beitr. Algebra Geom.* (2022), `https://doi.org/10.1007/s13366-022-00651-1`

[12] ODEHNAL, B., A Triad of Circles Externally Tangent to the Nine-Point Circle and Internally Tangent to Two Sides of a Triangle, *J. Geom. and Graph.*, **18**(1) (2014), 61–71.

[13] SHARP, J., Artzt parabolas of a triangle, *Math. Gaz.* **99**(546) (2015), 444–463, `https://doi.org/10.1017/mag.2015.81`

[14] SODDY, F., The Kiss Precise, *Nature* **183**(1021) (1936), `https://doi.org/10.1038/1371021a0`

[15] THÉBAULT, V., Parabolas Associated with a Triangle, *Amer. Math. Monthly* 64(1) (1957), 10–16, `https://doi.org/10.2307/2309078`

[16] WEISSTEIN, E. W., *CRC concise encyclopedia of mathematics (2nd edition)*, Boca Raton, FL: Chapman and Hall/CRC, 2002, `https://doi.org/10.1201/9781420035223`

[17] YIU, P., *Introduction to the Geometry of the Triangle*, Florida Atlantic University lecture notes, 2001, `https://bit.ly/3okGXSJ`

[18] YIU, P., The Clawson point and excircles, Department of Mathematics, Florida Atlantic University, 1999.

**Ronaldo Garcia**
orcid.org/0000-0001-8876-6956
e-mail: ragarcia@ufg.br

Universidade Federal de Goiás
Instituto de Matemática e Estatística
BR-74001970 Goiânia, GO, Brazil

**Liliana G. Gheorghe**
orcid.org/0000-0003-3922-0177
e-mail: liliana@dmat.ufpe.br

Federal Univ. of Pernambuco, Brazil

**Peter Moses**
e-mail: moparmatic@gmail.com

Moparmatic Inc., Worcestershire, England

**Dan Reznik**
orcid.org/0000-0002-0542-6014
e-mail: dreznik@gmail.com

Data Science Consulting, Rio De Janeiro, Brazil

https://doi.org/10.31896/k.26.3
Original scientific paper
Accepted 15. 11. 2022.

Boris Odehnal

# Pencils of Frégier Conics

**Pencils of Frégier Conics**

**ABSTRACT**

For each point $P$ on a conic $c$, the involution of right angles at $P$ induces an elliptic involution on $c$ whose center $F$ is called the Frégier point of $P$. Replacing the right angles at $P$ between assigned pairs of lines with an arbitrary angle $\phi$ yields a projective mapping of lines in the pencil about $P$, and thus, on $c$. The lines joining corresponding points on $c$ do no longer pass through a single point and envelop a conic $f$ which can be seen as the generalization of the Frégier point and shall be called a generalized Frégier conic. By varying the angle, we obtain a pencil of generalized Frégier conics which is a pencil of the third kind. We shall study the thus defined conics and discover, among other objects, general Poncelet triangle families.

**Key words:** conic, angle, projective mapping, Frégier point, Frégier conic, Poncelet porism, envelope

**MSC2020:** 51M04, 51N15, 14H50

**Pramenovi Frégierovih konika**

**SAŽETAK**

Za svaku točku $P$ na konici $c$, involucija pravih kutova u točki $P$ inducira eliptičnu involuciju na konici $c$ čije se središte $F$ zove Frégierova točka od $P$. Zamjena pravih kutova u točki $P$ između označenih krakova s proizvoljnim kutom $\phi$ vodi ka projektivnom preslikavanju u pramenu točke $P$, a tako i na konici $c$. Pravci koji povezuju odgovarajuće točke na konici $c$ više ne prolaze kroz jednu točku nego omataju koniku $f$ koja se vidi kao generalizacija Frégierove točke i zvat će se generalizirana Frégierova konika. Mijenjajući kut, dobivamo pramen generaliziranih Frégierovih konika koji je pramen treće vrste. Proučavat ćemo tako definirane konike i otkriti među ostalim i generalizirane familije Ponceletovih trokuta.

**Ključne riječi:** konika, kut, projektivno preslikavanje, Frégierova točka, Frégierova konika, Ponceletov porizam, omotaljka

## 1 Introduction

### 1.1 Known results, contributions of the present paper

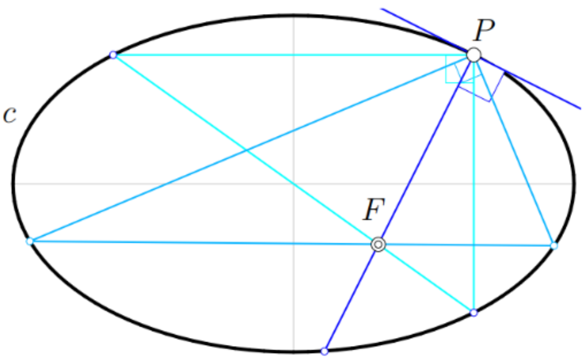


Figure 1: *The Frégier point $F$ is the center of the involution on $c$ that is induced by the involution of right angles at $P$.*

FRÉGIER's theorem in its original form says that *the chords of a conic $c$ which are seen from a point $P \in c$ under a right angle pass through one point $F$* (cf. [1, 6, 7] and see Fig. 1). The point $F$ is usually called the *Frégier point* of $P$.

If $P$ moves along $c$, then $F$ traces a conic $f$ (see Fig. 2) homothetic to $c$ with similarity factor $(a^2-b^2)/(a^2+b^2)$ (in the case of a non-circular ellipse, i.e., $a \neq b$) or $(a^2+b^2)/(a^2-b^2)$ (in the case of a non-equilateral hyperbola, i.e., $a \neq b$), where $a$ and $b$ are the semi-major and semi-minor axes lengths. For a parabola $c$, the conic $f$ is even congruent to $c$. The conic $f$ is sometimes called *Frégier conic* (see [7, 14]). However, the Frégier conic $f$ and $c$ are always of the same affine type.

According to [8, 13], a conic-shaped *generalized offset* to a conic $c$ with center (ellipse or hyperbola) can only be found by applying a multiple of the cube root of the curvature radius $\rho$ at $P$ on $c$'s normal at $P$ in order to find the corresponding point $P'$ of the generalized offset. In [13] it is shown that the distance function

$$k\sqrt[3]{\rho(t)}$$

is unique up to a constant $k \in \mathbb{R}$. The case of a parabola differs slightly, i.e., the distance function is no longer unique. Surprising enough, until now it is obviously not recognized what is illustrated in Fig. 2:

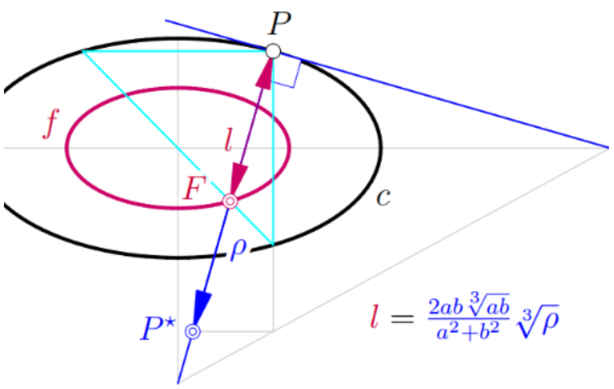


Figure 2: *The Frégier conic $f$ is a generalized offset of the conic $c$.*

**Theorem 1** *Frégier conics are conic-shaped generalized offsets (in the sense of* [8] *and* [13]*).*

**Proof.** We first recall that the Frégier point of a point $P \in c$ lies on $c$'s normal at $P$. Let $\rho$ denote the radius of curvature of $c$ at $P$ and let $l$ denote the distance between $P$ and its Frégier point, then it is elementary to verify that $\rho$ and $l$ are bound to

$$8a^4b^4\rho = (a^2 \pm b^2)^3 l^3,$$

where the plus stands for the ellipse and the minus for the hyperbola. Hence, the offset distance equals a multiple of the cube root of the curvature radius $\rho$ in both cases. For the parabola $x^2 = 2qy$ ($q \neq 0$) we find

$$8q^2\rho = l^3. \qquad \square$$

FRÉGIER's theorem can be considered a result of Euclidean geometry, for it involves right angles, or a result of projective geometry, since the Frégier point $F$ of a point $P$ on a conic $c$ is the center of the involution of right angles in the pencil about $P$ projected onto $c$, see [7].

Variants of FRÉGIER's theorem in higher dimensions do exist (see, e.g., [9, 17]). Further, connections to linear 2-parameter and 3-parameter families of conics are studied in [11]. FRÉGIER's theorem is also studied in relation to quadratic mappings recently in [17] and even earlier in [15].

In [16], the authors define a *Frégier involution* using right angles in Euclidean and non-Euclidean sense which gives rise to a possible generalization of FRÉGIER's theorem also in higher dimensions, but completely different from the approach made in [9]. Conics in non-Euclidean planes with singular Frégier conics are studied in [14]. Many relations of the Frégier point and FRÉGIER's theorem in Euclidean geometry to various construction tasks in connections with conics were disclosed, see [2, 3, 5, 12], to name just a few.

In this article, we replace the right angle which is usually the main ingredient of FRÉGIER's theorem by a different Euclidean angle $\phi \neq 0, \frac{\pi}{2}$ and study the chords cut out of $c$ by the legs of the rotating rigid angle (with vertex $P$ on $c$). Since the mapping that assigns to each line $g$ the rotated copy $g'$ with the fixed angle $\phi = \sphericalangle\, g, g'$ is a projectivity, we first show that the chords of $c$ that join pairs $(Q, Q')$ of assigned points envelope a conic. This does not depend on the affine type of $c$. These envelopes are then called *generalized Frégier conics*.

Although, we have this rather general result, the equations of the generalized Frégier conics of the three different affine types of base conics $c$ have to be elaborated separately. We will find that the generalized Frégier conics of a point $P \in c$ belong to a pencil of conics (of the third kind) which also contains the initial conic $c$ and the Frégier point $F$ as a limiting case. Further, the algebraic proofs of the results yield computational artifacts that allow for a geometric interpretation and give rise to general Poncelet porisms as described in [4].

The remainder of this section is dedicated to the technical details we use in the computational proofs and in the derivation of the equations of the generalized Frégier conics. Section 2 provides some general results and it is shown that the generalized Frégier conics form a pencil of the third kind. The proofs in Section 2 use synthetic reasoning. In Section 3, we shall derive the equations of the generalized Frégier conics. This enables us to show some more results on the variety of generalized Frégier conics. Along the way, we will discover some Poncelet families of triangles. Although we have to treat the different affine types of conics separately, we will lay down the computations in detail only for the case of the ellipse. This is done in order to make the presentation of results clear. In all other cases, we just point out what the differences are.

### 1.2 General setup and technical preliminaries

In order to describe points, we use inhomogeneous Cartesian coordinates $(x, y)$ in the Euclidean plane as well homogeneous coordinates $x_0 : x_1 : x_2$. These are linked by $x = x_1 x_0^{-1}$ and $y = x_2 x_0^{-1}$, provided that $x_0 \neq 0$, i.e., the point $x_0 : x_1 : x_2$ is not a point at infinity, and thus, it allows for a representation as $(x, y)$. The points at infinity (ideal points) lie on the line with the homogeneous equation $x_0 = 0$. Sometimes, we make use of the complex extension of the Euclidean plane. This leads to the finding that all Euclidean circles pass through the *absolute points* $I$ and $J = \overline{I}$ of Euclidean geometry with homogeneous coordinates

$$I = 0:1:\mathrm{i} \ \text{ and } \ J = 0:1:-\mathrm{i}.$$

Conversely, any conic through $I$ and $J$ is a Euclidean circle. The tangents from any circle's center $M$ to the circle are so-called *isotropic lines*, i.e., the joins $[M,I]$ and $[M,J]$ with the absolute points. Any two concentric circles touch each other at $I$ and $J$, and thus, they span a pencil of conics of the third kind.

We describe the three affine types of conics by their equations

$$\mathcal{E},\mathcal{H}: \frac{x^2}{a^2} \pm \frac{y^2}{b^2} = 1, \ \mathcal{P}: x^2 - 2qy = 0, \tag{1}$$

with respect to the standard frame assuming $a \neq b$, $a,b \in \mathbb{R}^+$, and $q \in \mathbb{R}\setminus\{0\}$. The computational proofs make use of their rational parametrizations

$$\begin{aligned} \mathbf{e}(t) &= \left(a\tfrac{1-t^2}{1+t^2}, b\tfrac{2t}{1+t^2}\right), \quad t \in \mathbb{R}, \\ \mathbf{h}(t) &= \left(a\tfrac{1+t^2}{1-t^2}, b\tfrac{2t}{1-t^2}\right), \quad t \in \mathbb{R}\setminus\{-1,1\}, \\ \mathbf{p}(t) &= \left(2qt, 2qt^2\right), \qquad t \in \mathbb{R}. \end{aligned} \tag{2}$$

At this point, we shall recall that for any conic there exists a huge variety of equivalent rational parametrizations. For example, the reparametrization $t \to \frac{a_{00}+a_{01}t}{a_{10}+a_{11}t}$ turns (2) in to an equivalent parametrizations and describe a projective mapping acting on the conic (provided that $a_{00}a_{11} - a_{10}a_{01} \neq 0$). In the computations, we should see that some geometric objects will then be described in a different way.

Later, we also need (Euclidean) rotation matrices. With the substitution

$$\cos\xi = \frac{1-x^2}{1+x^2} \ \text{ and } \ \sin\xi = \frac{2x}{1+x^2} \tag{3}$$

the rotation matrices $\mathbf{R}(\phi)$ can be given with rational entries as

$$\mathbf{R}(\phi) = \begin{pmatrix} \cos\phi & -\sin\phi \\ \sin\phi & \cos\phi \end{pmatrix} = \begin{pmatrix} \frac{1-f^2}{1+f^2} & \frac{-2f}{1+f^2} \\ \frac{2f}{1+f^2} & \frac{1-f^2}{1+f^2} \end{pmatrix}. \tag{4}$$

In the following, we assume that $\phi \neq 0, \pm\frac{\pi}{2}$ since we are interested in generalized Frégier conics different from the Frégier point. Further, $f \neq 0, \pm 1, \pm\mathrm{i}$ since these values correspond to $\phi \neq 0, \pm\frac{\pi}{2}$ and $\pm\mathrm{i}$ are the poles of the rational equivalents of sine and cosine, i.e., the poles of the arctangent. We will not repeatedly and explicitly write these assumptions any further.

## 2 Projective mappings on a conic

In this section, we shall have a closer look at projective mappings acting on conics. This will lead to a general and unifying result. In [7], we can find some results on projective mappings on conics and how to treat projective mappings on conics (especially involutive ones).

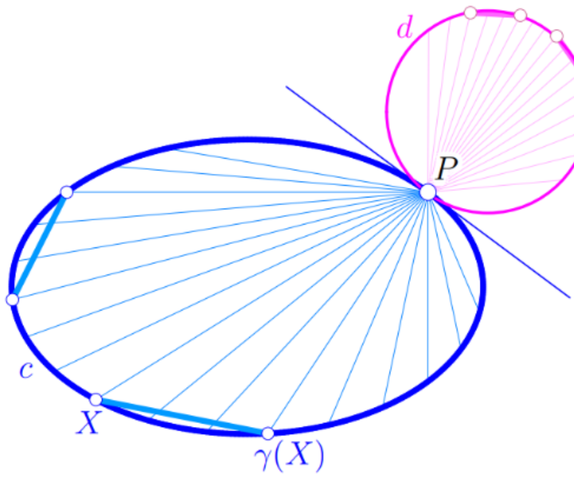


Figure 3: *The perspectivity $c \to d$ can be extended to a collineation $c \to d$.*

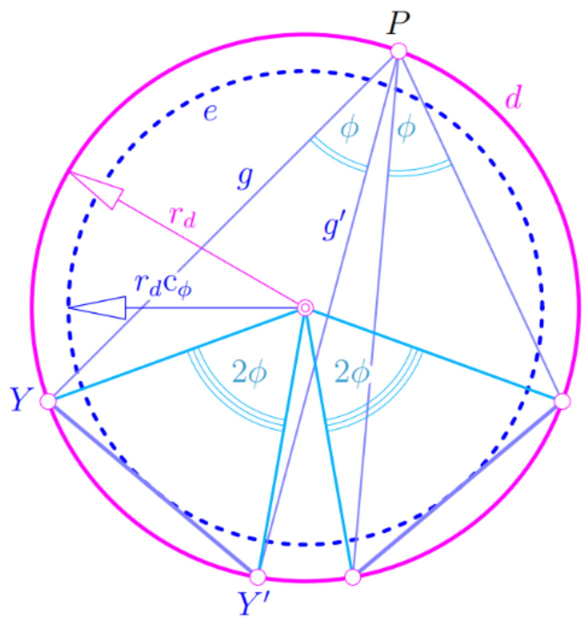


Figure 4: *The Frégier conic $e$ of $P \in d$ of the circle $d$ to the angle $\phi$ is a concentric circle.*

However, we need the following (apparently new) result:

**Theorem 2** *Let $c$ be a conic in a projective plane and $P$ be some point on $c$. Further, assume that $\gamma: c \to c$ is the non-involutive projective mapping acting on $c$ induced by the Euclidean rotation through a fixed angle $\phi \neq 0, \frac{\pi}{2}, \pi$ about $P$. Then, the chords $s = [X, \gamma(X)]$ of $c$ that join a each point $X \in c$ with its $\gamma$-image $\gamma(X) \in c$ envelope a conic $f$.*

**Proof.** We use a result from [7, p. 247]: The projective mapping on a line or in a pencil of lines can be transferred via a perspectivity onto a conic $c$, and *vice versa*. For that purpose the center $P$ of the perspectivity has to lie on the conic $c$ in order to guarantee for a one-to-one correspondence (between line/pencil and conic). Thus, a projective mapping on a conic $c$ can be transferred to any other conic $d$, for example, onto a circle $d$ (of radius $r_d$) that touches $c$ at $P$ (as illustrated in Fig. 3).
Now, the rotation about $P$ sends each line $g$ through $P$ to a line $g'$ through $P$ with $\sphericalangle\, g, g' = \phi$. Consequently, the projective mapping on $c$ is transferred to the projective mapping on $d$. From $P \in c, d$, each segment spanned by a point $Y$ and its image point $Y'$ is seen under the constant angle $\phi$, and thus, it is seen from the center of $d$ under the angle $2\phi$ (see Fig. 4). Therefore, the chords joining corresponding points envelop a circle $e$ concentric with $d$ and of radius $r_d \cos\phi$.
The perspectivity from $c \to d$ can be extended to a perspective collineation $\kappa$ with center $P$ that sends the envelope $e$ to a conic $f$, i.e., the generalized Frégier conic that touches $c'$ chords of assigned points. □

We have excluded the case of involutive projectivities, because then the envelope of the chords is the center of the involution on the conic (cf. [7, p. 251]).

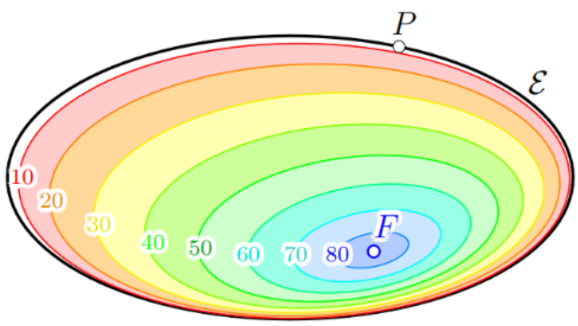


Figure 5: *Some generalized Frégier conics of $P \in \mathcal{E}$ ($\phi = 10°, \ldots, 80°$): For $\phi \to \frac{\pi}{2}$ the conics shrink to the Frégier point $F$ of $P$.*

With small modifications, Thm. 2 is valid for any projective mapping acting on $c$. The projective mapping $c$ mentioned in Thm. 2 is elliptic. However, the above result is true for elliptic, parabolic, and hyperbolic projectivities. There is something more important that we can deduce from Thm. 2:

**Theorem 3** *The generalized Frégier conics (for variable $\phi$) of a point $P$ on a conic $c$ form a pencil of conics of the third kind.*

**Proof.** We recall that the Frégier conics $e$ of the circle $d$ which is a collinear image of the initial conic $c$ form a pencil of concentric circles. This pencil consist of all conics that pass through the absolute points of Euclidean geometry sharing the isotropic tangents through the common center, and therefore, they form a pencil of conics of the third kind. The (perspective) collineation $\kappa$ (defined in the proof of Thm. 2) that sends $d$ back to $c$ maps all circles concentric with $d$ to the conics of a pencil of the third kind. □

It is clear that the initial conic $c$ is also a member of the pencil of generalized Frégier conics. Further, the Frégier point $F$ considered as the real intersection of a pair of complex conjugate lines is also a (singular) member of the pencil.
Fig. 5 shows some generalized Frégier conics of a point $P$ on an ellipse $\mathcal{E}$. The smaller the angle $\phi$, the shorter the chords of assigned points are, and therefore, the generalized Frégier conics come closer to the ellipse $\mathcal{E}$. If $\phi \to \frac{\pi}{2}$, then the conics shrink to the Frégier point $F$ of $P$.

## 3 Equations of Frégier conics

In this section, we compute the equations of the generalized Frégier conics. Unfortunately, we have to treat the three different affine types of conics separately. However, the generalized Frégier conics of all types of conics have some properties in common and we can simplify the description by leaving some things aside. The computational approach yields some results that could not be shown in a purely synthetic way.

### 3.1 Frégier conics of ellipses

Let an ellipse $\mathcal{E}$ be given by the equation (1). It means no restriction to assume that $a > b$ holds. The generic point $P$ on the ellipse $\mathcal{E}$ can be described by means of a real parameter $T$ as $P = \mathbf{e}(T)$ in (2).
The lines $g$ in the pencil shall be determined by choosing a second point $Q \in \mathcal{E}$ is given as $\mathbf{e}(U)$ with $U \neq T$ in (2). Hence, we obtain the equation of the chord $g := [P, Q]$ of $\mathcal{E}$ as

$$g : b(1-TU)\mathbf{x}+a(T+U)\mathbf{y}=b(1+TU). \tag{5}$$

If we rotate the normal vector

$$\mathbf{n} = (b(TU-1), -a(T+U))$$

through the angle $\phi \in (0, \frac{\pi}{2})$ either clockwise or counter clockwise, we obtain the normal vectors of those lines $g^+, g^-$ enclosing the angles $\pm\phi$ with $g$. The rotation is described by the multiplication of $\mathbf{n}$ with either of the matrices $\mathbf{R}(\phi)$ or $\mathbf{R}(-\phi)$ from (4).
Now, the lines $g^+$ and $g^-$ have the equations

$$\begin{aligned}g^+: &(1+T^2)\big((b(1-f^2)UT+2fa(T+U)+b(f^2-1))x+\\ &+(2TUbf+a(f^2-1)(T+U)-2fb)y\big)+\\ &+ab(1-f^2)(1+T^2)(1+TU)+\\ &+2a^2f(T+U)(T^2-1)-4b^2f(1+TU)T=0,\end{aligned}$$

and

$$\begin{aligned}g^-: &(1+T^2)\big((b(1-f^2)UT-2fa(T+U)+\\ &+bf^2-b)x+(-2TUbf+a(f^2-1)(T+U)+\\ &+2fb)y\big)+ab(1-f^2)(1+T^2)(1+TU)-\\ &-2a^2f(T+U)(1+T^2)+4b^2f(TU-1)T=0.\end{aligned}$$

The chords' endpoints $Q^+ = g^+ \cap \mathcal{E}$ and $Q^- = g^- \cap \mathcal{E}$ are

$$\begin{aligned}Q^+ =\, &b^2(a^2(f^2-1)^2+4b^2f^2)(1+T^2U^2)+\\ &+4abf(f^2-1)(a^2-b^2)(T+U)(1-TU)+\\ &+a^2(b^2(f^2-1)^2+4a^2f^2)(T^2+U^2)+\\ &+8f^2(a^2-b^2)(a^2+b^2)TU:\\ &:\big(ab(1-U)(1+T^2)(1-f^2)-(2b^2(1+T^2)+\\ &+2a^2(T^2+U)+2(a^2-b^2)T(1+U))f\big)\cdot\\ &\cdot\big(ab(1+T^2)(1+U)(f^2-1)-(2b^2(1-T^2)+\\ &+2a^2(T^2-U)-2(a^2-b^2)T(1-U))f\big):\\ &:\big(abU(1+T^2)(f^2-1)-(2a^2T^2+\\ &+2(a^2-b^2)UT+2b^2)f\big)\cdot\big(ab(1+T^2)\cdot\\ &\cdot(f^2-1)+(2b^2T^2U+2(a^2-b^2)T+2a^2U)f\big)\end{aligned}$$

and $Q^-$ admits a similar representation.
Now, we can state and prove:

**Theorem 4** *The lines $s^+ := [Q, Q^+]$ and $s^- := [Q, Q^-]$ envelop the same ellipse $\mathcal{F}_\mathcal{E}$.*
*The centers of all these ellipses trace an ellipse $\mathcal{M}$ homothetic to $\mathcal{E}$.*

**Proof.** The parametrizations of $Q^+$ and $Q^-$ enable us to derive the equations of the lines $s^+ = [Q, Q^+]$ and $s^- = [Q, Q^-]$. The computation of the envelopes is now straight forward: We eliminate $U$ from the equations of $s^-$ and $s^+$ and we can immediately see that both families of lines envelop the same curve with the equation

$$\begin{aligned}\mathcal{F}_\mathcal{E}: &b^2({s_\phi}^2{c_\tau}^2\varepsilon^2-4a^2b^2)\mathbf{x}^2+\\ &+a^2((a^2+b^2)^2-{s_\tau}^2{s_\phi}^2\varepsilon^2)\mathbf{y}^2+\\ &-2abf^2 s_\tau c_\tau(1+c_\phi)^2\varepsilon^2\mathbf{xy}+\\ &-2ab(a^4-b^4){s_\phi}^2(bc_\tau\mathbf{x}-as_\tau\mathbf{y})+\\ &-a^2b^2(c_\phi(a^2+b^2)^2-\varepsilon^2))=0,\end{aligned} \tag{6}$$

where we changed back to the trigonometric representation. For the sake of simplicity, we have set

$$\begin{aligned}s_\phi &:= \sin\phi,\ c_\phi := \cos\phi,\\ s_\tau &:= \sin\tau,\ c_\tau := \cos\tau,\end{aligned}$$

and $\varepsilon^2 := a^2 - b^2$ is the square of the linear excentricity of the ellipse $\mathcal{E}$. In order to show that the curves $\mathcal{F}_\mathcal{E}$ are ellipses, we find their centers as

$$\mathbf{m}(T) = \frac{f^2(a^4-b^4)}{(a^2f^2+b^2)(b^2f^2+a^2)}\mathbf{e}(-T)$$

(with $\mathbf{e}$ from (2)) which parametrizes the ellipse $\mathcal{M}$ mentioned above. Obviously, $\mathcal{M}$ is homothetic to $\mathcal{E}$ and its semi-axes lengths are

$$\begin{aligned}\text{major} &= \frac{af^2(a^4-b^4)}{(a^2f^2+b^2)(b^2f^2+a^2)},\\ \text{minor} &= \frac{bf^2(a^4-b^4)}{(a^2f^2+b^2)(b^2f^2+a^2)},\end{aligned}$$

provided $b < a$. Their ratio equals $a : b$ and they never vanish as long as $a \neq b$. □

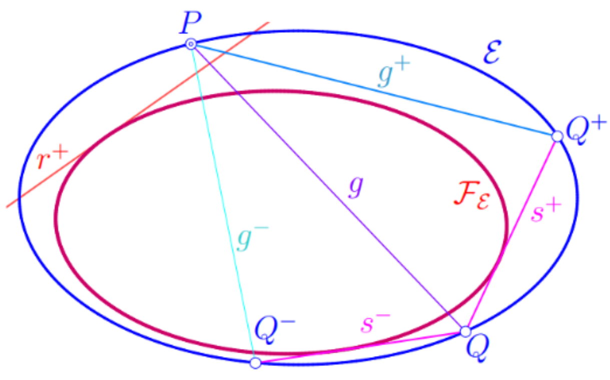


Figure 6: *Both chords $s^+$, $s^-$ envelop the same conic $\mathcal{F}_\mathcal{E}$.*

The fact that the generalized Frégier conics of an ellipse are always ellipses can also be deduced from the construction used in the proof of Thm. 2: For real rotation angles $\phi$, the envelopes of the chords are in the interior of the auxiliary circle $d$. The collineation $d \to c$ with center $P$ maps these interior circles to conics in the interior of the ellipse $c$ (or $\mathcal{E}$, respectively). Hence, the generalized Frégier conics of an ellipse can only be ellipses.

Only if we allow the rotation angle $\phi$ to be a pure imaginary number, the radii of the envelopes of $d$'s chords can become arbitrarily large:

$$r_d \cos(\mathrm{i}\phi) = r_d \cosh\phi \geq r_d,$$

and thus, there exist outer generalized Frégier conics of any affine type but not corresponding to real angles.
The Frégier ellipses (6) constitute a pencil of conics of the third kind (cf. Thm. 3). All conics in this pencil touch each other in a pair of complex conjugate points

$$B_1 = \left( a\frac{(a^2+b^2)(1-T^2)+4ab\mathrm{i}T}{(1+T^2)(a^2-b^2)}, 2b\frac{ab\mathrm{i}(1-T^2)-(a^2+b^2)T}{(1+T^2)(a^2-b^2))} \right),$$

and $B_2 = \overline{B_1}$. These points are the collinear images of the absolute points of Euclidean geometry common to all circles concentric with the auxiliary circle $d$ used in the proof of Thms. 2 and 3. Since, the points $B_1$ and $B_2$ are each others complex conjugates they span a real line

$$p:\ \varepsilon^2(b(1-T^2)x - 2aTy) = ab(a^2+b^2)(1+T^2) \qquad (7)$$

which is the polar line of the Frégier point

$$F = \frac{a^2-b^2}{a^2+b^2}\left(\frac{a(1-T^2)}{1+T^2}, \frac{-2bT}{1+T^2}\right). \qquad (8)$$

with pivot point $P \in c$. The line $p$ given by (7) is sometimes called the *Frégier* line of $P$ with respect to $c$ (cf. [15]). The Frégier line (with multiplicity two) is a singular conic in the pencil of generalized Frégier conics.
The following can also be shown:

**Theorem 5** *For variable point $P \in \mathcal{E}$, the Frégier ellipses $\mathcal{F}_{\mathcal{E}}$ envelop two ellipses $\mathcal{E}_i$, $\mathcal{E}_e$ which are homothetic to $\mathcal{E}$.*

**Proof.** The elimination of the parameter $T$ from the equation (6) of $\mathcal{F}_{\mathcal{E}}$ and its derivative with respect to $T$ yields

$$\mathcal{E}_o:\ \frac{x^2}{a^2} + \frac{y^2}{b^2} = \frac{(b^2f^2-a^2)^2}{(b^2f^2+a^2)^2},$$
$$\mathcal{E}_i:\ \frac{x^2}{a^2} + \frac{y^2}{b^2} = \frac{(a^2f^2-b^2)^2}{(a^2f^2+b^2)^2}.$$

Obviously, $\mathcal{E}_o$ and $\mathcal{E}_i$ are concentric with $\mathcal{E}$, there axes are parallel to those of $\mathcal{E}$, and since the semi-axes lengths of the latter ellipses are

$$a_i = a\frac{a^2-b^2f^2}{b^2f^2+a^2},\quad b_i = b\frac{a^2-b^2f^2}{b^2f^2+a^2}$$
and
$$a_o = a\frac{a^2f^2-b^2}{a^2f^2+b^2},\quad b_o = b\frac{a^2f^2-b^2}{a^2f^2+b^2}.$$

The ratio of both pairs of semi-axes lengths equals $a/b$. □

The outer and inner envelope $\mathcal{E}_o$ and $\mathcal{E}_i$ coincide if $f = \pm 1$ and become the ordinary Frégier conic being the trace (8) of the Frégier points of $\mathcal{E}$.
Fig. 7 shows the two ellipses $\mathcal{E}_o$ and $\mathcal{E}_i$ comprising the envelope of the Frégier ellipses of $\mathcal{E}$.

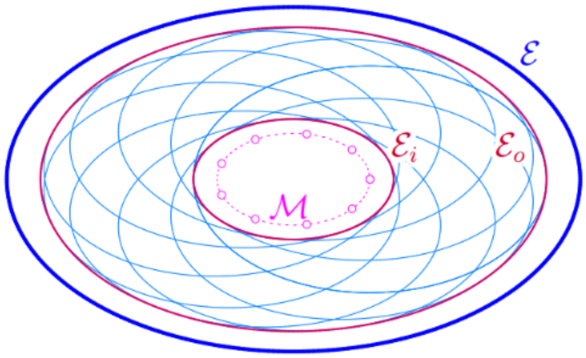


Figure 7: *The envelope of the generalized Frégier conics of the ellipse $\mathcal{E}$ consists of an outer ellipse $\mathcal{E}_o$ and an inner ellipse $\mathcal{E}_i$.*

The sketch of the computational proof of Thm. 4 hides a detail: The resultant of the equation of $s^+$ and its derivative with respect to $U$ turns out to be the product of a polynomial of degree one (equation of a line $r^+$) and a polynomial of degree two (equation of $\mathcal{F}_{\mathcal{E}}$). This is also the case with $s^-$ (yielding the equation of a line $r^- \neq r^+$ and the equation of $\mathcal{F}_{\mathcal{E}}$). However, the two resultants share the quadratic factor describing $\mathcal{F}_{\mathcal{E}}$ and differ in the linear parts. The lines $r^+$ and $r^-$ belong to the pencil about $(-a, 0)$ (the left principal vertex of $\mathcal{E}$ which corresponds to the parameter value $T = \infty$) and their equations are

$$r^+, r^-:\ b(\varepsilon^2 \mathrm{s}_\tau \sin\phi \pm 2ab\mathrm{c}_\phi)\mathbf{x} + a\sin\phi(\varepsilon^2\mathrm{c}_\tau + a^2 + b^2)\mathbf{y} +$$
$$+ ab(\varepsilon^2\mathrm{s}_\tau \sin\phi \pm 2ab\mathrm{c}_\phi) = 0.$$

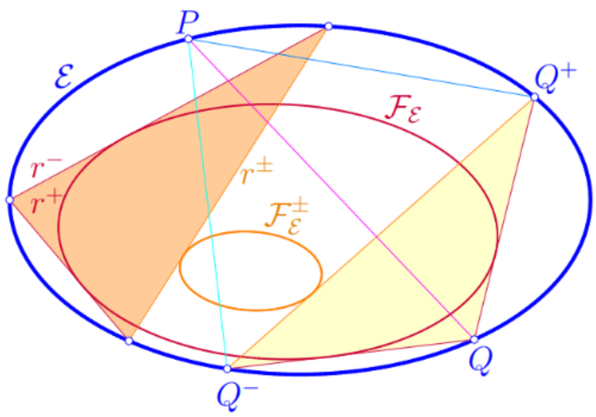


Figure 8: *The triangle built by $r^+$, $r^-$, $r^\pm$ already indicates the existence of a poristic family of triangles interscribed between $\mathcal{E}$ and the Frégier ellipses $\mathcal{F}_{\mathcal{E}}$ and $\mathcal{F}_{\mathcal{E}}^\pm$.*

From the computational point of view, the lines $r^+$ and $r^-$ do not have any further meaning. It is quite the opposite from the geometric point of view as we shall see soon.
The vertex of the pencil depends on the parametrization (2) and can be replaced with any other point on $\mathcal{E}$ (simply by substituting any linear rational function for $T$).
It is by no means surprising that the lines $s^{\pm} := [Q^-, Q^+]$ also envelop a conic $\mathcal{F}^{\pm}_{\mathcal{E}}$ since $\sphericalangle\, g^-g = \sphericalangle\, gg^+ = \frac{1}{2}\sphericalangle\, g^-g^+$. Further, a computational proof of the latter fact (comparable to that of Thm. 4) would also produce the equation of a line $r^{\pm}$ which is tangent to the Frégier ellipse $\mathcal{F}^{\pm}_{\mathcal{E}}$.
At this point, we emphasize that the respective coefficient matrices of the conics satisfy

$$\mathcal{F}^{\pm}_{\mathcal{E}} = \mathcal{F}_{\mathcal{E}}\mathcal{E}^{-1}\mathcal{F}_{\mathcal{E}},$$

which identifies $\mathcal{F}^{\pm}_{\mathcal{E}}$ as the *conjugate conic of* $\mathcal{E}$ with respect to $\mathcal{F}_{\mathcal{E}}$ in the sense of [10]. Also in that sense, the conics $\mathcal{E}$ and $\mathcal{F}_{\mathcal{E}}$ span an *exponential pencil* of conics which also contains $\mathcal{F}^{\pm}_{\mathcal{E}}$. Because of the nestedness of $\mathcal{E}$, $\mathcal{F}_{\mathcal{E}}$, and $\mathcal{F}^{\pm}_{\mathcal{E}}$, the exponential pencil has a point shaped limit which equals the Frégier point $F$ given by (8). This holds in the like manner for the generalized Frégier conics of hyperbolae and parabolae.
There exists a triple $(r^+, r^-, r^{\pm})$ of lines which are the sides of a triangle interscribed between $\mathcal{E}$, $\mathcal{F}_{\mathcal{E}}$, and $\mathcal{F}^{\pm}_{\mathcal{E}}$ independent of the choice of $P \in \mathcal{E}$. This gives rise to the following:

**Theorem 6** *The triangles bounded by the lines $r^+$, $r^-$, $r^{\pm}$ form a one-parameter family of triangles interscribed between the conic $\mathcal{E}$ and the Frégier ellipses $\mathcal{F}_{\mathcal{E}}$ and $\mathcal{F}^{\pm}_{\mathcal{E}}$. The triangles form a Poncelet family.*

**Proof.** We only have to show that the conics $\mathcal{E}$, $\mathcal{F}_{\mathcal{E}}$, and $\mathcal{F}^{\pm}_{\mathcal{E}}$ belong to a linear pencil (cf. [7, p. 259]) in order to meet the requirements of a general Poncelet porism (cf. [4]).
This can either be done by referring to Thm. 3 according to which the two Frégier conics to angles $\phi$ and $2\phi$ belong to a pencil of conics (of the third kind) or by means of computation:
For that purpose, we homogenize the equations of $\mathcal{E}$, $\mathcal{F}_{\mathcal{E}}$, and $\mathcal{F}^{\pm}_{\mathcal{E}}$, extract the coefficient matrices, and find that they are linearly dependent since

$$\begin{aligned}&\big(4(1-f^2)^2\,\mathcal{F}_{\mathcal{E}}-\mathcal{F}^{\pm}_{\mathcal{E}}\big)(1+f^2)^{-1} =\\ &= a^4b^4(3f^2-1)(f^2-3)^2(1+T^2)^2\,\mathcal{E},\end{aligned} \tag{9}$$

provided that $f \neq \pm 1$. In the cases $f = \pm\sqrt{3}, \pm 1/\sqrt{3}$, i.e., $\phi \neq \pm\frac{\pi}{6}$, the Frégier ellipses $\mathcal{F}_{\mathcal{E}}$ and $\mathcal{F}^{\pm}_{\mathcal{E}}$ coincide. □

We have shown that $\mathcal{F}_{\mathcal{E}}$, $\mathcal{F}^{\pm}_{\mathcal{E}}$, $\mathcal{E}$ belong to one pencil of conics. This is a pencil of the third kind that contains the two singular conics. The first of which is a line with multiplicity two:

$$\varepsilon^2\big(b(T^2-1)\mathbf{x}+2aT\mathbf{y}\big) = ab(a^2+b^2)(1+T^2).$$

The second one is a pair of complex conjugate lines concurring in the (real) Frégier point (8) with directions

$$\frac{x}{y} = \pm\frac{\mathrm{ib}}{2\mathrm{a}}\,\frac{(a^2+b^2)(1-T^2)+4ab\mathrm{i}T}{ab(T^2-1)-\mathrm{i}(a^2+b^2)T}.$$

This pair of complex conjugate lines is the image of the isotropic lines through the center of $d$ under the perspective collineation $d \to c$ used in the proof of Thm. 2.

### 3.2 Frégier conics of hyperbolae

In analogy to the previous section, we assume that a hyperbola $\mathcal{H}$ is given by the middle equation of (1) with real semi-axes $a, b$. The vertex of the rotating angle(s) is now $P = \mathbf{h}(T)$ with $\mathbf{h}$ from (2) where $T \in \mathbb{R}\setminus\{-1,1\}$.
Again, the point $Q$ is obtained by assuming $Q = \mathbf{h}(U)$ with $T \neq U$ and the chords $g := [P,Q]$ of $\mathcal{H}$ have an equation similar to that of $\mathcal{E}$ in (5). Now, the chords' normal vectors are proportional to

$$\mathbf{n} = \big(b(1+TU), -a(T+U)\big).$$

The normal vectors of the legs $g^+$ and $g^-$ of the moving angles attached to $g$ are found by applying the linear mappings induced by the matrices $\mathbf{R}(\phi)$ and $\mathbf{R}(-\phi)$ from (4).
This allows us to write down the equations of $g^+$ and $g^-$, compute the points $Q^+$, $Q^-$, and furthermore, to determine the envelopes of the lines $s^+ := [Q, Q^+]$, $s^- := [Q, Q^-]$, and $s^{\pm} := [Q^-, Q^+]$, and we find $\mathcal{F}^+_{\mathcal{H}} = \mathcal{F}^-_{\mathcal{H}} = \mathcal{F}_{\mathcal{H}}$ with the equation

$$\begin{aligned}\mathcal{F}_{\mathcal{H}} :\big(&(a^2-b^2f^2)(a^2f^2-b^2)(1+T^4)+\\ &+2(a^2b^2(1+f^2)^2+\varepsilon^2f^2)T^2\big)\mathbf{x}^2+\\ &+\big(a^2b^2(1+f^2)^2(1+T^4)+\\ &+2(2\varepsilon^2f^2-a^2b^2(1+f^2)^2)T^2\big)\mathbf{y}^2+\\ &+4a^2b\varepsilon^2f^2T(1+T^2)\mathbf{x}\mathbf{y}+\\ &-2ab^2(a^2-b^2)\varepsilon f^2(1-T^4)\mathbf{x}+\\ &-4a^2b(a^2-b^2)\varepsilon f^2T(1-T^2)\mathbf{y}+\\ &+a^2b^2(a^2f^2+b^2)\cdot(b^2f^2+a^2)(1-T^2)^2=0,\end{aligned} \tag{10}$$

where $\varepsilon^2 = a^2+b^2$ is the square of the linear excentricity of the hyperbola $\mathcal{H}$.
Analogously to Thm. 4, we can formulate

**Theorem 7** *The lines $s^+$ and $s^-$ envelop the same conic $\mathcal{F}_{\mathcal{H}}$, the generalized Frégier conic of the hyperbola $\mathcal{H}$. The generalized Frégier conics $\mathcal{F}_{\mathcal{H}}$ of a hyperbola $\mathcal{H}$ can be conics of any affine type.*

**Proof.** Since the determinant of the quadratic term of (10) equals

$$D_{12} := 4a^4b^4(1+f^2)^2(a^2-b^2f^2)^3\cdot(a^2f^2-b^2)^3(1-T^2)^4$$

and vanishes exactly if $f=\pm\frac{a}{b},\pm\frac{b}{a}$, the generalized Frégier conics in these particular four cases coincide and the equation of $\mathcal{F}_{\mathcal{H}}$ simplifies to

$$\begin{aligned}&(a^2+b^2)^2(2bT\mathbf{x}+a(1+T^2)\mathbf{y})^2+\\&-2ab(1-T^2)(b(a^4-b^4)(1+T^2)\mathbf{x}+\\&+2aT(a^4-b^4)\mathbf{y}-ab(a^4+b^4)(1-T^2))=0.\end{aligned}$$

The latter equation describes a parabola with ideal point

$$0:-a(1+T^2):2bT$$

(for all four values of $f$). For proper choices of $f$, $D_{12}$ can be positive as well as negative, and therefore, the generalized Frégier conics $\mathcal{F}_{\mathcal{H}}$ of $\mathcal{H}$ can also be ellipses and hyperbolae. Using the collineation applied in the proof of Thm. 2, we can also argue that all affine types of conics can show up here as generalized Frégier conics.
The Frégier conics of hyperbolae are regular since the determinant of the homogeneous equation equals

$$D_{012} := -8a^{10}b^{10}(1-f^2)^2(1+f^2)^4(1-T^2)^6$$

which vanishes only if $f=\pm1$ (right angle, Frégier point) or if $T=\pm1$ (which can be avoided by reparametrizing $\mathcal{H}$). □

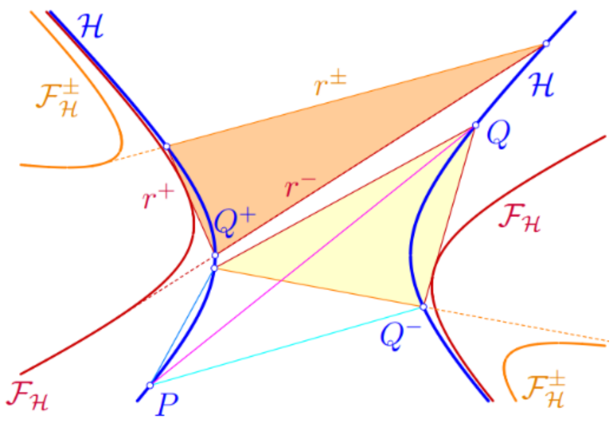


Figure 9: *Two triangles from the Poncelet family interscribed between $\mathcal{H}$, $\mathcal{F}_{\mathcal{H}}$, and $\mathcal{F}^{\pm}_{\mathcal{H}}$.*

The one-parameter family of generalized Frégier conics of a hyperbola shows a behaviour similar to that of an ellipse. Comparable to Thm. 5, we can show:

**Theorem 8** *For variable point $P\in\mathcal{H}$, the generalized Frégier conics $\mathcal{F}_{\mathcal{H}}$ envelop two hyperbolae $\mathcal{H}_i$, $\mathcal{H}_o$ which are homothetic to $\mathcal{H}$.*

**Proof.** We eliminate the parameter $T$ from the equation (10) of the generalized Frégier conics $\mathcal{F}_{\mathcal{H}}$ and of the derivatives of (10) with respect to $T$. This elimination yields besides the equations $ay\mp bx=0$ of $\mathcal{H}$'s asymptotes, the hyperbola $\mathcal{H}$, and a further hyperbola $\mathcal{H}'$ that does not contribute to the envelope.
The two components of the envelope are two hyperbolae

$$\begin{aligned}\mathcal{H}_i:\ \frac{x^2}{a^2}-\frac{y^2}{b^2}&=\frac{(b^2f^2+a^2)^2}{(b^2f^2-a^2)^2},\\ \mathcal{H}_o:\ \frac{x^2}{a^2}-\frac{y^2}{b^2}&=\frac{(a^2f^2+b^2)^2}{(a^2f^2-b^2)^2}.\end{aligned}$$

It is obvious that $\mathcal{H}_i$ and $\mathcal{H}_o$ are homothetic to $\mathcal{H}$. Their semi-axes are

$$a_o=a\frac{b^2f^2+a^2}{a^2-b^2f^2},\quad b_o=b\frac{b^2f^2+a^2}{a^2-b^2f^2}$$
and
$$a_i=a\frac{a^2f^2+b^2}{a^2f^2-b^2},\quad b_i=b\frac{a^2f^2+b^2}{a^2f^2-b^2}$$

(provided that $f\neq\pm\frac{a}{b},\pm\frac{b}{a}$) and the axes ratio equals $a/b$. □

It is a rather simple task to show that the centers of the generalized Frégier conics move on a hyperbola $\mathcal{M}$ homothetic to $\mathcal{H}$ with semi-axes

$$\begin{aligned}\text{principal}&=\frac{af^2(a^4+b^4)}{(a^2-b^2f^2)(a^2f^2-b^2)},\\ \text{auxiliary}&=\frac{bf^2(a^4+b^4)}{(a^2-b^2f^2)(a^2f^2-b^2)},\end{aligned}$$

provided that $f\neq\pm\frac{a}{b},\pm\frac{b}{a}$.
In the previous section, we have seen that the computation of the generalized Frégier conics as the envelopes of chords of a conic produced straight lines as some by-product. These lines depend on the parametrization of the initial conic, but nevertheless, they allow us to conclude that there exist general Poncelet families of triangles interscribed between $\mathcal{H}$ and the generalized Frégier conics $\mathcal{F}_{\mathcal{H}}$ and $\mathcal{F}^{\pm}_{\mathcal{H}}$.
Therefore, and without repeating the similar computations, and in analogy to Thm. 6, we can state:

**Theorem 9** *The hyperbola $\mathcal{H}$ and the pair of generalized Frégier conics $\mathcal{F}_{\mathcal{H}}$ and $\mathcal{F}^{\pm}_{\mathcal{H}}$ admit an interscribed one-parameter family of triangles,* i.e., *a one-parameter family of billiards with two caustics.*

According to Thm. 3 and because of

$$\begin{aligned}&\mathcal{F}^{\pm}_{\mathcal{H}}-4(1-f^2)^3\mathcal{F}_{\mathcal{H}}=\\&\quad=(3f^2-1)(f^2-3)(1+f^2)^2(1-T^2)^2a^4b^4\mathcal{H}\end{aligned}$$

the conics $\mathcal{H}$, $\mathcal{F}_{\mathcal{H}}$, and $\mathcal{F}^{\pm}_{\mathcal{H}}$ belong to a pencil of conics.

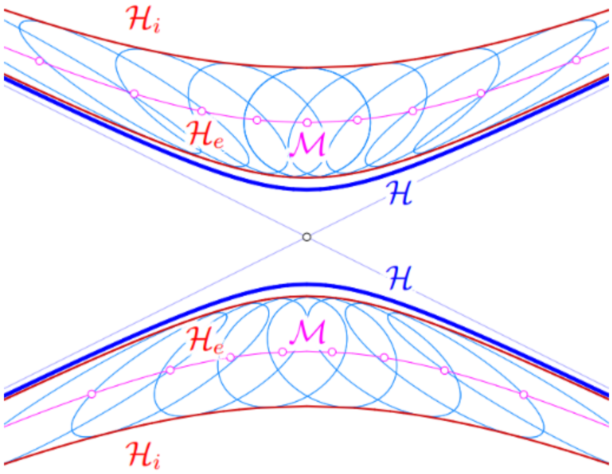


Figure 10: *Frégier conics of a hyperbola can be ellipses. In any case, the Frégier conics of a hyperbola $\mathcal{H}$ envelop two hyperbolae $\mathcal{H}_i$ and $\mathcal{H}_e$ (homothetic to $\mathcal{H}$) and with their centers on a further homothetic hyperbola $\mathcal{M}$.*

### 3.3 Frégier conics of parabolae

Finally, we assume that the parabola $\mathcal{P}$ is given by the third equation in (1). Now, we let $P = \mathbf{p}(T)$ and $Q = \mathbf{p}(U)$ with $T, U \in \mathbb{R}$ and $T \neq U$ be two points on $\mathcal{P}$ spanning the line $g = [P, Q]$ rotating about $P$ through $\phi$. With (4) applied to the normal vector

$$\mathbf{n} = (T+U, -1),$$

we find the line $g^+$ with the equation

$$\begin{aligned} g^+ : &((T+U)(f^2-1)+2f)\mathbf{x} + (2(T+U)f - f^2+1)\mathbf{y} = \\ &= 2pT(U(f^2-1)+2fT(T+U)+2f) \end{aligned} \tag{11}$$

and the line $g^-$ admits a similar representation. The lines $g^+$ and $g^-$ intersect $\mathcal{P}$ in the points $Q^+, Q^- \neq P$ where

$$Q^+ = 2p\left(\frac{U(f^2-1)-2f(T+U)T-2f}{2f(T+U)+f^2-1}, \frac{(2f(T+U)T+U(1-f^2)+2f)^2}{(2f(T+U)+f^2-1)^2}\right). \tag{12}$$

The point $Q^-$ admits a similar coordinate representation. This yields the equations of the chords $s^- := [Q, Q^-]$, $s^+ := [Q, Q^-]$, and $s^\pm := [Q^-, Q^+]$, where

$$\begin{aligned} s^+ : &2(f(T^2-U^2)+U(1-f^2)+f)\mathbf{x} + \\ &+ (2f(T+U)+f^2-1)\mathbf{y} = \\ &= 2pU(2f(T+U)T+U(1-f^2)+2f), \end{aligned} \tag{13}$$

and the equations of the other chords $s^-$ and $s^\pm$ can be given in a similar form.
We compute their envelopes and find again that the Frégier conics $\mathcal{F}_{\mathcal{P}}^- = \mathcal{F}_{\mathcal{P}}^+ =: \mathcal{F}_{\mathcal{P}}$ are identic. An equation of the parabola's generalized Frégier conics can be given as

$$\begin{aligned} \mathcal{F}_{\mathcal{P}} : &(4T^2f^2+(1+f^2)^2)\mathbf{x}^2 + 4f^2T\mathbf{xy} + f^2\mathbf{y}^2 + \\ &+ 8qf^2T(1+T^2)\mathbf{x} - 2q(f^4-2T^2f^2+1)\mathbf{y} + \\ &+ 4q^2f^2(1+T^2)^2 = 0. \end{aligned} \tag{14}$$

Now, we can state (comparable to Thm. 4 and Thm. 7):

**Theorem 10** *The chords $s^+$ and $s^-$ cut out of a parabola $\mathcal{P}$ by congruent angles centered at a point $P \in \mathcal{P}$ envelope the same conic $\mathcal{F}_{\mathcal{P}}$ with the equation* (14).
*The generalized Frégier conics $\mathcal{F}_{\mathcal{P}}$ of a parabola $\mathcal{P}$ are ellipses if $\phi \in \mathbb{R}$.*

**Proof.** The chords' envelope is already given in (14). Since the determinant of the homogeneous equation of $\mathcal{F}_{\mathcal{P}}$ equals

$$D_{012} = -8q^2(1-f^2)^2(1+f^2)^4,$$

it never vanishes (for, by assumption $q \neq 0$, $f \neq 0, \pm 1, \pm \mathrm{i}$). Hence, the generalized Frégier conics of the parabola are always regular. The determinant of the quadratic term in the inhomogeneous equation (14) of $\mathcal{F}_{\mathcal{P}}$ equals

$$D_{12} = 4f^2(1+f^2)^2$$

and is always positive (provided $f \neq 0, \pm\mathrm{i}$, which is excluded from the very beginning). Hence, (14) describes ellipses independent of the choice of $f$ and $T$ (since $p \neq 0$, $f \neq \pm 1, \pm \mathrm{i}$). In order to verify the second part of the theorem, just discuss the quadratic part of (14). □

The centers of the ellipses (14) showing up as generalized Frégier conics are located on a parabola with the parametrization

$$(-2qT, f^{-2}q(2T^2f^2+f^4+1))$$

and the equation

$$\mathcal{P}_c : \; \mathbf{x}^2 - 2q\mathbf{y} = -2f^{-2}q^2(1+f^4).$$

Obviously, this parabola is congruent to $\mathcal{P}$. This parabola is also shown in Fig. 11.
Like in the case with the ellipse $\mathcal{E}$, the elimination process delivers two lines $r^+$ and $r^-$, which are parallel and tangent to $\mathcal{F}$ and have the equations

$$r^+, r^- : \; 2fpT \mp p(1-f^2) + f\mathbf{x} = 0. \tag{15}$$

The parallelity of $r^+$ and $r^-$ depends on the parametrization (2) of $\mathcal{P}$ since $t = \infty$ in the third equation of (2) yields the point $0 : 0 : 1 = r^+ \cap r^-$. A suitable linear rational reparametrization of the parabola (2) can move the point $r^+ \cap r^-$ to any other point on $\mathcal{P}$.

The double angle Frégier conic $\mathcal{F}_{\mathcal{P}}^{\pm}$ has the equation

$$\begin{aligned}\mathcal{F}_{\mathcal{P}}^{\pm}:\ &(16f^2(1-f^2)^2T^2+(1+f^2)^4)\mathbf{x}^2+\\&+16f^2(1-f^2)^2T\mathbf{xy}+4f^2(1-f^2)^2\mathbf{y}^2+\\&+32pf^2(1-f^2)^2T(1+T^2)\mathbf{x}+\\&+(16pf^2(1-f^2)^2T^2-\\&-2p(f^8-4f^6]+22f^4-4f^2+1))\mathbf{y}+\\&+16p^2f^2(1-f^2)^2(1+T^2)^2=0.\end{aligned}\tag{16}$$

which is regular as long as $f\neq\pm1\pm\sqrt{2}$ and consists of the given parabola $\mathcal{P}$ and the line

$$2pT^2+2T\mathbf{x}+\mathbf{y}=0$$

if $f=\pm1$. The additional line that comes along with the equation (16) of $\mathcal{F}_{\mathcal{P}}^{\pm}$ has the equation

$$r^{\pm}:2f^2(2T\mathbf{x}+\mathbf{y})=p((1-f^2)^2-4f^2T^2).\tag{17}$$

The three conics $\mathcal{P}$, $\mathcal{F}_{\mathcal{P}}$, and $\mathcal{F}_{\mathcal{P}}^{\pm}$ belong to the same pencil since the respective equations (1), (14), and (16) satisfy

$$(3f^2-1)(3-f^2)(1+f^2)^2\mathcal{P}=4(1-f^2)^2\mathcal{F}_{\mathcal{P}}+\mathcal{F}_{\mathcal{P}}^{\pm}.\tag{18}$$

The comparison of (9) and (18) shows that the latter does neither contain the parameter $q$ nor the curve parameter $T$, while (9) depends on the semi-axes of $\mathcal{E}$ and on the point $P$.

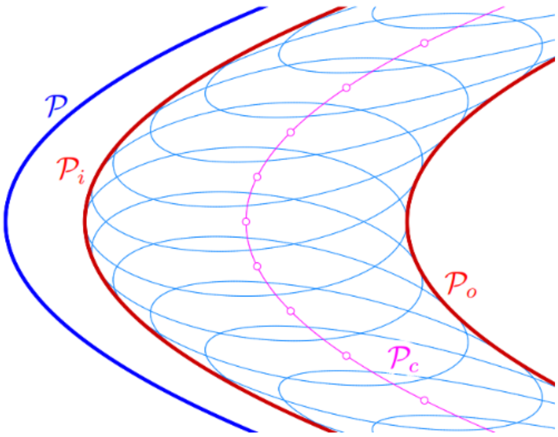


Figure 11: *The generalized Frégier conics of a parabola $\mathcal{P}$ envelop two parabolae $\mathcal{P}_i$ and $\mathcal{P}_o$ which are congruent to $\mathcal{P}$.*

Comparable to Thms. 5 and 8, we can show what is illustrated in Fig. 11:

**Theorem 11** *For variable point $P\in\mathcal{P}$, the generalized Frégier conics $\mathcal{F}_{\mathcal{P}}$ of a parabola* (1) *envelop a pair of congruent parabolas with the equations*

$$\begin{aligned}\mathcal{P}_o:\ &\mathbf{x}^2+4f^{-2}q^2=2q\mathbf{y},\\\mathcal{P}_i:\ &\mathbf{x}^2+4f^2q^2\ \ =2q\mathbf{y}\end{aligned}$$

*which are also congruent to $\mathcal{P}$.*

**Proof.** The computation of these two envelopes is straight forward. Since their quadratic part is a multiple of $x^2-2qy$ (as is the case with $\mathcal{P}$), they are congruent to each other and $\mathcal{P}$ as well. □

Because of the existence of one interscribed triangle bounded by the lines (15) and (17) between the conics $\mathcal{P}$, $\mathcal{F}_{\mathcal{P}}$, and $\mathcal{F}_{\mathcal{P}}^{\pm}$ (which belong to a pencil according to Thm. 3 and because of (18)), we have (cf. Thm. 6 and Thm. 9):

**Theorem 12** *The conics $\mathcal{P}$, $\mathcal{F}_{\mathcal{P}}$, and $\mathcal{F}_{\mathcal{P}}^{\pm}$ allow for a one-parameter family of interscribed triangles.*

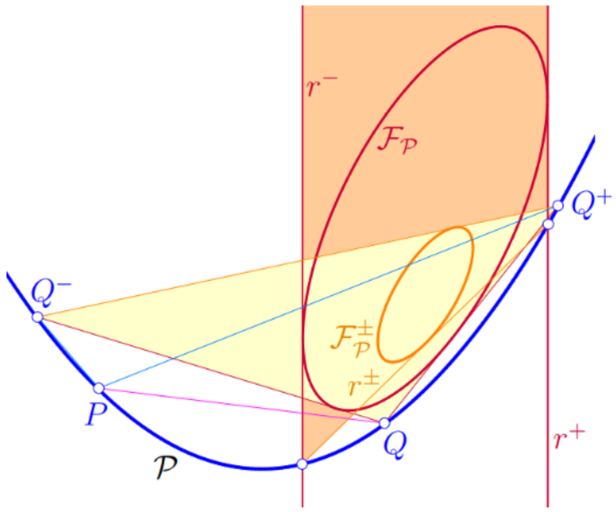


Figure 12: *Frégier conics $\mathcal{F}_{\mathcal{P}}$, $\mathcal{F}_{\mathcal{P}}^{\pm}$ related to a parabola $\mathcal{P}$.*

Fig. 12 illustrates that among the triangles in the Poncelet family described in Thm. 12 there are degenerate triangles with one vertex at infinity. It is more than one degenerate triangle since each vertex of the triangle can reach one of the positions of $r^+\cap\mathcal{P}$ or $r^-\cap\mathcal{P}$.

## 4 Concluding remarks

The generalized Frégier conics can be seen as a blow-up of the ordinary Frégier point just by replacing the right angle between assigned pairs of lines in the projective mapping at some point $P$ on a conic $c$. This blow-up "enlarges" or blows up the ordinary Frégier conic (the trace of the Frégier point if its pivot $P\in c$ is moving along $c$) to the two envelopes $\mathcal{E}_o$, $\mathcal{E}_i$ ($\mathcal{H}_o$, $\mathcal{H}_o$ or $\mathcal{P}_o$, $\mathcal{P}_i$). Of course, there are other ways to generalize or adapt Frégier's theorem. We shall postpone this to a future article.

The Poncelet families (one-parameter families of triangles interscribed in between some conics from a pencil) were found just occasionally since the lines bounding these triangles are by-products in the computation. The initial parametrizations (2) lead to just one *initial* triangle in the family. Any other (projectively equivalent) parametrization of the conics would have resulted in another triangle. However, one is enough since it was possible to show that the involved triple of conics $(\mathcal{E}, \mathcal{F}_{\mathcal{E}}, \mathcal{F}^{\pm}_{\mathcal{E}})$ (and also those related to the hyperbola and the parabola) belong to the same pencil.

## References


[1] AKOPYAN, A.V., ZASLAVSKY, A.A., *Geometry of Conics*, Mathematical World - Volume 26, AMS, 2007, `https://doi.org/10.1090/mawrld/026`

[2] BOUVAIST, R., Sur la détermination du centre de courbure en un point d'une conique, *Nouv. Ann.* **16**(4) (1916), 345–351.

[3] CIKOT, C.A., Over eene eigenschap van de ellips en haar analogon in de ellipsoïde, *Wisk. Tijdschr.* **3** (1907), 189–191.

[4] DEL CENTINA, A., Poncelet's Porism: a long story of renewed discoveries, I, *Arch. Hist. Exact Sci.* **70** (2016), 1–122, `https://doi.org/10.1007/s00407-015-0163-y`

[5] DEGEL, O., MAHRENHOLZ, J., GAEDECKE, W., Lösung zu 481 (Bd. XXIII, 80), *Arch. der Math. u. Phys.* **23**(3) (1915), 365–366.

[6] FRÉGIER, M., Thèorémes nouveaux sur les lignes et surfaces du second ordre, *Annales de Mathèmatiques pures et appliquèes*, tome 6 (1815-1816), 229–241.

[7] GLAESER, G, STACHEL, H., ODEHNAL, B., *The Universe of Conics.* From the ancient Greeks to 21st century developments. Springer-Spektrum, Springer-Verlag, Heidelberg, 2016, `https://doi.org/10.1007/978-3-662-45450-3`

[8] GRANERO RODRÍGUEZ, F., JIMENÉZ HERNÁNDEZ, F., DORIA IRIARTE, J.J., Constructing a family of conics by curvature-depending offsetting from a given conic, *Comput. Aided Geom. Design* **16** (1999), 793–815, `https://doi.org/10.1016/S0167-8396(99)00020-5`

[9] GREEN, H.G., PRIOR, L.E., Généralisation du point de Frégier pour des systèmes en involution sur des courbes de base unicursales, *Journal Ecole polytechn* **31**(2) (1933), 147–153.

[10] HALBEISEN, L., HUNGERBÜHLER, N., The exponential pencil of conics, *Beitr. Algebra Geom.* **59** (2018), 549–571, `https://doi.org/10.1007/s13366-017-0375-1`

[11] KRISHNASWAMI AYYANGAR, A.A., Theory of the general Frégier point, *Math. Gaz.* **20**(239) (1936), 191–198, `https://doi.org/10.2307/3608070`

[12] MAGRON, P., Sur le point de Frégier dans l'hyperbole, *Nouv. Ann.* **13**(4) (1913), 145–149.

[13] SCHRÖCKER, H.-P., A Family of Conics an Three Special Ruled Surfaces, *Beitr. Algebra Geom.* **42**(2) (2001), 531–545.

[14] SCHRÖCKER, H.-P., Singular Fégier Conics in Non-Euclidean Geometry, *J. Geom. Graph.* **21**(2) (2017), 201–208.

[15] TUMMERS, J.H., Quelques théorèmes par rapport au point de Frégier, *Chr. Huygens* **9** (1931), 201–205.

[16] WEISS, G., Frégier points revisited, *Proceedings of the Czeck-Slovak Conference on Geometry and Graphics* 2018, 277–286.

[17] WEISS, G., PECH, P., A quadratic mapping related to Frégier's theorem and some generalisations, *J. Geom. Graph.* **25**(1) (2021), 127–137.



**Boris Odehnal**
orcid.org/0000-0002-7265-5132
e-mail: boris.odehnal@uni-ak.ac.at
University of Applied Arts Vienna
Oskar-Kokoschka-Platz 2, A-1010 Vienna, Austria

https://doi.org/10.31896/k.26.4
Original scientific paper
Accepted 10. 11. 2022.

**HELLMUTH STACHEL**

# A Triple of Projective Billiards

**A Triple of Projective Billiards**

**ABSTRACT**

A projective billiard is a polygon in the real projective plane with a circumconic and an inconic. Similar to the classical billiards in conics, the intersection points between the extended sides of a projective billiard are located on a family of conics which form the associated Poncelet grid. We extend the projective billiard by the inner and outer billiard and disclose various relations between the associated grids and the diagonals, in particular other triples of projective billiards.

**Key words:** ellipse, billiard, caustic, Poncelet grid, billiard motion

**MSC2020:** 51N35

**Trojka projektivnih biljara**

**SAŽETAK**

Projektivni biljar je poligon u realnoj projektivnoj ravnini koji ima upisanu i opisanu koniku. Poput klasičnih biljara u konikama, sjecišta produljenih stranica projektivnog biljara se nalaze na familiji konika koje tvore pridruženu Ponceletovu mrežu. Proširujemo projektivni biljar unutarnjim i vanjskim biljarom i otkrivamo mnoštvo veza između pridruženih mreža i dijagonala, posebice drugih trojki projektivnih biljara.

**Ključne riječi:** elipsa, biljar, kaustika, Ponceletova mreža, biljarsko kretanje

## 1 Introduction

A *billiard* is the trajectory of a mass point in a domain called *billiard table* with ideal physical reflections in the boundary. Already for two centuries, billiards in ellipses (see Figures 1, 2, 8) and their projectively equivalent counterparts have attracted the attention of mathematicians, beginning with J.-V. Poncelet [4] and C.G.J. Jacobi [3] and continued, e.g., by S. Tabachnikov, who addresses in his book [10] a wide variety of themes around this topic. Computer animations carried out recently by D. Reznik [5] stimulated a new vivid interest on these well studied objects.

We focus on projective generalizations called *projective billiards*. This term stands for planar polygons $P_1P_2P_3\dots$ with a circumconic $e$ and an inconic $c$ called *caustic*. Not all projective billiards are projectively equivalent to Euclidean billiards (see, e.g., Figure 9), and not in all cases exist periodical polygons between the conics $e$ and $c$. However, in all cases the intersection points between extended sides define a family of conics which form the associated *Poncelet grid*. The goal of this paper is to demonstrate that in a quite natural way any given projective billiard defines two more projective billiards with associated Poncelet grids. It will be demonstrated that not only the conics of these grids, but also configurations of related lines deserve our interest.

It needs to be pointed out, that the computation of the billiards' vertices can only be carried out either iteratively or with the help of Jacobian elliptic functions (see, e.g., [8]). Therefore, it is not straightforward to obtain results on vertices and their respective $j$-th followers for any given integer $j > 1$. Often such assertions are equivalent to identities in terms of elliptic functions (see, e.g., [9, Section 5]).

**Structure of the article.** In Section 2 we introduce the three Poncelet grids associated respectively with a projective billiard and its inner and outer polygons. Section 3 is devoted to the conics $e^{(j)}$, $c^{(j)}$, and $r^{(j)}$ of the three grids. In Section 4 we recall results on the envelopes of diagonals and determine the points of contact. Finally in Section 5, we study the configuration of the $l$-th diagonals of the projective billiards inscribed respectively in $e^{(j)}$, $c^{(j)}$, and $r^{(j)}$.

## 2 A triple of Poncelet grids

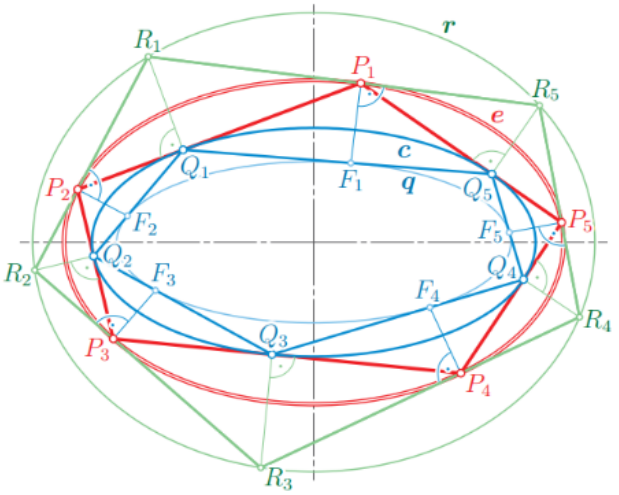


Figure 1: *Periodic billiard $P_1P_2\dots P_5$ inscribed in the ellipse $e$ along with the polygon $Q_1Q_2\dots Q_5$ of contact points with an ellipse $c$ as caustic, the polygon $F_1F_2\dots F_5$ of contact points with $q$, and the polygon $R_1R_2\dots \in r$ which is polar to $P_1P_2\dots P_5$ w.r.t. $e$.*

Let $P_1P_2P_3\dots$ be a polygon with circumconic $e$ and inconic $c$ in the real projective plane. Then there exists an associated Poncelet grid. We follow the notation in [7] and denote intersection points between extended sides[1] for $i,j=1,2,\dots$ as

$$S_i^{(j)} := \begin{cases} [P_{i-k-1},P_{i-k}]\cap[P_{i+k},P_{i+k+1}] & \text{for } j=2k, \text{ and} \\ [P_{i-k},P_{i-k+1}]\cap[P_{i+k},P_{i+k+1}] & \text{for } j=2k-1\,. \end{cases} \tag{1}$$

For fixed $j$, the points $S_1^{(j)},S_2^{(j)},\dots$ are located on a conic $e^{(j)}$ which belongs to the dual pencil (*range*, in brief) spanned by $e$ and $c$. This is due to a result of M. Chasles in 1843 (note, e.g., [7, Theorem 3.5]).

If the polygon $P_1P_2\dots$ is $N$-periodic, then we can confine to $1\le j\le[\frac{N-3}{2}]$, since for even $N$ the locus $e^{(j)}$ with $j=\frac{N-2}{2}$ is a line which has the same pole with respect to (w.r.t., for short) $e$ and $c$. Under the *billiard motion* of $P_1P_2\dots$, i.e., the variation of the vertices along the circumconic $e$ while $c$ remains fixed, each conic $e^{(j)}$ of the Poncelet grid remains fixed as well (note [7, Theorem 3.6]).[2]

In the classical case of a Euclidean billiard $P_1P_2\dots$ in a conic $e$, the conics $e^{(j)}$ are confocal with $e$ and the caustic $c$ (Figure 2). If for a given ellipse $e$ the caustic $c$ is an ellipse, then the billiard is called *elliptic* and the conics $e$ and $c$ intersect in two pairs of complex conjugate points. Otherwise we obtain a *hyperbolic* billiard with a hyperbola as caustic (Figures 6 and 7). Then the two conics share four real points.

### 2.1 The outer polygon

The tangents $t_{P_1},t_{P_2},\dots$ to the circumconic $e$ at the vertices $P_1,P_2,\dots$ of a projective billiard define a polygon $R_1R_2\dots$ called *outer polygon* in [5]. This polygon is polar to $P_1P_2\dots$ w.r.t. $e$ and therefore inscribed in a conic $r$ which is polar to $c$ w.r.t. $e$ (Figure 1). Similar to (1), the vertices $R_i^{(j)}$ of the associated Poncelet grid are points of intersection between tangents to $e$ and denoted for $j=1,2,\dots$ as given below:

$$R_i^{(j)} := \begin{cases} t_{P_{i-k}}\cap t_{P_{i+k+1}} & \text{for } j=2k, \text{ and} \\ t_{P_{i-k}}\cap t_{P_{i+k}} & \text{for } j=2k-1, \end{cases}$$

$$= \begin{cases} [R_{i-k-1},R_{i-k}]\cap[R_{i+k},R_{i+k+1}] & \text{for } j=2k, \text{ and} \\ [R_{i-k-1},R_{i-k}]\cap[R_{i+k-1},P_{i+k}] & \text{for } j=2k-1, \end{cases} \tag{2}$$

hence $k=\left[\frac{j+1}{2}\right]$ (note Figure 2).

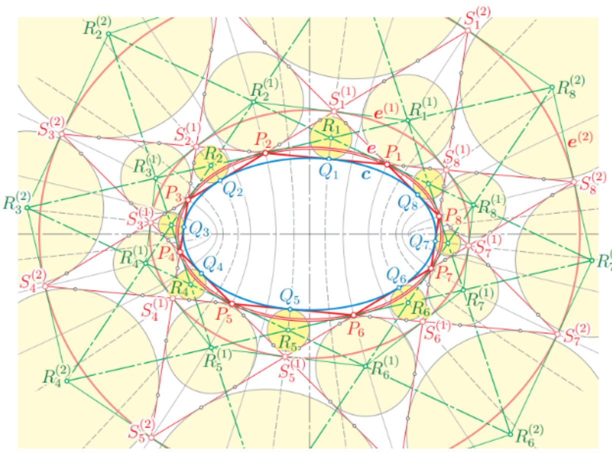

Figure 2: *Periodic billiard $P_1P_2\dots P_8$ in the ellipse $e$ with the net of tangent lines to $e$ at the vertices.*

### 2.2 The inner polygon

Beside the Poncelet grids associated with the pairs of conics $(e,c)$ and $(r,e)$, there is a third Poncelet grid. This time we focus on the polygon of contact points $Q_1,Q_2,\dots$ of the sides of $P_1P_2\dots$ with the caustic $c$. The polygon $Q_1Q_2\dots$

[1] Note that $XY$ denotes the segment bounded by the points $X$ and $Y$, while $[X,Y]$ denotes the connecting line.

[2] Beside the conics $e^{(j)}$, $j=1,2,\dots$, the Poncelet grid contains a second family of conics. In the case of classical billiards with ellipses $e$, $c$ and $e^{(j)}$, the remaining conics are confocal hyperbolas (see, e.g., [7, Figures 5 or 6]) which vary under the billiard motion. However, here we focus only on $e^{(j)}$.

is called *inner polygon* in [5]. The vertices of the associated Poncelet grid are defined as

$$Q_i^{(j)} := \begin{cases} [Q_{i-k-1}, Q_{i-k}] \cap [Q_{i+k}, Q_{i+k+1}] & \text{for } j = 2k, \\ [Q_{i-k-1}, Q_{i-k}] \cap [Q_{i+k-1}, Q_{i+k}] & \text{for } j = 2k-1 \end{cases} \tag{3}$$

(note Figure 4).

The extended sides of the polygon $Q_1Q_2\ldots$ envelop a conic $q$ which is polar to $e$ w.r.t. $c$. The line $[Q_{i-1}, Q_i]$ contacts $q$ at the $c$-pole $F_i$ of the tangent $t_{P_i}$ to $e$ at $P_i$. Therefore, in the case of a Euclidean billiard it is the point of intersection between the chord $[Q_{i-1}, Q_i]$ and the normal to $e$ at $P_i$ (Figure 1). The latter is the locus of poles of the tangent $t_{P_i}$ w.r.t. the conics of the confocal family.

**Lemma 1** *Referring to the previous notation, the circumconic $r$ of the polygon $R_1R_2\ldots$ with sides tangent to $e$ at $P_i$ is polar to $c$ w.r.t. $e$. The inconic $q$ of the polygon $Q_1Q_2\ldots$ with circumconic $c$ is polar to $e$ w.r.t. $c$. In the billiard case (Figure 1), $R_iQ_i$ is orthogonal to $c$ at $Q_i$, and $F_iP_i$ is orthogonal to $e$ at $P_i$.*

Lemma 1 reveals that also the conics $q$ and $r$ are invariant under the billiard motion along $e$. Clearly, if the original projective billiard $P_1P_2\ldots$ is periodic, then $Q_1Q_2\ldots$ and $R_1R_2\ldots$ are periodic, too.

A polygon with circumconic $e$ and inconic $c$ can be periodic even when the two conics share two real and two complex conjugate points. An example is depicted in Figures 5 and 9 with the two conics as circles. Such polygons $P_1P_2\ldots$ are called *bicentric*. They were first treated in 1828 by Jacobi [3] in the case where $c$ lies in the interior of $e$. In [6] various invariants of bicentric polygons are proved for the case that the circles $e$ and $c$ are either nested or disjoint.

## 3 More projective billiards in the three Poncelet grids

In the case of Euclidean billiards $P_1P_2\ldots$ in the plane or on the sphere (see [7, Fig. 7]), the tangents to $e$ at $P_i$ and those to $e^{(j)}$ at $S_i^{(j)}$ are angle bisectors of extended sides of $P_1P_2\ldots$. Therefore, the net of extended sides of $P_1P_2\ldots$ is *circular* with the points $R_i^{(j)}$ as centers of incircles of quadrilaterals (Figure 2). This result dates back to [1] in 2018. Below we present a generalization.

**Theorem 1** *Given a projective billiard $P_1P_2\ldots$, then for each $j = 1, 2, \ldots$ the vertex $R_i^{(j)}$ of the Poncelet grid associated with the outer polygon $R_1R_2\ldots$ is located on the tangents to $e^{(j)}$ at $S_i^{(j)}$ and $S_{i+1}^{(j)}$. The points $R_1^{(j)}, R_2^{(j)}, \ldots$ belong to a conic $r^{(j)}$ which is contained in the range spanned by $e$ and $r$. The polar conic of $r^{(j)}$ w.r.t. $e^{(j)}$ is the envelope of the extended sides of the polygon $S_1^{(j)}S_2^{(j)}\ldots$.*

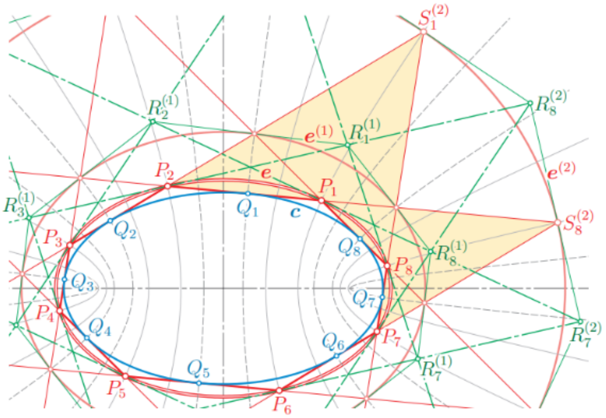


Figure 3: *$N$-periodic billiard with $N = 8$. In the proof of Theorem 1 we focus on the quadrilateral formed by the tangents from $S_1^{(2)}$ and $S_8^{(2)}$ to the caustic $c$.*

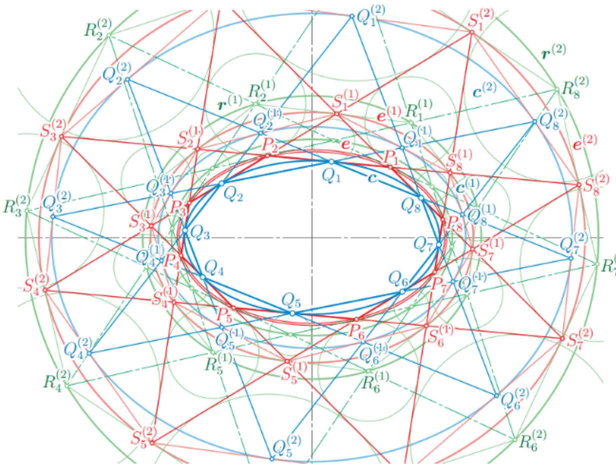

Figure 4: *The contact points of the sides of the polygon $S_i^{(j)}S_{i+1}^{(j)}\ldots$ with their envelope $c^{(j)}$ are the vertices $Q_i^{(j)}$ of the Poncelet grid associated with $Q_1Q_2\ldots$. In other words, the projective billiard $S_i^{(j)}S_{i+1}^{(j)}\ldots$ has $Q_1^{(j)}Q_2^{(j)}\ldots$ as its inner billiard.*

**Proof.** According to (1), the extended sides $[P_i, P_{i+1}]$ and $[P_{i+j+1}, P_{i+j+2}]$ through $S_{i+k}^{(j)}$ for $k = \left[\frac{j+1}{2}\right]$ and $[P_{i-1}, P_i]$ and $[P_{i+j}, P_{i+j+1}]$ through $S_{i+k-1}^{(j)}$ form a quadrilateral with $P_i, P_{i+j+1} \in e$ and $S_{i+k-1}^{(j)}, S_{i+k}^{(j)} \in e^{(j)}$ as pairs of opposite vertices (see the case $j = 2$, $N = 8$ and $i = 7$ in Figure 3). All four sides are tangents of the caustic $c$, while the conics and $e$, $e^{(j)}$ and $c$ belong to a range. According to the mentioned result by Chasles and its extension in [7, Theorem 3.5]), the tangents to $e$ at $P_i$ and $P_{i+j+1}$ and the tangents to $e^{(j)}$ at $S^{(j)}_{i+k-1}$ and $S^{(j)}_{i+k}$ are concurrent. By (2), their meeting point is $R^{(j)}_{i+k-1}$ (see Figure 2). After increasing all subscripts by 1, we obtain the analogue result for $R^{(j)}_{i+k}$.

The Poncelet grid associated with $R_1R_2\dots$ contains conics $r^{(j)}$ passing through the vertices $R^{(j)}_1, R^{(j)}_2, \dots$. All conics $r^{(j)}$ belong to the range spanned by $e$ and $r$ and are motion invariant, too. Since the polar line of $R^{(j)}_i \in r^{(j)}$ w.r.t. $e^{(j)}$ is the line $[S^{(j)}_i, S^{(j)}_{i+1}]$, the polar conic $c^{(j)}$ of $r^{(j)}$ w.r.t. $e^{(j)}$ envelops the polygon $S^{(j)}_1S^{(j)}_2\dots$. $\square$

**Theorem 2** *Referring to the previous notation, the sides of the polygon $S^{(j)}_1S^{(j)}_2\dots$ contact the enveloping conic $c^{(j)}$ at the vertices $Q^{(j)}_1, Q^{(j)}_2, \dots$. Hence, the envelope $c^{(j)}$ coincides with the conic of the Poncelet grid associated with $Q_1Q_2\dots$ (Figure 4).*

**Proof.** We replace the polygon $P_1P_2\dots$ inscribed in $e$ and circumscribed to $c$ by the polygon $R_1R_2\dots$ inscribed in $r$ and circumscribed to $e$. Then by virtue of Theorem 1, the side $[R^{(j)}_i, R^{(j)}_{i+1}]$ contacts the envelope $e^{(j)}$ at the point $S^{(j)}_i$. This implies for our original polygon $P_1P_2\dots$ that $[S^{(j)}_i, S^{(j)}_{i+1}]$ contacts the envelope $c^{(j)}$ at the vertex $Q^{(j)}_i$ of the Poncelet grid associated with the $j$-th diagonals of $Q_1Q_2\dots$. $\square$

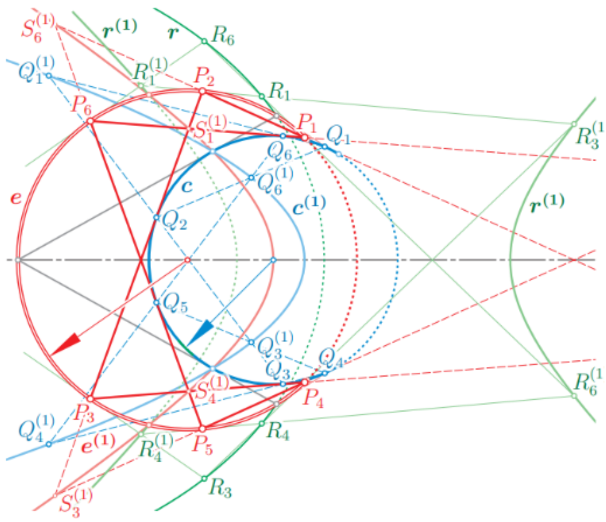


Figure 5: *Periodic projective billiard $P_1P_2\dots P_6$ in the bicentric case with the hyperbolas $e^{(1)}$ (red), $r^{(1)}$ (green), $c^{(1)}$ (blue), and the ellipse $r$ (green).*

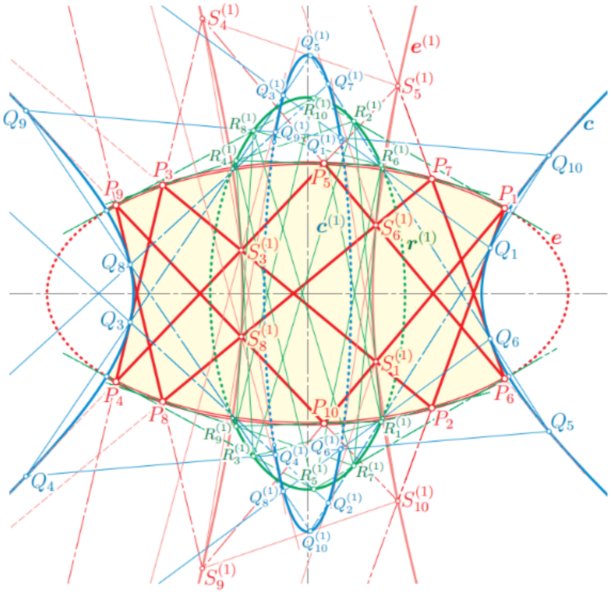


Figure 6: *A periodic hyperbolic billiard $P_1P_2\dots P_{10}$ along with the polygons $S^{(1)}_1S^{(1)}_2\dots S^{(1)}_{10}$ (red), $Q^{(1)}_1Q^{(1)}_2\dots Q^{(1)}_{10}$ (blue), $R^{(1)}_1R^{(1)}_2\dots R^{(1)}_{10}$ (green), and the respective circumconics $e^{(1)}$, $c^{(1)}$ and $r^{(1)}$.*

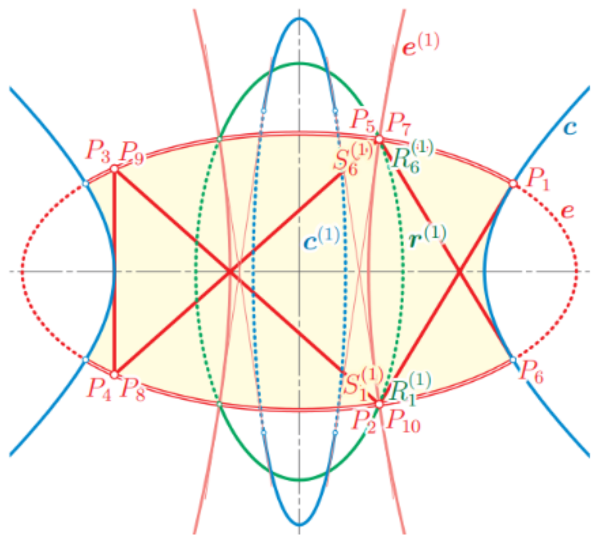


Figure 7: *Twofold pose of a periodic hyperbolic billiard $P_1P_2\dots P_{10}$ with $c^{(1)}$, $e^{(1)}$, and $r^{(1)}$.*

**Corollary 1** *Let $P_1P_2\dots$ be a projective billiard with $R_1R_2\dots$ and $Q_1Q_2\dots$ as respective outer and inner polygon. Then for fixed $j\in\{1,2,\dots\}$, the vertices $S^{(j)}_1, S^{(j)}_2, \dots$ on the conic $e^{(j)}$ of the Poncelet grid associated with $P_1P_2\dots$ form another projective billiard with the polygons $R^{(j)}_1R^{(j)}_2\dots$ as outer billiard with circumconic $r^{(j)}$ and*

*$Q_1^{(j)}Q_2^{(j)}\dots$ as inner billiard with the inconic $c^{(j)}$, which is polar to $r^{(j)}$ w.r.t. $e^{(j)}$.*

The Figures 5–7 illustrate that the triples $(c^{(j)},e^{(j)},r^{(j)})$ can look quite different in comparison with $(c^{(1)},e^{(1)},r^{(1)})$ or $(c^{(2)},e^{(2)},r^{(2)})$ in Figure 4.

As shown at the hyperbolic billiard in Figure 6, the conic $r^{(1)}$ passes through the intersection points of the hyperbola $e^{(1)}$ with $e$. This follows from particular poses with a twofold covered billiard (see Figure 7): When $P_1 \in e$ is specified at an intersection point[3] with the caustic $c$, then $P_2$ coincides with $P_{10}$ as well as with $S_1^{(1)}$ and $R_1^{(1)}$. There is a general statement in the background:

**Theorem 3** *Referring to the previous notation, for each $j = 1,2,\dots$ the conics $r^{(j)}$, $e^{(j)}$ and $e$ belong to a pencil. The same is true for the three conics $e^{(j)}$, $c^{(j)}$ and $c$ (Figure 5).*

**Proof.** We argue with help of the complex extension of the real projective plane. Whenever the point $R_{i+k}^{(j)} = t_{P_i} \cap t_{P_{i+j}}$ for $k = [\frac{j+1}{2}]$ is located on $e$, then follows $R_{i+k}^{(j)} = P_i = P_{i+j}$ and consequently $S_{j+k} = [P_{i-1},P_i] \cap [P_{i+j},P_{i+j+1}] = R_{i+k}^{(j)}$. This means that each point of intersection between $e$ and $r^{(j)}$ belongs also to $e^{(j)}$. Therefore, if $e$ and $r^{(j)}$ share four mutually different points, then $e^{(j)}$ belongs to the pencil spanned by $r^{(j)}$ and $e$.

The remaining cases with intersection points of higher order between $r^{(j)}$ and $e$ can be seen respectively as a limit where some of the four intersection points tend to coincidence. It cannot happen that in the limit the symmetric coefficient matrices of the three conics become linearly independent when everywhere else in the neighborhood they are linearly dependent.

The second statement follows just by replacing the triple $(r^{(j)},e^{(j)},e)$ by $(e^{(j)},c^{(j)},c)$. □

## 4 Diagonals

In view of the envelopes of the $j$-th diagonals $[P_i,P_{i+j+1}]$ of our polygon $P_1P_2P_3\dots$, we recall from [9] a result which was first stated in 1822 by V.-P. Poncelet [4] and reproved in 1828 by C.G.J. Jacobi for the case of nested circles $e$ and $c$. Moreover, we recall from [9] how to find the enveloping points. However, the proofs of the Theorems 1 and 2 in [9] cover only the cases of elliptic and hyperbolic billiards, where affine scalings are available between involved conics. The following theorem addresses the general case.

**Theorem 4** *Let $P_1P_2P_3\dots$ be a polygon inscribed in the conic $e$ and circumscribed to the conic $c$ with contact points $Q_1,Q_2,Q_3,\dots$. Then for fixed $j = 1,2,\dots$, the envelope of the $j$-diagonals $[P_i,P_{i+j+1}]$ is a conic $h_{e|j}$ included in the pencil spanned by $e$ and $c$, provided that in the particular case of $N$-periodic billiards with even $N$ holds $j \le [\frac{N-3}{2}]$.*
*The diagonal $[P_i,P_{i+j+1}]$ contacts $h_{e|j}$ at the intersection with the adjacent $j$-th diagonals $[Q_{i-1},Q_{i+j}]$ and $[Q_i,Q_{i+j+1}]$ of the inner billiard $Q_1Q_2Q_3\dots$ (Figures 8 or 9).*

**Proof.** (i) According to (1), the extended sides $[P_i,P_{i+1}]$ and $[P_{i+j+1},P_{i+j+2}]$ intersect at the point $S_{i+k+1}^{(j)}$, $k := [\frac{j}{2}]$, on the conic $e^{(j)}$, which belongs to the range spanned by $e$ and $c$. The restriction on $j$ in the periodic case as mentioned in Theorem 4 excludes the case where $e^{(j)}$ is a line.

The polarity in the caustic $c$ transforms this into the following statement: The connecting lines $[Q_i,Q_{i+j+1}]$ envelop a conic $h_{c|j}$ which belongs to the pencil spanned by $c$ and the polar conic $q$ of $e$ w.r.t. $c$ (Figures 1 and 8). In order to obtain the first part of our statement, it is sufficient to replace the polygon $Q_1Q_2Q_3\dots$ inscribed in $c$ and circumscribed to $q$ by the original polygon $P_1P_2P_3\dots$ with the circumconic $e$ and the inconic $c$.

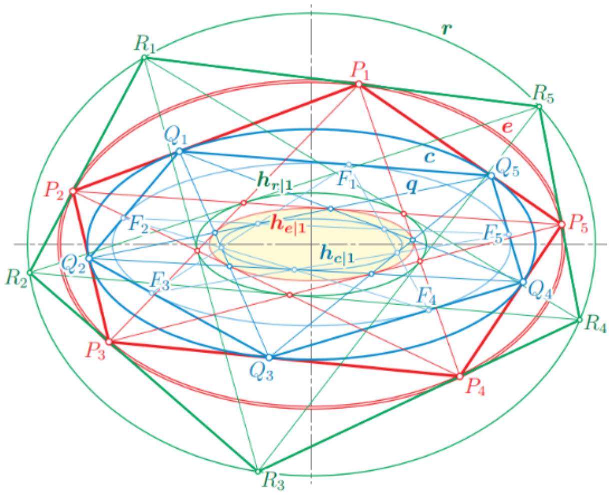


Figure 8: *Envelopes $h_{e|1}$, $h_{c|1}$ and $h_{r|1}$ of the diagonals of the periodic elliptic billiard $P_1P_2\dots P_5$ and of its inner and outer polygons $Q_1Q_2\dots$ and $R_1R_2\dots$. Triples of these diagonals together with that of $F_1F_2\dots$ meet at 15 points in the interior of $P_1P_2\dots$.*

[3]Twofold covered poses of projective billiards arise when one vertex is specified either as a point of intersection between the circumconic $e$ and the inconic $c$ or as the contact point with a common tangent between $e$ and $c$ (note the gray pose in Figure 5).

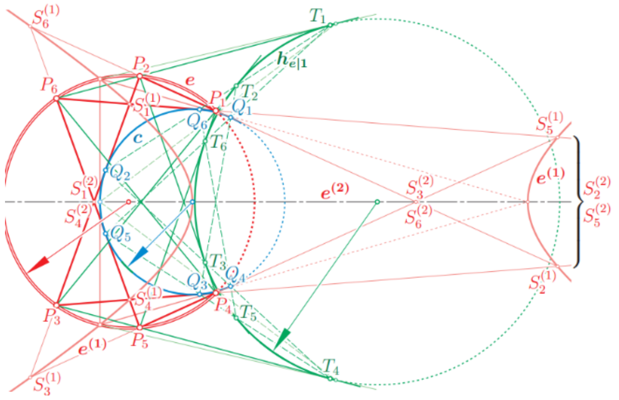


Figure 9: *In the bicentric case with circumcircle $e$ and intersecting incircle $c$ (blue) the envelope of the first diagonals (green solid) of the periodic polygon $P_1P_2\dots P_6$ is the circle $h_{e|1}$ (green) with contact points $T_1, T_2, \dots$. The hyperbola $e^{(1)}$ (pink) and the diameter $e^{(2)}$ belong to the associated Poncelet grid.*

(ii) The point of contact between $[Q_i, Q_{i+j+1}]$ and the envelope $h_{c|j}$ is the $c$-pole of the tangent to $e^{(j)}$ at $S^{(j)}_{i+k+1}$. By virtue of Theorem 1, this tangent passes through $R^{(j)}_{i+k}$ and $R^{(j)}_{i+k+1}$. Hence, the requested point of contact is the meeting point of the polar lines of $S^{(j)}_{i+k+1}$, $R^{(j)}_{i+k}$ and $R^{(j)}_{i+k+1}$ w.r.t. $c$.

The $c$-polar line of $S^{(j)}_{i+k+1}$ is the diagonal $[Q_i, Q_{i+j+1}]$. Since by (2) the point $R^{(j)}_{i+k}$ is the intersection of the tangents to $e$ at $P_i$ and $P_{i+j+1}$, the $c$-polar of $R^{(j)}_{i+k}$ connects the contact points $F_i$ and $F_{i+j+1}$ of respective sides of the polygon $Q_1Q_2\dots$ with its envelope $q$. After increasing all subscripts by 1, we obtain $[F_{i+1}, F_{i+j+2}]$ as the $c$-polar of $R^{(j)}_{i+k+1}$.

In order to prove the second claim, it is sufficient to replace the polygon $Q_1Q_2\dots$ with the inconic $q$ by the polygon $P_1P_2\dots$ with the inconic $c$ and the contact point $F_{i+1}$ of the side $[Q_i, Q_{i+1}]$ by the contact point $Q_i$ of the side $[P_i, P_{i+1}]$. □

In Figure 8, the particular case $j = 1$ is depicted along with the configuration of the $j$-th diagonals of $R_1R_2\dots$, $P_1P_2\dots$, $Q_1Q_2\dots$, and $F_1F_2\dots$ with triples of concurrent lines. The depicted enveloping conics $h_{r|1}$, $h_{e|1}$ and $h_{c|1}$ of the $j$-th diagonals of $R_1R_2\dots$, $P_1P_2\dots$ and $Q_1Q_2\dots$ in Figure 8 reveal that we obtain a sequence of triples of conics like $(r, e, c)$. This reminds on sequences of billiards as presented in [2].

**Corollary 2** *Let $P_1P_2\dots$ be a projective billiard with $R_1R_2\dots$ and $Q_1Q_2\dots$ as outer and inner polygon, while $F_1, F_2, \dots$ are the contact points of the inner polygon with its inconic $q$. Then the $j$-th diagonals of $Q_1Q_2\dots$ are the sides of another projective billiard, where the $j$-th diagonals of $P_1P_2\dots$ are the sides of the outer polygon and that of $F_1F_2\dots$ sides of the inner polygon (Figure 8).*

For later use we record a consequence of the Theorems 2 and 4:

**Lemma 2** *Referring to the previous notation, the conic $h_{e|j}$ is polar to $c^{(j)}$ w.r.t. the caustic $c$. The enveloping point of $[S^{(j)}_i, S^{(j)}_{i+1}]$ is the $c$-pole*

$$\begin{cases} Q^{(j)}_i \;\; \text{of} \;\; d := [P_{i-k}, P_{i+k+1}] & \text{for} \;\; j = 2k, \text{ and} \\ Q^{(j)}_{i+1} \;\; \text{of} \;\; d := [P_{i-k+1}, P_{i+k+1}] & \text{for} \;\; j = 2k-1\,. \end{cases}$$

*The line $d$ is a $j$-th diagonal of $P_1P_2P_3\dots$ and a diagonal of the quadrilateral consisting of the tangents drawn from $S^{(j)}_i$ and $S^{(j)}_{i+1}$ to the caustic $c$.*

The composition of the polarities in $c$ and $e$ is a collinear transformation $\kappa$. It takes $Q_i$ to $R_i$ and by (3) and (2) $Q^{(j)}_i$ to $R^{(j)}_i$ for all $i$. Moreover, it sends $c$ to $r$ and $c^{(j)}$ via $h_{e|j}$ to $r^{(j)}$ and the envelope of the $j$-th diagonals of $Q_1Q_2\dots$ to the envelope of $j$-th diagonals of $R_1R_2\dots$ (Figure 8). Lines with equal poles w.r.t. $e$ and $c$ remain fixed under $\kappa$ as for example the axes of symmetry of $e$ in the case of classical billiards.

## 5 Configurations of lines related to the Poncelet grids

The term ‘Poncelet grid’ usually stands for a configuration of conics, which are confocal in the particular case of Euclidean billiards. Below we demonstrate that a Poncelet grid is also combined with a configuration of lines.

The following theorem deals with the $l$-th diagonals of the polygon $S^{(j)}_1S^{(j)}_2\dots$ inscribed in the conic $e^{(j)}$ of the Poncelet grid associated with $P_1P_2\dots$ and circumscribed to the conic $c^{(j)}$. Note that in the case $l = j$ we obtain extensions of the sides of the original billiard $P_1P_2\dots$.

**Theorem 5** *The $l$-th diagonal $[S^{(j)}_i, S^{(j)}_{i+l+1}]$ of the polygon $S^{(j)}_1S^{(j)}_2\dots$ inscribed in $e^{(j)}$ contains three meeting points of at least five $l$-th diagonals of other polygons of the three involved grids (Figure 10):*

(i) *The contact point with the envelope of the $l$-th diagonals of $S^{(j)}_1S^{(j)}_2\dots$ is common to $[Q^{(j)}_{i-1}, Q^{(j)}_{i+l}]$, $[Q^{(j)}_i, Q^{(j)}_{i+l+1}]$ as well as for $j = 2k$ to $[Q_{i-k-1}, Q_{i-k+l}]$ and $[Q_{i+k}, Q_{i+k+l+1}]$ and for $j = 2k-1$ to $[Q_{i-k}, Q_{i-k+l+1}]$ and $[Q_{i+k}, Q_{i+k+l+1}]$.*

(ii) *The intersection point with the preceding diagonal*

*$[S_{i-1}^{(j)}, S_{i+l}^{(j)}]$ belongs also to $[R_{i-1}^{(j)}, R_{i+l}^{(j)}]$, as well as for even $j$ to $[P_{i-k-1}, P_{i-k+l}]$ and $[P_{i+k}, P_{i+k+l+1}]$ and in the odd case to $[P_{i-k-1}, P_{i-k+l}]$ and $[P_{i+k-1}, P_{i+k+l}]$. A similar result holds for the follower $[S_{i+1}^{(j)}, S_{i+l+2}^{(j)}]$.*

**Proof.** (i) The first statement is a direct consequence of Theorem 4, applied to the projective billiard $S_1^{(j)} S_2^{(j)} \dots$ with the circumconic $e^{(j)}$ and the inconic $c^{(j)}$.

In order to prove the second statement of (i), we apply Lemma 2 to the polygon $S_i^{(j)} S_{i+l+1}^{(j)} S_{i+2(l+1)}^{(j)} \dots \in e^{(j)}$, which is formed by $l$-th diagonals of $S_1^{(j)} S_2^{(j)} \dots$, but also by diagonals of a certain type in the polygon (or the union of polygons) with the caustic $c$ and the side lines $[S_i^{(j)}, S_{i+j+1}^{(j)}]$. Hence, the contact point of $[S_i^{(j)}, S_{i+l+1}^{(j)}]$ with the envelope of the $l$-th diagonals is the $c$-pole of a diagonal in the quadrilateral formed by the tangents drawn from $S_i^{(j)}$ and $S_{i+l+1}^{(j)}$ to $c$. According to (1), these tangents contact $c$ respectively

$$\begin{cases} \text{for } \; j = 2k \quad \text{at } Q_{i-k-1}, Q_{i+k} \text{ and } Q_{i-k+l}, Q_{i+k+l+1}, \\ \text{for } \; j = 2k-1 \quad \text{at } Q_{i-k}, Q_{i+k} \text{ and } Q_{i-k+l+1}, Q_{i+k+l+1}. \end{cases}$$

Due to the rules of the polarity w.r.t. $c$, the requested pole is the intersection of the connections of respective contact points, i.e., $[Q_{i-k-1}, Q_{i-k+l}] \cap [Q_{i+k}, Q_{i+k+l+1}]$ for even $j$ and $[Q_{i-k}, Q_{i-k+l+1}] \cap [Q_{i+k}, Q_{i+k+l+1}]$ for odd $j$.

(ii) From Theorem 4 applied to $r^{(j)}$ and $e^{(j)}$ follows that the contact point of $[R_{i-1}^{(j)}, R_{i+l}^{(j)}]$ with the envelope of the $l$-th diagonals of $R_1^{(j)} R_2^{(j)} \dots$ is common to $[S_{i-1}^{(j)}, S_{i+l}^{(j)}]$ and $[S_i^{(j)}, S_{i+l+1}^{(j)}]$.

In order to prove the second statement, we replace in Lemma 2 the pair of conics $(c, e^{(j)})$ by $(e, r^{(j)})$ and apply this result to the polygons $R_i^{(j)} R_{i+l+1}^{(j)} R_{i+2(l+1)}^{(j)} \dots$ formed by $l$-th diagonals of $R_1^{(j)} R_2^{(j)} \dots$. Hence, the contact point of $[R_{i-1}^{(j)}, R_{i+l}^{(j)}]$ with the envelope of these $l$-th diagonals is the $e$-pole of a diagonal $d$ in the quadrilateral formed by the tangents drawn from $R_{i-1}^{(j)}$ and $R_{i+l}^{(j)}$ to $e$. According to (2), the requested diagonal $d$ of the quadrilateral connects the points

$$t_{P_{i-k-1}} \cap t_{P_{i-k+l}} \quad \text{and} \quad \begin{cases} t_{P_{i+k}} \cap t_{P_{i+k+l+1}} & \text{for } \; j = 2k, \\ t_{P_{i+k-1}} \cap t_{P_{i+k+l}} & \text{for } \; j = 2k-1, \end{cases}$$

The $e$-pole of $d$ is the intersection of the connections of respective contact points with $e$, which confirms the claim. □

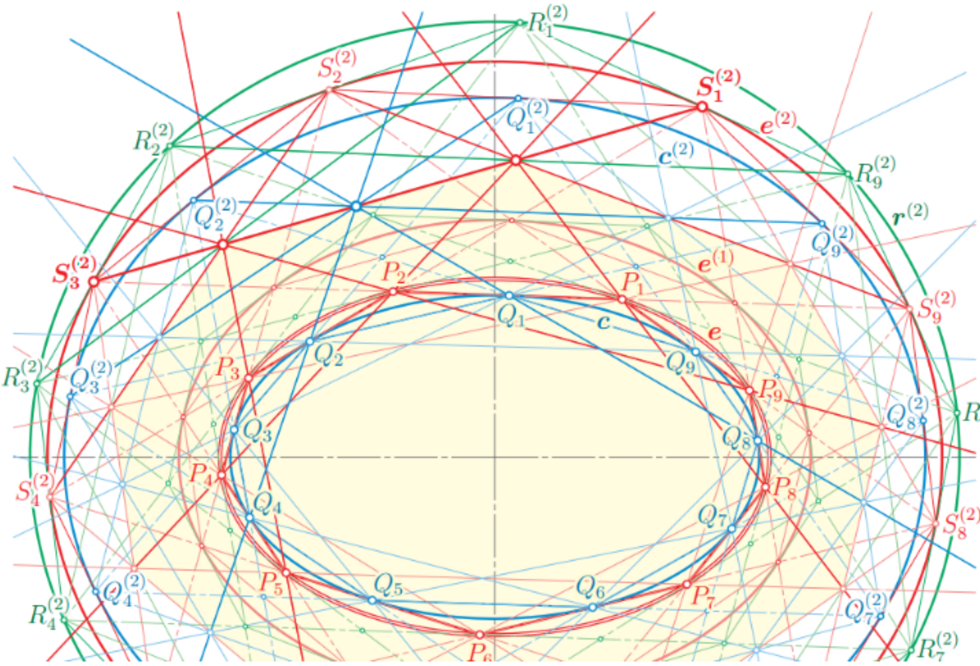


Figure 10: *Each $l$-th diagonal $[S_i^{(j)}, S_{i+l+1}^{(j)}]$ of the projective billiard $S_1^{(j)} S_2^{(j)} \dots$ in $e^{(j)}$ contains three meeting points with at least four other $l$-th diagonals of involved polygons (Theorem 5). Here the case $j = 2$ and $l = 1$ of a periodic elliptic billiard $P_1 P_2 \dots P_9$ is depicted; note the diagonal $S_1^{(2)} S_3^{(2)}$ (red).*

## References

[1] AKOPYAN, A.W., BOBENKO, A.I., Incircular nets and confocal conics, *Trans. Amer. Math. Soc.* **370**(4) (2018), 2825–2854, `https://doi.org/10.1090/tran/7292`

[2] GARCIA, R., REZNIK, D., A matryoshka of Brocard porisms, *Europ. J. Math.* **8** (2022), 308–329, `https://doi.org/10.1007/s40879-022-00529-5`

[3] JACOBI, C.G.J., Ueber die Anwendung der elliptischen Transcendenten auf ein bekanntes Problem der Elementargeometrie, *Crelle's Journal* **3**(4) (1828), 376–389, `https://doi.org/10.1515/crll.1828.3.376`

[4] PONCELET, J.-V., *Traité des propriétées projective des figures*, Tome premier, Bachelier, Libraire, Paris 1822. deuxième edition, Gauthier-Villiars, Imprimeur-Libraire, Paris 1865.

[5] REZNIK, D., GARCIA, R., KOILLER, J., Fifty New Invariants of N-Periodics in the Elliptic Billiard, *Arnold Math. J.* **7**(2) (2021), `https://doi.org/10.1007/s40598-021-00174-y`

[6] ROITMAN, P., GARCIA, R., REZNIK, D., New Invariants of Poncelet-Jacobi Bicentric Polygons, *Arnold Math J.* **7** (2021), 619–637, `https://doi.org/10.1007/s40598-021-00188-6`

[7] STACHEL, H., The Geometry of Billiards in Ellipses and their Poncelet Grids, *J. Geom.* **112**(40) (2021), `https://doi.org/10.1007/s00022-021-00606-2`

[8] STACHEL, H., On the Motion of Billiards in Ellipses, *Europ. J. Math.* **8**(4) (2022), (Special Issue: New Developments in Integrable Systems), 1602–1622, `https://doi.org/10.1007/s40879-021-00524-2`

[9] STACHEL, H., On the Diagonals of Billiards, In L.-Y. Cheng (ed): ICGG 2022 – *Proceedings of the 20th International Conference on Geometry and Graphics*, Lecture Notes on Data Engineering and Communication Technologies, vol. 146, Springer, Cham 2023, 19–33, `https://doi.org/10.1007/978-3-031-13588-0_2`

[10] TABACHNIKOV, S., *Geometry and Billiards.* American Mathematical Society, Providence/Rhode Island 2005, `http://dx.doi.org/10.1090/stml/030`

**Hellmuth Stachel**
orcid.org/0000-0001-5300-4978
e-mail: stachel@dmg.tuwien.ac.at
Vienna University of Technology
Institute of Discrete Mathematics and Geometry
Wiedner Hauptstraße 8-10, A-1040 Wien, Austria

https://doi.org/10.31896/k.26.5
Original scientific paper
Accepted 28. 11. 2022.

Hans Dirnböck
Gunter Weiss

# János Bolyai's Angle Trisection Revisited

Dedicated to Professor Hellmuth Stachel on the occasion of his 80th birthday

**János Bolyai's Angle Trisection Revisited**

**ABSTRACT**

J. Bolyai proposed an elegant recipe for the angle trisection via the intersection of the arcs of the unit circle with that of an equilateral hyperbola $c$. It seems worthwhile to investigate the geometric background of this recipe and use it as the basic idea for finding the $n^{th}$ part of a given angle. In this paper, we shall apply this idea for the trivial case $n=4$, and for 5. Following Bolyai in the case 5, one has to intersect the unit circle with cubic curve $c$. There, and in the cases $n \geq 5$, we find only numerical solutions, which shows the limitation of Bolyai's method. Therefore, we propose another construction based on epicycloids inscribed to the unit circle. By this method is even possible to construct the $(\frac{n}{m})^{th}$ part of a given angle.

**Key words:** angle trisection, angle $n$-section, equilateral hyperbola, cubic, epicycloid

**MSC2020:** 51-03, 51M04, 51M15, 51N20, 53A04, 53A17

**Ponovno razmatranje trisekcije kuta metodom Jánosa Bolyaija**

**SAŽETAK**

J. Bolyai je predložio elegantnu metodu za trisekciju kuta određivanjem sjecišta lukova jedinične kružnice s lukovima jednakostranične hiperbole $c$. Vrijedno je istražiti geometrijsku pozadinu ovog postupka te ga koristiti kao temeljnu ideju za pronalaženje $n$-tog dijela zadanog kuta. U ovom radu primijenit ćemo navedenu ideju u trivijalnom slučaju $n=4$, te za $n=5$. Slijedeći Bolyaija, u slučaju $n=5$ jediničnu kružnicu treba presjeći kubnom krivuljom $c$. U tom slučaju, kao i u slučajevima $n \geq 5$, nalazimo samo numerička rješenja, što pokazuje ograničenost Bolyaijeve metode. Stoga predlažemo i drugu konstrukciju, ovaj put utemeljenu na epicikloidi upisanoj jediničnoj kružnici. Ovom metodom moguće je čak konstruirati $\frac{n}{m}$-ti dio zadanog kuta.

**Ključne riječi:** trisekcija kuta, $n$-sekcija kuta, jednakostranična hiperbola, kubna krivulja, epicikloida

## 1 Angle trisection according to János Bolyai

P. Staeckel mentions in his book [3] about the geometric investigations of Wolfgang and Johann Bolyai on page 234 that "J. Bolyai delt with the angle trisection, as can be found on a slip of paper dating back to the early days of him". We present this passage from Staeckel's book in Figure 1a, b:

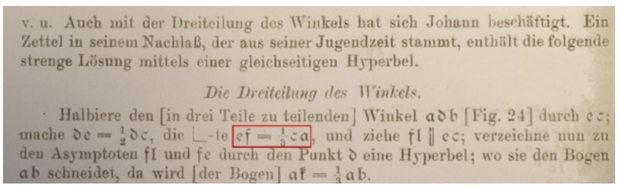
v. u. Auch mit der Dreiteilung des Winkels hat sich Johann beschäftigt. Ein Zettel in seinem Nachlaß, der aus seiner Jugendzeit stammt, enthält die folgende strenge Lösung mittels einer gleichseitigen Hyperbel.

*Die Dreiteilung des Winkels.*

Halbiere den [in drei Teile zu teilenden] Winkel adb [Fig. 24] durch ec; mache $de = \frac{1}{2}dc$, die ⌞-te $\boxed{ef = \frac{1}{3}ca}$, und ziehe $fl \parallel ec$; verzeichne nun zu den Asymptoten fl und fe durch den Punkt d eine Hyperbel; wo sie den Bogen ab schneidet, da wird [der Bogen] $ak = \frac{1}{3}ab$.

Figure 1a: *Reproduction of the text concerning the angle-trisection of [3, p.234].*

A translation of the text in Figure 1a would read as follows:

*The trisection of an angle*
*Halve the angle adb (Fig. 24) [to be divided into three parts] by ec; make now $de = \frac{1}{2}dc$, (make) the (normal)* ⌞ $\boxed{ef = \frac{1}{3}ca}$ *and draw $fl \| ec$; draw now a hyperbola through point d and with asymptotes $fl$ and $fe$; where it intersects the arc ab, the arc ak becomes $\frac{1}{3}ab$.*

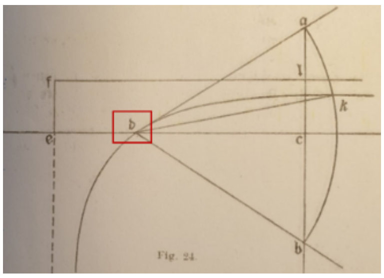


Figure 1b: *Reproduction of Fig. 24 of [3, p.234] concerning the angle-trisection.*

Figure "Fig. 24" does not exactly correspond with the"text", so there are misprints, as indicated by red rectangles. In "Fig. 24" point $b$, the centre of arc $ab$, should be labelled as "$d$", and in the text the term $ef = \frac{1}{3}ca$ should be replaced by $ef = \frac{1}{2}ca$.

Besides the mentioned recipe there is no further explanation or justification for it. János Bolyai (∗1802,†1860) was familiar with some Projective Geometry and the properties of conics. Therefore, one can suppose that, among geometers and mathematicians of his time, these subjects were generally known and a detailed explanation of the recipe could have been omitted. Nowadays, as mathematicians more or less disregard Classical Geometry, analytical treatment of Bolyai's construction can prove that the recipe is correct, but such proof does not show, why it is correct and how it was invented. The following chapter presents one possible idea, that J. Bolyai could have had in mind as a basis for his recipe.

## 2 Presumable geometric background of János Bolyai's angle trisection

We start with the unit circle $u$ in the Eucliden plane, which, as "Gauss plane", also models the affine line of complex numbers $\mathbb{C}$. Let an angle $\angle AOB$, with $O$ the center of $u$ and $A,B \in u$, have the measure $\measuredangle AOB = 3\alpha$, and we use halve line $OA$ as "real axis" in the Gauss plane. Then the complex number $z := \cos\alpha + i.\sin\alpha$ describes point $B$, and the cubic roots of $z$ become $\sqrt[3]{z}_p := \cos(\frac{3\alpha}{3} + p.\frac{2\pi}{3}) + i.\sin(\frac{3\alpha}{3} + p.\frac{2\pi}{3})$, $p = 0,1,2$. These three complex numbers describe points $P_0,P_1,P_2 \in u$ forming an equilateral triangle and solving the demanded trisection of $\angle AOB$. Having the idea to intersect $c$ with an algebraic curve through $P_0,P_1,P_2$ one could use a conic for this purpose. There exist a two-parameter set of conics through $P_0,P_1,P_2$, and we can choose one, which is somehow connected with the givens. For example, choosing orthogonal asymptote-directions in addition to $P_0,P_1,P_2$ selects equilateral hyperbolae $h$ in that set. Equilateral hyperbolae have the well-known nice property, that with any three points $P_0,P_1,P_2$ of such a hyperbola $h$ the orthocentre $O$ of triangle $P_0,P_1,P_2$ is also a point of $h$, see e.g. [2, p. 54]. This theorem seems to be stated first by Charles Brianchon (∗1783,†1864) and Jean Poncelet (∗1788,†1867), which were contemporaries of J. Bolyai. So, he could have been familiar with this theorem. Within the pencil of equilateral hyperbolae $h$ we take that one having line $OA$ as one of the asymptote-directions, see Figure 2. Therewith $h$ is described by

$$xy - ax - by = 0. \tag{1}$$

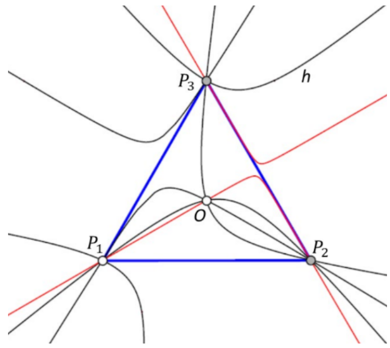


Figure 2: *Equilateral hyperbolae h through vertices of an equilateral triangle and its center O.*

Because of $\cos 3\alpha = 4(\cos\alpha)^3 - 3\cos\alpha$ and $-\sin 3\alpha = 4(\sin\alpha)^3 - 3\sin\alpha$, what we abbreviate by $V := 4x^3 - 3x$, resp. $-W := 4y^3 - 3y$, $(x := \cos\alpha, y := \sin\alpha, V^2 + W^2 = 1, x^2 + y^2 = 1)$, it follows that the intersection of $h$ with the unit circle $u$ must fulfil the conditions

$$(4x^3 - 3x - V)(x - S) = 0 \wedge (4y^3 - 3y + W)(y - T) = 0. \tag{2}$$

Thereby the additional fourth intersection point $Q$ has the coordinates $(S,T)$ with $S^2 + T^2 = 1$. We express $y$ resp. $x$ in (1) by $y = \frac{ax}{x-b}$ resp. $x = \frac{by}{y-a}$ and put these expressions into the equation of the unit circle $u$ receiving the fourth order equations

$$\begin{aligned} &y^4 - 2ay^3 - y^2(a^2 + b^2 - 1) + 2ay - b^2 = 0 \\ &x^4 - 2bx^3 - x^2(a^2 + b^2 - 1) + 2by - a^2 = 0). \end{aligned} \tag{3}$$

Comparing coefficients of (3) with those of (2) delivers

$$T = 2b, W = 2b, S = 2a, V = -2a, \tag{4}$$

such that $h$ has midpoint $M = (-\frac{1}{2}\cos 3\alpha, \frac{1}{2}\sin 3\alpha)$. The fourth intersection point has the coordinates $(S,T) = (-\cos 3\alpha, \sin 3\alpha)$ and is therefore diameter endpoint opposite to $O$. From the polar form of (1), and specialising with the coordinates of the origin $O = (0,0)$, it follows for the tangent $t_O$ of $h$ in $O$ that

$$t_O \ldots by = -ax \ldots y = x\tan 3\alpha, \tag{5}$$

such that $t_O$ has exactly the slope of the given angle, which is trisected by $h$.

We collect and visualise the mentioned properties of $h$ in Figure 3. In connection with angle trisection we shall call this special equilateral hyperbola $h$ the "Bolyai-hyperbola".

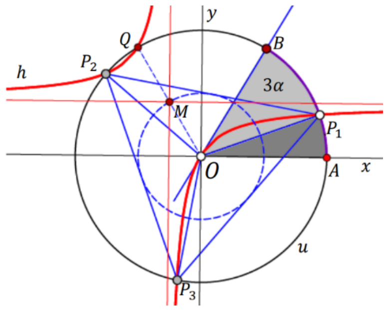


Figure 3: *Angle trisection as the intersection of the unit circle u with the "Bolyai-hyperbola" h.*

A consequence of the properties of the Bolyai-hyperbola $h$ follows

**Theorem 1 ([2, p.55])** *A circle $c$ with its midpoint at an arbitrary point $P$ of an equilateral hyperbola $h$ and passing through the opposite point $Q$ of $P$ on $h$ intersects $h$, besides in $Q$, in vertices of an equilateral triangle.*

It is not quite clear, who discovered the property of equilateral hyperbolae mentioned in Theorem 1. For example, it seems to be known already to H. Brocard in [1], but nowadays it cannot be considered as "widely known".

## 3 The $n-$section of an angle based on Bolyai's method

We follow the idea of J. Bolyai, when looking for the $n^{th}$ part of a given angle $\alpha$. As in chapter 2 we start with the $n^{th}$ root of a complex unit number $z := \cos\alpha + i.\sin\alpha$ describing a point $B$ at the unit circle $u$. The $n^{th}$ roots of $z$ become

$$\sqrt[n]{z}_p := \cos(\frac{\alpha}{n} + p.\frac{2\pi}{n}) + i.\sin(\frac{\alpha}{n} + p.\frac{2\pi}{n}), \qquad p = 0, 1, \ldots, n-1. \tag{6}$$

These $n$ complex numbers describe points $P_0, P_1, \ldots, P_{n-1} \in u$ forming a regular $n-$gon. If $n$ is the product of primes and their powers, it is obvious that one proceeds consecutively. For example, let $n = n_1 \cdot n_2 \cdot \ldots \cdot n_j$ (with $n_1 \geq n_2 \geq \ldots \geq n_j$), then the first stage delivers an $n_1-$gon with vertices $P_i$, the next stage delivers $n_2-$gons to each angle defined by $P_i$. In total one receives an $n_1 n_2-$gon with vertices $P_{i,j}$, and so on until we finally get an $n_1 n_2 \ldots n_j-$gon with vertices $P_{i,j,\ldots,k}$.

Even so it is trivial, we shall deal with "halving an angle" as a first example. According to (6) there will be two solutions $P_1, P_2$, which are opposite points of the unit circle $u$. Following J. Bolyai we need an algebraic curve, which intersects $u$ in the two points $P_1, P_2$. As a suitable curve of minimal degree we can take a line $g$, which passes through the centre $O$ of $u$, see Figure 4. Given an angle $2\alpha$ we put

$$\begin{aligned} &g \ldots y.\cos\alpha = x\sin\alpha, \\ &\cos 2\alpha = 2\cos^2\alpha - 1 =: V, \\ &\sin 2\alpha = 2\sin\alpha\cos\alpha =: W. \end{aligned} \tag{7}$$

Therefore, as $u \ldots x^2 + y^2 = 1$, the intersection points $g \cap u = \{P_1, P_2\}$ with

$$\begin{aligned} P_1 &= \left(+\sqrt{\frac{1}{2}(1+V)}, +\sqrt{\frac{1}{2}(1-W)}\right) =: (V_1, W_1) \\ P_2 &= \left(-\sqrt{\frac{1}{2}(1+V)}, -\sqrt{\frac{1}{2}(1-W)}\right) =: (-V_1, -W_1) \end{aligned} \tag{8}$$

and the solution angles are $\alpha_1 = \angle AOP_1$, $\alpha_2 = \angle AOP_2$, (with $A = (1,0)$).

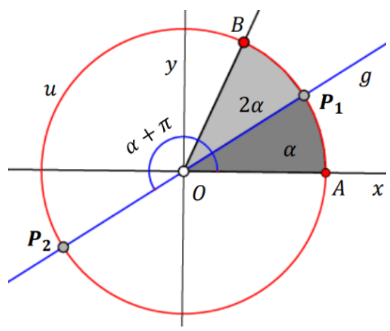


Figure 4: *Angle bisection as intersections of the unit circle u with the "Bolyai-line" g.*

If $n = 4 = 2 \cdot 2$, we can continue applying the halving procedure for the angles $\alpha_1, \alpha_2$. But we could also try a direct approach, too. We know already that the four solution points $P_j$ must form a square inscribed to $u$. As a simple curve $c$, which intersects $u$ in these points, we still can use a conic. The square of points $P_j$ defines a pencil of concentric and coaxial conics. Along the lines of case $n = 3$, we can choose a "clever" conic within that pencil, namely, the degenerate one forming the diagonals of the square, see Figure 5.
Thus $c$ is the product of the equations of two orthogonal lines:

$$c \ldots (y - kx)\left(y + \frac{1}{k}x\right) = 0, \quad k \in \mathbb{R}. \tag{9}$$

From (6) we get

$$\begin{aligned} &\cos 4\alpha = 8\cos^4\alpha - 8\cos^2\alpha + 1 =: V \\ &\sin 4\alpha = 4\sin\alpha\cos\alpha(2\cos^2\alpha - 1) =: W, \end{aligned} \tag{10}$$

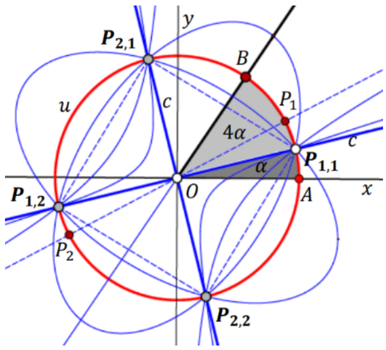


Figure 5: *Angle quadri-section as the intersection of the unit circle u with the degenerate "Bolyai-conic" c. The intermediate angle bisection and the pencil of conics through the solution points $P_{i,j}$ is shown, too.*

and we immediately can see that $\sin 4\alpha = 2\sin 2\alpha \cos 2\alpha$, $cos 4\alpha = \cos^2 2\alpha - sin^2 2\alpha$. Even so it could be calculated in a much shorter way, we want to show the general principle with this example. Rewriting (9) and (10) we get

$$\begin{aligned}
&c \ldots x^2 + Kxy - y^2 = 0, \quad (K := (k^2-1)/k),\\
&V = 8x^4 - 8x^2 + 1\\
&W = 4xy(2x^2 - 1)\\
&u \ldots x^2 + y^2 = 1. \qquad (11)
\end{aligned}$$

From these four equations we calculate $K$ resp. $k$:
From $K = -(2x^2-1)/x\sqrt{1-x^2}$ follows

$$K^2 = \frac{4x^4 - 4x^2 + \frac{1}{2} + \frac{1}{2}}{x^2 - x^4 - \frac{1}{8} + \frac{1}{8}} = \frac{4(V+1)}{1-V}, \quad K_{1,2} = \pm 2\sqrt{\frac{1+V}{1-V}},$$

whereof we finally get four values for the slopes $k$. By considering the third equation of (11) we combine the correct sine-values $y_j$ to the four cosine-values $x_i$, such that the points $P_i = (x_i, y_i)$ indeed will form a square.
We see that in the case of $n = 4$ the calculation of the algebraic problem is reducible and leads to consecutively extracting two roots. This means that the essential procedure concerns prime numbers n, as already noticed at the beginning of this chapter.

## 4 Finding the fifth of a given angle with Bolyai's method

As a non-trivial example, we now shall deal with the case $n = 5$. Here we expect a regular pentagon as the solution inscribed to the unit circle $u$. As five points already define a single conic, in our case the circle $u$, a low-degree curve through this pentagon surely must be at least a cubic $c$. There occurs an additional intersection point $Q = (S,T) \in u$, which, for special cases of the given angle $5\alpha$, might coincide with a point $P_i$. The set of planar cubic curves is 9-dimensional. This means that cubics through a pentagon still form a four-dimensional set and the first task would be to find a "clever" specimen within this set for our intersection purpose.

### 4.1 Cubics through the origin

Let $B = (\cos 5\alpha, \sin 5\alpha) = (V, W)$, and let, as a first try, $c$ pass through the origin $O$. Let one ideal point $U$ of $c$ be the that of the $y-$axis. This means that $c$ has an asymptote parallel to $y$. The consequences are some simplifications of the general equation of $c$:

$$x^3 + bx^2y + cxy^2 + ex^2 + fxy + gy^2 + hx + jy = 0. \qquad (12)$$

Because of

$$\begin{aligned}
&\cos 5\alpha = 16\cos^5\alpha - 20\cos^3\alpha + 5\cos\alpha,\\
&\sin 5\alpha = 16\sin^5\alpha - 20\sin^3\alpha + 5\sin\alpha, \qquad (13)
\end{aligned}$$

and by putting $\cos\alpha := x$, $\sin\alpha =: y$, ($x^2 + y^2 = 1$, which is the equation of $u$), we finally must compare (12) with

$$\begin{aligned}
&(16x^5 - 20x^3 + 5x - V)(x - S) = 0\\
&(16y^5 - 20y^3 + 5y - W)(x - T) = 0. \qquad (14)
\end{aligned}$$

We can eliminate $y$ in (12) by replacing $y^2$ in (12) by $1 - x^2$, by separating the terms, where $y$ occurs linearly, from the others, and finally squaring the resulting equation:

$$\begin{aligned}
&y(bx^2 + fx + j) =\\
&= -x^3 - cx(1-x^2) - g(1-x^2) - ex^2 - hx =\\
&= x^3(c-1) + x^2(g-e) - x(c+h) - g. \qquad (15)
\end{aligned}$$

By squaring, and again replacing $y^2$ by $1 - x^2$, we receive an equation of degree 6 in $x$. Thereby we abbreviate $c - 1 =: C$, $g - e =: E$, $c + h =: H$. The left side of (15) becomes

$$\begin{aligned}
&(1-x^2)(b^2x^4 + 2bfx^3 + (f^2 + 2bj)x^2 + 2fjx + j^2) =\\
&= -b^2x^6 - 2bfx^5 + (b^2 - 2bj - f^2)x^4 + 2f(b-j)x^3 +\\
&\quad + (f^2 + 2bj - j^2)x^2 + 2fjx + j^2.
\end{aligned}$$

The right side of (15) becomes

$$\begin{aligned}
&C^2x^6 + 2CEx^5 + (E^2 - 2CH)x^4 - (2EH + 2Cg)x^3 +\\
&+ (H^2 - 2Eg)x^2 + 2Hgx + g^2.
\end{aligned}$$

Both sides together deliver the equation

$$\begin{aligned}
&(b^2 + C^2)x^6 + 2(CE + bf)x^5 +\\
&+ (E^2 - 2CH - b^2 + 2bj + f^2)x^4 -\\
&- (2EH + 2Cg - 2bf + 2fj)x^3 +\\
&+ (H^2 - 2Eg - f^2 - 2bj + j^2)x^2 +\\
&+ 2(Hg - fj)x + (g^2 - j^2) = 0, \qquad (16)
\end{aligned}$$

and now we can compare (16) with

$$16x^6-16Sx^5-20x^4+20Sx^3+5x^2-(5S+V)x+VS=0. \tag{17}$$

The same way we eliminate $x$ in (12) and square the following equation:

$$x(y^2(1+c)+fy+h)=by^3+y^2(e-g)-y(b+j)-e.$$

Abbreviating $g-e=:E$, $b+j=:J$ we get

$$\begin{aligned}&(b^2+C^2)y^6+2(Cf-bE)y^5+\\&+(-C^2+E^2+2hC+f^2)y^4+\\&+(2EJ-2be-fC+fh)y^3+\\&+(2eE-2Ch+J^2-f^2+h^2)y^2+\\&+2(eJ-fh)y+(e^2-h^2)=0\end{aligned} \tag{18}$$

and can compare it with

$$16y^6-16Ty^5-20y^4+20Ty^3+5y^2-(5T+W)y+WT=0. \tag{19}$$

We collect the coefficients of equations (16) to (19) in the Table 1.

The 14 equations are not independent, the equations (0)-(6) resp. (0')-(6') alone allows us to express the coefficients $b,\dots,j$ of the cubic $c$ as functions of $V,W$ and $S,T$.

We see that the conditions of type (0)...(6') are quadratic equations in the unknowns $b,c,e,f,g,h,j,S,T$ and the givens $V,W$. They can be interpreted as hyperquadrics $Q_j^{(2)}$ in an 11-dimensional affine space $\mathbf{A}^{11}$, whereby $Q_0^{(2)}$ and $Q_1^{(2)}$ are the hypercylinders with equations $V^2+W^2=1$ resp. $S^2+T^2=1$.

When we use $V,W(V)$ as parameters, we finally will get a curve as intersection $Q_j^{(2)}\cap\dots\cap Q_k^{(2)}$, which represents a one-parameter set of cubics $c$. Obviously, to a fixed parameter pair $V_0,W(V_0)$ there will be, in the algebraic sense, up to 32 solutions of cubics $c(V_0)$. Figure 6 (left) shows an example of one solution of the cubics $c$ belonging to the given angle $5\alpha=98°$. To each given angle $5\alpha$ the calculations must be performed individually.

A similar calculation is performed for cubics having the ideal point of the $y-$axis as inflection point. Figure 6 (right) shows an example of this kind calculated to an angle $5\alpha=60°$.

| Equ. No. | Degr. | Coeff. (16) | Coef. (17) | Equ. No. | Degr. | Coeff. (18) | Coef. (19) |
|---|---|---|---|---|---|---|---|
| (6) | $x^6$ | $b^2+(1-c^2)$ | 16 | (6') | $y^6$ | $b^2+(c-1)^2$ | 16 |
| (5) | $x^5$ | $2((1-c)(e-g)+bf)$ | $-16S$ | (5') | $y^5$ | $2((c-1)f-b(g-e))$ | $-16T$ |
| (4) | $x^4$ | $(e-g)^2+2(1-c)(c+h)$ $-b^2+2bj+f^2$ | $-20$ | (4') | $y^4$ | $-(c-1)^2+(g-e)^2$ $+2(c-1)(h+1)$ $-2b(b+j)+f^2$ | $-20$ |
| (3) | $x^3$ | $2(e-g)(c+h)$ $+2(1-c)g-2bf+2fj$ | $20S$ | (3') | $y^3$ | $2(g-e)(b+j)$ $-2be-2f(c-1)$ $+f(h+1)$ | $20T$ |
| (2) | $x^2$ | $2(c+h)^2+2g(e-g)$ $-f^2-2bj+j^2$ | 5 | (2') | $y^2$ | $2e(g-e)$ $2(h+1)(c+1)$ $+(b+j)^2-f^2$ $+(h+1)^2$ | 5 |
| (1) | $x^1$ | $2((c+h)g-fj)$ | $-5S-V$ | (1') | $y^1$ | $2(e(b+j)-f(h+1))$ | $-5T-W$ |
| (0) | $x^0$ | $g^2-j^2$ | $VS$ | (0') | $y^0$ | $e^2-h^2$ | $WT$ |

Table 1: *Coefficients of (16) - (19) for the comparing procedure*

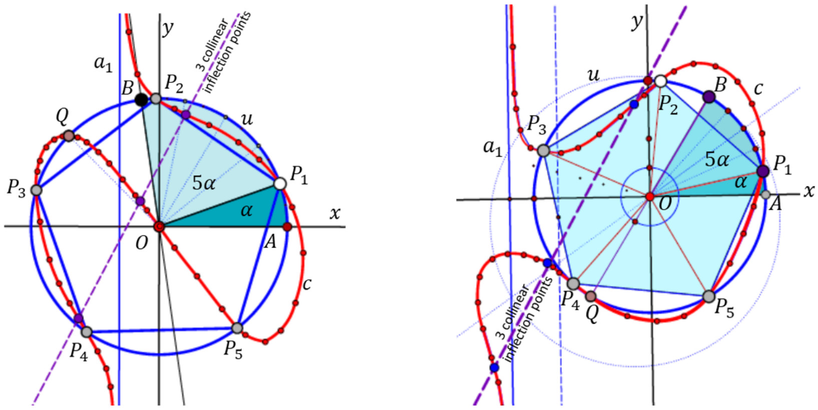


Figure 6: *Numerically gained solutions of "quinti-sectioning" the given angle $\angle AOB = 5\alpha$.*

### 4.2 Cubics with three given ideal points

One of the key-conditions of Bolyai's recipe is that all the "Bolyai hyperbolas" have the same ideal points and therefore are similar. In a *new approach* we focus at cubics $c(V)$ with the same triplet of ideal points. Note that the ideal points of $c(V)$ must be different from those of the unit circle. Let us try with three real ideal points $U_1 = (0,1,0)\mathbb{R}$, $U_2 = (0,0,1)\mathbb{R}$, $U_3 = (0,-1,1)\mathbb{R}$, (here we use homogeneous coordinates $(x_0,x_1,x_2)\mathbb{R}$ instead of affine coordinates $(1,x,y) =: (x,y)$). The equation of the general cubic c through these ideal points $U_i$ becomes

$$x^2y + xy^2 + ex^2 + fxy + gy^2 + hx + jy + k = 0. \tag{20}$$

The tangents $a_i$ at $U_i$, i.e. the asymptotes of $c$, are

$$a_1 \dots y = -e, \quad a_2 \dots x = -g, \quad a_3 \dots y = -x + e - f + g. \tag{21}$$

When we demand that $U_3$ shall be an inflection point of $c$, i.e. $a_3$ is an inflection asymptote, the coefficients $e, \dots, k$ fulfil the conditions

$$e^2 - g^2 - ef + fg + h - j = 0 \dots Q^{(2)}_{a_3}, \tag{22}$$

$$g(e-f)^2 + 2(e-f)g^2 + g^2 + (e-f+g)j + k = 0 \dots Q^{(3)}_{a_3}.$$

We shall compare (20) with (17) based on the condition $x^2 + y^2 = 1$. From (20) follows

$$(x^2 + fx + j) = x^3 - x^2(e-g) - x(1+h) - (g+k). \tag{23}$$

We abbreviate $e-g =: G$, $h+1 =: H$, $g+k =: K$ and square (23), we finally receive

$$2x^6 + 2(f-G)x^5 + (G^2 - 2H - 1 + f^2 + 2j)x^4 +$$
$$+ 2(GH - K - f + fj)x^3 + (H^2 + 2GK - f^2 + j^2 - 2j)x^2 +$$
$$+ (2HK - 2fj)x + (K^2 - j^2) = 0. \tag{24}$$

Similarly, we shall compare (19) with (20) based on condition $x^2 + y^2 = 1$. From (20) follows now $-x(y^2 + fy + h) = (1-y^2)y + e(1-y^2) + gy^2 + jy + k$ and when we abbreviate again $e-g =: G$, $j+1 =: J$, $e+k =: E$, we get

$$x(y^2 + fy + h) = y^3 + Gy^2 - Jy - E, \tag{25}$$

and by squaring this it becomes

$$2y^6 + 2(f-G)y^5 + (G^2 - 2J - 1 + f^2 + 2h)y^4 +$$
$$+ 2(GJ - E - f + fh)y^3 + (J^2 - 2EG - f^2 + h^2 - 2h)y^2 +$$
$$+ 2(EJ - fh)y + (E^2 - h^2) = 0. \tag{26}$$

By putting "(4)=(4')" and "(2)=(2')" we get $h = j$ and $g = e$ such that (20) simplifies to

$$x^2y + xy^2 + ex^2 + fxy + ey^2 + hx + hy + k = 0,$$

but again, we only get numerical solutions, (see Figure 7), as we must intersect hyperquadrics (and hyperplanes) in an 11-dimensional affine space. None of the results are such that there exists a one-parameter set of similar cubics. This allows at least to

**Conjecture 1** *There is no irreducible cubic carrying a one-parameter set of regular pentagons.*

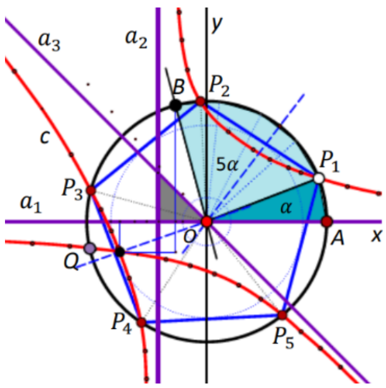


Figure 7: *Numerically gained solutions of "quinti-sectioning" the given angle $\angle AOB = 5\alpha = 105°$ with help of a cubic with three real asymptotes.*

| Equ. No. | Degr. | Coeff. (24) | Coef. (17) | Equ. No. | Degr. | Coeff. (26) | Coef. (19) |
|---|---|---|---|---|---|---|---|
| (6) | $x^6$ | $2$ | $16$ | (6') | $y^6$ | $2$ | $16$ |
| (5) | $x^5$ | $2(f-G)$ | $-16S$ | (5') | $y^5$ | $2(f-G)$ | $-16T$ |
| (4) | $x^4$ | $G^2-2H-1+f^2+2j$ | $-20$ | (4') | $y^4$ | $G^2-2J-1+f^2+2h$ | $-20$ |
| (3) | $x^3$ | $2(GH-K-f+fj)$ | $20S$ | (3') | $y^3$ | $2(GJ-E-f+fh)$ | $20T$ |
| (2) | $x^2$ | $H^2+2GK-f^2$ $+j^2-2j$ | $-5$ | (2') | $y^2$ | $2(J^2-2EG-f^2$ $+h^2-2h)$ | $-5$ |
| (1) | $x^1$ | $2(HK-fj)$ | $-5S-V$ | (1') | $y^1$ | $2(EJ-fh)$ | $-5T-W$ |
| (0) | $x^0$ | $K^2-j^2$ | $SV$ | (0') | $y^0$ | $E^2-h^2$ | $TW$ |

Table 2: *Coefficients of (24), (26) for the comparing procedure with (17), (19)*

### 4.3 Reducible cubics through regular pentagons

We try now with a conic $c$, which should pass through four points of the regular solution pentagon, and a line $l$ through its fifth point. Thereby $c$ and $l$ shall have the ideal point $(0,0,1)\mathbb{R}$ of the $y-$axis in common. Here we will get, in general, five solutions, as there are five possibilities for $l$ (and for $c$). But here, too, the explicit calculation turns out to become lengthy and results in numerical gained solutions, see Figure 8 showing solutions with a reducible cubic splitting into a hyperbola $c$ and a line $l$ parallel to the $y-$axis.

We note that within the pencil of conics $P_2,\ldots,P_5$ there is a special hyperbola $c$ passing through the origin $O$. It is symmetric to $OP_1$, its asymptotes include $120°$, and its midpoint's $M$ distance from the origin is one-third of the radius of (unit) circle $u$, (see Figure 9 showing $c$ in the standard position $5\alpha=0$). We used it already in Figure 8, but now we will add line $OA$ as the linear component $l$ of the reducible cubic $c$ in standard position and rotate this cubic $c$ according to the given angle $5\alpha$.

Hyperbola $c$ and line $l$ in standard position have the equations

$$c\ldots 3x^2+2x-y^2=0,\quad l\ldots y=0. \tag{27}$$

We rotate by angle $\varphi$, and we abbreviate $\sin\varphi=:s$, $\cos\varphi=:t$ to get the formulas shorter and better readable. We know already that $\varphi$ must turn out to become the solution angle $\alpha$. The rotated version of (27) reads as

$$c\ldots(3t^2-s^2)x^2+8stxy-(2s^2-t^2)y^2+2tx+2sy=0,$$
$$l\ldots sx-ty=0. \tag{28}$$

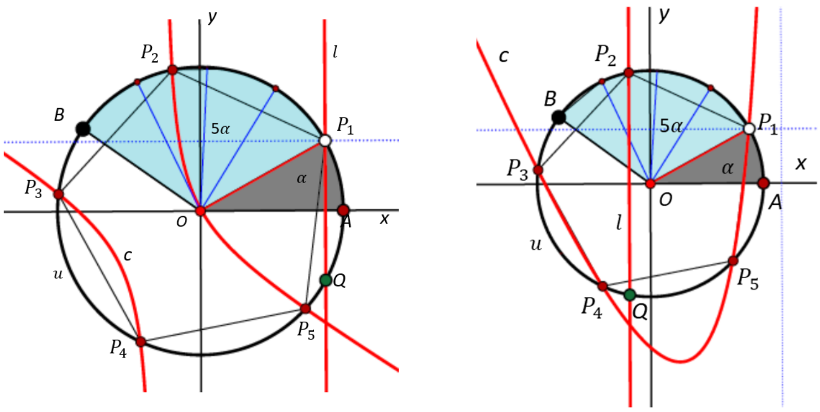


Figure 8: *Numerically gained solutions of "quinti-sectioning" the given angle $\angle AOB=5\alpha$ with help of a reducible cubic with a line component $l$ parallel $y$.*

| Equ. | $x^6$ | $x^5$ | $x^4$ | $x^3$ | $x^2$. | $x^1$ | $x^0$ |
|---|---|---|---|---|---|---|---|
| (17) | 16 | $-16U$ | $-20$ | $+20U$ | $+5$ | $-(5U+V)$ | $+UV$ |
| "(29)²" | 16 | $16t$ | ... | ... | ... | ... | $-t^2(16t^4-20t^2+5t)$ |

Table 3: *Comparison of the coefficients of the squared equation (29) with those of (17)*

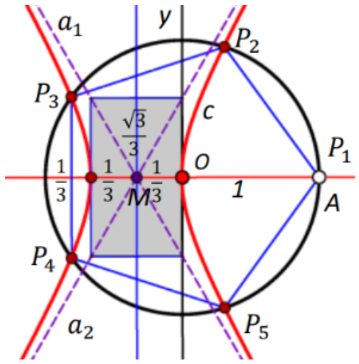


Figure 9: *Hyperbola $c$ through $O, P_2, \ldots, P_5$ in standard position.*

With $3t^2 - s^2 = 4t^2 - 1$ and $3s^2 - t^2 = 4s^2 - 1$ we find the equation of the reducible cubic $c$ as

$$s(4t^2-1)x^3 + 3t(4s^2-1)x^2y - 3s(4t^2-1)xy^2 - \\ - t(4s^2-1)y^3 + 2stx^2 + 2(1-2t^2)xy - 2sty^2 = 0. \qquad (29)$$

Following the procedure used in the former chapters, we again put $y^2 = 1 - x^2$ and separate terms containing $y$ from those containing only $x^k$, $k = 0, \ldots, 3$. By squaring this equation, we finally receive an equation of 6$^{\text{th}}$ degree in the variable $x$ and with coefficients being functions of $s$ and $t$, which are the only unknowns. Therefore, it is enough to consider the coefficients of $x^6$, $x^5$, and $x^0$ for connecting $s, t$ with the given cosine $V$ of polynomial (17), see table 3.
From the coefficients of $x^6$ follows that the proportionality factor of the two equations (17) and "(29)²" is 1. From $x^5$ we get $U = -t$, as expected, and from $x^0$ we receive the polynomial (13). Therefore, we end up with a tautology: To get the rotation angle we have to solve the original equation (13) $\cos 5\alpha = 16\cos^5\alpha - 20\cos^3\alpha + 5\cos\alpha$.
All the presented attempts to get sort of a standard cubic to solve the 5-section of an angle failed.
**Result:** The $n-$section ($n \geq 5$) of an angle $n\alpha$ based on Bolyai's method to intersect the unit circle with an algebraic curve $c$ of suitable degree leads to calculating the coefficients of an equation of $c$ individually to each given angle $n\alpha$.

**Remark 1** *Angle trisection, as one of the classical cubic problems, is only graphically solved via intersecting the unit circle with Bolyai's equilateral hyperbola. An exact solution should solve an equation of the third degree, too. In the following chapter, we present a possibility for a graphic solution using well-known properties of epicycloids.*

## 5 $p-$sectioning an angle using epicycloids

A generally applicable graphical solution of $p-$sectioning ($p \in \mathbb{Q}$) a given angle can be based on epicycloids, see e.g. [4, p.156] and [5]. Due to a theorem of F.E. Eckhardt (c.f. [4]) the line connecting the points $B$ and $P_1$, which move along the unit circle $u$ with speed $p\alpha$ resp. $\alpha$ envelops an epicycloid $e$ with the parameter representation

$$e \ldots \begin{pmatrix} x \\ y \end{pmatrix} = \frac{1}{p+1} \begin{pmatrix} p\cos\alpha + \cos(p\alpha) \\ p\sin\alpha + \sin(p\alpha) \end{pmatrix}. \qquad (30)$$

Such a cycloid admits two kinematic generations with circles $m$ and $m'$ rolling on a fixed circle $f$. The radii $r_f$, $r_m$, $r'_m$ of fixed circle $f$ and moving circles $m$ and $m'$ are therewith

$$r_f = \frac{1-p}{1+p}, \quad r_m = \frac{p}{1+p}, \quad r'_m = \frac{1}{1+p}. \qquad (31)$$

The following Figures 10, 11 and 12 show examples of such graphical angle p-sections. Thereby some additional properties of cycloids become obvious:
In both cases shown in Figure 10, the angle bisection and trisection, we notice that, besides of two orthogonal tangents $t_1, t_2$, resp. three tangents $t_1, t_2, t_3$ (inclosing 120° angles) intersect the (unit) circle $u$ in the solution points $P_1$, $P_2$, resp. $P_1$, $P_2$, $P_3$. There occurs an additional tangent $t$ with no meaning for the bisection problem. Figure 11 shows these properties, too. In all cases the touching points $E_j$ of $t_j$ with the epicycloids $e$ are the intersection points of the moving circle $m'$ (center $M' \in OB$) with $t_j$. The intersection of $m'$ with the additional tangent $t$ is not a point of epicycloid $e$. The segments $[E_jM']$ are parallel to the solution segments $[OP_j]$. The circle $u$ is an "orthoptic locus" of the cardioid $e$ (Figure 10 (left)) and, as a consequence of the "angle at circumference theorem", $u$ is a "multi-isoptic locus" of the epicycloids $e$ (Figure 10 (right) and Figure 11). The points

$E_j$ form a regular $n-$gon inscribed to $e$ and $m'$, such that this $n-$gon moves along $e$, when $B$ moves along the circle $u$. (By the way, this well-known property of epitrochoids has the "Wankel-motor" as a technical application, see e.g. [6].) Figure 12 shows examples of $p-$sectioning an angle for the cases $p = \frac{2}{5}$ and $p = \frac{3}{5}$. Here we find in fact the same properties as described above.
For $p = \frac{2}{5}$ it follows from (31) that $r_f = \frac{3}{7}$ , $r_m = \frac{2}{7}$ , $r'_m = \frac{5}{7}$, and for $p = \frac{3}{5}$ we get that $r_f = \frac{1}{4}$, $r_m = \frac{3}{8}$, $r'_m = \frac{5}{8}$. The cycloids $e$ have threefold resp. twofold symmetry, and again, a regular pentagon can move in $e$.

We collect these results in

**Theorem 2** *Let $\varphi = \angle AOB$ be the main value of a given angle, (A, B points of the (unit) circle u), and let e be the $p-$epicycloid with fixed circle f (radius $\frac{1-p}{1+p}$) concentric with u and A as vertex. Then one can construct the $p^{th}$ part(s) ($p \in \mathbb{Q}$) of $\varphi$ by drawing the tangents $t_j$ from B to e and intersect them with u. The intersection points $P_j$ forming a regular polygon define the solution angles $\angle AOP_j$. The circumcircle u of e is a multi-isoptic locus for the epicycloid e.*

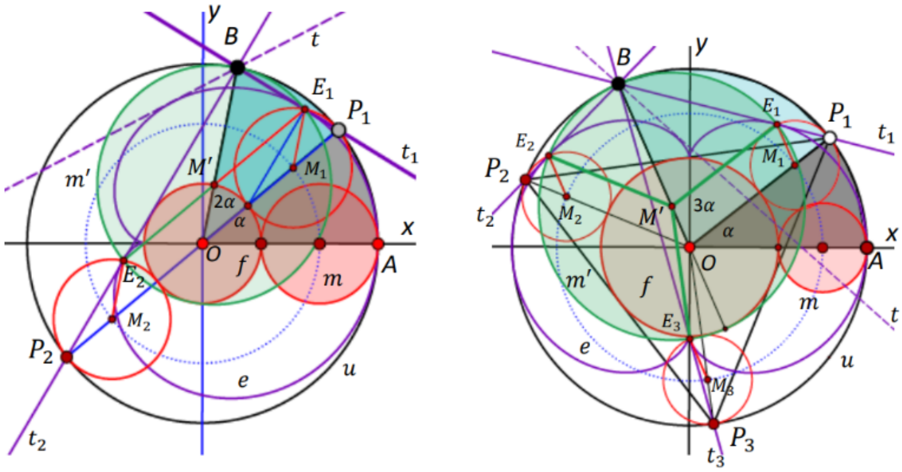

Figure 10: *Angle bisection and trisection with help of a cardioid resp. a nephroid.*

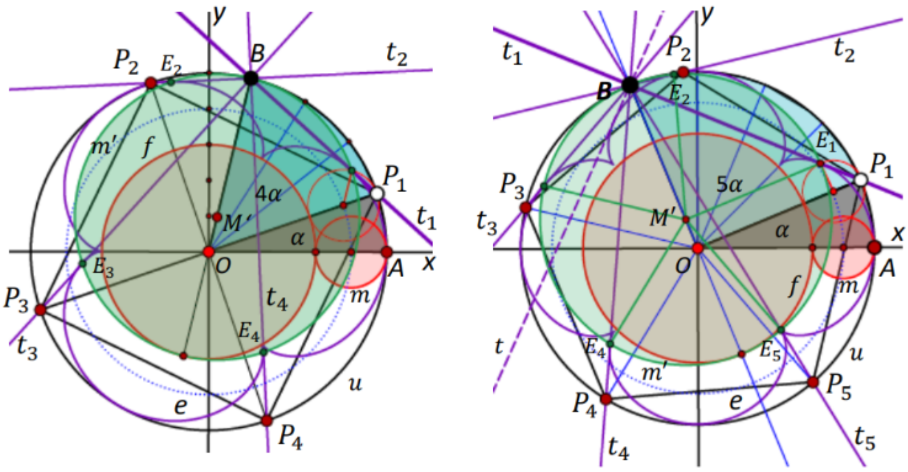

Figure 11: *Angle 4-section and 5-section with help of epicycloids.*

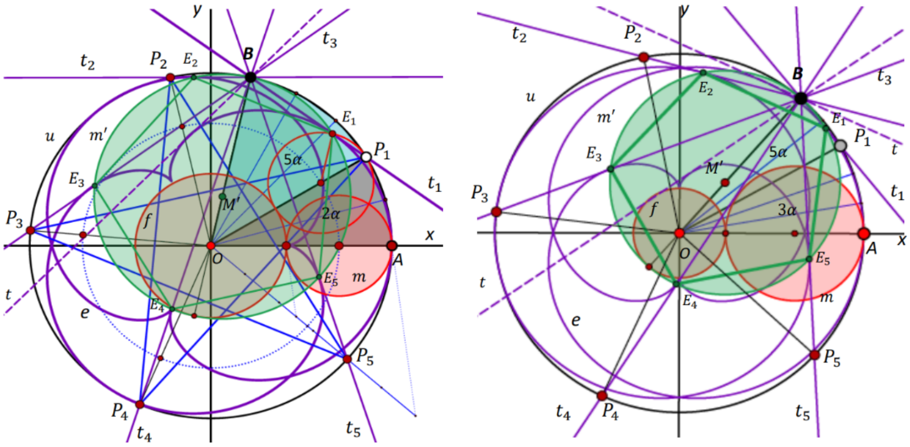


Figure 12: *The* $\frac{2}{5}$ *and* $\frac{3}{5}$ *of an angle with help of epicycloids.*

## 6 Conclusion

In this paper, we tried to "explain" Bolyai's classical method of angle trisection and extend it to $n-$ resp. $p-$sectioning an angle, ($n \in \mathbb{N}$, $p \in \mathbb{Q}$). While the trisection uses an equilateral hyperbola in standard position, the $5-$section must use cubics (or curves of higher degree), which have to be calculated individually to each given angle $5\alpha$. An equilateral hyperbola $c$ allows a "similarity-motion" of an equilateral triangle, such that its vertices move along $c$. We could not find a cubic $c$ allowing a similarity- motion to a regular pentagon, such that its vertices move along $c$. Therefore, this extension of Bolyai's method has no practical application and is finally adapted to replacing $c$ with epicycloids $e$ in the standard position. For $p \in \mathbb{Q}$ these epicycloids $e$ are closed, and they admit a congruence motion of regular $p-$stars, such that their vertices move along $e$, a well-known property, which is basic for Wankel motors. Obviously, because of the theorem of the angle at circumference, the circumcircle $u$ of $e$ is a "multi-isoptic locus" for $e$. Finally, one might add that this "epicycloid-method" also works for $p \in \mathbb{R}$, but in such cases, one should restrict the construction to the main value $P_1 \in u$.

## References


[1] BROCARD, H., *Nouvelle Correspondance Mathematique*, 1877.

[2] SCHAAL, H., Euklidische und pseudoeuklidische Sätze über Kreis und gleichseitige Hyperbel, *Elem. D. Math.* **19**(3) (1964), 53–56, Birkhäuser, Basel.

[3] STAECKEL, P., *Wolfgang und Johann Bolyai - Geometrische Untersuchungen*, Part 2, B.G. Teubner, Leipzig & Berlin 1913.

[4] WUNDERLICH, W., *Ebene Kinematik*, Hochschultaschenbücher 447, B. I. Mannheim/Wien/Zürich 1970.

[5] Epicycloid: `https://en.wikipedia.org/wiki/Epicycloid`

[6] Wankelmotor: `https://de.wikipedia.org/wiki/Wankelmotor`



**Hans Dirnböck**

Am Rautkogel 15, 9061 Klagenfurt-Woelfnitz, Austria

**Gunter Weiss**
e-mail: weissgunter@gmx.at

University of Technology Vienna,
Karlsplatz 13, 1040 Vienna, Austria

University of Technology Dresden,
Helmholtzstrße 10, 01069 Dresden, Germany

https://doi.org/10.31896/k.26.6
Review
Accepted 30. 11. 2022.

**VLADIMIR VOLENEC**
**EMA JURKIN**
**MARIJA ŠIMIĆ HORVATH**

# A Complete Quadrilateral in Rectangular Coordinates

**A Complete Quadrilateral in Rectangular Coordinates**

**ABSTRACT**

A complete quadrilateral in the Euclidean plane is studied. The geometry of such quadrilateral is almost as rich as the geometry of a triangle, so there are lot of associated points, lines and conics. Hereby, the study was performed in the rectangular coordinates, symmetrically on all four sides of the quadrilateral with four parameters $a,b,c,d$. In this paper we will study the properties of some points, lines and circles associated to the quadrilateral. All these properties are well known, but here they are all proved by the same method. During this process, still some new results have appeared.

**Key words:** Euclidean plane, complete quadrilateral, parabola

**MSC2020:** 51N20

**Potpuni četverostran u pravokutnim koordinatama**

**SAŽETAK**

U radu proučavamo potpuni četverostran u euklidskoj ravnini. Poput trokuta i potpuni četverostran ima mnogo zanimljivih svojstava te pridruženih točaka, pravaca i konika. Ovdje je proučavanje provedeno korištenjem pravokutnih koordinata, simetrično po sve četiri stranice četverostrana s četiri parametra $a,b,c,d$. Proučavamo svojstva točaka, pravaca i kružnica pridruženih četverostranu. Gotovo sve tvrdnje prikazane u ovom radu su dobro poznate, ali su se ipak ponegdje usput pojavili i neki novi rezultati.

**Ključne riječi:** euklidska ravnina, potpuni četverostran, parabola

## 1 Motivation

The focus of this paper is the geometry of a complete quadrilateral in the Euclidean plane. Such a geometry is almost as rich as the geometry of a triangle, so there are lot of associated points, lines and conics. The facts given in the paper are well known, but the idea of the paper is to prove them all by the same method. Hence, the study is performed in the rectangular coordinates, symmetrically on all four sides of the quadrilateral with four parameters $a,b,c,d$. During this process, still some new results have appeared.

We mention only the literature where the facts and the statements are presented for the first time.

Previously known statements are included in the text and given in italic while the new results are given in the form of theorem.

## 2 Introduction

A complete quadrilateral, or just a *quadrilateral* $\mathcal{ABCD}$ is a set of four lines $\mathcal{A}$, $\mathcal{B}$, $\mathcal{C}$, $\mathcal{D}$ in the Euclidean plane, where none of two lines are parallel and no three of which are concurrent. Lines $\mathcal{A}$, $\mathcal{B}$, $\mathcal{C}$, $\mathcal{D}$ are *sides* of that quadrilateral, and intersections of the pairs of lines are its *vertices*. Pairs of vertices $T_{AB} = \mathcal{A}\cap\mathcal{B}$, $T_{CD} = \mathcal{C}\cap\mathcal{D}$; $T_{AC} = \mathcal{A}\cap\mathcal{C}$, $T_{BD} = \mathcal{B}\cap\mathcal{D}$; $T_{AD} = \mathcal{A}\cap\mathcal{D}$, $T_{BC} = \mathcal{B}\cap\mathcal{C}$ are pairs of *opposite vertices*, and their connecting lines $\mathcal{U} = T_{AB}T_{CD}$, $\mathcal{V} = T_{AC}T_{BD}$, $\mathcal{W} = T_{AD}T_{BC}$ are *diagonals* of that quadrilateral. Intersection points $U = \mathcal{V}\cap\mathcal{W}$, $V = \mathcal{W}\cap\mathcal{U}$, $W = \mathcal{U}\cap\mathcal{V}$ are *diagonal points* and a triangle formed by diagonal points and diagonals is a *diagonal triangle* of a quadrilateral. Only one parabola $\mathcal{P}$ can be inscribed to the quadrilateral $\mathcal{ABCD}$ and let it touches the sides of the

quadrilateral at the points $A$, $B$, $C$, $D$. An axis and a vertex tangent of that parabola is taken as $x$-axis and $y$-axis of the coordinate system. Then, taking any metrical unit for length the equation of that parabola is $y^2 = 2px$. That parabola has the point $(\frac{p}{2}, 0)$ as a focus and the line $x = -\frac{p}{2}$ as the directrix. Without loss of generality, we can take the metrical unit for length in a way that $p = 2$ is valid. The size of some object is not important, but only its shape and mutually position to the similarity. The diagonal triangle is autopolar with respect to the parabola $\mathcal{P}$, i.e. lines $\mathcal{U}$, $\mathcal{V}$, $\mathcal{W}$ are polars of points $U, V, W$ with respect to parabola.
Hence, we can take that inscribed parabola $\mathcal{P}$ of the quadrilateral $\mathcal{ABCD}$ has the equation

$$\mathcal{P} \ldots y^2 = 4x, \tag{1}$$

so its focus is point $S = (1, 0)$, the directrix $\mathcal{H}$ is $x = -1$. The polarity with respect to the parabola $\mathcal{P}$ maps any point $T_0 = (x_0, y_0)$ to the line $\mathcal{T}_0$ with the equation $y_0 y = 2x + 2x_0$, the polar line of the point $T_0$. For the contact points of the parabola $\mathcal{P}$ with the sides of the quadrilateral the following points are taken

$$A = (a^2, 2a), B = (b^2, 2b), C = (c^2, 2c), D = (d^2, 2d). \tag{2}$$

The tangent lines of the parabola at the points $A, B, C, D$ are lines $\mathcal{A}$, $\mathcal{B}$, $\mathcal{C}$, $\mathcal{D}$ with equations

$$\begin{aligned} &\mathcal{A} \ldots ay = x + a^2, \quad \mathcal{B} \ldots by = x + b^2, \\ &\mathcal{C} \ldots cy = x + c^2, \quad \mathcal{D} \ldots dy = x + d^2, \end{aligned} \tag{3}$$

because on the example of the polar line for the point $A$ we get the equation $2ay = 2x + 2a^2$. For the vertices of the quadrilateral $\mathcal{ABCD}$ we get the following forms

$$\begin{aligned} &T_{AB} = (ab, a+b), T_{AC} = (ac, a+c), T_{AD} = (ad, a+d), \\ &T_{CD} = (cd, c+d), T_{BD} = (bd, b+d), T_{BC} = (bc, b+c). \end{aligned} \tag{4}$$

The diagonals are

$$\begin{aligned} \mathcal{U} &= T_{AB}T_{CD} \ldots (cd - ab)y \\ &\quad = (c + d - a - b)x + (a + b)cd - ab(c + d), \\ \mathcal{V} &= T_{AC}T_{BD} \ldots (bd - ac)y \\ &\quad = (b + d - a - c)x + (a + c)bd - ac(b + d), \\ \mathcal{W} &= T_{AD}T_{BC} \ldots (bc - ad)y \\ &\quad = (b + c - a - d)x + (a + d)bc - ad(b + c), \end{aligned} \tag{5}$$

and diagonal points

$$\begin{aligned} U &= \left( \frac{(a+b)cd - ab(c+d)}{c+d-a-b}, 2\frac{cd - ab}{c+d-a-b} \right), \\ V &= \left( \frac{(a+c)bd - ac(b+d)}{b+d-a-c}, 2\frac{bd - ac}{b+d-a-c} \right), \\ W &= \left( \frac{(a+d)bc - ad(b+c)}{b+c-a-d}, 2\frac{bc - ad}{b+c-a-d} \right). \end{aligned} \tag{6}$$

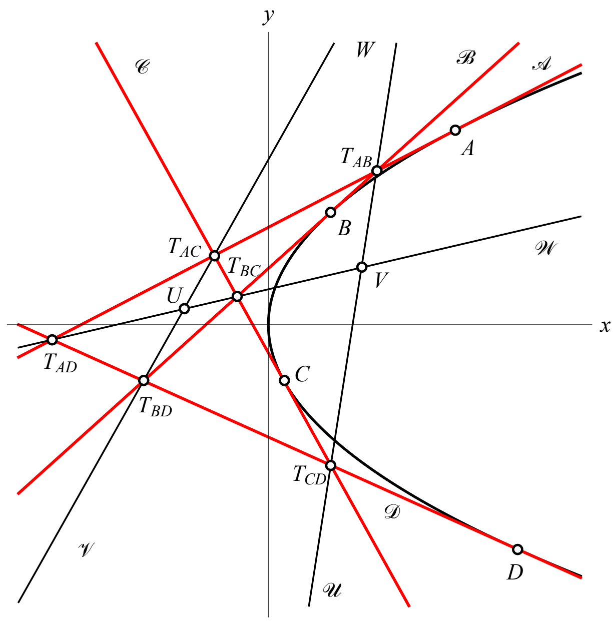


Figure 1: *A complete quadrilateral* $\mathcal{ABCD}$

There is a complete quadrilateral $\mathcal{ABCD}$ on Figure 1.
Let denote basic symmetric functions of the parameters $a, b, c, d$ by $s, q, r$ and $p$, so that

$$\begin{aligned} &s = a + b + c + d, \quad q = ab + ac + ad + bc + bd + cd, \\ &r = abc + abd + acd + bcd, \quad p = abcd \end{aligned}$$

are valid.

We will often use and labels $\alpha = a^2 + 1$, $\beta = b^2 + 1$, $\gamma = c^2 + 1$, $\delta = d^2 + 1$.

## 3 On a complete quadrilateral

Hereby, we will give many well known results on a complete quadrilateral $\mathcal{ABCD}$, as well as few new results. Connecting line $AB$ from (2) is the line with the equation $2x - (a + b)y + 2ab = 0$ that is fullfilled by coordinates of the point $U$ from (6). Similarly computation is valid for others connecting lines of the points $A$, $B$, $C$ and $D$. Hence, *a complete quadrangle ABCD has the same diagonal triangle UVW as the quadrilateral* $\mathcal{ABCD}$, see [43].
The midpoints of pairs of points $T_{AB}, T_{CD}$; $T_{AC}, T_{BD}$; $T_{AD}, T_{BC}$ from (4) are following points

$$\begin{aligned} &U_0 = \left( \frac{1}{2}(ab + cd), \frac{1}{2}s \right), \quad V_0 = \left( \frac{1}{2}(ac + bd), \frac{1}{2}s \right), \\ &W_0 = \left( \frac{1}{2}(ad + bc), \frac{1}{2}s \right) \end{aligned} \tag{7}$$

and obviously they lie on the line $\mathcal{N}$ with the equation

$$\mathcal{N}\ldots y=\frac{1}{2}s. \tag{8}$$

There are lots of names for this line, here we will call it a *median* of the quadrilateral $\mathcal{ABCD}$. It was mentioned for the first time in [9], an its existence was proved in [16]. Out of formulas (7) the following formulas for directed lengths follow

$$V_0W_0=\frac{1}{2}(a-b)(d-c),\quad W_0U_0=\frac{1}{2}(a-c)(b-d),$$
$$U_0V_0=\frac{1}{2}(a-d)(c-b). \tag{9}$$

The centroid of six points from (4) and the centroid of four points from (2) are points

$$T=(\frac{1}{6}q,\frac{1}{2}s),\quad T'=(\frac{1}{4}(s^2-2q),\frac{1}{2}s) \tag{10}$$

that are incident with $\mathcal{N}$.

In [33] the following statement is proved:
*Areas of two triangles whose bases are two diagonals of the quadrilateral, and common vertex is any of two additional vertices of that quadrilateral, are related as segments on the median of the quadrilateral from the midpoints of these two vertices to the midpoints of two diagonals mentioned before.*
That means that areas of triangles $T_{AB}T_{AC}T_{BD}$ and $T_{AB}T_{AD}T_{BC}$, as well as areas of triangles $T_{CD}T_{AC}T_{BD}$ and $T_{CD}T_{AD}T_{BC}$ are related as directed lengths $U_0V_0$ and $U_0W_0$, and there are two more such examples. Areas of triangles $T_{AB}T_{AC}T_{BD}$ and $T_{AB}T_{AD}T_{BC}$ are $\frac{1}{2}(a-b)(a-d)(b-c)$ and $\frac{1}{2}(a-b)(a-c)(b-d)$, and areas of $T_{CD}T_{AC}T_{BD}$ and $T_{CD}T_{AD}T_{BC}$ are $\frac{1}{2}(c-d)(a-d)(b-c)$ and $\frac{1}{2}(c-d)(a-c)(b-d)$ while directed lengths $U_0V_0$ and $U_0W_0$ according to (9) are equal $\dfrac{1}{2}(a-d)(c-b)$ and $\dfrac{1}{2}(a-c)(d-b)$. So, all three mentioned ratios are equal to $\dfrac{(a-d)(b-c)}{(a-c)(b-d)}$, that is actually the cross ratio $(abdc)$. In another two examples two cross ratios are $(acbd)$ and $(adcb)$.
In the quadrilateral $\mathcal{ABCD}$ we can observe three quadrangles $T_{AC}T_{AD}T_{BD}T_{BC}$, $T_{AB}T_{AD}T_{CD}T_{BC}$, and $T_{AB}T_{AC}T_{CD}T_{BD}$, one of them is convex, one concave, and one crossed. Centroids of these quadrangles are points

$$T_u=\Big(\frac{1}{4}(ac+ad+bc+bd),\frac{1}{2}s\Big),$$
$$T_v=\Big(\frac{1}{4}(ab+ad+bc+cd),\frac{1}{2}s\Big),$$
$$T_w=\Big(\frac{1}{4}(ab+ac+bd+cd),\frac{1}{2}s\Big)$$

incident with the median $\mathcal{N}$. For the directed lengths on that line we have the equalities

$$T_vT_w=\frac{1}{4}(a-b)(c-d),$$
$$T_wT_u=\frac{1}{4}(a-c)(d-b),$$
$$T_uT_v=\frac{1}{4}(a-d)(b-c),$$

so because of the equality (9) we get $V_0W_0=-2T_vT_w$, $W_0U_0=-2T_wT_u$, $U_0V_0=-2T_uT_v$ that is a result given in [32].
If for oriented lengths equalities $T_{AB}T_{AD}=uT_{AB}T_{AC}$, $T_{AB}T_{BC}=vT_{AB}T_{BD}$ are valid, then easily we get equalities $\dfrac{b-d}{b-c}=u$, $\dfrac{a-c}{a-d}=v$. If the number $w$ is such that $U_0W_0=wU_0V_0$ is fulfilled, then because of (9)

$$w=\frac{(a-c)(d-b)}{(a-d)(c-b)}=uv$$

follows. This is result from [38].
Let the points $B_1$ and $C_1$ be points on lines $\mathcal{B}$ and $\mathcal{C}$ so that for the directed lengths the equalities $T_{AB}B_1=T_{BC}T_{BD}$, $T_{AC}C_1=T_{BC}T_{CD}$ are valid. Then out of (4) we get points $B_1$ and $C_1$ of the form

$$B_1=(ab+bd-bc,a+b-c+d),$$
$$C_1=(ac+cd-bc,a-b+c+d).$$

The line $B_1C_1$ has the equation $2x-(a+d)y+(a+d)^2-(a+d)(b+c)+2bc=0$, and its intersections $A_1$ and $D_1$ with lines $\mathcal{A}$ and $\mathcal{D}$ with equations (3) are points having ordinates

$$\frac{1}{d-a}[d^2+2ad-a^2-(a+d)(b+c)+2bc],$$
$$\frac{1}{a-d}[a^2+2ad-d^2-(a+d)(b+c)+2bc],$$

so the midpoint of these points $A_1$ and $D_1$ has an ordinate $a+d$, the midpoint of $B_1$ and $C_1$ has the same ordinate as well. Because of that *directed lengths $A_1B_1$ and $C_1D_1$ are equal*. This statement we find in [35]. We see that: *the common midpoint of the line segments $A_1D_1$ and $B_1C_1$ is incident with the diameter of the parabola $\mathcal{P}$ through the point $T_{AD}$*. There are five more analogous statements where we find common midpoints of the pairs of line segments on diameters of parabola $\mathcal{P}$ through other five vertices of the quadrilateral $\mathcal{ABCD}$.
The median $\mathcal{N}$ with the equation $y=\frac{1}{2}(a+b+c+d)$ intersects the line $\mathcal{A}$ with the equation $ay=x+a^2$ in the point $\mathcal{A}\cap\mathcal{N}=(\frac{1}{2}(ab+ac+ad-a^2),\frac{1}{2}(a+b+c+d))$, and a midpoint of that point and point $T_{BC}=(bc,b+c)$ is the point

$$\Big(\frac{1}{4}(ab+ac+ad-a^2+2bc),\frac{1}{4}(a+3b+3c+d)\Big).$$

This midpoint is incident with the line

$$2x-(a+b+c-d)y+\frac{1}{4}(3a^2+3b^2+3c^2-d^2+2ab+$$
$$+2ac+2bc-2ad-2bd-2cd)=0.$$

Midpoints of the pairs $\mathcal{B}\cap\mathcal{N}, T_{AC}$ and $\mathcal{C}\cap\mathcal{N}, T_{AB}$ are incident with it as well. Hence, that line is a median of the quadrilateral $\mathcal{ABCN}$. Its intersection with the line $\mathcal{N}$ is the point $(\frac{1}{2}(4q-s^2), \frac{1}{2}s)$ that is incident with medians of quadrilaterals $\mathcal{ABDN}$, $\mathcal{ACDN}$, $\mathcal{BCDN}$. It is point $QL-P23$ in [43].

Points symmetric to intersections of the given line with sides of given triangle with respect to the midpoints of these lines are incident with one line that are said to be *reciprocal* to given line with respect to given triangle.

Let us determine the line $\mathcal{D}'$ reciprocal to the line $\mathcal{D}$ with respect to trilateral $\mathcal{ABC}$. A point on the line $\mathcal{A}$ symmetric to the point $T_{AD}$ with respect to the midpoints $T_{AB}$ and $T_{AC}$ is of the form $(ab+ac-ad, a+b+c-d)$. Out of symmetry on $a,b,c$ of the ordinate of that point we conclude that the same ordinate is achieved in a similar procedure with lines $\mathcal{B}$ and $\mathcal{C}$. So, *the equation of $\mathcal{D}'$ is $y=a+b+c-d$ and it is parallel to the median $\mathcal{N}$ of the quadrilateral $\mathcal{ABCD}$.* This statement is coming from both [17] and [31]. Analogously, lines $\mathcal{A}', \mathcal{B}', \mathcal{C}'$ reciprocal to lines $\mathcal{A}$, $\mathcal{B}$, $\mathcal{C}$ with respect to trilaterals $\mathcal{BCD}$, $\mathcal{ACD}$, $\mathcal{ABD}$ have equations $y=-a+b+c+d$, $y=a-b+c+d$, $y=a+b-c+d$. Adding up these four equations, we find $4y=2(a+b+c+d)$, i.e. the equation $y=\frac{1}{2}s$ of the median $\mathcal{N}$. Hence, the median of the quadrilateral $\mathcal{ABCD}$ is so-called *centroid line* of the lines $\mathcal{A}', \mathcal{B}', \mathcal{C}', \mathcal{D}'$.

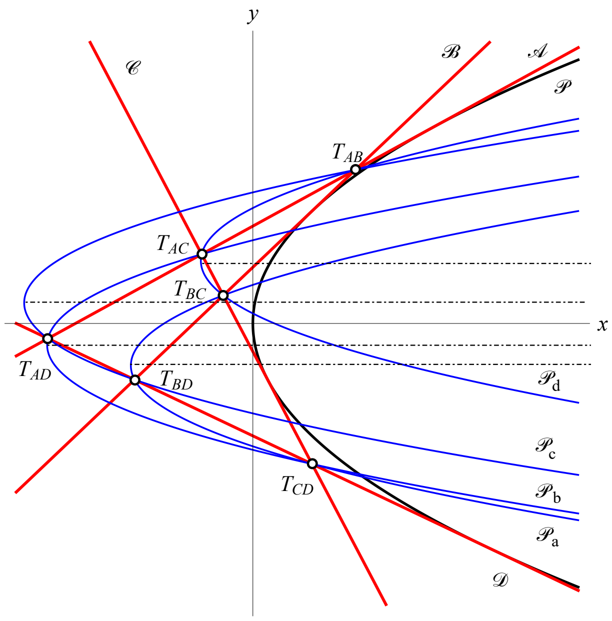


Figure 2: *Parabolas circumscribed to trilaterals*

*Lines $\mathcal{D}$ and $\mathcal{D}'$ are reciprocal with respect to trilateral* $\mathcal{ABC}$ and that relationship is symmetric on that two lines, so as *the line $\mathcal{D}'$ is parallel to the median of the quadrilateral $\mathcal{ABCD}$, then and the line $\mathcal{D}$ is parallel to the median of the quadrilateral $\mathcal{ABCD}'$.* Similar is valid for the other sides of the quadrilateral $\mathcal{ABCD}$ and their reciprocal lines $\mathcal{A}'$, $\mathcal{B}'$, $\mathcal{C}'$. This statement is found in [39].

In [12] it is stated:

*Parabolas inscribed to trilaterals formed by three sides of the quadrilateral with axes parallel to the axis of parabola inscribed to that quadrilateral arises from this inscribed parabola by using translations.*

The statement is not quite correct.

Namely, parabola $\mathcal{P}_d$ with equation

$$y^2-(a+b+c)y=x-ab-ac-bc$$

is incident with points $T_{AB}, T_{AC}, T_{BC}$, i. e. it is circumscribed to the trilateral $\mathcal{ABC}$, and it has an axis parallel to the axis of $\mathcal{P}$, but its parameter is equal to the quarter of the parameter of $\mathcal{P}$. See Figure 2. Hence the following theorem is valid:

**Theorem 1** *The parabolas $\mathcal{P}_a$, $\mathcal{P}_b$, $\mathcal{P}_c$, $\mathcal{P}_d$ inscribed to trilaterals $\mathcal{BCD}$, $\mathcal{ACD}$, $\mathcal{ABD}$, $\mathcal{ABC}$ arise from each other by translations. The parameter of these parabolas is equal to the quarter of the parameter of $\mathcal{P}$ .*

For example, substituting

$$x \to x+\frac{1}{4}(c-d)(2a+2b-c-d),$$
$$y \to y+\frac{1}{2}(c-d)$$

the equation of $\mathcal{P}_d$ turns into $y^2-(a+b+d)y=x-ab-ad-bd$ that is the equation of $\mathcal{P}_c$.

A parabola with an equation $12x=9y^2-6sy+4q$ passes through the centroid $G_d=(\frac{1}{3}(ab+ac+bc), \frac{2}{3}(a+b+c))$ of the trilateral $\mathcal{ABC}$, and then through centroids of other three trilaterals of the quadrilateral $\mathcal{ABCD}$. A vertex of this parabola is the point $(\frac{1}{12}(4q-s^2), \frac{1}{3}s)$, and its axis has the equation $y=\frac{1}{3}s$, so *the distance from the focus $S$ of the quadrilateral $\mathcal{ABCD}$ to its median is equal to three halves of the distance from this focus to this parabola.* This statement is from [5] and [6].

The parabola $\mathcal{P}$ inscribed to the quadrilateral $\mathcal{ABCD}$ is circumscribed to the quadrangle $ABCD$. However, there is one more parabola circumscribed to that quadrangle. It is parabola with the equation

$$x^2-\frac{1}{2}sxy+\frac{1}{16}s^2y^2+(q-\frac{1}{4}s^2)x-\frac{1}{2}ry+p=0,$$

because for example for the point $A=(a^2,2a)$ we get equality $a^4-a^3s+a^2q-ar+p=0$. The square part of previous equation is $\frac{1}{16}(4x-sy)^2$, so it follows that the axis of this parabola has the slope $\frac{4}{s}$. The slope of connecting line of the focus $S=(1,0)$ and the intersection point $Q=(-1,\frac{1}{2}s)$ of the median and the directrix is equal to $\frac{-s}{4}$. It proves that *the axis of studied parabola is perpendicular to the connecting line SQ*, see [43].

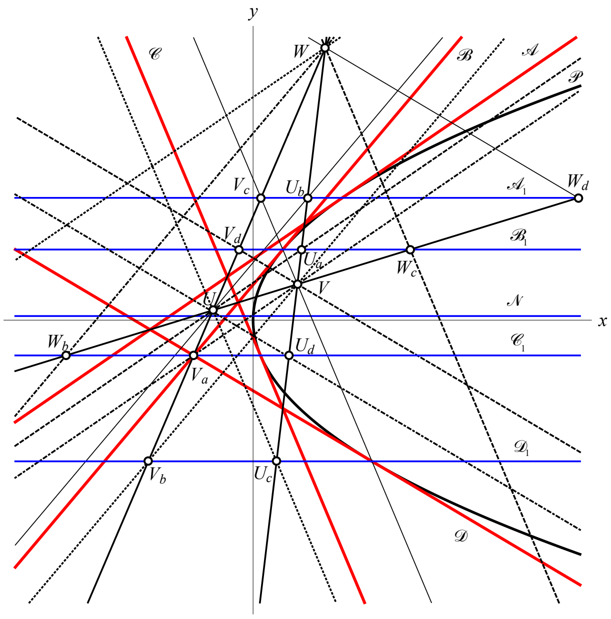


Figure 3: *Lines $\mathcal{A}_1$, $\mathcal{B}_1$, $\mathcal{C}_1$, $\mathcal{D}_1$ are parallel to the median $\mathcal{N}$*

A line through the point $U$ from (6), parallel to the line $\mathcal{B}$ has the equation

$$(c+d-a-b)(x-by)=2ab^2+acd-abc-abd-bcd$$

and intersects the line $\mathcal{U}$ from (5) in the point $\mathcal{U}_b$ with coordinates

$$x=\frac{1}{c+d-a-b}(abc+abd+acd-bcd-2a^2b),$$
$$y=2a.$$

Analogously, a line parallel to the line $\mathcal{C}$ and incident with $V$ intersects a line $\mathcal{V}$ in the point $V_c$ with coordinates

$$x=\frac{1}{b+d-a-c}(abc+abd+acd-bcd-2a^2c),$$
$$y=2a,$$

and the line parallel to the line $\mathcal{D}$ and incident with $W$ intersects a line $\mathcal{W}$ in the point $W_d$ with coordinates

$$x=\frac{1}{b+c-a-d}(abc+abd+acd-bcd-2a^2d),$$
$$y=2a.$$

*The points $U_b,V_c,W_d$ are incident with one line $\mathcal{A}_1$ with the equation $y=2a$. Analogously, sets of three similar points $U_a,V_d,W_c$; $U_d,V_a,W_b$; $U_c,V_b,W_a$ are incident with lines $\mathcal{B}_1$, $\mathcal{C}_1$, $\mathcal{D}_1$, respectively, and lines $\mathcal{A}_1$, $\mathcal{B}_1$, $\mathcal{C}_1$, $\mathcal{D}_1$ are parallel (see Figure 3).* This is statement from [26]. During this process, the new result has appeared:

**Theorem 2** *All four lines $\mathcal{A}_1$, $\mathcal{B}_1$, $\mathcal{C}_1$, $\mathcal{D}_1$ are parallel to the median $\mathcal{N}$ of the quadrilateral $\mathcal{ABCD}$, and the median is their centroid line.*

Altitudes from the vertices $T_{BC},T_{AC},T_{AB}$ in the triangle $T_{BC}T_{AC}T_{AB}$ have equations $y=-ax+b+c+abc$, $y=-bx+a+c+abc$, $y=-cx+a+b+abc$ and they are intersected in the point $H_d=(-1,a+b+c+abc)$ that is orthocenter of that triangle, i. e. of the trilateral $\mathcal{ABC}$. Similarly, orthocenters of trilaterals $\mathcal{ABD}$, $\mathcal{ACD}$, $\mathcal{BCD}$ are points

$$H_c=(-1,a+b+d+abd),$$
$$H_b=(-1,a+c+d+acd),$$
$$H_a=(-1,b+c+d+bcd).$$

All four orthocenters lie on the line $\mathcal{H}$ with the equation

$$\mathcal{H}\ldots x=-1, \tag{11}$$

which is the directrix of the inscribed parabola $\mathcal{P}$ of the quadrilateral $\mathcal{ABCD}$ and they have the centroid $G_h=(-1,\frac{1}{4}(3s+r))$. The statement that *these four orthocenters are incident with one line* is given in [37] without proof. The proof is given in [23]. In the literature, the line $\mathcal{H}$ has many names, herein we will call it a *directrix* of the quadrilateral $\mathcal{ABCD}$. The intersection point of the median and the directrix of the quadrilateral $\mathcal{ABCD}$ is the point

$$Q=(-1,\frac{1}{2}s) \tag{12}$$

which is called $QL-P7$ Newton-Steiner point in [43]. The midpoint of this point and the focus $S=(1,0)$ is the point $(0,\frac{1}{4}s)$ that is in [43] denoted by $QL-P19$.
The line through $H_a=(-1,b+c+d+bcd)$, parallel to the line $\mathcal{A}$ has the equation $x-ay+1+ab+ac+ad+abcd=0$ and goes through the point $(-1-ab-abcd,c+d)$ where the line $\mathcal{H}_b$, parallel to $\mathcal{B}$ passes as well. The line through $H_a$, perpendicular to $\mathcal{A}$ has the equation $ax+y=-a+b+c+d+bcd$ and goes through the point $(-2-cd,a+b+c+d+acd+bcd)$, through which the line perpendicular to $\mathcal{B}$ through the point $H_b$ passes as well. The connecting line of two obtained points has the equation

$$(a+b)x+(1-ab)y+a+b-c-d+a^2b+ab^2+$$
$$+abc+abd+a^2bcd+ab^2cd=0$$

and passes through the point $(-2-abcd,a+b+c+d)$. Five analogous lines are incident with that point as well.

Hence, *quadrilaterals, that are formed by the lines that passes through points $H_a$, $H_b$, $H_c$, $H_d$, parallel to lines $\mathcal{A},\mathcal{B},\mathcal{C},\mathcal{D}$, and perpendicular to these lines, are perspective.* A centre of the perspectivity is the point $(-p-2,s)$, which in [43] is called $QL-P21$ adjunct orthocenter homothetic center, although this is not homothecy. The point $(-1-ab-abcd,c+d)$ and the point $T_{AB}=(ab,a+b)$ have for the midpoint the point $(\frac{1}{2}(1+abcd),\frac{1}{2}(a+b+c+d))$, and similar is valid for five more pairs of corresponding points. It means that *the quadrilateral, formed by parallels to $\mathcal{A},\mathcal{B},\mathcal{C},\mathcal{D}$ through the points $H_a$, $H_b$, $H_c$, $H_d$ is symmetric to the quadrilateral $\mathcal{ABCD}$ with respect to the point $(-\frac{1}{2}(1+p),\frac{1}{2}s)$ that is in [43] called $QL-P20$ orthocenter homothetic center. It is obviously incident with the median $\mathcal{N}$.*

In the quadrilateral $T_{AB}T_{BC}T_{BD}T_{AD}$ perpendiculars from points $T_{AC}$ and $T_{BC}$ to the line $\mathcal{D}$ pass through orthocenters $H_a$ and $H_b$ of trilaterals $\mathcal{BCD}$ and $\mathcal{ACD}$, hence the perpendicular from the midpoint of the side $T_{AC}T_{BC}$ to the opposite side $T_{BD}T_{AD}$ passes through the midpoint of $H_a$ and $H_b$. In the same way, the perpendiculars from $T_{BD}$ and $T_{AD}$ to the line $\mathcal{D}$ pass through the orthocenters $H_a$ and $H_b$ and because of that the perpendicular from the midpoint of $T_{BD}T_{AD}$ to the opposite side $T_{AC}T_{BC}$ passes through the midpoint of $H_a$ and $H_b$. So, *for the pair of opposite sides $T_{AC}T_{BC}$, $T_{BD}T_{AD}$ perpendiculars from the midpoint of the each of them to the opposite side are intersected in one point on the directrix, which is the midpoint of $H_a$ and $H_b$.* In the same way it is shown that for *the pair of opposite sides $T_{AC}T_{AD}$, $T_{BD}T_{BC}$ perpendiculars from the midpoint of the each of them to the opposite side are intersected in one point on the directrix, which is the midpoint of $H_c$ and $H_d$.* Analogously it is valid for the quadrangles $T_{AB}T_{AD}T_{CD}T_{BC}$ and $T_{AB}T_{AC}T_{CD}T_{BD}$, so we get four more times per two lines, that are intersected in midpoints of pairs of orthocenters $H_a,H_c$ and $H_b,H_d$, and $H_a,H_d$ and $H_b,H_c$.
The distance of the focus $S$ of the quadrilateral $\mathcal{ABCD}$ to its median $\mathcal{N}$ and to its directrix $\mathcal{H}$ are equal to $\frac{1}{2}s$ and 1, so their ratio is $\frac{1}{2}s=\frac{1}{2}(a+b+c+d)$. However, for example the line $\mathcal{A}$ has an equality $\cot\angle(\mathcal{N},\mathcal{A})=a$, so that *the ratio we have mentioned is equal to* $\frac{1}{2}[\cot\angle(\mathcal{N},\mathcal{A})+\cot\angle(\mathcal{N},\mathcal{B})+\cot\angle(\mathcal{N},\mathcal{C})+\cot\angle(\mathcal{N},\mathcal{D})]$ that is statement found in [27].

If $\mathcal{L}$ is line having equation $y=mx+n$, then the perpendicular from $T_{AB}$ to that line has the equation $x+my=ab+am+bm$, and the intersection point of that two lines has the coordinates $x=\frac{1}{\eta}(am+bm-mn+ab), y=\frac{1}{\eta}(am^2+bm^2+abm+n)$, where $\eta=m^2+1$. The perpendicular from that intersection point to line $\mathcal{C}$ has the equation $\eta(cx+y)=acm+bcm-cmn+abc+am^2+bm^2+abm+n$. It can be checked that this line passes through the point with coordinates

$$x=-\frac{1}{\eta}(m^2+mn), \tag{13}$$
$$y=\frac{1}{\eta}[(a+b+c)m^2+(ab+ac+bc)m+abc+n].$$

The perpendiculars to lines $\mathcal{A}$ and $\mathcal{B}$ from pedals of perpendiculars from points $T_{BC}$ and $T_{AC}$ to the line $\mathcal{L}$ are incident with the point (13).
Because of that this point is an orthopole of the line $\mathcal{L}$ with respect to the trilateral $\mathcal{ABC}$. Similarly, the same is valid for the trilaterals $\mathcal{BCD}$, $\mathcal{ACD}$, $\mathcal{ABD}$. Hence, *all four orthopoles are incident with the line having equation $x=-\frac{1}{\eta}(m^2+mn)$ that is perpendicular to the median of the quadrilateral $\mathcal{ABCD}$.* This statement is from [21]. *If for the line $\mathcal{L}$ the line $\mathcal{D}$ is taken, then $m=\frac{1}{d}, n=d, \eta=\frac{1}{\delta}\cdot d^2$ are valid, so for the orthopole of the line $\mathcal{D}$ with respect to the trilateral $\mathcal{ABC}$ we get the point*

$$O_d=\Big(-1,\frac{1}{\delta}[a+b+c+(ab+ac+bc)d+abcd^2+d^3]\Big), \tag{14}$$

*that is incident with the directrix of the quadrilateral $\mathcal{ABCD}$ as well as the analogous orthopoles of lines $\mathcal{A},\mathcal{B},\mathcal{C}$ with respect to the trilaterals $\mathcal{BCD}$, $\mathcal{ACD}$, $\mathcal{ABD}$.* This statement is coming from [18]. The same statement can be found in [28], but herein the author observes on these orthopoles as radical centers of pedal circles on the lines $\mathcal{A},\mathcal{B},\mathcal{C},\mathcal{D}$ with respect to trilaterals $\mathcal{BCD}$, $\mathcal{ACD}$, $\mathcal{ABD}$, $\mathcal{ABC}$, what is in accordance with so-called Lemoyne's theorem (see [18]).
In the previous proof it was assumed that $m\neq 0$. Let the line $\mathcal{L}$ be parallel with the median and with the equation $y=n$. The pedal point of the perpendicular from the point $T_{AB}$ to that line is the point $(ab,n)$, and perpendicular from that point to the line $\mathcal{C}$ has the equation $cx+y=abc+n$. This perpendicular, and two more analogous perpendiculars, are incident with the point $(0,abc+n)$ that is an orthopole of $\mathcal{L}$ with respect to the trilateral $\mathcal{ABC}$. This orthopole and orthoploes of the line $\mathcal{L}$ with respect to trilaterals $\mathcal{BCD}$, $\mathcal{ACD}$, $\mathcal{ABD}$ are incident with the $y$-axis, the vertex tangent of the parabola $\mathcal{P}$.
Let us study any line $\mathcal{L}$ parallel to the directrix with the equation $x=l$. The pedal point of the perpendicular from $T_{AB}$ to that line is the point $(l,a+b)$, and the perpendicular from that point to the line $\mathcal{C}$ has the equation $cx+y=cl+a+b$ and obviously it passes through the point $(l-1,a+b+c)$, that is orthopole of the line $\mathcal{L}$ with respect to the trilateral $\mathcal{ABC}$. As well as other three orthopoles of $\mathcal{L}$ with respect to the trilateral $\mathcal{ABD}$, $\mathcal{ACD}$, $\mathcal{BCD}$, it is incident to the line with the equation $x=l-1$, parallel to the median of $\mathcal{ABCD}$ and the line $\mathcal{L}$. Particularly, *there*

*are orthopoles of the vertex tangent of the parabola $\mathcal{P}$ with respect to trilateras $\mathcal{ABC}$, $\mathcal{ABD}$, $\mathcal{ACD}$, $\mathcal{BCD}$ on the directrix*. These statements are in [43] but they are atributed to S. Kirikami.

The line $\mathcal{L}'$, where orthopoles of the given line $\mathcal{L}$ with respect to the trilaterals $\mathcal{BCD}$, $\mathcal{ACD}$, $\mathcal{ABD}$, $\mathcal{ABC}$ are lying, is called an *orthopolar line* of the line $\mathcal{L}$ with respect to the quadrilateral $\mathcal{ABCD}$.

Earlier, we found out that the line $\mathcal{L}$ with the equation $y = mx+n$ has the orthopolar $\mathcal{L}'$ with the equation $x = -\frac{1}{\eta}(m^2+mn)$, that line $\mathcal{L}$ with the equation $y = n$ has the orthopolar $\mathcal{L}'$ with the equation $x = 0$, and the line $\mathcal{L}$ with the equation $x = l$ has the orthopolar $\mathcal{L}'$ with the equation $x = l-1$. The tangent at the point $(m^2, -2m)$ at parabola $\mathcal{P}$ has the equation $x+my+m^2 = 0$ and it is perpendicular to the given line $\mathcal{L}$ with the equation $y = mx+n$. These two lines has the intersection with the abscissa $x = -\frac{1}{\eta}(m^2+mn)$, that lies on the line $\mathcal{L}'$. The tangent line of the parabola $\mathcal{P}$ at the point $(t^2, 2t)$ has the equation $ty = x+t^2$, i.e. $m = \frac{1}{t}$, $n = t$. Because of that the orthopolar of that tangent has the equation $x = -1$, and that is directrix $\mathcal{H}$. So, *the orthopolar of any tangent of the parabola $\mathcal{P}$ is the directrix $\mathcal{H}$*. If the line $\mathcal{L}$ passes through the focus $S$, then it has the equation $y = m(x-1)$, and for it $n = -m$ is valid and orthopolar $\mathcal{L}'$ has the equation $x = 0$ and that is vertex tangent $\mathcal{Y}$ of the parabola $\mathcal{P}$.

Let $\mathcal{P}''$ be parabola, with the same focus $S = (1,0)$ and the same axis as parabola $\mathcal{P}$. If its directrix has the equation $x = t$, then that parabola $\mathcal{P}''$ has the equation $(x-1)^2+y^2 = (x-t)^2$, that after simplifying, reaches the form $y^2 = 2(1-t)x+t^2-1$. The intersections of this parabola and parabola $\mathcal{P}$ with equation $y^2 = 4x$ are the points $(x', y') = (\frac{1}{2}(t-1), \pm\sqrt{2(t-1)})$, where $t > 1$. Tangents at these points to both parabolas have the slopes $\frac{2}{y'}$ and $\frac{1-t}{y'}$, whose product is equal to $-1$, because $y'^2 = 2(t-1)$. That is the reason why those two parabolas are orthogonal which is special case of very well known fact that confocal conics are orthogonal. Let $(x'', y'')$ be any point of parabola $\mathcal{P}''$. Tangent at this point to this parabola has the equation $yy' = (1-t)(x+x'')+t^2-1$, so because of it $m = \frac{1-t}{y''}, n = 1-ty''(x''-t-1)$ are valid and we get

$$\begin{aligned} y''^2(m^2+mn) &= (1-t)^2(x''-t), \\ y''^2(m^2+1) &= (1-t)^2+y''^2 \\ &= (1-t)^2+2(1-t)x''+t^2-1 \\ &= 2(1-t)(x''-t), \end{aligned}$$

where we use the equality $y''^2 = 2(1-t)x''+t^2-1$, because the point $(x'', y'')$ is incident with parabola $\mathcal{P}''$. Because of this $-\frac{1}{\eta}(m^2+mn) = \frac{1}{2}(t-1)$ is valid, so each tangent line of parabola $\mathcal{P}$ has the same orthopolar with the equation $x = \frac{1}{2}(t-1)$ that passes through the intersections $(\frac{1}{2}(t-1), \pm\sqrt{2(t-1)})$ of parabolas $\mathcal{P}$ and $\mathcal{P}''$. Hence, *all lines with the same orthopolar $\mathcal{L}$ perpendicular to median $\mathcal{N}$ are tangents to parabola $\mathcal{P}''$ which has the same focus and the same axis as parabola $\mathcal{P}$ and it is orthogonal to it at the intersection points with the line $\mathcal{L}'$*. These statements found in [43] are attributed to T. Q. Hung. The line $\mathcal{L}'$ with the equation $x = \frac{1}{2}(t-1)$ is the bisector of directrices of $\mathcal{P}$ and $\mathcal{P}'$ that have equations $x = -1$ and $x = t$.

The circle $\mathcal{S}_d$ through the points $T_{BC}, T_{AC}, T_{AB}$ from (4), i.e. the circumscribed circle to the trilateral $\mathcal{ABC}$, has the equation

$$\begin{aligned} &x^2+y^2-(ab+ac+bc+1)x-(a+b+c-abc)y+ \\ &+ab+ac+bc = 0, \end{aligned} \tag{15}$$

the center

$$S_d = \Big(\frac{1}{2}(ab+ac+bc+1), \frac{1}{2}(a+b+c-abc)\Big), \tag{16}$$

and the radius $\rho_d$ given by $4\rho_d{}^2 = (ab+ac+bc-1)^2+(a+b+c-abc)^2$, that is actually the formula

$$4\rho_d{}^2 = (a^2+1)(b^2+1)(c^2+1). \tag{17}$$

The circles $\mathcal{S}_a, \mathcal{S}_b, \mathcal{S}_c$ circumscribed to trilaterals $\mathcal{BCD}$, $\mathcal{ACD}$, $\mathcal{ABD}$, respectively, have the similar equations. The circle (15) passes through the point

$$S = (1,0), \tag{18}$$

that is focus of inscribed parabola $\mathcal{P}$ of the quadrilateral $\mathcal{ABCD}$, here we will call it a *focus* of this quadrilateral, although there are different names in the literature. W. Wallace has the fact that *four mentioned circles are incident with one point* in [34].

The point $P20 = (-\frac{1}{2}(p+1), \frac{1}{2}s)$ is the midpoint of the focus $S = (1,0)$ and the point $P21 = (-p-2, s)$, and the point $P19 = (0, \frac{1}{4}s)$ is the midpoint of the point $S$ and the point $Q$ from (12), because of that *lines $P20P19$ and $P21Q$ are parallel* (see [43]).

The line through the point $T_{BC}$ parallel to $\mathcal{A}$ has the equation $x-ay = bc-ab-ac$, and a connecting line $AS$ of the points $A = (a^2, 2a)$ and $S = (1,0)$ has the equation $2ax+(1-a^2)y = 2a$. Those lines are intersected in

$$\begin{aligned} &\Big(\frac{1}{\alpha}(a^3b+a^3c-a^2bc+2a^2-ab-ac+bc), \\ &\frac{1}{\alpha}(2a-2abc+2a^2b+2a^2c)\Big) \end{aligned}$$

that lies on the circle $\mathcal{S}_d$ with the equation (15). Hence, *the parallel line to the line $\mathcal{A}$ through the point $T_{BC}$ intersects the circle $\mathcal{S}_d$ residually (except at the point $T_{BC}$) at the point on the line AS, and then by analogy, the other two intersection points of the circles $\mathcal{S}_b$ and $\mathcal{S}_c$ with lines through the points $T_{CD}$ and $T_{BD}$ parallel to the line $\mathcal{A}$ are incident with* *that line too. Similarly, we have three points each on lines BS, CS and DS.* This is statement from [7] and [8].

The line $\mathcal{A}$ with the equation $x-ay+a^2=0$ intersects the $y$-axis with the equation $x=0$ at the point $(0,a)$, and line through this point has generally the equation $mx-y+a=0$. The bisector of this line and the axis $y$-axis has the equation $\frac{1}{\sqrt{\eta}}(mx-y+a)\pm x=0$, where $\eta=m^2+1$, i.e. the equation $(m\pm\sqrt{\eta})x-y+a=0$ holds. This bisector is the same as the line $\mathcal{A}$ under the condition $a(m\pm\sqrt{m^2+1})=1$, out of which $m=\frac{1}{2a}(1-a^2)$. That's the reason why the line symmetric to the $y$-axis with respect to the line $\mathcal{A}$ has the equation $(a^2-1)x+2ay=2a^2$. The line symmetric to the $y$-axis with respect to the line $\mathcal{B}$ has the equation $(b^2-1)x+2by=2b^2$, and these two lines have the intersection $(\frac{2ab}{ab+1},\frac{a+b}{ab+1})$. This intersection point lies on the line with the equation $(a+b)x+(1-ab)y=a+b$, where the points $S=(1,0)$ and $T_{AB}=(ab,a+b)$ lie as well. Hence, *the line $ST_{AB}$ passes through the intersection of lines, that are symmetrical to the lines $\mathcal{A}$ and $\mathcal{B}$ with respect to the y-axis, a vertex tangent of parabola $\mathcal{P}$. Similar statement is valid for the lines $ST_{AC},ST_{AD},ST_{BC},ST_{BD},ST_{CD}$.* These statements are in [43] attributed to S. Kirikami.

*The perpendicular from the point $S=(0,1)$ to the line $\mathcal{A}$ has the equation $ax+y=a$, the parallel line $\mathcal{H}_{ab}$ with directrix $\mathcal{H}$ through the point $T_{CD}$ has the equation $x=cd$, and the intersection point of these lines is the point $(cd,a-acd)$, that lies on the circle $S_b$* with the equation $x^2+y^2-(ac+ad+cd+1)x-(a+c+d-acd)y+ac+ad+cd=0$, analogous to the one in (15). Similar to this, *the perpendicular from the point S to the line $\mathcal{B}$ intersects the line $\mathcal{H}_{ab}$ in the point $(cd,b-bcd)$ that lies on the circle $\mathcal{S}_b$. There are five more analogous lines $\mathcal{H}_{ac},\mathcal{H}_{ad},\mathcal{H}_{bc},\mathcal{H}_{bd},\mathcal{H}_{cd}$ with similar properties.* This is the statement in [31].

The circle $\mathcal{E}_d$ with the equation

$$2x^2+2y^2-(ab+ac+bc-1)x-(3a+3b+3c+abc)y+$$
$$+(a+b+c)(a+b+c+abc)=0$$

passes through the midpoint $(\frac{1}{2}a(b+c),\frac{1}{2}(2a+b+c))$ of the points $T_{AB}$ and $T_{AC}$. Because of symmetry on $a,b,c$ it is Euler's circle of the triangle $T_{AB}T_{AC}T_{BC}$, i. e. the trilateral $\mathcal{ABC}$. It intersects the $y$-axis i.e. the vertex tangent of parabola $\mathcal{P}$, in the points $Y_d=(0,a+b+c)$ and $Y'_d=(0,\frac{1}{2}(a+b+c+abc))$. The circle with the equation

$$2x^2+2y^2-(ab+ac-bc+1)x-(3a+b+c+abc)y+$$
$$+a(a+b+c+abc)=0$$

passes through the midpoint of $T_{AB}$ and $T_{AC}$, but it is incident with the midpoint $(\frac{1}{2}(ab+1),\frac{1}{2}(a+b))$ of points $S$ and $T_{AB}$ as well, so because of symmetry on $b$ and $c$ it is Euler's circle of the triangle $ST_{AB}T_{AC}$. It intersects the $y$-axis in the points $(0,a)$ and $Y'_d=(0,\frac{1}{2}(a+b+c+abc))$. Because of symmetry on $a,b,c$ it follows that the point $Y'_d$ lies on Euler's circles of the triangle $ST_{AB}T_{BC}$ and the triangle $ST_{AC}T_{BC}$, that intersects the $y$-axis residually at the point $(0,b)$ and $(0,c)$, respectively. The point $S'_d=(ab+ac+bc,a+b+c-abc)$ is symmetric to the point $S=(1,0)$ with respect to the point $S_d$ from (16). The normal from that point to the line $\mathcal{A}$ with the equation $x-ay=-a^2$ has the equation $ax+y=a^2b+a^2c+a+b+c$ and intersects the line $\mathcal{A}$ at the point $(ab+ac,a+b+c)$. The symmetry of the ordinate of this point on $a,b,c$ means that the line with the equation $y=a+b+c$ is Wallace's line of the point $S'_d$ diametrically opposite to the focus $S$ on the circle $\mathcal{S}_d$, with respect to the triangle $T_{AB}T_{AC}T_{BC}$, i. e. the trilateral $\mathcal{ABC}$. That line passes through the point $Y_d=(0,a+b+c)$ and parallel to the median of the quadrilateral $\mathcal{ABCD}$. To summarize: *The Wallace's line of the point $S'_d$ diametrically opposite to the focus S on the circle $\mathcal{S}_d$, passes through an intersection point of the Euler's circle $\mathcal{E}_d$ of trilateral $\mathcal{ABC}$ and the vertex tangent of parabola $\mathcal{P}$. It is parallel to the median $\mathcal{N}$ of the quadrilateral $\mathcal{ABCD}$.* Analogous statements are valid for Euler's circles of trilaterals $\mathcal{ABD}$, $\mathcal{ACD}$, $\mathcal{BCD}$. Here we proved the statements taken from [**?**].

Let us the equations of $\mathcal{S}_d$ and $\mathcal{S}_c$ add after multiplying them by parameters $u$ and $v$ where $u+v=1$. We get the equation of the circle

$$x^2+y^2-[ab+(a+b)t+1]x-[a+b+(1-ab)t]y+$$
$$+ab+(a+b)t=0,$$

where $t=uc+vd$. It is easy to see that this circle passes through the points $(at,a+t)$ and $(bt,b+t)$ that are reached as the linear combinations $uT_{AC}+vT_{AD}$ and $uT_{BC}+vT_{BD}$. Hence, the statement from [20] is valid: *every circle through the focus S and the vertex $T_{AB}$ intersects lines $\mathcal{A}$ and $\mathcal{B}$ at the points that divide the segments $T_{AC}T_{AD}$, $T_{BC}T_{BD}$ in the same ratios.*

The line connecting $S_d$ from (16) with the point $T_{AB}$ from (4) has a slope $\frac{c-a-b-abc}{ac+bc-ab+1}$ and it is parallel to the line $\mathcal{D}$ that has slope $\frac{1}{d}$ under the condition $ab+cd-(a+b)(c+d)=1+abcd$, then because of symmetry on pairs of parameters $a,b$ and $c,d$ the following statements follow: *if $S_dT_{AB}$ is parallel to $\mathcal{D}$ then $S_cT_{AB}$ is parallel to $\mathcal{C}$, $S_aT_{CD}$ is parallel to $\mathcal{A}$, and $S_bT_{CD}$ is parallel to $\mathcal{B}$.* This statement is in [22]. Analogously, the following statement is valid:

**Theorem 3** *If $S_dT_{AB}$ is perpendicular to $\mathcal{D}$, the statements that $S_cT_{AB}$ is perpendicular to $\mathcal{C}$, $S_aT_{CD}$ is perpendicular to $\mathcal{A}$, and $S_bT_{CD}$ is perpendicular to $\mathcal{B}$ follow. The statement is valid for the other two possibilities of pairs on $a,b,c,d$.*

*The circle with the equation*

$$x^2+y^2-\frac{1}{2}(3+ab+ac+ad+bc+bd+cd-abcd)x-$$
$$-\frac{1}{2}(a+b+c+d-abc-abd-acd-bcd)y+$$
$$+\frac{1}{2}(1+ab+ac+ad+bc+bd+cd-abcd)=0$$

*passes through the point $S_d$ from (16), and because of symmetry on $a,b,c,d$ it passes through $S_b,S_c,S_d$.* For the first time, this statement is found in [29]. That circle is usually called Miquel's circle, but here we will call it the *central circle* of the quadrilateral $\mathcal{ABCD}$. Its equation can be written as

$$\mathcal{M}\ldots x^2+y^2-\frac{1}{2}(3+q-p)x+\frac{1}{2}(r-s)y-\frac{1}{2}(1+q-p)=0. \tag{19}$$

Obviously, it follows that it is incident with the focus $S$ from (18). Its center is the point

$$M=(\frac{1}{4}(3+q-p),\frac{1}{4}(s-r)) \tag{20}$$

that we will call a *central point* of the $\mathcal{ABCD}$, and its radius $\rho$ is given by formula $16\rho^2=(1-q+p)^2+(s-r)^2$. However, because $(a^2+1)(b^2+1)(c^2+1)(d^2+1)=(1-q+p)^2+(s-r)^2$ is valid, there is following formula

$$16\rho^2=(a^2+1)(b^2+1)(c^2+1)(d^2+1). \tag{21}$$

The line $x+dx=d^2$ is symmetric line to the line $\mathcal{D}$ with respect to the axis $\mathcal{X}$ of parabola $\mathcal{P}$. The line parallel to this line and passing through $S_d$ from (16) has the equation $x+dy=\frac{1}{2}(1+q-p)$ and intersects the axis $\mathcal{X}$ in the point $(\frac{1}{2}(1+q-p),0)$ which is because of symmetry on $a,b,c,d$ incident with the lines that pass through $S_a,S_b,S_c$ and that are parallel to the lines symmetric to $\mathcal{A},\mathcal{B},\mathcal{C}$ with respect to the axis $\mathcal{X}$. *This point is incident with the central circle $\mathcal{M}$* from (19). This result is attributed to R. Bouvaist in [40].

Bisectors of the segments $T_{AC}T_{BC}$ and $T_{AD}T_{BD}$ have the equations

$$cx+y=\frac{1}{2}(ac+bc)c+\frac{1}{2}(a+b+2c),$$
$$dx+y=\frac{1}{2}(ad+bd)d+\frac{1}{2}(a+b+2d)$$

and the intersection point

$$T'_{AB}=\Big(\frac{1}{2}(a+b)(c+d)+1,\frac{1}{2}(a+b)(1-cd)\Big),$$

that is incident with the circle (19). The bisectors of the segments $T'_{AC}T'_{AD}$ and $T'_{BC}T'_{BD}$ are intersected in the point

$$T'_{CD}=\Big(\frac{1}{2}(a+b)(c+d)+1,\frac{1}{2}(c+d)(1-ab)\Big),$$

on the same circle. The line $T'_{AB}T'_{CD}$ with the equation $x=\frac{1}{2}(a+b)(c+d)+1$ is parallel to the directrix $\mathcal{H}$. Similarly, we get two more lines $T'_{AC}T'_{BD}$ and $T'_{AD}T'_{BC}$ parallel to $\mathcal{H}$. A line parallel to the median through the point $T'_{AB}$ has the equation $y=\frac{1}{2}(a+b)(1-cd)$, and a connecting line of the point $T_{AB}$ with the focus $S$ has the equation $(a+b)x+(1-ab)y=a+b$, and the intersection point of these lines is the point

$$T''_{AB}=\Big(\frac{1}{2}(1+ab+cd-abcd),\frac{1}{2}(a+b)(1-cd)\Big).$$

The midpoint of the points $T''_{AB}$ and $T'_{CD}$ is the central point $M$ of the quadrilateral, so *the point $T''_{AB}$ is diametrically opposite to the point $T'_{CD}$ on the central circle $\mathcal{M}$. Similarly, there are five more diameters $T''_{AC}T'_{BD},T''_{AD}T'_{BC}$, $T''_{BC}T'_{AD},T''_{BD}T'_{AC},T''_{CD}T'_{AB}$ of the circle $\mathcal{M}$.* These results are found in [31].

The line parallel to the line $\mathcal{D}$ through the point $T_{AB}=(ab,a+b)$ has the equation $x-dy=ab-ad-bd$, a connecting line of the points $S=(1,0)$ and $T_{CD}=(cd,c+d)$ has the equation $(c+d)x+(1-cd)y=c+d$, and an intersection point of these two lines is the point with coordinates

$$x=\frac{1}{\delta}(cd-1)(ad+bd-ab)+cd+d^2,$$
$$y=\frac{1}{\delta}(c+d)(1-ab+ad+bd).$$

It is easy to check that this point is incident to the circle $\mathcal{S}_d$ with equation (15). Similarly, it is valid for two more points on the circle $\mathcal{S}_d$ so the statement, [13], that *parallels to $\mathcal{D}$ through the vertices of the trilateral $\mathcal{ABC}$ intersect a circumscribed circle of the trilateral at the points, whose connecting lines to opposite vertices of the quadrilateral $\mathcal{ABCD}$ are incident with the focus of this quadrilateral* holds. Similarly, it is valid for all other trilaterals of the quadrilateral.

If two lines $\mathcal{L}$ and $\mathcal{L}'$ have slopes $\frac{m}{n}$ and $\frac{m'}{n'}$, then for the oriented angle $\angle(\mathcal{L},\mathcal{L}')$ the following formula is valid

$$\tan\angle(\mathcal{L},\mathcal{L}')=\frac{m'n-mn'}{mm'+nn'}. \tag{22}$$

Lines $ST_{AB}$ and $ST_{AC}$ have slopes $\frac{a+b}{ab-1}$ and $\frac{c+d}{cd-1}$. If $k=\frac{k}{1}$ is the slope of the line $\mathcal{T}$, then according to (22) we get

$$\tan\angle(ST_{AB},\mathcal{T})=\frac{k(ab-1)-a-b}{ab-1+k(a+b)},$$
$$\tan\angle(\mathcal{T},ST_{CD})=\frac{k(cd-1)-c-d}{cd-1+k(c+d)}.$$

The line $\mathcal{T}$ is the bisector of the lines $ST_{AB}$ and $ST_{CD}$ under the condition

$$\frac{k(ab-1)-a-b}{ab-1+k(a+b)}+\frac{k(cd-1)-c-d}{cd-1+k(c+d)}=0,$$

that by simplifying is of the form

$$(r-s)k^2+2(p-q+1)k+s-r=0. \tag{23}$$

Symmetry on $a,b,c,d$ means that the line $\mathcal{T}$ is then the bisector of lines $ST_{AC},ST_{BD}$ and $ST_{AD},ST_{BC}$ as well. If $k_1$ and $k_2$ are slopes of the bisectors $\mathcal{T}_1$ and $\mathcal{T}_2$ of mentioned three pairs of lines, we have equalities

$$k_1+k_2=2\frac{p-q+1}{s-r}, \quad k_1k_2=-1.$$

The line with the equation $y=k(x-1)$ is incident with the point $S$ and its another intersection $T_d$ with the circle $\mathcal{S}_d$ from (15) has coordinates

$$x=\frac{1}{\kappa}[k^2+(a+b+c-abc)k+ab+ac+bc],$$
$$y=\frac{1}{\kappa}[(a+b+c-abc)k^2+(ab+ac+bc-1)k],$$

where $\kappa=k^2+1$. If that line is one bisector of $\mathcal{T}_1$ and $\mathcal{T}_2$, then in previous mentioned formulas it should be taken $k=k_1$, $k=k_2$, respectively. For other intersections $T_{d,1}$ and $T_{d,2}$ of lines $\mathcal{T}_1$ and $\mathcal{T}_2$ with the circle $\mathcal{S}_d$ we get

$$\begin{aligned}\kappa_1\kappa_2(x_2-x_1)&=({k_1}^2+1)[{k_2}^2+(a+b+c-abc)k_2+\\&+ab+ac+bc]-({k_2}^2+1)[{k_1}^2+(a+b+c-abc)k_1+\\&+ab+ac+bc]=(k_1-k_2)[(a+b+c-abc)k_1k_2+\\&+(ab+ac+bc-1)(k_1+k_2)-(a+b+c-abc)]=\\&=(k_1-k_2)[2\frac{p-q+1}{s-r}(ab+ac+bc-1)-\\&-2(a+b+c-abc)],\end{aligned}$$

$$\begin{aligned}\kappa_1\kappa_2(y_2-y_1)&=({k_1}^2+1)[(a+b+c-abc){k_2}^2+\\&+(ab+ac+bc-1)k_2]-({k_2}^2+1)[(a+b+c-\\&-abc){k_1}^2+(ab+ac+bc-1)k_1]=(k_1-k_2)[ab+\\&+ac+bc-1)k_1k_2-(a+b+c-abc)(k_1+k_2)-\\&-(ab+ac+bc-1)]=(k_1-k_2)[-2(ab+ac+bc-\\&-1)-2\frac{p-q+1}{s-r}(a+b+c-abc).\end{aligned}$$

so the line $T_{d,1}T_{d,2}$ has the slope

$$\frac{-(ab+ac+bc-1)(s-r)-(a+b+c-abc)(p-q+1)}{(ab+ac+bc-1)(p-q+1)-(a+b+c-abc)(s-r)},$$

that is equal to $-d$, because of

$$\begin{aligned}&-(ab+ac+bc-1)(s-r)-(a+b+c-abc)(p-q+1)+\\&+d(ab+ac+bc-1)(p-q+1)-\\&-d(a+b+c-abc)(s-r)=0.\end{aligned}$$

That means that this line is perpendicular to the line $\mathcal{D}$, and because of lines $\mathcal{T}_1$ and $\mathcal{T}_2$, it is diameter of the circle $\mathcal{S}_d$. Similarly, it is valid for the intersections of $\mathcal{T}_1$ and $\mathcal{T}_2$ with circles $\mathcal{S}_a$, $\mathcal{S}_b$, $\mathcal{S}_c$. We proved the statement from [40] saying:

*Diameters of the circles $\mathcal{S}_a,\mathcal{S}_b,\mathcal{S}_c,\mathcal{S}_d$ perpendicular to the lines $\mathcal{A},\mathcal{B},\mathcal{C},\mathcal{D}$, respectively, intersects these circles in two points each, one of points lies on one bisector, and the other one on the other bisector of pairs of lines $ST_{AB},ST_{CD}$; $ST_{AC},ST_{BD}$ and $ST_{AD},ST_{BC}$.*

Lines $\mathcal{T}_1$ and $\mathcal{T}_2$ are so- called *Steiner's axes* of the quadrilateral $\mathcal{ABCD}$. Because of (23) they have equation

$$y=\frac{1}{r-s}[-(p-q+1)\pm\sqrt{(p-q+1)^2+(r-s)^2}](x-1).$$

The line $SM$ has the slope $\frac{r-s}{p-q+1}$, and bisectors of pairs of lines $ST_{AB},ST_{CD}$; $ST_{AC},ST_{BD}$ and $ST_{AD},ST_{BC}$ have the slope $k$ under the condition (23). For the tangent of an angle of that bisector to the line $SM$, and according to (22), we get $\frac{r-s-k(p-q+1)}{k(r-s)+p-q+1}$, that is equal to $k$ because of (23). That is the tangent of an angle of the axis $\mathcal{X}$ to this bisector. *It means that the line SM and the axis of parabola $\mathcal{P}$ are symmetric with respect to the mentioned bisector*, and that is statement from [13].

Bisectors of the sides $\mathcal{A}$ and $\mathcal{B}$ have the equations

$$\frac{1}{\sqrt{\alpha}}(x-ay+a^2)\pm\frac{1}{\sqrt{\beta}}(x-by+b^2)=0,$$

and pairs of these two lines has the equation $\beta(x-ay+a^2)^2-\alpha(x-by+b^2)^2=0$. We find the abscissae of intersections of this degenerated conics with the median $y=\frac{1}{2}s$. If we put $y=\frac{1}{2}s$ in the previous equation then coefficients next to $x^2$ and $x$ are $\beta-\alpha=-(a^2-b^2)$ and $\beta(2a^2-as)-\alpha(2b^2-bs)=2(a^2-b^2)+(ab-1)s(a-b)$, respectively, so for solutions of this equation we have equality $(x_1+x_2)=\frac{1}{a+b}(2a+2b-s-abs)$. *Because of that the midpoint $P_{AB}$ of these two intersections has the form $(\frac{1}{2(a+b)}(a+b-c-d+abs),\frac{1}{2}s)$ and it is easy to check that is collinear to the points $S=(1,0)$ and $T_{AB}=(ab,a+b)$. Similarly, it is valid for five more lines analogous to the line $T_{AB}P_{AB}$ through the focus S.* This statement can be found in [25]. That pair of bisectors of $\mathcal{A}$ and $\mathcal{B}$ intersects the axis of inscribed parabola with equation $y=0$ in the points whose abscissae are solutions of the equation $\beta(x+a^2)^2-\alpha(x+b^2)^2=0$, for them we get $x_1+x_2=2$, so these points are symmetric with respect to the focus $S=(1,0)$. That is result of [25] as well. In that paper it is proved that *the focus and point at infinity of the median are isogonal with respect to each of four trilaterals of the quadrilateral $\mathcal{ABCD}$.* For proof of this statement it is enough to prove that for example the line $ST_{AB}$ and parallel to the median $\mathcal{N}$ through the point $T_{AB}$ are lines isogonal with respect to $\mathcal{A}$ and $\mathcal{B}$, i. e. the angle of lines $\mathcal{N}$ and $\mathcal{A}$

is equal to the angle of lines $\mathcal{B}$ and $ST_{AB}$. It easily follows from the fact that these lines have slopes equal to $0 = \frac{0}{1}$ and $\frac{1}{a}$, and $\frac{1}{b}$ and $\frac{a+b}{ab-1}$, so both of these angles have the tangent angle equal to $\frac{1}{a}$ due to (22). However, [7] has already had this statement.

The point $M_d = (\frac{1}{2}(ab+ac+bc+1), \frac{1}{2}d(1-ab-ac-bc))$ is incident with the central circle (19) and with the line having equation $dx+y-d=0$, that passes through the focus $S=(1,0)$ and it is perpendicular to the line $\mathcal{D}$. Because points $M_d$ and $S_d$ from (15) have the same abscissa, then *the line $M_dS_d$ is parallel to the directrix $\mathcal{H}$ of the quadrilateral $\mathcal{ABCD}$, the same is valid for analogous lines $M_aS_a$, $M_bS_b$, $M_cS_c$.* This is result in [1].

The perpendiculars from the points $T_{AB}$ and $T_{AC}$ to the lines $\mathcal{B}$ and $\mathcal{C}$ has equations $bx+y=ab^2+a+b$, $cx+y=ac^2+a+c$, and the intersection point is the point $(ab+ac+1, a-abc)$. That point is incident with the circle $\mathcal{S}'_a$ with equation

$$x^2+y^2-(ab+ac+ad-abcd+2)x-$$
$$-(a-abc-abd-acd)y+ab+ac+ad-abcd+1=0.$$

The intersection points of perpendiculars from points $T_{AB}$ and $T_{AD}$ to the lines $\mathcal{B}$ and $\mathcal{D}$ as well as from points $T_{AC}$ and $T_{AD}$ to lines $\mathcal{C}$ and $\mathcal{D}$ are incident with $\mathcal{S}'_a$. The circle $\mathcal{S}'_a$ obviously is incident to the focus $S=(1,0)$. The center of that circle is the point

$$S'_a = \Big(\frac{1}{2}(ab+ac+ad-abcd+2), \frac{1}{2}(a-abc-abd-acd)\Big).$$

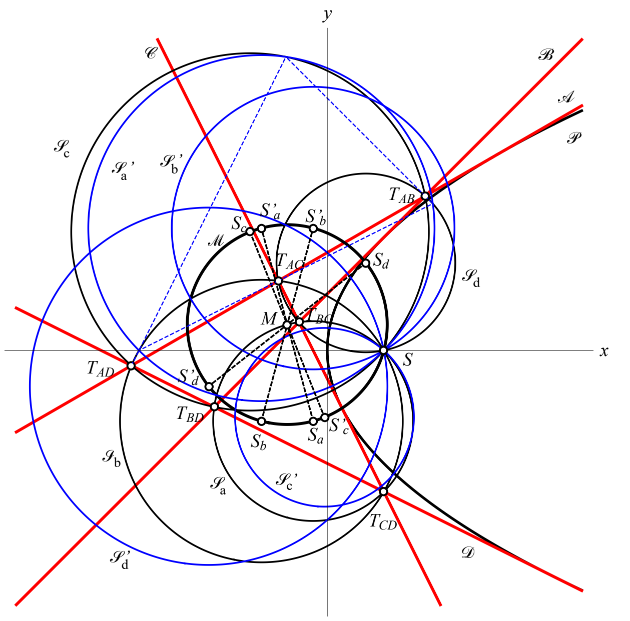


Figure 4: *Points $S'_a, S'_b, S'_c, S'_d$ are incident to the central circle $\mathcal{M}$*

The midpoint of $S'_a$ and $S_a$ from formula analogous to the formula (15) is the point $M$ from (20), the center of the central circle, so the point $S'_a$ together with the point $S_a$ is incident with that circle. Analogously, there are three more points on the central circle. The statement that *there are circles $\mathcal{S}'_a, \mathcal{S}'_b, \mathcal{S}'_c, \mathcal{S}'_d$ incident to the central circle* can be found in [43] and it is attributed to A. Hatzipolakis. Hereby, we have found out (see Figure 4) :

**Theorem 4** *The line segments $S_aS'_a, S_bS'_b, S_cS'_c, S_dS'_d$ are diameters of the central circle $\mathcal{M}$.*

Let us study now the quadrilateral $\mathcal{ABCD}'$ where $\mathcal{D}'$ is the reciprocal line to the line $\mathcal{D}$ with respect to the trilateral $\mathcal{ABC}$. The intersection point of the line $\mathcal{D}'$ and the line $\mathcal{A}$ is the point $(ab+ac-ad, a+b+c-d)$, and for the lines $\mathcal{D}'$ and $\mathcal{B}$ is the point $(ab+bc-bd, a+b+c-d)$. Two of these points and the point $T_{AB}=(ab, a+b)$ are incident to the circle

$$x^2+y^2-(2ab+ac+bc-ad-bd)x-(2a+2b+c-d-$$
$$-abc+abd)y+a^2b^2+(a+b)(a+b+c-d)=0$$

with the center $(\frac{1}{2}(2ab+ac+bc-ad-bd), \frac{1}{2}(2a+2b+c-d-abc+abd))$. This center is incident to the circle with equation

$$2x^2+2y^2-(3ab+3ac+3bc-ad-bd-cd+1+$$
$$+abcd)x-(3a+3b+3c-d-3abdc+abd+acd+$$
$$+bcd)y+a^2b^2c^2+a^2b^2+a^2c^2+b^2c^2+abcd)+$$
$$+a^2+b^2+c^2+3ad+3bd+3cd-ad-bd-cd=0,$$

and a center

$$S''_d = \Big(\frac{1}{4}(3ab+3ac+3bc-ad-bd-cd+1+abcd),$$
$$\frac{1}{4}(3a+3b+3c-d-3abc+abd+acd+bcd)\Big).$$

Out of symmetry on $a,b,c,d$ it follows that this circle is the central circle of the quadrilateral $\mathcal{ABCD}'$, so it passes through the point $S_d$. However, the midpoint of $S''_d$ and the point $M$ from (20) is the point $S_d$ from (16). Because of that the central circles of quadrilaterals $\mathcal{ABCD}$ and $\mathcal{ABCD}'$ tangent each other in the point $S_d$ and they are congruent. Similarly, it is valid for the following pairs of quadrilaterals $\mathcal{ABCD}$ and $\mathcal{ABC}'\mathcal{D}$; $\mathcal{ABCD}$ and $\mathcal{AB}'\mathcal{CD}$; and $\mathcal{ABCD}$ and $\mathcal{A}'\mathcal{BCD}$. Hence, *all five quadrilaterals $\mathcal{ABCD}$, $\mathcal{A}'\mathcal{BCD}$, $\mathcal{AB}'\mathcal{CD}$, $\mathcal{ABC}'\mathcal{D}$, $\mathcal{ABCD}'$ have the congruent central circles and the central circle of the quadrilateral $\mathcal{ABCD}$ tangents other four circles in circumcenters of trilaterals $\mathcal{BCD}$, $\mathcal{ACD}$, $\mathcal{ABD}$, $\mathcal{ABC}$.* These statements come from [2]. *If this circles have the radius $\rho$, then there is the circle of the radius $3\rho$ that is concentric to the central circle of the quadrilateral $\mathcal{ABCD}$, that other*

*four circles touch inside.* The statement is found in [41].
The line $\mathcal{A}$ with the equation (3) intersects the directrix $\mathcal{H}$ with the equation $x=-1$ at the point $A'=(-1,\frac{1}{a}(a^2-1))$. The connecting line of this point to the focus $S=(1,0)$ has the equation $(a^2-1)x+2ay=a^2-1$. *The altitude from the vertex $T_{BC}$ in the trilateral $\mathcal{ABC}$ has the equation $ax+y=b+c+abc$, the intersection point of these two lines is the point*

$$N_{D,A}=\Big(\frac{1}{\alpha}(1-a^2+2ab+2ac+2a^2bc),\\ \frac{1}{\alpha}(b-a+a^3+abc-a^2b-a^2c-a^3bc)\Big)$$

*for which we can check that it is incident to circumscribed circle $\mathcal{S}_d$ of this trilateral with equation (15). Analogously, the line $SA'$ intersects the altitudes to the side $\mathcal{A}$ in trilaterals $\mathcal{ABD}$ and $\mathcal{ACD}$ in the points $N_{C,A}$ and $N_{B,A}$, that are incident with the circumscribed circle of these trilaterals, respectively. Analogously, it is valid and for the lines $SB'$, $SC'$, $SD'$, where $B'$, $C'$, $D'$ are intersection points of the directrix $\mathcal{H}$ with the sides $\mathcal{B},\mathcal{C},\mathcal{D}$.* These statements are from [10].
The pedal $F$ of the normal from the focus $S$ to the directrix of the quadrilateral $\mathcal{ABCD}$ has coordinates $(-1,0)$, and point $S'$ that is diametrically opposite to the focus $S=(1,0)$ with respect to the central circle $\mathcal{M}$ has coordinates

$$S'=\left(\frac{1+q-p}{2},\frac{s-r}{2}\right).$$

Lines $FT_{AB}$ and $S'T_{CD}$ have equations

$$(a+b)x-(ab+1)y+a+b=0,$$
$$(c+d-a-b+r)x+(1+q-p-2cd)y=\\ =cd(c+d-a-b+r)+(c+d)(1+q-p-2cd),$$

respectively, and they are intersected in the point with coordinates

$$x=\\ \frac{(a+b)\left[c^2+d^2+c^2d^2+2cd+2p+cdp-1+ab(c^2+d^2-1)\right]}{(c+d)(a^2b^2+a^2+b^2+4ab+1)}-\\ -\frac{(c+d)(a^2+b^2-a^2b^2-1)}{(c+d)(a^2b^2+a^2+b^2+4ab+1)},$$
$$y=\\ \frac{(a+b)\left[(a+b)(c^2d^2+c^2+d^2+2cd-1)+2(c+d)(ab+1)\right]}{(c+d)(a^2b^2+a^2+b^2+4ab+1)}.$$

It can be checked that these coordinates fullfil the equation

$$(c+d)(x^2+y^2-1)-(c^2d^2+c^2+d^2+2cd-1)y=0$$

of the circle $SFT_{CD}$. Analogously, we can prove the rest of five statements.

Hence, the statement given in [19] is proved: *Let $F$ be the pedal of the normal from the focus $S$ to directrix of the quadrilateral $\mathcal{ABCD}$. Lines $FT_{AB}$, $FT_{AC}$, $FT_{AD}$, $FT_{BC}$, $FT_{BD}$ and $FT_{CD}$ intersect the circles $SFT_{CD}$, $SFT_{BD}$, $SFT_{BC}$, $SFT_{AD}$, $SFT_{AC}$ and $SFT_{AB}$ (except in $F$) in the points whose connecting lines with the points $T_{CD}$, $T_{BD}$, $T_{BC}$, $T_{AD}$, $T_{AC}$ and $T_{AB}$, respectively, pass through one point $S'$. This point $S'$ is diametrically opposite to the focus $S$ on the central circle.*
The line through points $T_{BC}$ from (4) and $S_d$ from (16) has the equation

$$(abc-a+b+c)x+(ab+ac-bc+1)y=\\ =ab^2c^2+ab^2+ac^2+abc+b+c.$$

Similarly, the line $T_{BD}S_c$ has the equation

$$(abd-a+b+c)x+(ab+ad-bd+1)y=\\ =ab^2d^2+ab^2+ad^2+abd+b+d \quad (24)$$

and for the intersection of these two lines we get the point with coordinates

$$S_A=(\frac{1}{\alpha}[a(abc+abd+acd-bcd+b+c+d)+1],\\ \frac{a}{\alpha}(-abcd+ab+ac+ad-bc-bd-cd+1)). \quad (25)$$

Because of symmetry of these coordinates on $b,c,d$ it follows that the line $T_{CD}S_b$ is incident to this point.
The central circle $\mathcal{M}$ with the equation (19) and circumscribed circle $\mathcal{S}_a$ of the trilateral $\mathcal{BCD}$ with equation $x^2+y^2-(bc+bd+cd+1)x-(b+c+d-bcd)y+bc+bd+cd=0$, analogous to the (15), have radical axis with the equation

$$(1+ab+ac+ad-bc-bd-cd-abcd)x+\\ +(a-b-c-d-abc-abd-acd+bcd)y+\\ +bc+bd+cd-ab-ac-ad-1+abcd=0.$$

The point $S_A$ from (25) is incident to this line, and as this point is incident to the circle $\mathcal{M}$, it is incident to the circle $\mathcal{S}_a$ as well. Similarly, it is valid for points $S_B,S_C,S_D$. Hence, *points $S_A,S_B,S_C,S_D$ are actually another intersection points of the circle $\mathcal{M}$ with circumscribed circle of trilaterals $\mathcal{BCD}$, $\mathcal{ACD}$, $\mathcal{ABD}$, $\mathcal{ABC}$.* A statement found in [24]: *lines $T_{BC}S_d,T_{BD}S_c,T_{CD}S_b$ are intersected in one point $S_A$ and there are three analogous points $S_B,S_C,S_D$, and these four points are incident with central circle.* On the other hand, in [30] it is proved that *these points are incident to corresponding circles $\mathcal{S}_a,\mathcal{S}_b,\mathcal{S}_c,\mathcal{S}_d$.* However, all these statements are found in [11] even earlier.

The line $SS_A$ has a slope

$$\frac{-ap+a(ab+ac+ad-bc-bd-cd)+a}{a(abc+abd+acd-bcd)+a(b+c+d-a)}=$$
$$-\frac{p-ab-ac-ad+bc+bd+cd-1}{abc+abd+acd-bcd+b+c+d-a}.$$

On the other hand, the connecting line of the point $M$ from (20) and $S_a$ from the formula analogous to the formula (15) has a slope

$$\frac{2(b+c+d-bcd)-(s-r)}{2(bc+bd+cd+1)-(3+q+p)}=$$
$$\frac{b+c+d-a+abc+abd+acd-bcd}{bc+bd+cd-ab-ac-ad+p-1},$$

so these two lines are perpendicular. The line $MS_a$ has the equation

$$\begin{aligned}&2(b+c+d-a+abc+abd+acd-bcd)x+\\&+2(1-abcd+ab+ac+ad-bc-bd-cd)y=\\&=bcdp+a(b^2c^2+b^2d^2+c^2d^2)+\\&+a(b+c+d)^2-2bcd-a+2(b+c+d).\end{aligned}$$

The midpoint of the point $S=(1,0)$ and the point $S_A$ from (25) has coordinates

$$\begin{aligned}x&=\frac{1}{2\alpha}[a(abc+abd+acd-bcd)+a(a+b+c+d)+2],\\y&=\frac{1}{2\alpha}[-a^2bcd+a(ab+ac+ad-bc-bd-cd)+a].\end{aligned}$$

It is easy to check that this point is incident with the line $MS_a$. Hence, *points $S$ and $S_A$ are symmetric with respect to the diameter $MS_a$ of the central circle*, and the point $S$ is incident with that circle, so because of that the point $S_A$ is incident to that circle as we have already proved it. In the same way, *pairs of points $S,S_B$; $S,S_C$; $S,S_D$ are symmetric with respect to lines $MS_b,MS_c,MS_d$*, respectively.
The perpendicular line from the point

$$\begin{aligned}S_D=\Big(&\frac{1}{\delta}[d(abd+acd+bcd-abc+a+b+c)+1],\\&\frac{d}{\delta}(-abcd+ad+bd+cd-ab-ac-bc+1)\Big)\end{aligned}$$

analogous to the point $S_A$ from (25) to the line $\mathcal{A}$ has the equation

$$\begin{aligned}&\delta(ax+y)=ad(abd+acd+bcd-abc+a+b+c)+a+\\&+d(-abcd+ad+bd+cd-ab-ac-bc+1)\end{aligned}$$

and it intersects the line $\mathcal{A}$ with the equation $\delta(x-ay)=-a^2d^2-a^2$ in the point with the coordinates

$$\begin{aligned}x=&\frac{1}{\alpha\delta}(a^3bd^2+a^3cd^2-a^3bcd+a^3d+abd^2)+\\&+\frac{1}{\alpha\delta}(acd^2-abcd+ad)\\y=&\frac{1}{\alpha\delta}(a^2bd^2+a^2cd^2-a^2bcd+a^3d^2+a^2d+ad^2)+\\&+\frac{1}{\alpha\delta}(bd^2+cd^2+a^3-bcd+a+d).\end{aligned}$$

This point is incident to the line $\mathcal{P}_D$ with the equation

$$\delta(x-dy)=(ab+ac+bc-ad-bd-cd)d^2-abcd-d^2.$$

The symmetry of this equation on $a,b,c$ means that on this line there are pedals of the perpendicular lines from the point $S_D$ to the lines $\mathcal{B}$ and $\mathcal{C}$, so $\mathcal{P}_D$ is Wallace's line of $S_D$ with respect to the trilateral $\mathcal{ABC}$. We see that this line is parallel to the line $\mathcal{D}$, as well as *Wallace's lines $\mathcal{P}_A,\mathcal{P}_B,\mathcal{P}_C$ of the points $S_A,S_B,S_C$ with respect to trilaterals $\mathcal{BCD}$, $\mathcal{ACD}$, $\mathcal{ABD}$ parallel to the lines $\mathcal{A}$, $\mathcal{B}$, $\mathcal{C}$*, respectively. This result is found in [15] and [14].
The line $ST_{CD}$ has the equation $(c+d)x+(1-cd)y=c+d$. It is incident with the point

$$S_{CD}=\Big(\frac{1}{2}(1+ab+cd-abcd),\frac{1}{2}(c+d)(1-ab)\Big)\qquad(26)$$

that is incident with the circle $\mathcal{M}$ from (19). Because of that $S_{CD}$ is another intersection (one is $S$) of this circle with the line $ST_{CD}$. The circle $\mathcal{S}_{CD}$ with the equation

$$\begin{aligned}&x^2+y^2-(1+ab+cd-abcd)x-(c+d)(1-ab)y+\\&+cd(1+ab-abcd)-ab(c+d)^2=0\end{aligned}\qquad(27)$$

has the center $S_{CD}$ and the radius $\rho_{CD}$ given by $\rho_{CD}{}^2=(ab+1)^2(c^2+1)(d^2+1)$. It can be checked that this circle passes through $T_{CD}=(cd,c+d)$ and through the point $S_A$ from (25), and because of symmetry on $a$ and $b$ it is incident with $S_B$. Hence, the circle $\mathcal{S}_{CD}$ with the center $S_{CD}$ passes through the points $T_{CD},S_A,S_B$.

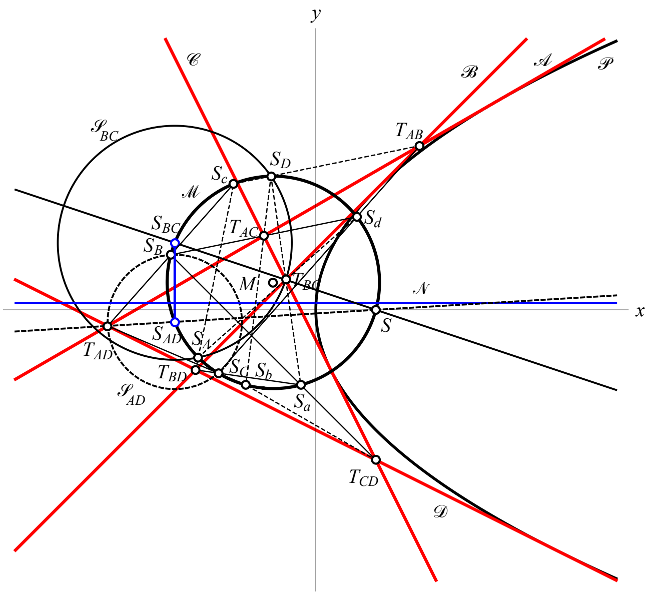


Figure 5: *An illustration of Theorem 5 on the example of the line $S_{AD}S_{BC}$*

Therefore, *if $S_{AB}, S_{AC}, S_{AD}, S_{BC}, S_{BD}, S_{CD}$ are another intersections of the circle $\mathcal{M}$ (one is $S$) with lines $ST_{AB}, ST_{AC}, ST_{AD}, ST_{BC}, ST_{BD}, ST_{CD}$, then there are circles $\mathcal{S}_{AB}, \mathcal{S}_{AC}, \mathcal{S}_{AD}, \mathcal{S}_{BC}, \mathcal{S}_{BD}, \mathcal{S}_{CD}$ with the centers $S_{AB}, S_{AC}, S_{AD}, S_{BC}, S_{BD}, S_{CD}$, that passes through the triples of points $T_{AB}, S_C, S_D$; $T_{AC}, S_B, S_D$; $T_{AD}, S_B, S_C$; $T_{BC}, S_A, S_D$; $T_{BD}, S_A, S_C$; $T_{CD}, S_A, S_B$, respectively.* The point $S_{AB}$ has the same abscissa as the point $S_{CD}$ in (26), so the line $S_{AB}S_{CD}$ has the equation $x = \frac{1}{2}(1+ab+cd-abcd)$ and it is perpendicular to the median of the quadrilateral $\mathcal{ABCD}$. Hence, our new result is:

**Theorem 5** *If $S_{AB}, S_{AC}, S_{AD}, S_{BC}, S_{BD}, S_{CD}$ are another intersections of the circle $\mathcal{M}$ (one is $S$) with lines $ST_{AB}, ST_{AC}, ST_{AD}, ST_{BC}, ST_{BD}, ST_{CD}$ then lines $S_{AB}S_{CD}$, $S_{AC}S_{BD}$ and $S_{AD}S_{BC}$ are perpendicular to the median of the quadrilateral $\mathcal{ABCD}$.*

Let us find another intersection (except $T_{CD}$) of the line $\mathcal{C}$ and the circle $\mathcal{S}_{CD}$. Putting $x = cy - c^2$ in the equation (27), simplifying and dropping off the factor $c^2+1$, we get ordinate from the equation $y^2 - (2c+d-abc)y + (c+d)(c-abd) = 0$. The solution $y = c+d$ corresponds to the point $T_{CD}$, and another solution $y = c - abd$ gives $x = -abcd$, i.e. another intersection is the point $T_{CE} = (-p, c-abd)$. The circle $\mathcal{S}_{CD}$ is incident with it as well as circles $\mathcal{S}_{AC}$ and $\mathcal{S}_{BC}$ because of symmetry on $a, b, d$. This point is incident with the line $\mathcal{E}$ with the equation $x = -p$ which is perpendicular to the median $\mathcal{N}$ of the quadrilateral $\mathcal{ABCD}$. This line intersects $\mathcal{A}$, $\mathcal{B}$, $\mathcal{D}$ in the points $T_{AE} = (-p, a-bcd)$, $T_{BE} = (-p, b-acd)$, $T_{DE} = (-p, d-abc)$, which triplets of circles $\mathcal{S}_{AB}$, $\mathcal{S}_{AC}$, $\mathcal{S}_{AD}$; $\mathcal{S}_{AB}$, $\mathcal{S}_{BC}$, $\mathcal{S}_{BD}$; $\mathcal{S}_{AD}$, $\mathcal{S}_{BD}$, $\mathcal{S}_{CD}$, respectively, are incident with. Let us study a quadrilateral $\mathcal{ABCE}$. *The circle $\mathcal{S}_{AB}$ is incident with $T_{AB}, T_{AE}, T_{BE}$, so it is circumscribed circle to the trilateral $\mathcal{ABE}$. Similarly, the circles $\mathcal{S}_{AC}$ and $\mathcal{S}_{BC}$ are circumscribed circles to the trilaterals $\mathcal{ACE}$ and $\mathcal{BCE}$. We know from earlier that $\mathcal{S}_d$ is the circumscribed circle to $\mathcal{ABC}$. All of these four circles are incident to the point $S_D$ so it is the focus of the quadrilateral $\mathcal{ABCE}$. The centers of these circles are incident with the central circle $\mathcal{M}$, then this circle is the central circle of this quadrilateral as well. Similarly, quadrilaterals $\mathcal{ABDE}$, $\mathcal{ACDE}$, $\mathcal{BCDE}$ have focuses $S_C, S_B, S_A$, and the central circle is the circle $\mathcal{M}$ as well.* These statements are found in [36].

Hereby, we give the new result. Points $T_{AB} = (ab, a+b)$ and $T_{CE} = (-p, c-abd)$ have the midpoint $(\frac{1}{2}(ab-abcd), \frac{1}{2}(a+b+c-abd)$ that is incident with the line $\mathcal{N}_d$ with the equation $y + dx = \frac{1}{2}(a+b+c-abcd^2)$. Because of symmetry on $a, b, c$ this line is incident with midpoints of pairs of points $T_{AC}, T_{BE}$ and $T_{BC}, T_{AE}$, so $\mathcal{N}_d$ is the median of the quadrilateral $\mathcal{ABCE}$. It is perpendicular to the line $\mathcal{D}$. Similarly, it is valid for medians $\mathcal{N}_a$, $\mathcal{N}_b$, $\mathcal{N}_c$. So:

**Theorem 6** *Medians $\mathcal{N}_a$, $\mathcal{N}_b$, $\mathcal{N}_c$, $\mathcal{N}_d$ of the quadrilaterals $\mathcal{BCDE}$, $\mathcal{ACDE}$, $\mathcal{ABDE}$, $\mathcal{ABCE}$ are perpendicular to $\mathcal{A}, \mathcal{B}, \mathcal{C}, \mathcal{D}$ and intersect median $\mathcal{N}$ in one point*

$$N = \left(-\frac{1}{2}(p+1), \frac{1}{2}s\right). \tag{28}$$

For Theorem 6 see Figure 6.

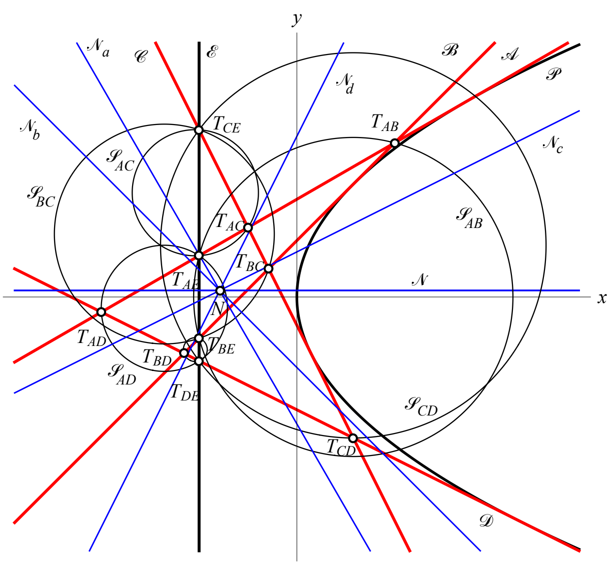


Figure 6: *Medians $\mathcal{N}_a$, $\mathcal{N}_b$, $\mathcal{N}_c$, $\mathcal{N}_d$, and $\mathcal{N}$ are intersected in the point $N$*

The line $T_{BD}S_c$ has the equation (24) and it is easy to check that is incident to $S_A$ from (25), and similarly, lines $T_{BC}S_d$ and $T_{CD}S_b$ pass through the point $S_A$. The point $T_{CE} = (-abcd, c - abd)$ and the point

$$S_{AC} = \Big(\frac{1}{2}(1 + ac + bd - abcd), \frac{1}{2}(a + c)(1 - bd)\Big) \tag{29}$$

that we achieve out of the formula (26) by a substitution $a \leftrightarrow d$, are incident with the line with the equation $(c-a)x + (1+ac)y = c - abd + ac^2 - abc^2d$, that is incident with the point $S_A$. The lines $T_{BE}S_{AB}$ and $T_{DE}S_{AD}$ are incident with $S_A$ as well. Hence, the points $S_d$, $S_c$, $S_b$, $S_{AB}$, $S_{AC}$, $S_{AD}$ are another intersections of the central circle $\mathcal{M}$ and connecting lines of the focus $S_A$ and vertices $T_{BC}, T_{BD}, T_{CD}, T_{BE}, T_{CE}, T_{DE}$ of the quadrilateral $\mathcal{BCDE}$.
The point $S_d$ from (16) is analogous to the point

$$S_c = \Big(\frac{1}{2}(ab + ad + bd + 1), \frac{1}{2}(a + b + d - abd)\Big). \tag{30}$$

It is easy to see that the connecting line $S_cS_{AC}$ have a slope equal to $\frac{1}{a}$, so that line is parallel to the line $\mathcal{A}$, i.e. it is perpendicular to the median $\mathcal{N}_a$ of the quadrilateral $\mathcal{BCDE}$. The same is valid for the lines $S_bS_{AB}$ and $S_dS_{AD}$. Analogous properties are valid for the quadrilaterals $\mathcal{ACDE}$, $\mathcal{ABDE}$ and $\mathcal{ABCE}$. The perpendicular line from the point $T_{AE} = (-p, a - bcd)$ to the line $\mathcal{B}$ has the equation $bx + y - a + bcd + ab^2cd = 0$, and a perpendicular line from the point $T_{BE}$ to the line $\mathcal{A}$ has the equation $ax + y - b + acd + a^2bcd = 0$. These two lines are intersected in the point $H_{ab} = (-abcd - cd - 1, a + b)$ which is the orthocenter of the trilateral $\mathcal{ABE}$. Hence, it is incident with directricies $\mathcal{H}_c$ and $\mathcal{H}_d$ of $\mathcal{ABDE}$ and $\mathcal{ABCE}$ that are perpendicular to the medians of these quadrilaterals and parallel to the lines $\mathcal{C}$ and $\mathcal{D}$, respectively. However, the midpoint of the point $T_{CD} = (cd, c + d)$ and the point $H_{ab}$ is the point $N$ from (28). Because of that lines $\mathcal{H}_c$ and $\mathcal{H}_d$ are symmetric to the lines $\mathcal{C}$ and $\mathcal{D}$ with respect to the point $N$. Analogously, lines $\mathcal{H}_a$ and $\mathcal{H}_b$ are symmetric to the lines $\mathcal{A}$ and $\mathcal{B}$ with respect to the point $N$. The directrix $\mathcal{H}$ of the quadrilateral $\mathcal{ABCD}$ with the equation $x = -1$ and the line $\mathcal{E}$ with the equation $x = -p$ are symmetric with respect to the point $N$. It means that the pentagonals $\mathcal{ABCDE}$ and $\mathcal{H}_a\mathcal{H}_b\mathcal{H}_c\mathcal{H}_d\mathcal{H}$ are symmetric with respect to the point $N$. The orthocenter $H_a = (-1, b + c + d + bcd)$ of the trilateral $\mathcal{BCD}$ and the intersection point $T_{AE} = (-p, a - bcd)$ of lines $\mathcal{A}$ and $\mathcal{E}$ have the midpoint $N$ from (28). Similarly, it is valid for the pairs of points $H_b, T_{BE}$; $H_c, T_{CE}$; $H_d, T_{DE}$. We have already proved that the orthocenter $H_{ab}$ of the trilateral $\mathcal{ABE}$ and the point $T_{CD}$ have the same midpoint $N$.
There is a statement from [3] and [4]:
*To every quadrilateral the fifth line can be joined so that there is a point, which is common midpoint of ten segments with one endpoint in an intersection point of any two lines of these five and the another endpoint in the orthocenter of the triangle formed by the rest three lines.*
The line $\mathcal{A}$ intersects the directrix $\mathcal{H}$ in the point $A' = (-1, \frac{1}{a}(a^2 - 1))$, and the midpoint of this point and the point $T_{BC} = (bc, b + c)$ is the point $(\frac{1}{2}(bc - 1), \frac{1}{2a}(a^2 + ab + ac - 1)$. This midpoint is incident with the line $\mathcal{N}'_d$ with the equation

$$x + abcy = \frac{1}{2}[abc(a + b + c) - 1]. \tag{31}$$

Symmetry of this equation on $a, b, c$ means that two more analogous midpoint are incident with the line $\mathcal{N}'_d$, so that line is the median of the quadrilateral $\mathcal{ABCH}$. It is incident with the point $N$ from (28), and because of symmetry on $a, b, c, d$, medians of quadrilaterals $\mathcal{ABDH}$, $\mathcal{ACDH}$, $\mathcal{BCDH}$ are incident with that point $N$ as well. This point is incident to the median $\mathcal{N}$ of the quadrilateral $\mathcal{ABCD}$. The fact that *these five medians are intersected in one point* can be found in [42]. However, we see that this point is the same point as the point $N$ from (28), so we give the new result:

**Theorem 7** *All medians of even nine quadrilaterals $\mathcal{ABCD}$, $\mathcal{ABCE}$, $\mathcal{ABDE}$, $\mathcal{ACDE}$, $\mathcal{BCDE}$, $\mathcal{ABCH}$, $\mathcal{ABDH}$, $\mathcal{ACDH}$, $\mathcal{BCDH}$ are intersected in the point $N$.*

See Figure 7.

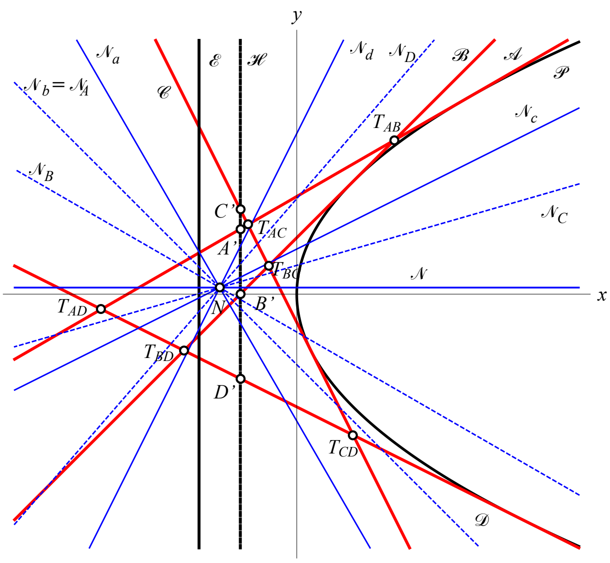


Figure 7: *Medians of quadrilaterals $\mathcal{ABCD}$, $\mathcal{ABCE}$, $\mathcal{ABDE}$, $\mathcal{ACDE}$, $\mathcal{BCDE}$, $\mathcal{ABCH}$, $\mathcal{ABDH}$, $\mathcal{ACDH}$, $\mathcal{BCDH}$ are intersected in the point $N$*

There are many more claims that are not presented in this paper and we plan to deal with them in the next paper.

## References


[1] Blanchard, R., Question 3755, *Mathesis* **65** (1956), 503., solutions par R. Goormaghtigh et R. Deaux, **67** (1958), 377–379.

[2] Blanchard, R., Note, *Mathesis* **55** (1945), 119.

[3] Bricard, R., Question 2433, *Nouv. Ann. Math.* (4) **19** (1919), 472. without a solution

[4] Bouvaist, R., Sur une configuration de cinq droites, *Mathesis* **56** (1947), 33–35.

[5] Clawson, J.W., 509. Points, lines and circles connected with the complete quadrilateral, *Math. Gaz.* **9**(129) (1917), 85–88, `https://doi.org/10.2307/3603503`

[6] Clawson, J.W., Problem 2898, *Amer. Math. Monthly* **28**(5) (1921), 228., `https://doi.org/10.2307/2973761`, solution by the proposer, **29**(5) (1922), 230–231, `https://doi.org/10.2307/2299751`

[7] Clawson, J.W., The complete quadrilateral, *Ann. of Math.* **20**(4) (1919), 232–261, `https://doi.org/10.2307/1967118`

[8] Clawson, J.W., Problem 2921, *Amer. Math. Monthly* **28**(10) (1921), 392., `https://doi.org/10.1080/00029890.1921.11986070`, solution by A. Pelletier, **30**(6) (1923), 339, `https://doi.org/10.2307/2300286`

[9] Connor, J.T., Ladies' Diary, 1795.

[10] Cunningham, A., On the circle perpend-feet pencil and orthocentrical axis of a complete quadrilateral, *Mess. Math.* **21** (1891-92), 188–191.

[11] Davies, T.S., Question 555, *Math. Repository* (2) **6** (1835), 229–234.

[12] Deaux, R., Note, *Mathesis* **61** (1952), 14–16.

[13] Deaux, R., Involution de Möbius et point de Miquel, *Mathesis* **55** (1945), 223–230.

[14] Demir, H., Problem 4818, *Amer. Math. Monthly* **65**(10) (1958), 779., `https://doi.org/10.1080/00029890.1958.11992001`, solution by proposer **66**(8) (1959), 732–733, `https://doi.org/10.2307/2309371`

[15] Gallatly, W., The modern geometry of triangle, Hodgson, London 1910, 27.

[16] Gauss, C.F., Bestimmung der grössten Ellipse, welche die vier Seiten eines gegebenen Vierecks berührt, **22** (1810), 112–121.

[17] Gibbins, N.M., Points connected with the complete quadrilateral, *Math. Gaz.* **24**(260) (1940), 165–168, `https://doi.org/10.2307/3605707`

[18] Goormaghitigh, R., Lemoyne's theorem, *Scripta Math.* **18** (1952), 182–184.

[19] Goormaghitigh, R., Question 3830, *Mathesis* **67** (1958), 111., généralisation par R. Blanchard, **68** (1959), 287–288.

[20] Grinberg, D., From the complete quadrilateral to the Droz-Farny theorem, preprint, 2005, 10.

[21] Guillotin, R., Sur le cercle de Lemoyne d'une droite, *Mathesis* **64** (1955), 280–281.

[22] Guillotin, R., Question 3602, *Mathesis* **62** (1953), 191., solutions M. Durieu and W. Barbenson, **63** (1954), 192–193.

[23] Heinen, F., Auflösung der Aufgaben and Beweis der Lehrsätze 5-9 in Isten Hefte S. 96 und 29-33. im 2ten Hefte S. 191 des 2ten Baudes dieses Journals, J. Reine *Angew. Math* **3** (1828), 285–300, `https://doi.org/10.1515/crll.1828.3.285`

[24] Hermes, O., Question 476, *Nouv. Ann. Math.* **18** (1959), 171.

[25] Marchand, J., Géométrie du quadrilatère complet, *Bull. Soc. Vaudoise Sci. Nat.* **59** (1937), 251–270.

[26] Ono, T., Question 2258, *Nouv. Ann. Math.* (4) **15** (1915), 432., solution par R. Bouvaist, (4) **18** (1918), 114–115.

[27] Opperman, A., Premiers éléments d'une théorie du quadrilatère complet, Gauthier-Villars, Paris 1919, p. 43.

[28] Pita, J.Y., Sobre la recta de los nueve puntos, *Gac. Mat.* **34** (1982), 92–98.

[29] Puissant, Théorème, *Corresp. Ecole Imp. Polytechn.* **1** (1806), 193.

[30] Pujet, A., É. Francoise, Solution de la question 476, *Nouv. Ann. Math.* **18** (1859), 359–362.

[31] Ripert, L., Notes sur le quadrilatère, *Assoc. Franc. Avane. Sci.* **30** (1901), 106–118.

[32] Rochat, Démonstration du théorème énoncé à la paige 232 de ce volume, et de quelques autres propriétés du quadrilatère, *Ann. de Math.*, **1** (1810-11), 314–316.

[33] SCHLÖMILCH, O., Über das vollständige Viereck, *Ber. Verh. Kön. Sächs. Ges. Wiss. Leipzig*, **6** (1854), 4–13.

[34] SCOTICUS, Question 86, *Math. Repository* (2) **1** (1806), 169–170, solution by G. Pickering and J. Cavill

[35] SISKAKIS, A., Problem 1224, *Math. Mag.* **58** (1985), 238., solution by B. Poonen and H. Eves, **59** (1986), 246–247.

[36] SPORER, B., Geometrische Sätze, *Zeitschr. Math. Phys.* **31** (1886), 43–49.

[37] STEINER, J., Théorème sur le quadrilatère complet, *Ann. de Math.* **18** (1827-28), 302–304., Ges. Werke, I, 223–224.

[38] YAMOUT, J., Problem E 3299, *Amer. Math. Monthly* **95** (1988), 954., solution by H. Kappus, **98** (1991), 60.

[39] THÉBAULT, V., Sur des plans associés à un tétraèdre, *Ann. Soc. Sci. Bruxelles*, **66** (1952), 111-118; *Mathesis* **62** (1953), suppl. 8 pp.

[40] THÉBAULT, V., Sur le quadrilatère complet, *C.R. Acad. Sci. Paris* **217** (1943), 97–99.

[41] THÉBAULT, V., Question 3348, *Mathesis* **56** (1947), 243., solution par J. Andersson, **61** (1952), 62.

[42] THÉBAULT, V., Sur le quadrilatère complet, *Mathesis* **51** (1937), 187–191, 242–243.

[43] TIENHOVEN, C., Encyclopedia of Quadri-Figures, `https://chrisvantienhoven.nl/mathematics/encyclopedia`

**Vladimir Volenec**
orcid.org/0000-0001-7418-8972
e-mail: volenec@math.hr

University of Zagreb, Faculty of Science
Bijenička cesta 30, HR-10000 Zagreb, Croatia

**Ema Jurkin**
orcid.org/0000-0002-8658-5446
e-mail: ema.jurkin@rgn.unizg.hr

University of Zagreb
Faculty of Mining, Geology and Petroleum Engineering
Pierottijeva 6, HR-10000 Zagreb, Croatia

**Marija Šimić Horvath**
orcid.org/0000-0001-9190-5371
e-mail: marija.simic@arhitekt.hr

University of Zagreb, Faculty of Architecture
Kačićeva 26, HR-10000 Zagreb, Croatia

# INSTRUCTIONS FOR AUTHORS

**SCOPE.** "KoG" publishes scientific and professional papers from the fields of geometry, applied geometry and computer graphics.

**SUBMISSION.** Scientific papers submitted to this journal should be written in English, professional papers should be written in Croatian or English. The papers have not been published or submitted for publication elsewhere.
The manuscript should be sent in PDF format via e-mail to the editor:

Ema Jurkin
ema.jurkin@rgn.unizg.hr

The first page should contain the article title, author and coauthor names, affiliation, a short abstract in English, a list of keywords and the Mathematical subject classification.

**UPON ACCEPTANCE.** After the manuscript has been accepted for publication authors are requested to send its LaTex file via e-mail to the address:

ema.jurkin@rgn.unizg.hr

Figures should be titled by the figure number that match to the figure number in the text of the paper.

The corresponding author and coauthors will receive hard copies of the issue free of charge.

# How to get KoG?

The easiest way to get your copy of KoG is by contacting the editor's office:

Marija Šimić Horvath
marija.simic@arhitekt.hr
Faculty of Architecture
Kačićeva 26, 10 000 Zagreb, Croatia
Tel: (+385 1) 4639 176

The price of the issue is €15 + mailing expenses €5 for European countries and €10 for other parts of the world.

The amount is payable to:

| | |
|---|---|
| ACCOUNT NAME: | Hrvatsko društvo za geometriju i grafiku<br>Kačićeva 26, 10000 Zagreb, Croatia |
| IBAN: | HR8623600001101517436 |

ISSN 1331-1611
9 771331 161005